Inaugural dissertation

for obtaining the doctoral degree of the

Combined Faculty of Mathematics, Engineering and Natural Sciences

of the

Ruprecht-Karls-University Heidelberg, Germany

Presented by M.Sc. Tobias Riedl

born in: Baden bei Wien, Austria 21st of April 1993

Oral examination: 8th of April 2022

Deciphering the molecular regulation of the antiviral deaminase APOBEC3B

Referees:

Professor Doktor Ralf Bartenschlager

Professor Doktor Mathias Heikenwälder

Table of contents

1   Abbrevations

µL	**microlitre**
µm	micrometre
µM	micromolar
A20	**also TNFAIP3, Tumor necrosis factor, alpha-induced protein 3**
aa	amino acid(s)
ADV	adefovir dipivoxil
AGO (1/2/3/4)	argonaute protein (1/2/3/4)
AhR	aryl hydrocarbon receptor
AID	activation-induced cytidine deaminase
ALT	alanine aminotransferase
APE1/2	apurinic/apyrimidinic endonuclease1/2
APOBEC1	apolipoprotein B mRNA editing enzyme, catalytic polypeptide 1
APOBEC2	apolipoprotein B mRNA editing enzyme, catalytic polypeptide 2
APOBEC3A/A3A	apolipoproteins B mRNA editing catalytic polypeptide-like 3A
APOBEC3B/A3B	apolipoproteins B mRNA editing catalytic polypeptide-like 3B
APOBEC3G/A3G	apolipoproteins B mRNA editing catalytic polypeptide-like 3G
APOBEC4	apolipoprotein B mRNA editing enzyme, catalytic polypeptide 4
ARNT/HIF1β	aryl hydrocarbon receptor nuclear translocator/hypoxia induced factor 1 beta
ATCC	American Type Culture Collection
BAFFR	**B-cell activating factor receptor**
BCA	bicinchoninic acid
BCP	basal core promoter
BER	base-excision-repair
bHLH-PAS	basic helix–loop–helix Per–Arnt–Sim
BHQ	black hole quencher
BS1	a LTβR agonising antibody used in this PhD thesis
CAIX	**carbonic anhydrase IX (9)**
CAM	capsid assembly modulator
CAR-T	chimeric antigen receptor T-cells
Cas9	CRISPR associated protein 9
CBP/CREBBP	CREB-binding protein
cccDNA	covalently closed circular DNA
CD (30/40)	cluster of differentiation (30/40)
CDK6	cyclin dependent kinase 6
cDNA	complementary DNA
CHB	chronic hepatitis B
ChIP	chromatin immunoprecipitation

cIAP (1/2)	cellular inhibitor of apoptosis protein (1/2)
c-Met	tyrosine-Protein Kinase Met
CNV	copy number variation
c-Rel	V-Rel Avian Reticuloendotheliosis Viral Oncogene Homolog
CRISPR	clustered regularly interspaced short palindromic repeats
CTD	C-terminal domain
CV	central vein
CXCL10	C-X-C motif chemokine ligand 10
DAPI	**4′,6-diamidino-2-phenylindole**
DDB1	DNA damage-binding protein 1
DGCR8	DiGeorge syndrome critical region 8 Microprocessor Complex Subunit
DHBV	duck hepatitis B virus
DMOG	dimethyloxallyl glycine; inhibitor of PHD1/2/3
DMSO	dimethyl sulfoxide
DNA	deoxyribonucleic acid
dNTP	deoxynucleoside triphosphate
Dox	doxycycline
dr-HIF1α	degradation resistant HIF1α (carrying P402A/P564A mutations)
dsDNA	double stranded DNA
DTT	dithiothreitol
E2F (2/3)	**E2F transcription factor (2/3)**
E3	ubiquitin ligase
EASL	European Association for the Study of the Liver
EDTA	ethylenediaminetetraacetic acid
EGFR	epidermal growth factor receptor
EMA	European Medicines Agency
ER	endoplasmic reticulum
ETV	entecavir
EZH2	enhancer of zeste homolog 2
FCS	**fetal calf serum**
FG-4592	also Roxadustat; inhibitor of PHD1/2/3
FIH	factor inhibiting HIF-1
FITC	Fluorescein isothiocyanate
GS-9620	**Vesatolimod; TLR7 agonist**
H3K4Me3	**triple-methylated lysine 4 in histone H3**
HBcAg	HBV core antigen (viral capsid)
HBeAg	HBV e antigen (secreted viral protein)
HBsAg	HBV surface antigen (viral envelope)
HBSP	HBV spliced protein

HBV	hepatitis B virus
HBV ΔX	HBV lacking functional HBx
HBx	HBV X protein (transactivating viral protein)
HCC	hepatocellular carcinoma
HCl	hydrogen chloride
HDV	hepatitis delta virus
HEK293	human embryonic kidney 293 cells
HepAD38	HCC cell line, based on HepG2, which produces HBV
HepG2	HCC cell line
HIF (1/2/3α)	hypoxia induced factor (1/2/3 alpha)
HIV	human immunodeficiency virus
HO	hypoxia, 1% oxygen
HPRT	hypoxanthine phosphoribosyltransferase 1
HRE	HIF responsive element
HRP	horseraddish peroxydase
HSPG	heparan sulphate proteoglycan
ICC	**immunocytochemistry**
IFNα (2A)	interferon alpha (2A)
IFNγ	interferon gamma
IFNλ (1/2/3)	interferon lambda (1/2/3)
IHC	immunohistochemistry
IKK	inhibitor of kappa B kinase
IKKα	inhibitor of kappa B kinase alpha
IKKβ	inhibitor of kappa B kinase beta
IKKγ/NEMO	inhibitor of kappa B kinase gamma/NF-κB essential modulator
IL (-1β/6/17A)	interleukin (1 beta/6/17A)
IP	immunoprecipitation
ISH	in situ hybridisation
IU	interantional units
IκB (α)	inhibitor of kappa B (alpha)
kb	**kilobases**
KCl	potassium chloride
kDa	kilodalton
KEGG	Kyoto Encyclopedia of Genes and Genomes
L(-HBsAg)	**large HBV surface antigen**
LAM	lamivudine
LPS	lipopolysaccharide
LSEC	liver sinusoidal endothelial cells
LTα/β	lymphotoxin alpha/beta

LTβR	lymphotoxin beta receptor
M(-HBsAg)	**middle HBV surface antigen**
mg	milligram
MgCl2	magnesium chloride
miRNA	micro RNA
mL	millilitre
mM	millimolar
mmHg	millimetre of mercury
mRNA	messenger RNA
mRNP	messenger RNP; mRNA with bound proteins
MVB	multi vesicular body
NA	**nucleotide/nucleoside analogue**
NaCl	sodium chloride
NAP	nucleic acid polymer
NF-κB	nuclear factor kappa B
NF-κB1/p105/p50	nuclear factor kappa B p105 subunit 1
NF-κB2/p100/p52	nuclear factor kappa B p100 subunit 2
NIK	NF-κB inducing kinase
NLS	nulcear localisation signal
nm	nanometre
NO	normoxia, 20% oxygen
NT	non-treated
nt	nucleotide(s)
NTCP	sodium-taurocholate co-transporting polypeptide
NTD	N-terminal domain
ODD	**oxygen-dependent degradation domain**
ORF	open reading frame
PAM3CSK4	**Pam3CysSerLys4, a synthetic peptide; TLR2 agonist**
PBS	phosphate buffered saline
PEG	polyethylene glycol
PES	polyethersulfone
pgRNA	pre-genomic RNA
PHA-408	inhibitor of IKKβ
PHD (1/2/3)	prolyl hydroxylase (1/2/3)
PHH	primary human hepatocyte
pO_2	partial oxygen pressure
PolII	RNA polymerase II
PPAR	peroxisome proliferator-activated receptor
pre-miRNA	precursor miRNA

Pre-S1/Pre-S2/S	in-frame start codons for the HBsAg gene
pri-miRNA	primary miRNA
PVDF	polyvinylidene fluoride
pVHL	Von Hippel–Lindau tumour suppressor
qPCR	**quantitative PCR**
rcDNA	**relaxed circular DNA**
RelA (p65)	nuclear factor NF-kappa-B p65 subunit
RelB	V-Rel reticuloendotheliosis viral oncogene homolog B
rHBV	recombinant HBV
RHOT2	ras homolog family member T2
RIPA buffer	radioimmunoprecipitation assay buffer
RISC	RNA induced silencing complex
RNA	ribonucleic acid
rpm	rounds per minute
RT	reverse transcriptase
RT-qPCR	reverse transcription-qPCR
S(-HBsAg)	**small HBV surface antigen**
SBP	hepatitis B surface antigen binding protein
sgRNA	single guide RNA
siRNA	small interfering RNA
SMC (5/6)	structural maintenance of chromosomes protein (5/6)
SNP	Single nucleotide polymorphism
sRNA seq	small RNA sequencing
ssDNA	single standed DNA
subviral particle	SVP
SYBR	SYBR Green fluorescent DNA dye
TAF	**tenofovir alafenamide fumarate**
TAK1/MAP3K7	Mitogen-activated protein kinase kinase kinase 7
TDF	tenofovir disoproxil fumarate
Teno	tenofovir
THA	terminal hepatic arteriole
TLR (2/7/9)	toll-like receptor (2/7/9)
TLV	telbivudine
TNFR	TNFα receptor
TNFα	tumour necrosis factor alpha
TP	"terminal protein"-domain of the HBV polymerase
TPCA-1	also GW683965; inhibitor of IKKβ
TPV	terminal portal vein
TRAF (2/3)	TNF receptor associated factor (2/3)

Tris	tris(hydroxymethyl)aminomethane
TTR	transthyretin
TRPB	TAR RNA-binding protein
Tyr	tyrosine
UNG	**uracil-DNA glycosylase**
UTR	untranslated region
UV	ultra violet
Vif	**viral infectivity factor**
WHB	**woodchuck hepatitis virus**
WHO	World Health Organisation
YAP1	**YES-associated protein 1**

2   Summary

Although effective vaccines against the hepatitis B virus (HBV) are available, it remains a major global health burden. The World Health Organisation estimates that nearly 300 million people are infected with HBV as of 2019 and chronic carriers, suffering from chronic hepatitis B (CHB) are at high risk of developing end-stage liver disease, such as liver cirrhosis and liver cancer.

HBV has a complicated life cycle with 2 main steps [1]: (I) the establishment of the viral genome - the covalently closed circular DNA (cccDNA) - in the nucleus of infected hepatocytes, which is highly stable and used as the template for all viral RNAs, and (II) a reverse transcription step, which produces a replicative intermediate - the relaxed circular DNA (rcDNA) - from the pre-genomic RNA (pgRNA). In the clinic, CHB patients are often treated with nucleotide and nucleoside analogues (NAs), which efficiently block the reverse transcription and prevent spread of the virus. While these treatments can prevent the progression of the liver disease, they cannot cure the infection. Therefore, the development of resistance against NAs or being non-compliant to the treatment can result in a relapse of the infection.

The research group of Prof. Mathias Heikenwälder and colleagues were the first to show that the agonisation of the lymphotoxin beta receptor (LTβR) on the surface of hepatocytes with an antibody (named BS1) leads to the degradation of the cccDNA. Importantly, they presented evidence that the infection did not rebound after withdrawal of the LTβR agonist, which is the case for the treatment with NAs. The degradation of the cccDNA was dependent of the induction of the apolipoproteins B mRNA editing catalytic polypeptide-like 3B (APOBEC3B), an antiviral enzyme with cytidine deaminase activity, which efficiently edited cytosines to uracils within the cccDNA, eventually leading to the degradation of the cccDNA [2]. These findings represented a potential novel treatment option for CHB patients, allowing for a cure of the disease by directly targeting the viral genome and degrading it, therefore preventing viral rebound.

Aim 1: Deciphering transcriptional and post-transcriptional control of APOBEC3B

In this scientific context, I investigated key factors involved in the regulation of APOBEC3B on the transcriptional and post-transcriptional level. I used HBV infected and non-infected differentiated HepaRG (dHepaRG), treated or not with the LTβR agonist BS1. Further, CRISPR-Cas9-induced knock-out cell lines of dHepaRG, small interfering RNA, and micro RNA (miRNA) transfections into dHepaRG as well as kinase inhibitors were used to shed light on key molecular mechanisms involved in APOBEC3B regulation.

The data of this PhD thesis indicate that APOBEC3B induction is mediated by the nuclear factor kappa B (NF-κB), and that mainly the non-canonical NF-κB signalling, through RelB/p52 dimers, plays an important role in APOBEC3B induction. Furthermore, the miRNA hsa-miR-138-5p is a post-transcriptional repressor of APOBEC3B. Interference with NF-κB signalling and aberrant expression of hsa-miR-138-5p reduced inducibility of APOBEC3B by LTβR activation and prevented strong anti-cccDNA effects of the treatment.

I published these results as a co-first author in *Journal of Hepatology Reports* in August 2021 (DOI: 10.1016/j.jhepr.2021.100354) [3].

Aim 2: Hypoxia reduces antiviral effects of LTβR activation and offers a niche for HBV to avoid immune responses

Next, I deciphered how oxygen levels, sensed on a cellular level *inter alia* by hypoxia induced factor 1 alpha (HIF1α), affect APOBEC3B expression and anti-cccDNA effects of LTβR activation. To this end, I also used HBV infected and non-infected dHepaRG, treated or not with the LTβR agonist BS1. Transgenic dHepaRG cell lines, transfection of siRNAs, and pharmacological inhibition of proline hydroxylases (i.e. proteins involved in the destabilisation of HIF1α) were also used. In addition, I analysed histological stainings of liver sections of CHB patients. I identified HIF1α as a restriction factor for APOBEC3B induction by LTβR activation. RelB protein levels were reduced under high HIF1α protein levels, preventing efficient APOBEC3B induction and subsequent anti-cccDNA effects. My data indicated that liver areas presenting high levels of HIF1α can offer a reservoir for HBV *in vivo*, in which the virus can avoid immune-mediated clearance.

I published these results as a co-first author in *Hepatology* in April 2021 (DOI: 10.1002/hep.31902) [4].

3   Zusammenfassung

Obwohl effektive Vakzine verfügbar gegen das Hepatitis B Virus (HBV) verfügbar sind, bleibt dieses Virus ein ernstzunehmendes, globales Gesundheitsproblem. Die Weltgesundheitsorganisation (World Health Organisation, WHO), schätzt, dass im Jahr 2019 knapp 300 Millionen Personen mit HBV infiziert waren. Patienten, die an einer chronische Hepatitis B (CHB) leiden, weisen ein hohes Risiko auf, eine fatale Leberpathologie auszubilden, zum Beispiel eine Leberzirrhose oder Leberkrebs.

HBV hat einen komplizierten Lebenszyklus, den man grob in zwei wichtige Schritte einteilen kann [1]: (I) Die Etablierung der zirkulären, kovalent geschlossenen DNA (cccDNA, engl. covalently closed circular DNA) im Zellkern infizierter Hepatozyten, die sehr stabil ist und als Vorlage aller viralen mRNAs dient, und (II) ein reverser Transkriptions-Schritt, der die relaxierte, zirkuläre DNA (rcDNA, engl. Relaxed circular DNA) auf Grundlage der prägenomischen RNA (pgRNA) produziert. Klinisch werden CHB Patienten oft mit Nukleotid- und Nukleosid-Analoga (NA) behandelt, die mit hoher Effizienz die reverse Transkription von HBV inhibieren und dadurch die Vermehrung des Virus unterbinden. Diese Behandlung kann dazu beitragen, das Fortschreiten der Lebererkrankung zu verlangsamen oder zu stoppen, jedoch kann die Krankheit nicht komplett geheilt werden und bei einer Ausbildung von Resistenzen gegen die Behandlung oder dem nicht-Einhalten der Medikamenteneinnahme kann dazu führen, dass die Krankheit wieder ausbricht.

Die Arbeitsgruppe von Prof. Mathias Heikenwälder, zusammen mit Kollegen, war die erste, die zeigen konnte, dass die Agonisierung des Lymphotoxin beta Rezeptors (LTβR) mit einem Antikörper (genannt BS1) zu einer Degradierung der cccDNA führt. Des Weiteren konnte gezeigt werden, dass auch nach Beendigung der Behandlung die Erkrankung nicht mehr ausbrach, wie es bei der Behandlung mit NA der Fall war. Die Degradierung der cccDNA war abhängig von der Induktion des antiviralen Proteins apolipoproteins B mRNA editing catalytic polypeptide-like 3B (APOBEC3B), welches eine Cytidin-Deaminase Aktivität aufweist. Dieses Protein deaminierte Cytosine in der cccDNA zu Uracilen, was schlussendlich die Degradierung der cccDNA zur Folge hatte [2]. Diese Resultate könnten eine neue Behandlungsoption für CHB Patienten darstellen, die auch kurativ wirkt und nicht nur das Virus in der Ausbreitung hemmt, da die cccDNA direkt angegriffen und abgebaut wird was einen erneuten Ausbruch der verhindert.

Ziel 1: Entschlüsselung der transkriptionellen und post-transkriptionellen Expressionskontrolle von APOBEC3B

In dem wissenschaftlichen Kontext dieser PhD Thesis untersuchte ich Schlüsselfaktoren, die die APOBEC3B Expression auf der transkriptionellen und post-transkriptionellen Ebene

regulieren. Dafür verwendete ich HBV-infizierte und nicht-infizierte differenzierte HepaRG (dHepaRG) Zellen, die mit dem LTβR Agonisten BS1 behandelt wurden. Des Weiteren wurden CHRISPR-Cas9 induzierte Knock-Out dHepaRG verwendet; außerdem verwendete ich kurze, interferierende RNAs (siRNAs, engl. small interfering RNAs) und microRNAs (miRNAs), die in dHepaRG transfiziert wurden. Darüber hinaus wurden Kinase-Inhibitoren verwendet, um die molekularen Schlüsselmechanismen, die der APOBEC3B Regulierung zugrunde liegen, näher zu beleuchten.

Die Daten in dieser PhD Thesis verdeutlichen, dass die APOBEC3B Induktion vom nukleären Faktor kappa B (NF-κB) Signaltransduktionsweg abhängt und dass vorrangig der nicht-kanonische NF-κB Signaltransduktionsweg über RelB/p52 Dimere eine wichtige Rolle spielt. Darüber hinaus ist die miRNA hsa-miR-138-5p ein post-transkriptioneller Repressor von APOBEC3B. Die Blockade von NF-κB und die aberrante Expression von hsa-miR-138-5p reduzierte die Induzierbarkeit von APOBEC3B durch LTβR Aktivierung und verhinderte starke anti-cccDNA Effekte der Behandlung.

Ich konnte diese Ergebnisse als Ko-Erstautor in *Journal of Hepatology Reports* im August 2021 publizieren (DOI: 10.1016/j.jhepr.2021.100354) [3].

Ziel 2: Hypoxie reduziert antivirale Effekte der LTβR Aktivierung und schafft eine Nische für HBV, in der Immunreaktionen vermieden werden können

Als nächstes entschlüsselte ich, wie der Sauerstoffgehalt, der auf zellular Ebene unter anderem über den Hypoxia-induzierten Faktor 1 alpha (HIF1α) wahrgenommen wird, die APOBEC3B Expression und die anti-cccDNA Effekte der LTβR Aktivierung beeinflusst. Dazu verwendete ich ebenfalls HBV-infizierte und nicht-infizierte dHepaRG Zellen, die mit dem LTβR Agonisten BS1 behandelt wurden. Außerdem wurden transgene dHepaRG Linien verwendet, siRNA Transfektionen durchgeführt und dHepaRG mit Inhibitoren behandelt, die die Aktivität von Polin-Hydroxylasen blockieren, Proteine die in die Destabilisierung von HIF1α involviert sind. Ebenfalls habe ich histologische Färbungen von Lebern von CHB Patienten untersucht. Ich konnte HIF1α als Restriktionsfaktor für APOBEC3B Induktion durch LTβR Aktivierung identifizieren. RelB Protein Levels waren reduziert unter hohen HIF1α Proteinlevels, was eine effiziente APOBEC3B Induktion und anti-cccDNA Effekte verhinderte. Meine Daten weisen darauf hin, dass in Leberregionen mit hohen HIF1α Levels ein Reservoir für HBV darstellen können, in denen das Virus einem immun-vermittelten Abbau entgeht.

Ich konnte diese Ergebnisse als Ko-Erstautor in *Hepatology* im April 2021 publizieren (DOI: 10.1002/hep.31902) [4].

4   Introduction

4.1   Hepatitis B

4.1.1 Epidemiology

The World Health Organisation (WHO) estimates that nearly 300 million people are infected with Hepatitis B Virus (HBV) as of 2019, with around 1.5 million new infections per year. HBV chronic infection (chronic hepatitis B [CHB]) can cause severe long-term damage to the liver, including the development of liver cirrhosis and hepatocellular carcinoma (HCC). Taken together, chronic and acute infections with HBV cause nearly 900,000 deaths per year (WHO, 2019). Globally, between 3.5 and 5.6% of the population, based on different reports, are estimated to carry HBV, indicated by sero-positivity for the viral surface protein, (HBV surface antigen [HBsAg]) [5-7]. Locally, the endemic is sub-categorised in four groups: low seroprevalence (below 2%), low-intermediate (or low-moderate) seroprevalence (2-4.9%), high-intermediate (or high-moderate) seroprevalence (5-7.9%), and high seroprevalence (above 8%). The highest prevalence is found in sub-Saharan countries with prevalence rates above 8%) [8, 9] (**FIGURE 1a**).

Genetically, HBV was previously divided into eight well-known, different genotypes (A-H). but recently, two more genotypes, I and J, were also described [10-12]. On the nucleotide level, those genotypes can differ up to 7.5%. Interestingly, the HBV genotypes show a very distinct distribution and vary between regions (**FIGURE 1b**). Indeed, genotype C is mostly found in the Asian-Pacific region, while genotype E is most prevalent in Africa. The eight genotypes can further be divided into subtypes if the nucleotide sequence differences are above 4%. Furthermore, recombination between genotypes has been described in the literature [13, 14]. The different genotypes show correlations with different clinical features of the disease, as well as to a different response to treatments (**TABLE 1**); however, a clear and generalised connection between genotypes and those parameters has not been established yet. Resistance or reduced response to interferon (IFN) therapy, as well as increased mutation frequency in the core protein promoters were associated with the genotype C [15]. Furthermore, genotype C showed higher HBV DNA serum levels and a more severe liver disease in a Taiwanese population compared to genotype B, whereas genotype B seemed to induce HCC more strongly in young patients [13, 16]. A very particular association was found in genotype D with the mutations in the PreCore region of the HBV genome, which lead to the disruption of the HBV e antigen (HBeAg) open reading frame (ORF) and the loss of HBeAg secretion during the course of the infection [13, 17].

a
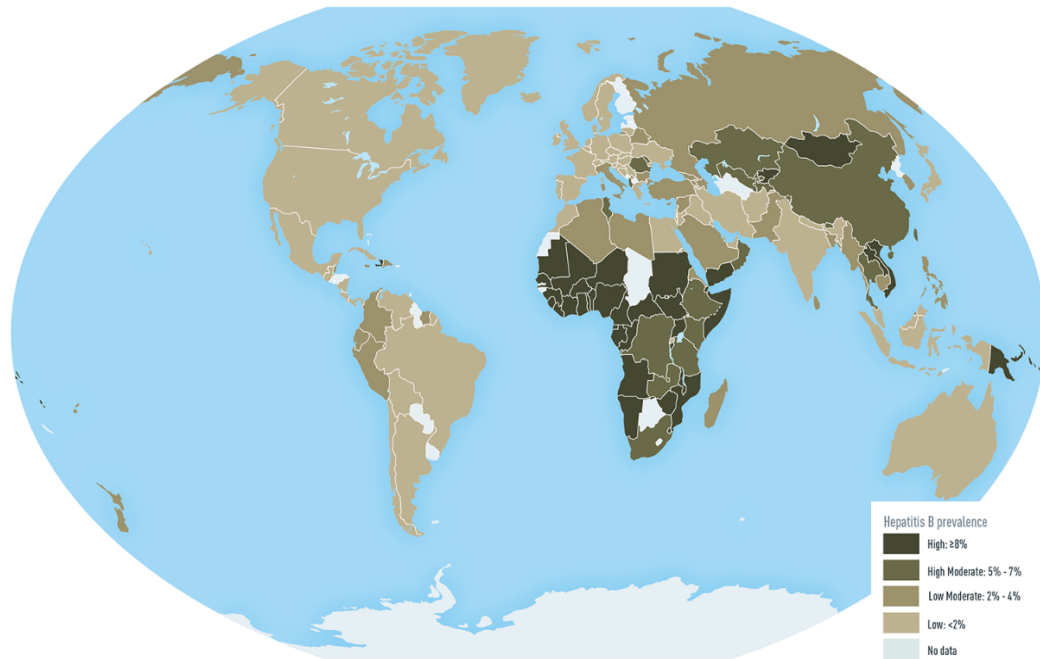
b
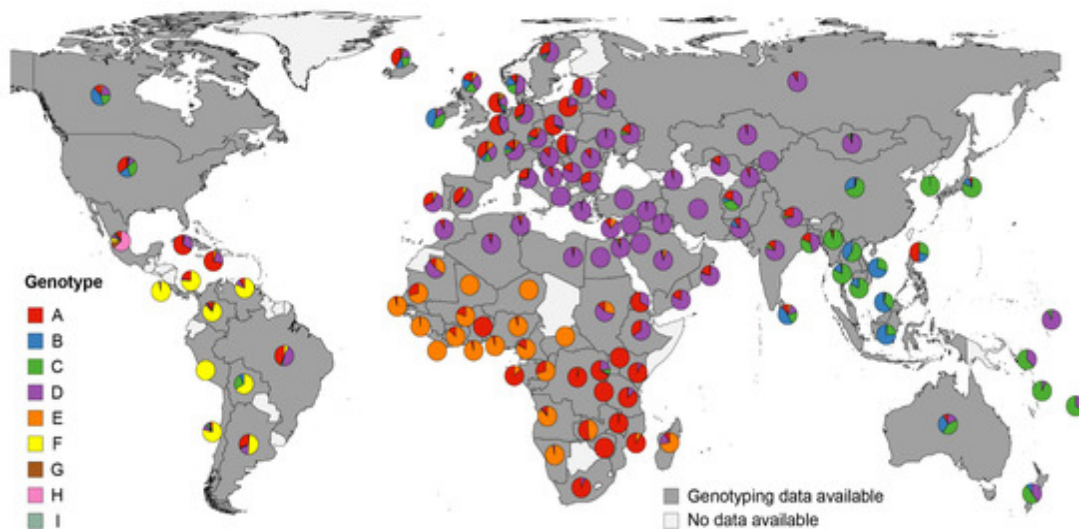
Figure 1: Distribution of HBV seroprevalence and genotypes worldwide
(a) (Adapted from Harris, CDC, Yellow Book 2020 and Schweitzer, *et al.* [7]) Seroprevalence of hepatitis B virus infections is classified into 4 groups: low (<2%), low moderate (2-4.9%), high moderate (5-7.9%), and high (>8%). **(b) (adapted from Lin, *et al.* [18])** The distribution of HBV genotypes worldwide. While genotype C is very prevalent in the Asia/Pacific region, genotype E is mainly found in sub-Saharan Africa, and genotype F is very prevalent in South- and Middle America.

The transmission of HBV can follow two distinct routes: vertically and horizontally [13], with different genotypes also showing a preference for the one or the other (**TABLE 1**). The vertical

transmission from the HBV positive mother to the child, either during birth or in the first months after birth mostly happens in zones of high prevalence. No significant infection rates of unborn children via placental transmission have been transcribed in the literature. The highest risk of vertical transmission is associated with mothers who suffer from an acute infection with HBV during the third trimester, have a high viral load and are positive for HBeAg. Horizontal transmission occurs between a HBV positive and a negative individual with no parent-child relation. Here, HBV is transmitted usually by infected blood (e.g. contaminated needles, blood transfusions), or by exchange of body fluids (e.g. during unprotected sexual contact) [19]. Importantly, the rates of developing a chronic or an acute HBV infection greatly differ between those infection routes, given that the HBV negative person is unvaccinated before primo infection. Indeed, 90% of infected new-borns will develop a chronic disease, while only around 5% of infected adults would develop a CHB [20]. Infected children and young adolescents develop a chronic infection between at around 23% and 10%, respectively [21].

Table 1: Clinical differences between different HBV genotypes (adapted from Rajoriya, N., *et al.* and Lin, C.-L., *et al.* [22, 23])

In the case of a lack of reliable data, cells are marked with a " - ".

Genotype	A		B	C	D	E-I
Sub-genotype	A1	A2				
Genome size	3,221 bp	3,221 bp	3,215 bp	3,215 bp	3,182 bp	E, F, H, I - 3,212 bp G - 3,248 bp I - 3,182 bp
HBV DNA levels	-	-	Low	High	-	-
Main mode of transmission	Horizontal	Vertical	Vertical	Vertical	Horizontal	Horizontal
HbAg positivity	Low	High	Low	High	Low	-
HBeAg seroconversion in natural history	Early	Early	Early	Late	Late	-
Progression to cirrhosis and HCC	High	Low	Lower rates of progression than C	High rate of progression	More severe liver disease than A, depending on the country	High rate of progression in F
Response rates to INFa	High	-	High	Low	Low	Low in G

4.1.2 HBV biology

4.1.2.1 Classification

HBV is a small DNA virus, measuring around 42 nanometre (nm) in diameter. Its partially double stranded genome is replicated via a unique reverse transcription step from a RNA intermediate. In the Baltimore classification, it therefore belongs to the group VII, namely "dsDNA (double stranded DNA) viruses which replicate via an RNA intermediate". HBV belongs to the Hepadnaviridae family, together with similar hepatotropic viruses like the duck hepatitis B virus (DHBV) and the woodchuck hepatitis virus (WHV). Both DHBV and WHV have thus been used to better understand Hepadnaviridae biology, and as surrogate models for HBV.

4.1.2.2   HBV genome and transcripts

The hepatitis B virus genome features only four ORFs (**FIGURE 2**) [24]. All HBV open reading frames are overlapping, leading to a highly compact genome of only 3.2 kilobases (kb).

- The **Pre-Core/Core ORF** contains two in-frame start codons. The pre-core ORF encodes the secreted HBeAg and the core ORF contains the information for the capsid antigen (HBV core antigen [HBcAg]).
- The **Polymerase ORF** represents around 80% of the viral genome and encodes the viral polymerase.
- The **Pre-S1/Pre-S2/S ORF** is completely embedded in the polymerase gene and contains 3 in-frame "ATG" start codons for the three HBV envelope proteins, hereafter called S-(small), M-(medium), and L-(large) HBsAg. These are transcribed from the first, second, and third start codon, respectively.
- The **X ORF** encodes the hepatitis B virus X protein (HBx).

Altogether, four viral promoters, two enhancers, and one cis-acting element regulate the transcription of the five major HBV transcripts [25] (**FIGURE 2**):

- The pre-genomic RNA (pgRNA; 3.5 kb), which represents the template for the translation of the viral polymerase, the core protein, and is, in addition, the template for the *de novo* synthesis of the HBV genome.
- The Pre-Core mRNA (3.5 kb) is only a few nucleotides longer than the pre-genomic RNA. It is the only transcript that fully covers the first ATG from the pre-Core ORF and therefore is important for the translation of the secreted HBeAg.
- The Pre-S1 mRNA (2.4 kb) is the template for L-HBsAg
- The Pre-S2/S mRNA (2.1 kb) is the template for M-HBsAg and S-HBsAg.
- The X mRNA (0.7 kb) is the template for HBx.

4.1.2.3   Viral proteins

Seven different HBV proteins are produced in infected cells. These proteins are the HBV polymerase, HBcAg, the pre-core protein, which is later processed to for the mature HBeAg, L-, M- and S-HBsAg, and HBx [26]. These proteins will be further described in this section. Another protein, that will not be further described here, that was found in liver samples of patients, is the HBV spliced protein, which is produced by alternative splicing of the pgRNA [27].
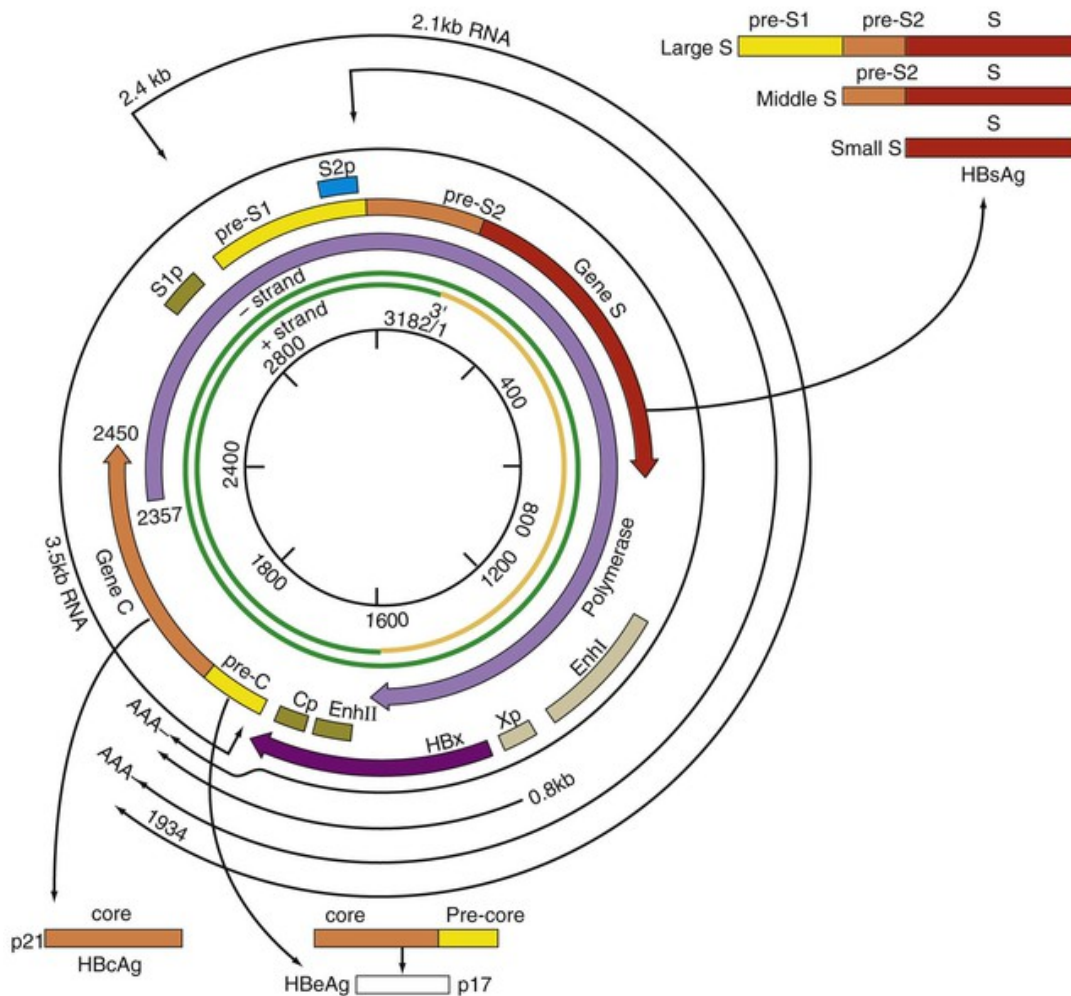
Figure 2: HBV has a highly compacted genome with overlapping open reading frames (adapted from https://oncohemakey.com/hepatitis-b-virus-and-hepatitis-delta-virus/ and from Murray, *et al.* **[28])**

The HBV genome contains 4 open reading frames (Pre-Core/Core, Polymerase, Pre-S1/Pre-S2/S, and X) and 4 promoters (Core promoter, Cp; Pre-S1 promoter, S1p; Pre-S2 promoter, S2p and the X promoter, Xp). Furthermore, 2 enhancer regions are indicated (EnhI and EnhII). Gene products of the Pre-Core/Core ORF are shown below, the 21 kD HBcAg at the left side and the 17 kD HBeAg at the right side. Gene products of the HBsAg ORF are shown at the right side. The large HBs, L-HBs, contains N-terminal extensions of the pre-S1 and pre-S2 region, the middle HBs contains an N-terminal extension of the pre-S2 region and the small HBs only contains the S region as the other two.

- **HBcAg**: The capsid protein is 183 amino acids (aa) long and has a molecular weight of 21 kilodalton (kDa). HBcAg naturally assembles into homodimers. Subsequently, to form the nucleocapsid, 90 to 120 homodimers assemble, containing the viral pgRNA and the polymerase. The two domains, the N- and C-terminal domain (NTD and CTD, respectively), have distinct functions. While the **NTD** is involved in the assembly of the protein into di- and multimeres, the **CTD** is involved in the pgRNA encapsidation. The maturation process of capsids is regulated by the phosphorylation status of the individual HBcAg molecules. Dephosphorylation induces DNA synthesis from the pgRNA and leads to the conformational reorganisation of the CTD. By this, binding sites to the envelope proteins are exposed and

mature virions are assembled [29, 30]. The CTD also features a nuclear localisation signal, enabling the nuclear import of capsids into the nucleus. Newly synthesised nucleocapsids can, if not enveloped and secreted, re-enter the nucleus thus increasing the nuclear pool of the viral genome [31]; this process is called recycling.

- **HBeAg**: Such as HBcAg, HBeAg is translated from the pre-core mRNA but present a 29 aa N-terminal extension as compared to HBcAg. First, a 25 kDa protein is produced, which is transported to the endoplasmic reticulum (ER), where the protein is processed. The CTD, which contains the NLS, is cleaved off the precursor by sequential cleaving events to form the mature HBeAg of 17 kDa, which can be secreted [32]. Although the expression of HBeAg is not necessary for the completion of the viral life cycle, as it was shown in *in vitro* studies [33], the presence of HBeAg in patient's serum is often used as a surrogate marker for active viral replication.

- **Polymerase**: The HBV polymerase is the only protein with enzymatic activity encoded by the viral genome. The protein is 230 aa in size and has a molecular weight of around 90 kDa. The protein itself can be divided into three parts with distinct functions. The **TP domain** is essential for the interaction with the "epsilon" ε-signal, or ε-loop, of the pgRNA. In the TP domain, a tyrosine (Tyr) covalently links the newly synthesised DNA to the polymerase [34]. The **RT domain** has both a reverse transcriptase activity and a DNA-dependent DNA polymerase activity. First it reverse transcribes the pgRNA, synthesising the minus-polarised DNA strand, followed by the partial synthesis of the plus strand, forming the HBV rcDNA (relaxed circular DNA). The RT domain lacks a 3'-5' exonuclease function and has therefore no proof-reading activity [35]. The **RNaseH domain** of the polymerase is responsible for the degradation of the pgRNA after the synthesis of the minus-strand. Furthermore, it is important for the generation of short RNA primers that are necessary for the initiation of the plus-strand synthesis [36].

- **HBsAg**: The three envelope proteins, S-, M- and L-HBsAg make up the outer layer of the mature virion. The proteins are 226 aa, 281 aa, and between 389 and 400 aa (depending on the strain) in size, respectively. Of these 3, S is the most abundant form of HBsAg found in infected cells [37]. All three forms of HBs are synthesised and mature in the ER and then assemble into hetero- and homodimeric complexes. Cysteins in the S domain play an essential role in this process to produce the mature envelope [38]. During its maturation process, L is myristoylated [39] and required for the attachment to and the entry via the sodium-taurocholate co-transporting polypeptide (NTCP) [40, 41]. Furthermore, L is required for the virion morphogenesis by the envelopment of nucleocapsids. Interestingly, while M is dispensable for virion secretion, S and L are required for this process [37].

Envelope proteins can also self-assemble into subviral particles (SVPs), which are also secreted. SVPs come in the flavour of either spheres, which mainly contain S and M and are

around 20 nm in diameter, or filaments of variable length and with around 22 nm in diameter (**FIGURE 3**). Those filaments also contain L [42-44]. In infected patients, the amount of SVPs found in serum is in large excess compared to infectious virions, the so-called Dane particle. On average, SVPs can be found from 1,000 up to 10,000 times more than Dane particles [45]). It is of high clinical importance that SNPs are present in large excess. Indeed, SVPs can reach levels up to 1 mg/mL in the blood and act as decoys for the recognition of HBsAg specific antibodies and cells of the adaptive immune system [44, 46].
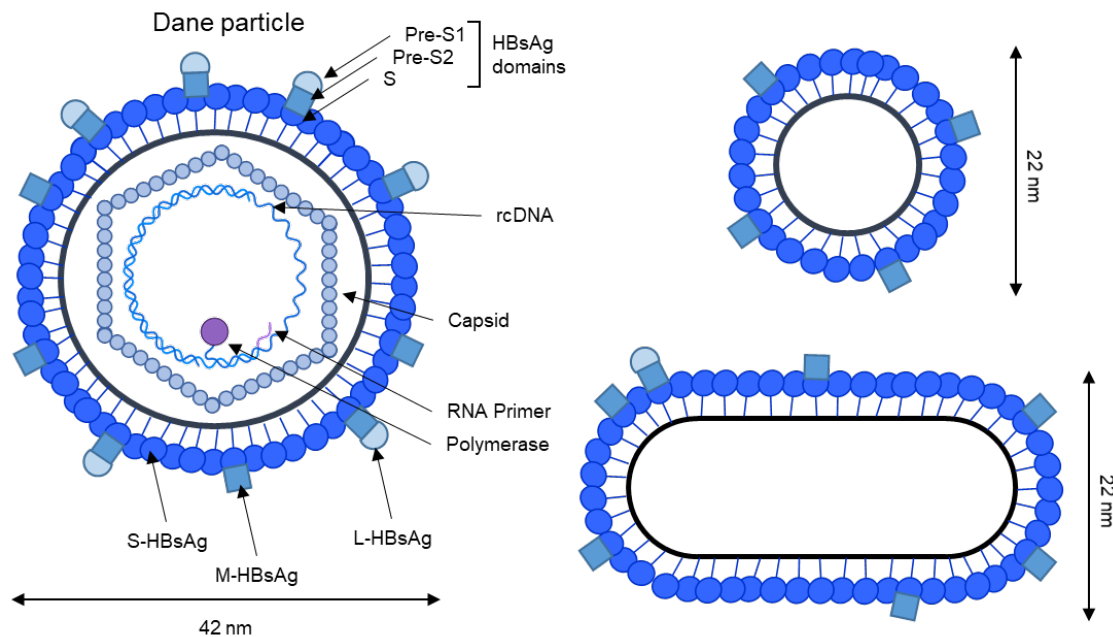

Figure 3: Secreted products of HBV (adapted from Herrscher, *et al.* [47])
Subviral particles come in the flavour of spheres with 22 nm in diameter or filaments of variable lengths, also with 22 nm in diameter. Dane particles, containing a nucleocapsid, are the infectious particles and are 42 nm in diameter.

- **HBx**: The HBV X protein is the smallest protein encoded on the viral genome. It is only 154 aa or 17 kDa in size. HBx is necessary for the maintenance of an open chromatin structure and active transcription from the viral genome and is therefore indispensable for replication as shown *in vitro* for HBV [48] and *in vivo* in the case of WHV [49]. 2 studies from the last decade suggest that HBx targets the host restriction factor of HBV, the structural maintenance of chromosomes protein 5/6 (SMC5/6) complex, for degradation. It has been proposed that the engagement of the DNA damage-binding protein 1 (DDB1)/E3 ubiquitin ligase complex by HBx leads to the ubiquitination of SMC5/6 and its proteasomal degradation [50, 51]. Another study describes the regulation of the nucleocapsid phosphorylation by HBx, which is also essential for efficient replication [52]). Furthermore, the X protein was described to trans-activate the promoters of the extrachromosomal HBV genome [25]. Besides these functions

of HBx on HBV itself, this protein was also described to directly modulate the host cell. Although HBx is not known to directly bind DNA, host gene regulation can be regulated by the interaction of HBx with cellular transcription factors [53]. In addition, HBx was shown to act on the host epigenome by interactions with histone modifying enzymes [54]. Wei and colleagues furthermore describe the X protein to be involved in the regulation of the cell cycle, the response to DNA damage, the apoptosis, and the modulation of the innate immune response [55, 56]. Given all those different potential targets for HBx in an infected hepatocyte, it is hardly surprising that HBx was suggested to play a role in the development of HBV-associated HCC [57].

4.1.3 Viral life cycle

4.1.3.1   Viral entry

L-HBsAg is necessary for the entry of HBV into hepatocytes. It can interact with heparan sulphate proteoglycans (HSPGs) [58, 59] and, as previously mentioned, mediate the entry into the hepatocyte via NTCP (**FIGURE 4, step 1**), which is expressed at the baso-lateral membrane of the cells [40, 41]. SPB, the hepatitis B surface antigen binding protein, was also suggested to play a role in the entry of HBV into the cell [60]. Furthermore, the epidermal growth factor receptor (EGFR) is a known co-receptor for HBV entry [61]. Internalisation is mediated by an endocytosis pathway [62-64]. A very recent publication proposes that both the clathrin-mediated endocytosis, as well as the clathrin-independent endocytosis pathways are involved in the internalisation of HBV, depending on the levels of liver sinusoidal endothelial cell (LSEC)-derived epidermal growth factor (EGF) [65].

4.1.3.2   Nuclear import and cccDNA formation

After internalisation, Dane particles end up in cytoplasmic vesicles. It is believed that the viral envelope fuses then with the membranes of the vesicles to release the nucleocapsid in the cytoplasm, however the exact mechanism remains elusive [1] (**FIGURE 4, step 2**). The nucleocapsid is then transported to the nucleus along the microtubules [66] and, via an importin-dependent mechanism, is imported into the nucleus through the nuclear pore complex [67, 68] (**FIGURE 4, step 3**). The HBV genome, at this point, is still present as the rcDNA, with a complete, but nicked minus-strand and a partially synthesised plus-strand. The polymerase is still attached to the 5'-end of the minus-strand and the RNA primer, used to prime the plus-strand synthesis, is still attached to the 5'-end thereof (depicted both in purple in **FIGURE 3**) [69, 70]. Both the polymerase and the RNA primer are then removed [71] and the cccDNA (covalently closed circular DNA) is formed (**FIGURE 4, step 4**), a process that

will not be discussed here *in extenso*. The cccDNA is a highly stable molecule and was estimated to have a half-life in patients of around nine months [72]. The cccDNA primarily stays as an episome, or a minichromosome. As such, it is decorated with histones and non-histone proteins and forms a chromatin-like structure [73, 74]) (**FIGURE 4, step 5**). The cccDNA is the central part of the viral life cycle, as it gives rise to all viral RNAs and therefore allows replication and spread of the virus. As noted, as an episome, the cccDNA has a high stability [75, 76] and can persist even after seroconversion from HBsAg to anti-HBsAg antibodies, which is a sign of functional cure [77, 78]), even if recycling of nucleocapsids from the cytoplasm to the nucleus is inhibited [79].

Nonetheless, the HBV genome can also integrate into the host genome. The latter is believed to happen in 10-100% of patients during HCC development, although it was not finally proven that the integration event is an inevitable cancer driver or just happens in a series of events that ultimately lead to cancer [26]. It was proposed that "wrongly" reverse transcribed, linear HBV genomes integrate into the host DNA through homologous recombination, at locations where the host DNA suffers from DNA double strand breaks [80] (**FIGURE 4, step 6**).

4.1.3.3 Encapsidation and rcDNA synthesis

All viral RNAs are transcribed from the cccDNA in an RNA polymerase II (PolII) dependent mechanism. The viral RNAs therefore contain a regular 5' cap structure and a poly-A tail. All RNAs are generally transcribed at ER-associated ribosomes (**FIGURE 4, step 7**).

The pgRNA contains the ORF for the viral polymerase. After translation, the viral polymerase recognises and binds to the ε-loop of the pgRNA, blocking its translation [81]. After the binding, the reverse transcription and the encapsidation of the emerging HBV DNA are thought to be ongoing in parallel [82] (**FIGURE 4, step 8**). The tyrosine residue Y63 serves as primer in the reverse transcription, covalently linking the polymerase to the emerging DNA molecule. A trinucleotide (GAA) is synthesised which switches template from the 5'-end to the 3'-end of the pgRNA. Then, the minus-strand is produced over the whole length of the pgRNA, with some additional terminal redundancy (**FIGURE 4, step 9**). Subsequently, the pgRNA is degraded by RNaseH activity, leaving only the 5'-end of the pgRNA behind. This short RNA primer binds to the minus-strand at the 3' direct repeat and initiates the synthesis of the plus-strand [83, 84] (**FIGURE 4, step 10**). A template switch of the polymerase navigates the elongation over the physical "gap" in the minus-strand by the redundant sequence in the minus-strand, allowing for the generation of the rcDNA. Note wise, the ongoing rcDNA synthesis leads to a maturation of the pgRNA containing capsids, from hyper-phosphorylated HBcAg molecules in the immature capsids to dephosphorylated ones at the end of the maturation and rcDNA synthesis process. The progressive dephosphorylation has functional

consequences for the capsids, with mature, dephosphorylated capsids having a higher affinity for envelopment with HBsAg and the secretion [46].

4.1.3.4 HBV morphogenesis

Encapsidated rcDNA can mainly have two different fates: the re-import into the nucleus to the formation of a cccDNA pool (**FIGURE 4, step 11**), or the secretion after the envelopment with HBsAg. The latter involves the assembly of virions on multi vesicular bodies [85] (**FIGURE 4, step 12**). Interestingly, the secretion of subviral particles follows a different secretion pathway via the ER and a general secretion pathway [44, 86] (**FIGURE 4, step 13**).
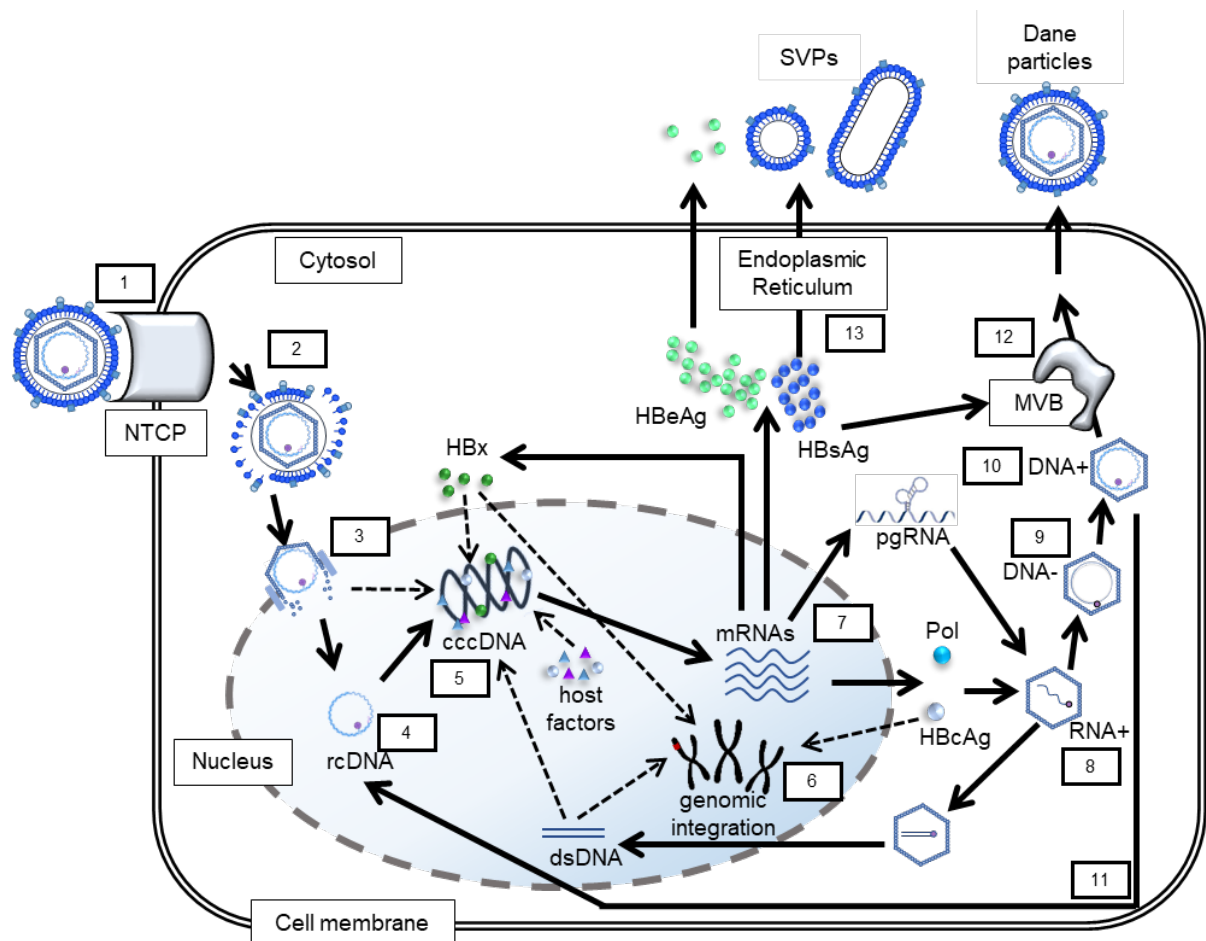
Figure 4: The HBV life cycle (adapted from Tsukuda, *et al.* and Wang, *et al.* [1, 87])
Detailed explanations for the individual steps and specific references are given in the text for the indicated numbers.

4.1.4 HBV Disease

Usually, the incubation period ranges from one to six months after exposure to the virus, before an infection can be clinically evidenced. In general, two forms of an HBV infection are distinguished, the acute and the chronic infection.

4.1.4.1   Acute HBV infection

An **acute HBV** infection, on the one hand, results in a majority of cases as an asymptomatic disease (ranging between 60 and 80%). This disease lasts between one and two weeks. An acute infection can develop into a fulminant hepatitis in less than 1% of cases, resulting often in an acute liver failure with high mortality rates. Already during the acute phase, antibodies against the core antigen are observed.

4.1.4.2   Chronic HBV infection

On the other hand, a **chronic hepatitis B** infection is defined by HBsAg sero-positivity for more than six months. The chronic disease is clinically divided into five phases of different durations (**FIGURE 5**) [88].
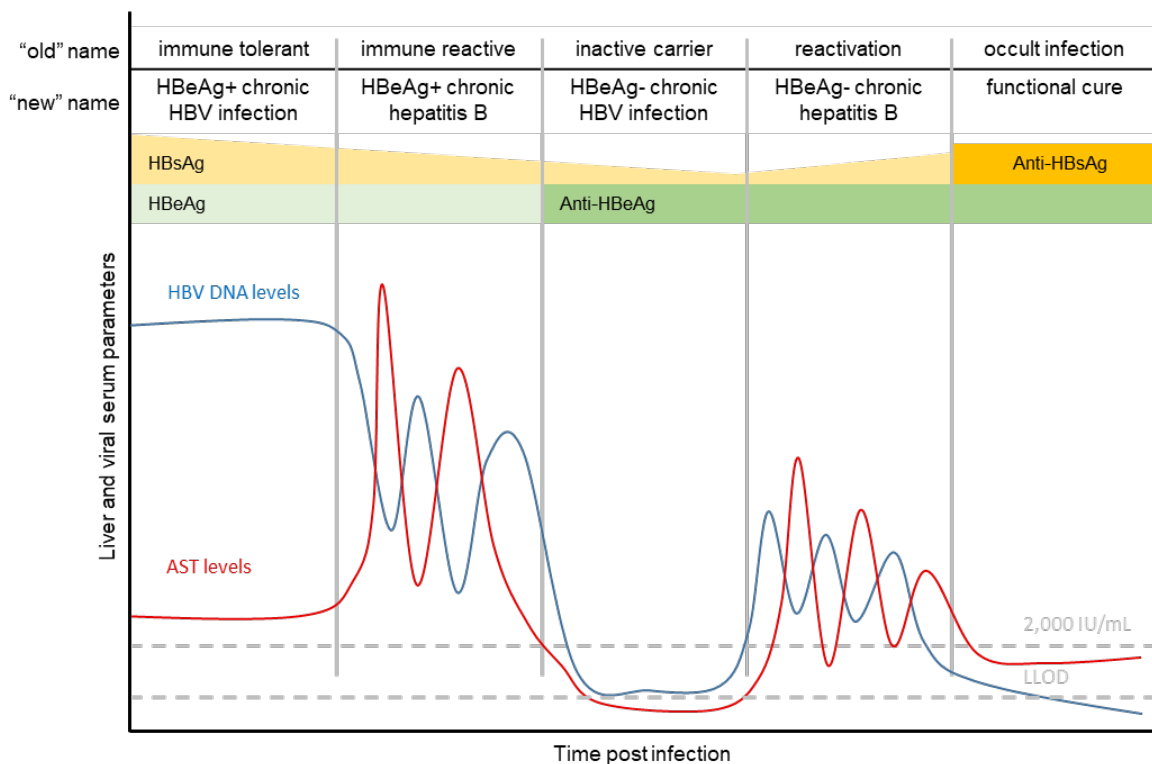

Figure 5: The natural history of the chronic HBV infection consists of 5 phases (adapted from Fanning, *et al.* [89])

Note that early after the first contact with HBV, and then throughout the course of the infection, serum anti-HBcAg antibodies can be measured. Exact times cannot be given, since the progress of the infection depends on different parameters (e.g. HBV genotype, treatment, individual host factors). IU=international units; LLOD=lowest level of detection.

- During the **"immune tolerant"** phase, viral replication reaches very high levels, characterised by high viremia (i.e. HBV DNA in the serum) and HBeAg positivity. Alanine aminotransferase (ALT) levels are low and minimal histological activity is observed, indicative of low to absent liver damage during this phase. Nevertheless, there have been some recent

challenges of the concept of the "immune tolerant" phase. Evidence suggested that liver damage, mediated by immune cells, can occur during this phase of the infection [90, 91], and that this phase should maybe rather be named "high replicative, low inflammatory" [92]. Furthermore, the integration of the viral genome, as well as clonal expansion of hepatocytes can occur already during this phase [93]. This suggests that the transformation of hepatocytes might already happen during this early phase of the infection, setting stone for HCC development later. The liver pathology during this phase is not easy to study since liver biopsies are rarely collected in the absence of liver damage. The new European Association for the Study of the Liver (EASL) guidelines suggest renaming this phase to "HBeAg-positive chronic HBV infection" [94].

- In the **"immune reactive"** phase of the disease, immune responses against the virus occur. Usually, after being high when entering this phase, the viremia eventually drops; ALT levels increase as a result of liver damage (e.g. through necroinflammation) caused by the immune system. Fibrosis is occurring frequently in this phase. The seroconversion from HBeAg to anti-HBeAg antibodies can occur, also HBV DNA suppression is observed in a part of the patients. The new name for this phase suggested by the EASL is "HBeAg-positive chronic hepatitis B" [94].

- Characteristic for the **"inactive carrier"** phase is usually the very low replicative activity of HBV (i.e. HBV DNA in the serum below 2,000 international units (IU)/mL) and the HBeAg seroconversion. Serum transaminases are low. In rare cases (only 1-3%), a seroconversion from HBsAg positivity to anti-HBsAg antibodies is observed. The infection of hepatocytes, however, is not eliminated during this phase and the liver disease is progressing. The new name for this phase, as suggested by the EASL, is "HBeAg-negative chronic HBV infection" [94].

- In the **"reactivation"** phase of the disease, flares of HBV DNA in the serum can be measured, co-occurring with increased levels of aminotransferase levels. HBeAg in serum remains undetectable. Usually mutations in the PreCore region of the HBV genome disrupt the HBeAg reading frame or mutations in the basal core promoter, which is driving the expression of HBeAg [95]. This phase should be called "HBeAg-negative chronic hepatitis B" according to the new guidelines of the EASL [94].

- During the **"occult infection"**, HBV DNA is still measurable in liver homogenate, with HBsAg levels being below the limit of detection in the serum [96]. HBV DNA might or might not be detected at low levels in the serum. Epigenetic silencing of the viral genome might be the reason for the low replicative activity during this phase [97].

In general, untreated patients progress to develop liver fibrosis, cirrhosis, and HCC. The pace of this progression can happen at different rates, depending on the phase of the infection. Usually, the progression during the inactive carrier phase is very slow, with less than 1% of

patients per year. The rate of progression, however, is much higher in patients in immune reactive phases. In HBeAg negative patients, the progression can be between 2% and 10% per year. Generally, CHB patients have a cumulative risk of cirrhosis development of 8% to 20%. Cirrhotic CHB patients suffer from high risk of end-stage liver disease like liver decompensation and HCC development [88]. HBeAg positive, cirrhotic patients suffer from a 3.6 times higher risk of developing HCC than HBeAg negative patients; also increased HBV DNA levels present a risk factor for the progression from cirrhosis to HCC. Globally, the outcome of a chronic HBV infection is determined by both host factors, like age, gender etc., and viral factors, including HBV DNA levels and the genotype [24].

4.1.4.3 Treatments against HBV

4.1.4.3.1 Vaccination

30 years ago, in 1981, the first HBV vaccine was commercialised. Back then, it was produced by purification of spheres (non-infectious particles) from the blood of CHB patients [98]. The current available vaccine, however, is a recombinant vaccine, first established around half a decade after the first generation was on the market. This second generation of anti-HBV vaccines shows a high efficiency (95%) in preventing the establishment of an HBV infection after the full immunisation cycle (three doses) and the presence of a minimal titre of anti-HBsAg antibodies in the serum (100 IU/L). Two studies from Taiwan show that the vaccination program is very important and effective. The HBsAg prevalence in children below 15 years dropped strongly in only 6 years from 9.8% to 1.3% (measured in 1988 and 1994, respectively) [99]. In another study, the decrease in the emergence of HCC in children from 6 to 14 years was reported as a consequence of the first vaccination campaign [100].

4.1.4.3.2 Antiviral treatments

Although this effective vaccine against HBV is available, as presented previously, HBV remains a major health problem worldwide, causing high numbers of deaths. Antiviral treatments show in part good effects in suppressing the spreading of the virus and improving the liver pathology and serological parameters. In this section, I will further look into the seven available treatment options against HBV; interferon alpha (IFNα, two formulations were used in the past, nowadays only the PEGylated formulation is available for HBV infections) and six different nucleoside or nucleotide analogues (NAs), that inhibit the viral polymerase.

IFNα, more specifically the isoform 2A, was first approved in 1991 for the treatment of CHB patients. While one formulation, Roferon®, was removed from the market in 2019 due to inferior effectiveness compared to the newer formulation; another one, Pegasys®, is still in use for patients. The latter one is the IFNα2A protein, bound to polyethylene glycol (PEG) of a molecular weight of around 40 kDa. This covalent conjugation increases the half-life in the

serum. Whereas a significant proportion of patients do not respond to IFNα treatment, and the suppressed infection might relapse after treatment stop [101, 102], responding patients show a reduced risk of developing end-stage liver disease and HCC when compared to non-responders [103]. Seroconversion is observed in 3%-7%, depending on the mode of therapy (if given as a monotherapy or together with NAs). In addition, the stage of the disease and the genotype might have an influence [104-106]. The relapse rate of HBV in IFNα treated patients is much lower when compared to NA treatments [107]. The exact mode of action of IFNα treatment on HBV is not fully understood yet, and several mechanisms were proposed. For example, it was described in *in vitro* and *in vivo* studies, that IFNα treatment can lead to cccDNA degradation or silencing [2, 108-110]), but several other activities are suggested.

The 6 different NAs all work on the viral polymerase. These direct acting antivirals prevent the polymerase from generating a cDNA from the pgRNA, efficiently stopping the spread of virus progeny. **Lamivudine** (LAM) was the first NA to be available for the treatment of CHB and could efficiently lower the HCC incidence in those patients [111-113]. However, this first generation of NA had a high rate of resistance development of the virus by point mutations in the viral polymerase [114]. **Adefovir dipivoxil** (ADV), the second NA to enter the market for treatment of CHB patients, was shown to be efficient even for LAM-resistant virus in patients [115, 116]. However, a severe drawback for ADV was its nephrotoxicity [117]. **Entecavir**, on the market in the USA since 2005, was the most potent direct-acting antiviral drug (DAA) against HBV at that time. It reduced serum ALT levels back to normal, improved liver histology, showed a higher rate HBeAg seroconversion than LAM [118] and also suppressed the infection better than ADV [119]. Importantly, mutation-induced resistance development against entecavir was much weaker than against LAM and ADV [120]. **Telbivudine** (TLV) also showed promising results in clinical trials and was superior to LAM treatment in nearly all measured parameters [121]. TLV is safe to use to prevent mother-to-child transmission, but due to the high rate of resistance development, it is rarely used [107]. **Tenofovir**, is given as a prodrug, either as tenofovir disoproxil fumarate (TDF) or as tenofovir alafenamide fumarate (TAF). It is the most recent NA used in the treatment of HBV. It shares structural similarities with ADV but outcompetes the older drug. Viral suppression, improvement of liver histology, and reduction of liver transaminase levels were all stronger in TDF treated patients than in ADV treated patients. Importantly, in 3% of TDF treated versus in 0% ADV treated patients, HBsAg seroconversion was achieved. Furthermore, after five years of treatment, no significant resistance development was observed [107].

Taken together, the closer look onto treatment options for CHB highlights a need for a treatment that can offer a "functional cure" (i.e. HBsAg seroconversion). NAs have to be given life-long, since treatment stop would allow the virus to spread again, and hardly lead to eradication or even immune system-mediated control of the infection. IFNα treatment suffers

from low responder rates and can have severe side effects [122]. As described previously, the HBV cccDNA is the essential and central part of the viral life cycle. The here mentioned treatments do not (in case of NAs) or only in a subset of responding patients (in the case of IFNα) lead to a decrease of cccDNA levels. Although viral suppression can be achieved with current treatments, a relapse may occur when the treatment is stopped. Therefore, there is an unbroken need of novel treatment options, especially in regards of targeting the cccDNA.

4.1.4.3.2 Experimental treatments under development

Previously, I presented the urgent need of novel therapeutic approaches to overcome a chronic HBV infection. Several drugs are now under investigation to prevent the disease and offer new ways to tackle the virus, for instance on the genomic level or on capsid assembly.

Entry inhibition of HBV into cells is facilitated by bulevirtide (Hepcludex). Bulevirtide is derived from the myristoylated Pre-S1 peptide and binds to NTCP, preventing HBV binding to its receptor [123]. In 2020, Bulevirtide was approved by the European Medicines Agency (EMA) as a treatment of hepatitis delta virus (HDV). This small virus is a satellite of HBV, needing the HBV envelope proteins to spread, since it does not produce any envelope on its own and cannot exit cells without it. By blocking the entry of HBV via NTCP into the cells, Bulevirtide also blocks HDV entry and showed very promising results in clinical studies [124]. Reduction in HBV levels, however, were only minor.

Transcriptional repression of the HBV episome could potentially achieve control of the virus. The epigenetic modification of the cccDNA might be facilitated by inhibiting the hypo-acetylation of the cccDNA-associated histones or induce the methylation thereof, as well as the cccDNA methylation *per se* [125].

Encapsidation modulation, generally achieved by the treatment with capsid assembly modulators (CAMs), can also prevent HBV from efficiently spreading or cccDNA from efficiently forming. As described previously, the HBV capsid formation is tightly coupled to the reverse transcription and rcDNA synthesis. Five different classes of CAMs were described: phenyl-propenamides, heteroaryldihydropyrimidines, sulfamoylbenzamides, sulfamoylpyr-roloamides, and glyoxamoylpyrroloxamides. In brief, the modulation of capsids can go in two different directions. The stabilisation of capsids, on the one hand, acts like a molecular glue that leads to faster capsid formation and therefore to empty capsids that form even in the absence of pgRNA and rcDNA synthesis. The destabilisation of capsids, on the other hand, can lead to the prevention of the efficient transport thereof to the nucleus, so that the rcDNA isn't placed there and cccDNA cannot form. Furthermore, freshly synthesised capsids can be destabilised, preventing the spread of the virus [126].

Viral assembly inhibition is a new class of molecules inhibiting the secretion of HBsAg and virion formation. Nucleic acid polymers (NAPs) were developed in the last decade, tested first

for duck hepatitis B virus infection [90, 123] and showed promising effects in pre-clinical evaluations [127]. NAPs were well tolerated in patients and showed good effects against both the HBV mono-infection and HBV/HDV superinfections, showing even increased rates of HBsAg seroconversions [127, 128].

cccDNA destabilisation is another potential treatment option against HBV. Sulfonamide compounds were shown in 2012 to inhibit cccDNA formation and prevent establishment of the infection [108]. In established infections, the use of engineered nucleases such as zinc-finger nucleases [129]) and the CRISPR/Cas9 system [124, 129] showed promising results in the targeting of the cccDNA and restriction of HBV replication.

While the described HBV treatment options target the virus directly, recent efforts showed very promising results in **activating the host immune system** to fight HBV. The effects of IFNα are mainly due to the restriction of the virus by effector proteins, induced by the immune stimulatory signal. The induction of those effectors can have several effects on the virus: the epigenetic repression and transcriptional control, control of RNA stability and translation rate or the restriction and degradation of cccDNA, or also a combination thereof. Activators of toll-like receptors (TLRs), for instance, showed promising results. *In vitro*, the TLR2 ligand PAM3CSK4 showed strong anti-HBV activity [130], as well as the TLR7 ligand GS-9620 [90, 123] whereas TLR9 agonist was the least efficient of those three [124].

Furthermore, some cytokines were shown to efficiently counteract the infection, *inter alia* the T-cell-derived cytokines type II interferon (IFNγ), tumour necrosis factor alpha (TNFα) [124], type III interferons (IFNλ1, -2, and -3), and other pro-inflammatory cytokines like interleukin (IL)-1β and IL-6 [124]. These cytokines showed a reduction in HBV RNA, total DNA, and also cccDNA levels, which is of high interest for the cure of patients. Finally, the lymphotoxin beta receptor (LTβR) agonist BS1, showed very strong effects against HBV. The activation of the LTβR leads to the induction of nuclear factor kappa B (NF-κB) signaling and the subsequent upregulation of apolipoprotein B mRNA editing enzyme catalytic subunit 3B (APOBEC3B, short A3B), an antiviral cytidine deaminase that eventually deaminates the HBV cccDNA, leading to the degradation thereof without cytopathic effects [129]. A3B induction, e.g. downstream of LTβR activation, presents a very interesting strategy to attack the HBV cccDNA. It was shown in patients that, in acute self-limited infection, A3B mRNA is induced, whereas in chronic HBV carriers, it is not [124]. Besides cytokines like TNFα, T-cells can also express the ligands of the LTβR to target hepatocytes, which leads to the degradation of cccDNA [130]. Based on these findings, I can speculate, that in patients with a chronic disease, which comes along with a (functional) loss of HBV-specific T-cells [131, 132], restoration of LTβR signaling and upregulation of A3B in hepatocytes could help eradicate the cccDNA in a T-cell independent manner.

4.2 APOBEC3B

4.2.1 General description

A3B belongs, together with six other members, to the sub-family of APOBEC3 (or A3) enzymes. This family of cytidine deaminases consists of A3A, -B, -C, -DE, -F, -G, and -H. All of those enzymes are related to activation-induced cytidine deaminase (AID), APOBEC1, APOBEC2, and APOBEC4, forming together the family of APOBEC enzymes.

As cytidine deaminases, APOBEC enzymes catalyse the reaction from a cytosine a uracil (C > U transitions) (**FIGURE 6a**). For the members of the APOBEC family, different functions were described, involved in diverse biological processes (e.g. somatic mutations during antibody maturation for AID). A3 enzymes, however, were mainly described for their antiviral activities.
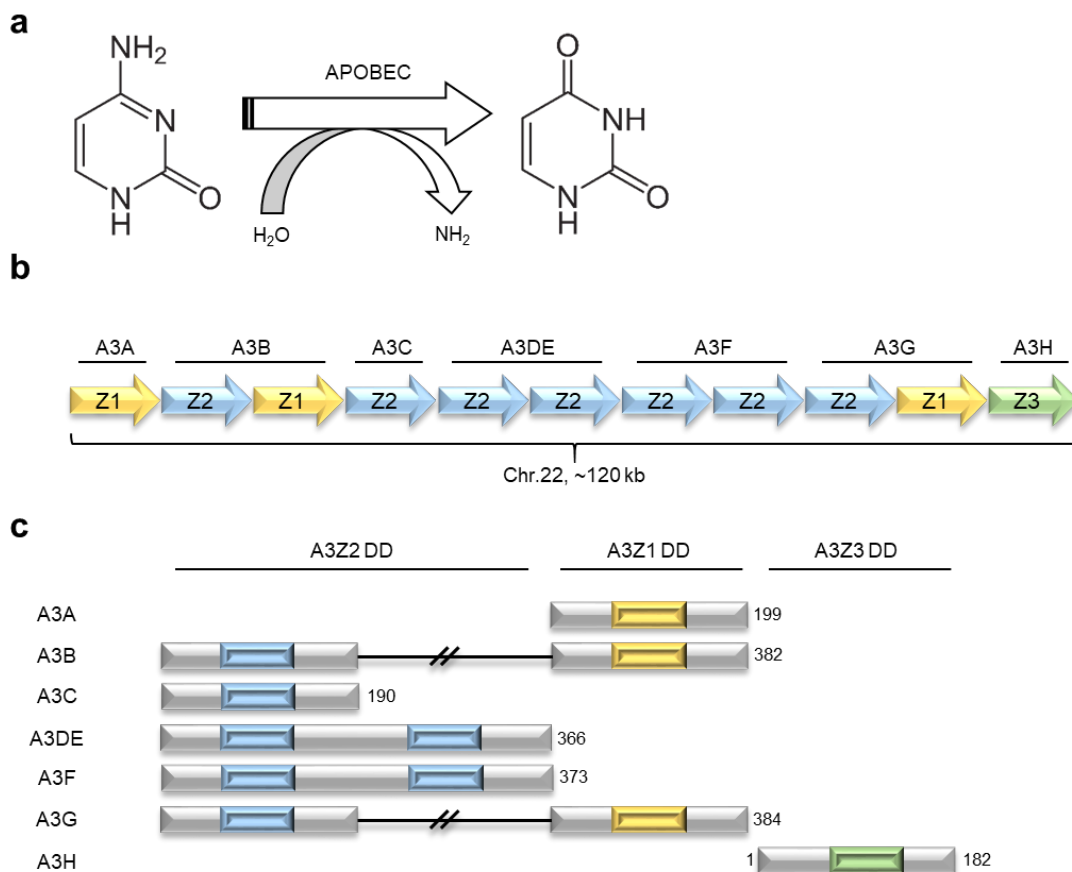

Figure 6: The APOBEC3 family consists of 7 members

(a) Schematic representation of the chemical reaction catalysed by APOBEC3 enzymes **(b) (adapted from Refsland, *et al.* [133])** The A3 locus on chromosome 22 spans around 120 kb. The A3 family members are arranged in tandem. **(c) (adapted from Vasudevan, *et al.* [134])** The A3 family contains members with only one or 2 deamination domains. Those domains, although similar, are of different origin and are divided into 3 subclasses, A3Z1 (yellow), A3Z2 (blue), or A3Z3 (green). Numbers indicate the last amino acid in each protein.

While A3G is most famous for the restriction of the human immunodeficiency virus (HIV) [135], the other A3 enzymes were also described to target a multitude of different viruses, as well as retro-elements of the human genome [136]. Generally, it is believed that single stranded DNA (ssDNA) which occurs during reverse transcription, genome duplication or potentially during transcription, is the main substrate for A3 enzymes [130], although A3 binding [137] and A3-mediated editing of RNA [138] was also described. The antiviral activity of A3 enzymes is a consequence of their cytidine deaminating activity towards the ssDNA. The deamination of cytosines in viral DNA leads to mutations, which cannot be efficiently repaired in the case of viral DNAs, potentially due to the lack of specific DNA repair mechanisms.

In the case of the human genome, uracils are recognised and excised by specific enzymes, which initiates the base-excision-repair (BER) pathway. First, an apurinic site (from where the uracil was excised, but the phosphor-diester backbone is still intact) is generated by the activity of DNA glycosylases (e.g. UNG or uracil-DNA glycosylase), which is recognised by Apurinic/apyrimidinic (AP) endonucleases (APE1 and APE2). APEs induce a single strand cleavage of the DNA backbone, which leads to a single strand resection and subsequent filling up of the strand with the correct nucleotides, followed by a ligation of the nick [139]. As previously mentioned, A3B can induce damage into HBV cccDNA which leads to the subsequent degradation of the cccDNA. The involvement of BER enzymes in the degradation of HIV cDNA was reported for HIV [140]; I therefore speculate, that if high number of uracils in a single cccDNA molecule are produced by A3B activity, the BER pathway would not repair it, but lead to "shattering" of the cccDNA. If at several sites of the cccDNA, uracils were excised and the backbone was cleaved, the cccDNA may fall apart. If this would happen in the case of the human genome, still homologous repair using the sister chromosome could guarantee genome integrity, however, this would not work in the case of the HBV cccDNA.

4.2.2 Genomic location and genetic history of A3B

While the murine genome only encodes a single A3 enzyme, the human genome encodes seven highly related A3 enzymes. The ORFs for those are arranged in a head-to-tail manner on chromosome 22 [141-144] (**FIGURE 6b**), likely to have arisen from tandem duplication and recombination by unequal crossover. While three of the A3 enzymes only contain a single deaminase domain (DD), A3B contains, like A3DE, A3F, and A3G, two deaminase domains (**FIGURE 6b-c**). There are three different A3 DD, named A3Z1-A3Z3, showing slight differences on the amino acid level around the catalytic centre. The emergence of two of those DDs in a single enzyme probably arose during the phylogenetic diversification in mammals. It is believed that the last common A3 enzyme only featured a single DD of each of those

different DD [133, 135, 145]. Note wise, the number of synonymous nucleotide substitutions is significantly lower in the A3 family than the number of non-synonymous nucleotide exchanges, suggesting that on this genomic locus a higher-than-average selective pressure is present [146, 147]).

4.2.3 Regulation of APOBEC3B expression

Other A3 family members were shown to be interferon-stimulated genes, for instance A3A and A3G [2, 148]. While some reports claim that A3B expression is as well regulated by IFN [149], recent evidence, together with my work, strongly suggests that nuclear factor kappa B (NF-κB) signalling is a strong driver of A3B expression [2-4, 150-152].

4.3   NF-κB signalling

NF-κB signalling is a highly conserved signalling pathway that is present in nearly all cells of the human body and is important for signal transduction during inflammation and in immunity [153]. Interestingly, it is so highly conserved that homologues of mammalian NF-κB were even found in very basal organisms, like cnidarians and single-celled protists [154]. The family of NF-κB proteins in mammals is made up of five related transcription factors: NF-κB1 (or p50), NF-κB2 (or p52), RelA, RelB, and c-Rel (**FIGURE 7a**). Those proteins can form diverse homo- and heterodimers to control gene transcription of NF-κB target genes by binding to a specific NF-κB recognition motif [155, 156]. In the absence of induction of the signalling, the NF-κB proteins are bound by inhibitory proteins, the inhibitor of kappa B family (IκB) in the cytoplasm of the cell, preventing them from the translocation to the nucleus [157]. NF-κB1 and NF-κB2 furthermore contain a C-terminal IκB-like domain, which prevents them from the nuclear translocation [158] (**FIGURE 7a**).

4.3.1 The classical/canonical NF-κB pathway

The canonical NF-κB signalling is mainly induced by the binding of various cytokines to their receptors, the activation of pattern-recognition receptors by their ligands, or by the activation of the B-cell or T-cell receptor (**FIGURE 7b, step 1**) [159], but also by cellular stress like reactive oxygen species and ultra-violet radiation [160]. Note wise, the canonical NF-κB signalling pathway does not rely on active production of any of the involved factors, all of them are available in the cytoplasm. Usually, the activation is very rapid and transient.

The induction of canonical NF-κB is facilitated by the phosphorylation of the IKK (inhibitor of kappa B kinase) complex (**FIGURE 7b, step 2**) by TAK1 (also known as Mitogen-activated protein kinase kinase kinase 7 or MAP3K7) [161]. This in turn leads to the activation of this complex, consisting of IKKα, IKKβ, and IKKγ (also known as NF-κB essential modulator or NEMO). This complex then phosphorylates IκB proteins (**FIGURE 7b, step 3**), which leads to their poly-ubiquitination and degradation via the proteasome (**FIGURE 7b, step 4**). IκB degradation then allows NF-κB dimers (for the classical pathway mainly RelA/p50 and c-Rel/p50, with p50 being the active form of NF-κB1), to translocate to the nucleus to bind recognition sites and activate transcription (**FIGURE 7b, step 5**) [162].

4.3.2 The alternative/non-canonical NF-κB pathway

The non-canonical NF-κB signalling is usually induced by a subset of TNFα receptor- (TNFR) family members, *inter alia* the BAFFR (B-cell activating factor receptor), cluster of differentiation 40 (CD40), and the LTβR (**FIGURE 7c, step 1**). Compared to the classical NF-κB signalling pathway, this pathway is rather activated by constant stimulation and relies on constant production of involved factors, mainly the NF-κB inducing kinase (NIK) [157].

Under homeostasis, NIK is constantly degraded. TNF receptor associated factor 3 (TRAF3) was shown to be responsible for this process [163] and induces the ubiquitination and subsequent proteasomal degradation of NIK in a TRAF2-, cIAP1-, and cIAP2- (cellular inhibitor of apoptosis protein 1 and 2, respectively) dependent manner [164].

Ligands binding to receptors activating the non-canonical pathway induce the linkage of the receptors on the cell surface into larger complexes, which further leads to the formation of a cIAP1/2 containing complex that induces the ubiquitination and degradation of TRAF2 and TRAF3. By this NIK will be stabilised and auto-phosphorylated [164]. Together with constant transcription and translation of NIK, the kinase accumulates in cells, which is a strong trigger for the phosphorylation and thereby activation of IKKα (**FIGURE 7c, step 2**), as well as the binding of IKKα to its substrate, NF-κB2 [165]. NF-κB2, when phosphorylated (**FIGURE 7c, step 3**), will be ubiquitinated and processed via the proteasome, to generate the active form, p52 [166] (**FIGURE 7c, step 4**). While the inactive form of NF-κB2, the non-processed p100 inhibits the translocation into the nucleus of the non-canonical NF-κB heterodimer RelB/p100, the emerging heterodimer RelB/p52 can translocate into the nucleus and initiate translation of NF-κB target genes (**FIGURE 7c, step 5**).
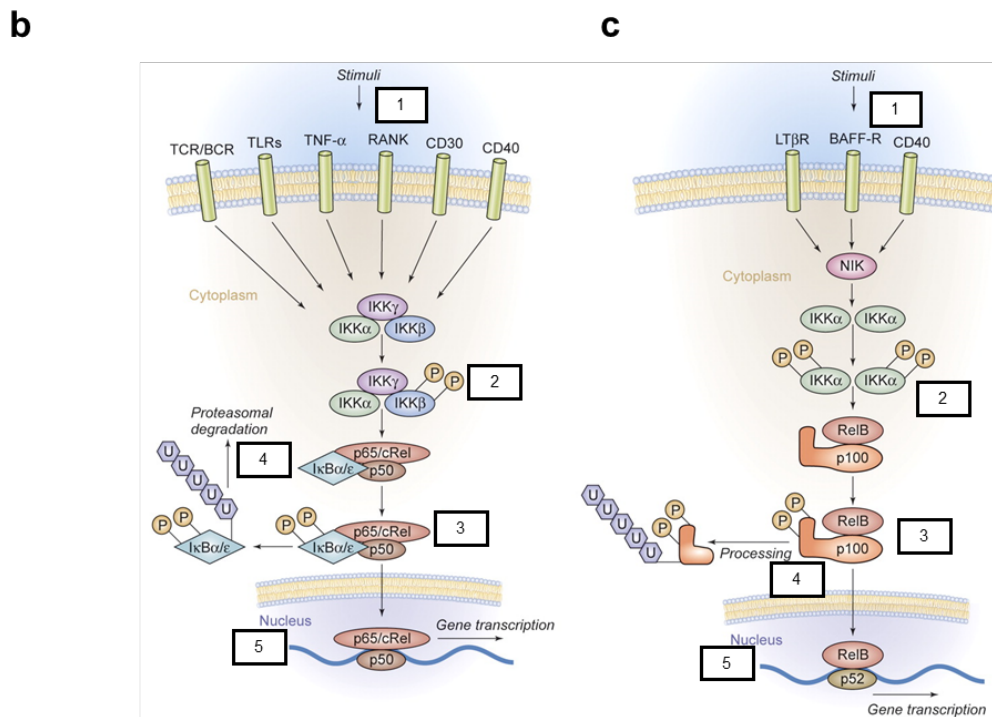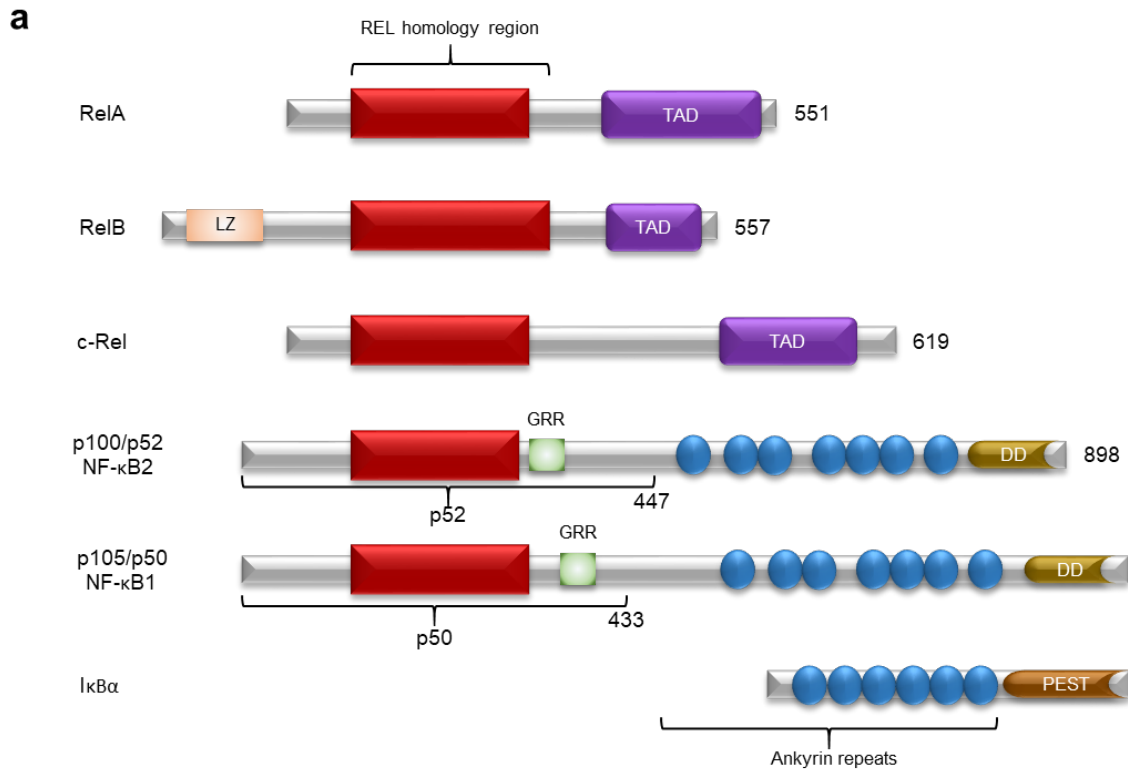
Figure 7: NF-κB signalling is an important signal transduction mechanism

(a) (adapted from Shehata [167]) The 5 NF-κB transcription factors are schematically shown, as well as one representation of a stereotypic IκB molecule, IκBα. The most important domains for each protein are indicated. DD, death domain; GRR, glycine-rich region; LZ, leucine-zipper; PEST, proline-, glutamic acid-, serine-, and threonine-rich region; TAD, transactivation domain. Numbers indicate the last amino acid in each protein. **(b-c) (Adapted from Jost, *et al.* [168])** Schematic representation of the (b) canonical and (c) non-canonical NF-κB signalling pathway. Detailed explanations for steps 1-5 are given in the text.

4.4 Micro RNAs

4.4.1 General description

Micro RNAs (miRNAs) are ~22 nucleotides (nt) long RNAs. These small, non-coding RNAs are involved in a multitude of biological processes and represent a level of post-transcriptional gene regulation by either repression of translation or degradation of target mRNAs (i.e. "silencing" of genes). In humans, the silencing of genes is usually mediated by base pairing of the miRNA to the 3'-UTR (untranslated region) of target mRNAs. Generally, this base-pairing to the 3'-UTR is "non-perfect", which means that not every miRNA nucleotide has a binding partner in the corresponding mRNA, although other far less common mechanisms were described [169].

The first miRNA that described in literature was the *C. elegans* miRNA "lin-4" [170], which plays an important role in the nematode's larval development. It was not for long that this novel class of small, non-coding RNAs became a large and vibrant field of research, which lead to the discovery of more and more miRNAs over time in a variety of species. Of note, it is now known that miRNAs play crucial roles at all stages of development and homeostasis, and dysregulation of particular miRNAs can be involved in numerous pathologies, particularly cancer [171]. In the following sections, I will focus on mammalian, especially human, miRNA biogenesis and the *homo sapiens* miRNA-138-5p (hsa-miR-138-5p), which I found to be involved in A3B regulation downstream of NF-κB signaling.

4.4.2 miRNA biogenesis

4.4.2.1 Transcription

In general, miRNAs are transcribed by PolII [172] (**Figure 8, step 1).** In humans, miRNAs are usually contained in intronic regions of both protein-coding and non-coding RNAs. However, also exonic miRNAs are found [173]. Polycistronic miRNAs were transcribed in cases where several miRNA loci are located in close proximity in the genome [174]. Of note, miRNAs are produced as a large primary miRNA-transcript (pri-miRNA) (**Figure 8, step 2**), which can, as mentioned, contain several mature miRNAs in stereotypic 3-dimensional hairpin structures. As PolII products, the miRNA transcription is dependent on transcription factors that regulate PolII activity and processing, as well as on epigenetic regulation [175-177]).

4.4.2.2 Nuclear processing

In the nucleus, the pri-miRNA is processed into the mature precursor miRNA (pre-miRNA) by an RNaseIII enzyme, DROSHA [178], which is active in a complex with DGCR8 (DiGeorge

syndrome critical region 8 Microprocessor Complex Subunit), the so called microprocessor complex [179] (**Figure 8, step 3**). The resulting pre-miRNA emerges from the previously mentioned, local hairpin structure, which consist of a stem of around 33-35 nucleotides in length and a terminal loop [178]. The microprocessor complex recognises sequence motifs embedded within the basal region of the stereotypical hairpin and probably a nucleotide sequence in the terminal loop [123, 180]. Then, the stem is cleaved around 11 nt away from the basal junction and around 22 nt away from the apical loop to form the mature pre-miRNA stem-loop structure [181]. After processing by the microprocessor complex, the pri-miRNA is exported from the nucleus via the nuclear pore in a exportin 5 and Ras-related nuclear protein dependent manner [182, 183] (**Figure 8, step 4**).

4.4.2.3   Cytoplasmic processing and RNA interference

In the cytoplasm, the pre-miRNA hairpin structure is recognised and processed by DICER1 [184-186]. DICER1 processing leads to the removal of the terminal loop and results in the liberation of an RNA duplex structure, each of which is around 22 nt in size (**Figure 8, step 5**). DICER1 shows preferential binding towards RNA structures with terminal overhangs of two 3' nt, which is the usual product of the nuclear DROSHA reaction [187]. DICER1 interacts with TAR RNA-binding protein (TRPB) which plays a role in pre-miRNA processing and controls the length of mature miRNAs [188, 189]

The two resulting miRNAs can be loaded into argonaute (AGO) proteins for RNA interference (RNAi) (**Figure 8, step 6**). Although at first, both miRNAs of the duplex are loaded, one miRNA is more prevalent and has a superior biological activity, so that it makes up 96%-99% of the miRNAs emerging from a duplex, while the other one is degraded. Nomenclature defines one strand as the 5' miRNA and the other one as the 3' miRNA, depending on the strand of the duplex the miRNA emerges from (e.g. hsa-miR-138-5p and hsa-miR-138-3p). The 4 human AGO proteins (AGO1-4) do not show a significant preference towards any miRNAs, as they are associated with highly comparable sets of miRNAs [190-193]. All of those AGO proteins can induce RNAi and mRNA decay, whereas AGO2 can slice mRNAs which are targeted by the miRNA [192, 194].

After the loading of the miRNA duplex into AGO proteins, the precursor RISC (pre-RISC, "RNA induced silencing complex") is formed, then the complex rapidly selects one of the strands to form the mature RISC. AGO2 could potentially cleave the passenger strand to only keep the active "guide" strand. However, this is only possible if there are no central mismatches in the duplex [192, 195]. Otherwise, as it is the case for AGO1, -3, and -4, which lack slicer activities, the miRNA duplex undergoes unwinding and is split up, induced by mismatches in the imperfect base pairing within it [125, 196]. The previously mentioned discrepancy between the relative abundances between the two strands of a miRNA duplex comes from the strand

selection process during AGO loading. The thermodynamic stability of the ends of the miRNAs is a strong determinant factor for the preference of AGO proteins for one strand over the other (the strand with a higher 5' instability is selected), as well as the presence for a uracil at position 1 [197, 198]. After the strand selection, the "guide" strand is kept in the RISC and the "passenger" strand is released and degraded rapidly (**Figure 8, step 7**). Guided by the miRNA, the RISC represses target mRNA translation and mRNA decay (**Figure 8, step 8**).
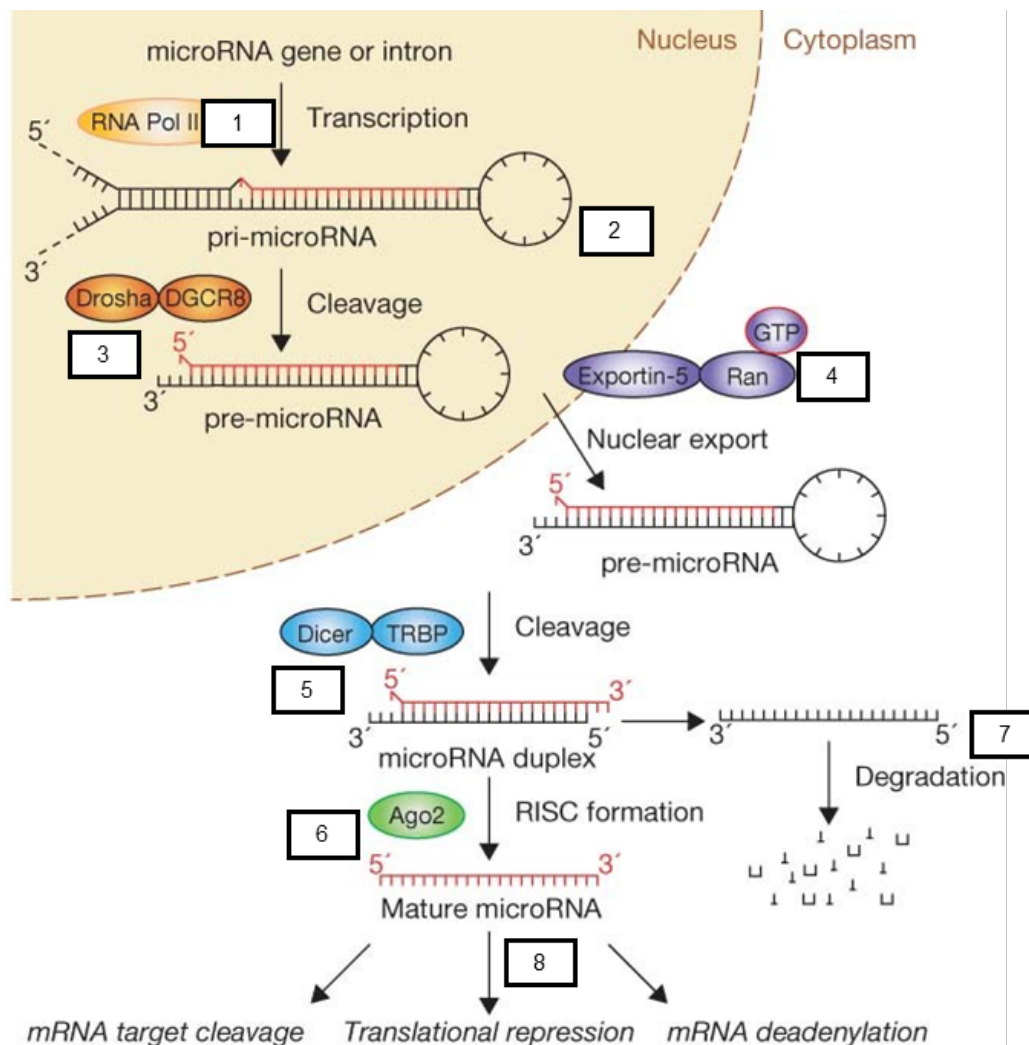

Figure 8: Figure 8 – miRNA biogenesis involves sequential processing by DROSHA and DICER1 (adapted from Winter, *et al.* [199])

Extensive explanation on individual steps are given in the text for the indicated numbers. In Brief: Primary miRNAs (pri-miRNAs) are translated mainly by RNA polymerase II (RNA Pol II) and contain the mature sequence in a distinct hairpin structure. This structure is recognised by the nuclear microprocessor complex, containing DROSHA and DGCR8, which cleave the hairpin structure off, which is exported from the nucleus as the precursor miRNA (pre-miRNA) by exportin-5 and RAN. In the cytoplasm, DICER chops off the loop of the pre-miRNA, releasing a duplex structure, which is loaded into argonaute (AGO) proteins, e.g. AGO2 as depicted here. One strand, the "guide", is selected in this process, while the "passenger" is released and degraded. The miRNA-AGO complex, also called RNA-induced silencing complex (RISC) then mediates post-transcriptional control of mRNAs by altering their stability and their translation rate.

4.4.3 hsa-miR-138

Hsa-miR-138 belongs to a miRNA family highly conserved in vertebrates. Hsa-miRNA-138-5p emerges, as previously discussed, from a heteroduplex with hsa-miR-138-3p. The latter, however, is only found at very low levels, indicating that it is the "passenger" strand, whereas hsa-miR-138-5p is the "guide" strand and therefore the active miRNA, which is involved in post-transcriptional control of target genes. Hsa-miR-138-5p can be expressed from 2 different genomic loci, one located on chromosome 3 and the other one on chromosome 16, giving rise to a pre-miR-138-1 and -2, respectively.

Hsa-miR-138-5p was shown to be dysregulated in different kinds of cancers (e.g. breast cancer). The gene regulation of hsa-miR-138 has been under investigation, and of now, several different regulatory mechanisms were discovered, including *inter alia* epigenetic regulation [200, 201], transcription factor-dependent regulation [202, 203], and hormone-dependent regulation [204].

The finding that hsa-miR-138 is frequently downregulated in cancer of different origin (e.g. gall bladder [205], thyroid carcinoma [206], lung cancer [207] or squamous cell carcinoma [208]), suggest its role as a tumour suppressor gene.

Cell proliferation is under control of hsa-miR-138, as it targets for instance YAP1 (YES-associated protein 1) [208] and c-Met (also called hepatocyte growth factor receptor, HGFR) [209]. Furthermore, the genes EZH2 (enhancer of zeste homolog 2), CDK6 (cyclin dependent kinase 6), E2F2 (E2F transcription factor 2), and E2F3 (E2F transcription factor 3) were shown to all be under control of hsa-miR-138, which also supresses cell proliferation.

EZH2 is also a regulator of invasion and metastasis by inducing the expression of E-cadherin [210], which is therefore also under control of hsa-miR-138. Furthermore, hsa-miR-138 represses the expression of ZEB2 (Zinc finger E-box-binding homeobox 2), which as well induces E-cadherin expression and can therefore promote tumour cell invasion [211, 212].

The here presented examples are just a glimpse of the variety of cellular functions under the control of hsa-miR-138. Elevated levels of hsa-miR-138 are usually linked to a better prognosis in cancers of different origin [213-215]. The link to A3B expression fits the role of hsa-miR-138 as a tumour suppressor, since elevated expression of a DNA-mutating enzyme could lead to somatic mutations and tumour initiation. Although the broad spectrum of hsa-miR-138 targets cannot be discussed here *in extenso*, it is of note that in literature a link between hsa-miR-138 and hypoxia induced factor 1α (HIF1α), one of the main responders to low intracellular oxygen levels, is described [216].

4.5   Hypoxia

The liver features an important anatomical and functional niche in the body, and liver function strongly affects *inter alia* the oxygen homeostasis. On the one hand, blood entering the liver via the terminal hepatic arteriole (THA) delivers highly oxygenated blood from the heart to the liver. On the other hand, through another afferent vessel, the terminal portal vein (TPV), oxygen-depleted blood from the gut flows to the liver (**FIGURE 9**). The mixed oxygenated and deoxygenated blood then directional flows towards the central vein (CV) of the hepatic lobule, generating a physiological oxygen gradient [217]. In literature, it is reported that the oxygen tension (also partial oxygen pressure, pO_2) of incoming, mixed blood from the heart via the THA and the gut (i.e. periportal) is around 60-65 mmHg (84–91 µM), whereas the pO_2 at the CV (i.e. pericentral) is around only 30-35 mmHg (42–49 µM) (**FIGURE 9**). As a comparison, the pO_2 on most other tissues falls between 74-104 mmHg and the pO_2 in venous blood is between 34-46 mmHg [217].

This gradient plays an important role for the generation of the "liver zonation", and hypoxia responses are usually not present in a healthy liver. Hepatocytes can differ substantially between different zones of the liver in their biochemical and functional properties. Periportal hepatocytes, receiving more oxygen, for instance also display a more oxidative metabolism than pericentral hepatocytes [126, 218].

Chronic liver disease, like a CHB, results in persistent damage to the liver, including cell death, regenerative proliferation, as well as activation of fibroblasts (hepatic stellate cells) and thereby fibrosis [131, 219, 220]. The production of an excessive amount of extracellular matrix (ECM) during progressing fibrosis can restrict the blood flow, thus generating lowly oxygenated areas, eventually leading to hypoxia [221].

4.5.1 Hypoxia induced factors

Hypoxia induced factors, or HIFs, belong to the basic helix–loop–helix Per–Arnt–Sim (bHLH-PAS) family of proteins. These proteins act as oxygen-dependent transcription factors that facilitate a response to low oxygen. Since cells eventually need oxygen for survival, HIFs help to optimise cellular biochemical functions for limited amounts of oxygen. For example, mitochondrial oxygen consumption is reduced [222] or the cellular metabolism is shifted towards anaerobic glucose metabolism [223].

HIFs form hetero-dimers between the alpha subunit, of which three different forms exist (HIF1α, HIF2α, and HIF3α) and a beta subunit, the aryl hydrocarbon receptor nuclear translocator (ARNT) - also called HIF1β [224, 225] (**FIGURE 10**). While HIF1α and ARNT are expressed ubiquitously through different tissues, the expression of HIF2α and HIF3α are more

restricted to a subset of cell lineages (vascular endothelium, liver parenchyma, kidney epithelial cells and thymus, cerebellar Purkinje cells, the corneal epithelium of the eye, respectively) [226].
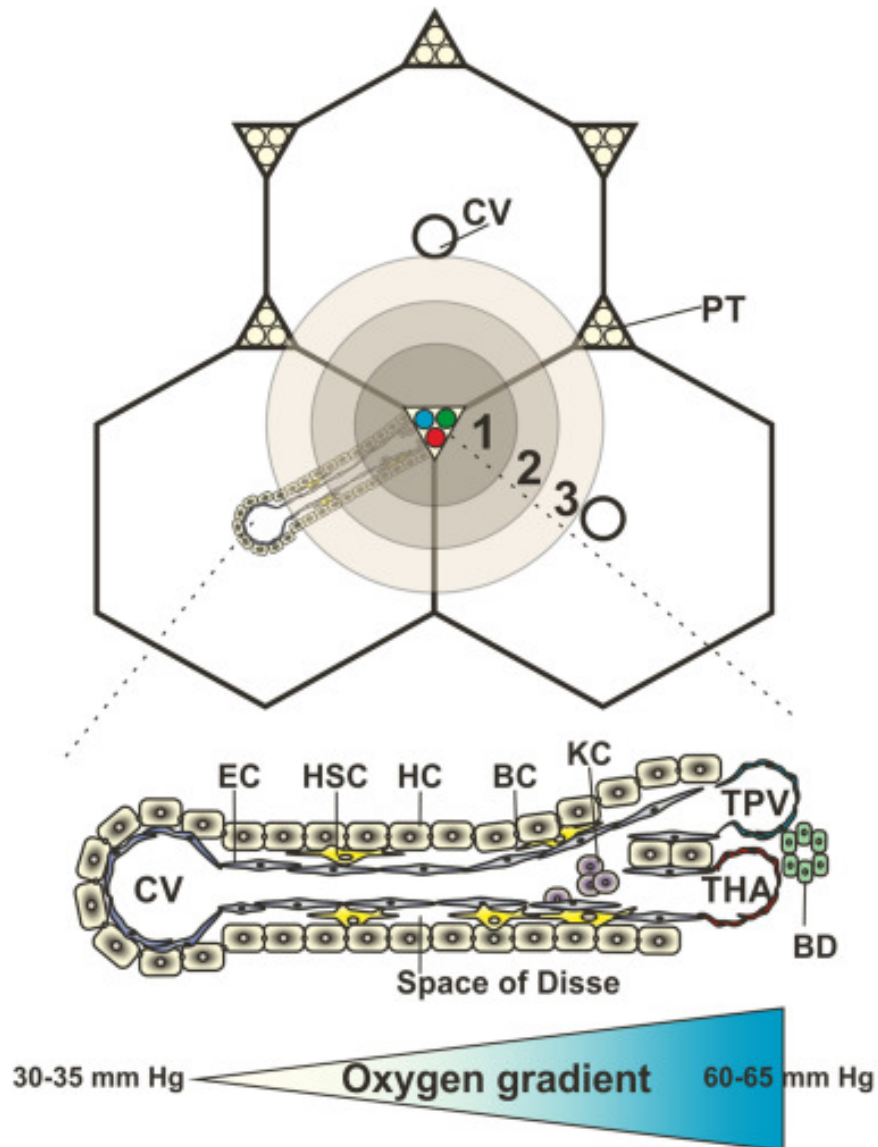

Figure 9: The liver features a unique anatomical architecture and a natural oxygen gradient. (adapted from Kietzmann [227])

Schematic representation of (upper panel) the liver micro architecture and (lower panel) the oxygen gradient along the sinusoids. The liver lobules have a hexagonal shape. The central vein (CV) is in the middle of the lobule and the portal triad (PT) sits at the corners of the hexagon. The portal triad consists of the terminal portal vein (TPV), the terminal hepatic arteriole (THA), and the bile duct (BD), which receives the bile transported via the bile canaliculi (BC). Along the sinusoids, 3 zones can be distinguished: (1) the periportal zone, (2) the intermediary zone, and (3) pericentral zone. Along the sinusoids, there is an oxygen gradient, ranging from 60-65 mm Hg pO_2 in the periportal region to 30-35 mm Hg pO_2 in the pericentral region. In those sinusoids, different cell types are present: Hepatocytes (HC), endothelial cells (EC), hepatic stellate cells (HSC), and Kupffer cells (KC).

4.5.2 Regulation of hypoxia responses

Prolyl hydroxylases (PHDs) 1, 2, and 3 are enzymes that strongly respond to hypoxic conditions, under which they lose their catalytic activity due to the lack of substrate (oxygen) [228]. Under normoxic, or physoxic conditions (when physiological levels of oxygen are present), PHDs attach hydroxyl groups to specific and well-conserved prolines in the oxygen-dependent degradation domain (ODD) (**FIGURE 10**) of HIF1α, HIF2α and HIF3α. In the case of human HIF1α, these prolines are P402 and P564 [229, 230]). The proline hydroxylation allows the Von Hippel–Lindau tumour suppressor (pVHL) to recognise and bind HIF1α. A pVHL-containing E3-ubiquitin ligase complex then targets HIF1α for proteasomal degradation by ubiquitination [231-233] (**FIGURE 10**). Another level of controlling HIF1α depends on FIH (factor inhibiting HIF1α, also named HIF1AN for HIF1α inhibitor), an asparaginyl hydroxylase, which can as well hydroxylate HIF1α at the position N803 and thereby prevent it's binding to p300/CREB-binding protein (CBP; also known as CREBBP), preventing the co-activation of HIF1α target genes [234].

If oxygen levels are low, however, PHDs reversibly lose their function in a dose-dependent manner [235, 236]. HIF1α protein is stabilised due to the lack of hydroxylation and can translocate into the nucleus, where it will bind, together with its subunit ARNT, to HIF responsive elements (HREs) to activate transcription of HIF target genes.

4.5.3 Hypoxia and immune responses

Hypoxia represents a big problem in cancer. Cancer cells, if suffering from hypoxia, and therefore having active HIF1α signalling, show reduced susceptibility to radio- and chemotherapy. In addition, hypoxia can negatively impact the immune responses, including *inter alia* the expression of pro-inflammatory cytokines and the response to them [237, 238].

4.5.3.1 HIF1α and NF-κB

In general, hypoxia was shown to be involved in several different immune processes, which will not be discussed *in extenso* here. However, it is important to mention that it was shown that between the HIF1α and the NF-κB, a well-conserved and central immune response pathway, there is a frequent cross talk during immune responses [239]. Between the two pathways, several activators, regulators, and also targets are shared [240].

It was already suggested in 1994 that hypoxia can induce NF-κB signalling [241], and in the following years, underlying mechanisms were studied further. It was found that the deactivation of PHD1 under hypoxia can increase IKKβ stability and enzymatic activity, enhancing IκBα phosphorylation and thereby NF-κB signalling [242]. Furthermore, there are

reports that link HIF1α mRNA production to active NF-κB signalling [243] in immune cells. Although several studies show that HIF1α and NF-κB positively influence one another (e.g. enhancing activity of myeloid cells) [244], some contradicting reports describe a negative influence of HIF1α/hypoxia on immune responses. Both *in vitro* and *in vivo* studies find that HIF1α can prevent NF-κB signalling and immune responses [129, 245]. All the different physical (e.g. RelB binding to ARNT, [246] and functional cross-talks (e.g. negative and positive feedback loops) between HIF1α and NF-κB signalling suggest a context specific regulation from those pathways, allowing cells to adapt to different situations [247].
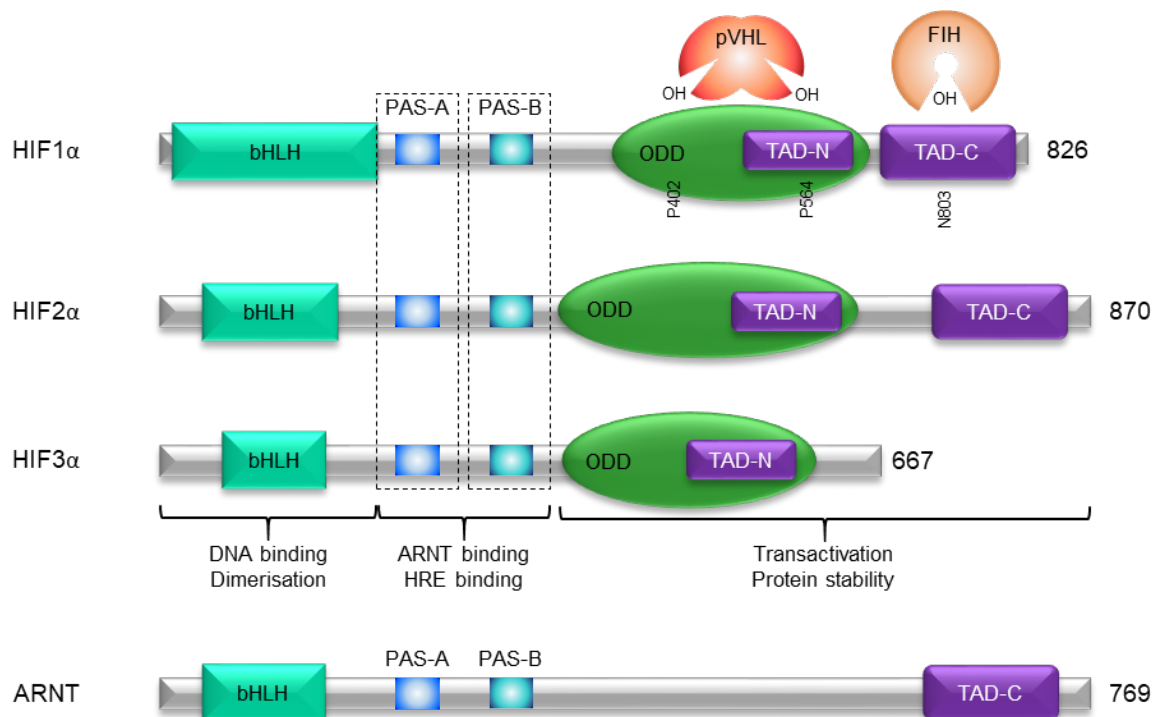

Figure 10: The hypoxia induced factor protein family are important oxygen sensors (adapted from Saint-Martin, *et al.* [248])

Schematic representation of the 4 proteins belonging to the HIF family, HIF1α, HIF2α, HIF3α, and ARNT. These proteins share common domains: (i) the basic helix-loop-helix (bHLH) domain which is involved in dimerisation and DNA binding; (ii) 2 central per-ARNT-sim (PAS) domains, PAS-A and -B, which are involved in the binding of HIF1α, -2α, and -3α to ARNT; (iii) domains involved in transactivation of target genes (TAD, transactivation domain, either N-terminal, TAD-N, or C-terminal, TAD-C) and the destabilisation/regulation of the of the proteins in the presence of oxygen (ODD, oxygen-dependent degradation domain). For HIF1α, the 2 prolines (P402 and P564), which are hydroxylated by PHDs in the presence of oxygen are indicated, as well as the asparagine N803, which is hydroxylated by FIH in the presence of oxygen. The Von Hippel Lindau-tumour suppressor protein (pVHL) recognising hydroxylated P402 and P564 is shown as well, which leads to the ubiquitination and the proteasomal degradation of HIF1α. Numbers indicate the last amino acid in each protein.

5   Hypothesis and aims

In the frame of this PhD theses I addressed two main questions. First, what are the molecular underpinnings of APOBEC3B expression control, both on a transcriptional and on a post-transcriptional level? Second, how does the microenvironmental oxygen levels influence APOBEC3B expression and subsequently antiviral responses mediated by APOBEC3B?

Aim 1: Deciphering transcriptional and post-transcriptional control of APOBEC3B

The first aim of my PhD thesis was to shed a light on cellular mechanisms involved in the transcriptional and post-transcriptional control of APOBEC3B expression and their relevance in the context of an HBV infection. To this end, I utilised cultured dHepaRG, which were infected with HBV and treated with the LTβR agonist BS1. Further, differently manipulated dHepaRG (e.g. knocked-down for specific genes, treated with kinase inhibitors and transfected with small, interfering RNAs (siRNAs)) were used.

To address the hypothesis, that manipulation of cellular pathways that are involved in the APOBEC3B induction in hepatocytes after LTβR activation can alter the anti-cccDNA effects of the treatment, the following questions, aims and milestones were defined:

1. Which signalling pathways triggered by LTβR activation are involved in APOBEC3B induction?

2. What are the expression dynamics of APOBEC3B induction? Is APOBEC3B expression controlled on a post-transcriptional level?

3. How does repression of APOBEC3B inducing pathways influence cccDNA degradation under LTβR activation?

4. Can manipulation of post-transcriptional regulators of APOBEC3B modify antiviral effects of LTβR activation?

5. Is HBV able to modulate APOBEC3B expression?

6. Can I find evidence that APOBEC3B induction leads to cccDNA degradation in a transcriptionally silent or a non-replicating HBV infection?

This study should allow an in-depth understanding of how the expression of the antiviral enzyme APOBEC3B is regulated in hepatocytes. Thus, it was envisioned that the found molecular mechanisms and how manipulation thereof could help to improve the APOBEC3B-mediated cccDNA degradation [3].

Aim 2: Hypoxia reduces antiviral effects of LTβR activation and offers a niche for HBV to avoid immune responses

The second aim of this PhD thesis was to investigate the influence of microenvironmental oxygen levels on LTβR activation-induced APOBEC3B induction and antiviral effects of the

treatment. To this end, dHepaRG were used and infected with HBV, treated with BS1 and cultured under hypoxic conditions. Additionally, siRNA transfection, transgene transduction and pharmacological inhibitors were utilised *in vitro* and human and murine liver specimen were analysed.

To address the hypothesis that hypoxia or other HIF1α stabilising conditions can impair efficient APOBEC3B induction and antiviral effects, the following questions, aims and milestones were defined:

1. Are high HIF1α levels correlated with higher viral load and lower APOBEC3B expression in CHB patients?

2. Is HIF1α stabilisation sufficient to block APOBEC3B induction and antiviral effects of LTβR activation *in vitro*? Is HIF2α also involved?

3. Does HIF1α stabilisation also block effects of other immune-stimulatory treatments?

4. What is the mechanism behind the effects of HIF1α stabilisation on LTβR agonisation-induced APOBEC3B upregulation?

5. What consequence on the "hypoxic proteome" has the removal of HIF1α? Is the hypoxic phenotype blocked or reverted to a normoxic phenotype?

This study allowed an in-depth analysis of the effects of HIF1α on the expression of the antiviral enzyme APOBEC3B. Thus, the data deepened current knowledge about the interplay of HIF1α signalling and NF-kB signalling and identified reduced RelB protein levels under HIF1α stabilisation as the reason for reduced antiviral activity of LTbR activation [4].

6   Methods

6.1   Cell Culture

Adapted from my written and experimental contribution in Faure-Dupuy*, Riedl*, *et al.* [34] and Riedl*, Faure-Dupuy*, *et al.* [4]: Culturing of was previously described [249]. These cells represent a non-transformed progenitor cell line that can be differentiated into hepatocytes. Briefly, proliferating cells were cultured in "growth medium", William's Medium E (Genaxxon), supplemented with 10% FetalClone II (Thermo Fisher), 1% Penicillin/Streptomycin (Gibco), 5 µg/ml insulin (Insuman Rapid; from Sanofi), and 5×10^{-5} M hydrocortisone hemisuccinate (Pfizer). After seeding, HepaRG were cultured for ten days in "growth medium". From the 11th day after seeding onwards, HepaRG were cultured for 13 days in "differentiation medium" and were just used in experiments after this differentiation process. "Differentiation medium" contains the same supplements as "growth medium", but additionally contains 1.8% DMSO. Medium was changed twice per week and cells were split weekly 1:6 using a trypsin/EDTA (ethylenediaminetetraacetic acid) solution (Sigma Aldrich).

HEK293T cells (ATCC CRL-3216; for the generation of lentiviral particles) and HEK293T/17 (ATCC CRL-11268; for luciferase activity assays) were cultured in DMEM (Gibco) supplemented with 10% FCS (Gibco) and 1% Penicillin/Streptomycin (Gibco). Cells were split three times per week 1:4 using a trypsin/EDTA solution.

Isolation and culture conditions of primary human hepatocytes (PHHs) was previously described [250]. Work with primary cells was approved by the local ethics committee (French ministerial authorisations [AC 2013-1871, DC 2013–1870, AFNOR NF 96 900 Sept 2011]). Written consent was obtained from all patients. HBV, HDV, or HIV chronically infected specimens were excluded.

Hypoxia experiments were carried out in the InVivO2 hypoxia working station (Baker Ruskinn) under 1% or 3% oxygen and 5% CO2, in a humidified atmosphere.

6.2   Treatments

Adapted from my written and experimental contribution in Faure-Dupuy*, Riedl*, *et al.* [34] and Riedl*, Faure-Dupuy*, *et al.* [4]: dHepaRG were stimulated with 0.5 µg/mL of BS1 (generous gift from Jeffrey Browning, Biogen/Idec). Furthermore, non-infected cells were treated either with 10 ng/mL of TNFα, 50 ng/mL of IL-17A (both RnD systems), or 100 ng/mL of lipopolysaccharide from S. minnesota R595 (LPS; from InVivogen), or left untreated. In HBV infected cells, the treatment of dHepaRG was carried out with 1,000 IU of IFNα2A (Roferon; from Roche), 800 IU of TNFα (RnD Systems), or 200 IU of IFNγ (RnD Systems). Furthermore,

dHepaRG were treated with 5 µM TPCA-1, 10 µM PHA-408, 0.1 µM tenofovir, 100 µM dimethyloxallyl glycine (DMOG) and 30 µM FG-4592 (all from Sigma Aldrich).

6.3   Plasmids

All sequences of primers used in this section are presented in Table 2.

Table 2: Primers for cloning and (RT-)qPCR analysis

	Forward primer	Reverse Primer
Cloning primers		
Luciferase Assays		
promoter_A3B	AAAACTCGAGGGACAGATAAAGACAGAGCAGC	AAAAAAGCTTGAAGCTCTGTGGTTTCACTTC
Mut-κB1	GACTCATAAGGCCCTAAAAGGTCACTTTAAGGAGGGCTGTCC	GGACAGCCCTCCTTAAAGTGACCTTTTAGGGCCTTATGAGTC
Mut-κB2	CATGAAGCACCCCAAAGCCTCCCACACCAATGCCTG	CAGGCATTGGTGTGGGAGGCTTTGGGGTGCTTCATG
APOBEC3A 3'UTR-luciferase	AGTCAGCGATCGCAATCAGGGAAACTGAAGGATGG	AGTCAGCGGCCGCGTGTTTGTGGAAACTCTTGCAATT
APOBEC3B 3'-UTR-luciferase	AGTCAGCGATCGCAATCAGGGAAACTGAAGGATGG	AGTCAGCGGCCGCGTGTTTGTGGAAACAATTATGGAAG
APOBEC3G 3' UTR-luciferase	AGTCAGCGATCGCAATCAGGGAAACTGAAGGATGG	AGTCAGCGGCCGCACAGAAAGATTTAGTATTTCATTTTATTCCTC
mutAPOBEC3B-delta-138-luciferase	GCTCACAGACGTCAGCAAAGCAATG	AGCTGGAGATGGTGGTGA
mutAPOBEC3G-delta-138-luciferase	GATCACAGACGTCAGCAAAGCAATGC	AGCTGGAGATGGTGGTGA
mutAPOBEC3A-SNP-138-luciferase	GCTCACAGACACCAGCAAAGC	AGCTGGAGATGGTGGTGA
miR-138	CGATCAGATCTAGCAGCACAAAGGCATCTCT	CGATCAAGCTTATGCTGCCTGTAGTGTGGTG
CRISPR Knock-outs		
NIK sgRNA	ACGCGTCTCACACCGGCTCCTTCGGAGAGGTGCACGTTTTAGAGCTAGAAATAGCAAGTT	ACGCGTCTCAAAACGGCTTTGCTGCGACGCTTTCCGGTGTTTCGTCCTTTCCAC
IKKb sgRNA	ACGCGTCTCACACCGGGTTTGCAAGCAGAAGGCGCGTTTTAGAGCTAGAAATAGCAAGTT	ACGCGTCTCAAAACTCGACTACTGGAGCTTCGGCCGGTGTTTCGTCCTTTCCAC
sgCtrl (non-targeting)	CACC GTTCCGCGTTACATAACTTA	AAAC TAAGTTATGTAACGCGGAAC
sgRNA sequencing	CCCCTCCCCCCAACTTCTC	
RT-qPCR primers		
A20	GGCTGCGTGTATTTTGGGAC	CGCTGGCTCGATCTGTTTGT
APOBEC3B	GACCCTTTGGTCCTTCGAC	GCACAGCCCCAGGAGAAG
APOBEC3B promoter	ACAGATAAAGACAGAGCAGCC	CCCAGGGCCTTATGAGTCATG
CAIX	GTCTCGCTTGGAAGAAATCGC	CACAGGGCGGTGTAGTCAG
CXCL10	TATTCCTGCAAGCCAATTTTGTC	TCTTGATGGCCTTCGATTCTG
HBV total RNA	GGAGGGATACATAGAGGTTCCTTGA	GTTGCCCGTTTGTCCTCTAATTC
HIF1a	TCATCAGTTGCCACTTCCACATA	CCATCATCTGTGAGAACCATAACAA
HIF2a	CAATGACAGCTGACAAGGAGAAG	CATGGGCCAGCTCATAGAAC
HPRT	TCAGGCAGTATAATCCAAAGATGGT	AGTCTGGCTTATATCCAACACTTCG
NF-κB2	GGGCCGAAAGACCTATCCC	CAGCTCCGAGCATTGCTTG
NIK	AGCAGAAGGAACTCCCCAAA	ATCACGTCATTCAGGATCTCCC
pgRNA	GGAGTGTGGATTCGCACTCCT	AGATTGAGATCTTCTGCGAC
RelB	CCGTTTCCAGGAGCACAGATGAA	GAGACACCAGGCGTGGCA
RHOT2	CTGCGGACTATCTCTCCCCTC	AAAAGGCTTTGCAGCTCCAC
tRFP	AACACCGAGATGCTGTACCC	CCGGGCATCTTGAGGTTCTT
VEGFa	GGGCCTCCGAAACCATGAA	AGCTGCGCTGATAGACATCC
HBV cccDNA (Taqman)	CCGTGTGCACTTCGCTTCA	GCACAGCTTGGAGGCTTGA
gDNA (Taqman)	TTCACCTCCCTCAGCACCAG	CCCAGCACTCACGATCAAGT

6.3.1 Plasmids for luciferase activity assays

Plasmids for luciferase assays were generously provided by Emmanuel Dejardin and Nicolas Gillet.

Adapted from my written and experimental contribution in Faure-Dupuy*, Riedl*, *et al.* [34]: In brief, NF-κB expression vectors were previously described [251]. To generate the A3B-promoter luciferase reporter vector, the backbone of pGL3-Basic (Promega) was digested with XhoI and HindIII; as well as a PCR amplicon generated with the primers promoter_A3B_forward and promoter_A3B_reverse. The digested amplicon was then ligated

into the backbone using T4 ligase (New England Biolabs). Single and double mutations of the kB sites 1 and 2 were generated using the primers Mut-kB1_forward and Mut-kB1_reverse or Mut-kB2_forward and Mut-kB2_reverse in a reaction with the Q5 Site-Directed Mutagenesis Kit (New England Biolabs). All restriction reactions were done with enzymes purchased from New England Biolabs.

For the 3'-UTR fusion experiments, the APOBEC3A, -B and -G sequences were generated in a PCR reaction with HEK293T genomic DNA as a template. The vector backbone (psiCHECK2, from Promega) and the PCR amplicons were then digested with AsisI and NotI and ligated to generate plasmids containing A3A, A3B and A3G 3'-UTRs downstream of a luciferase open reading frame. To mutate the predicted miR-138-5p recognition site in the 3'-UTRs of A3B and A3G, the Q5 Site-Directed Mutagenesis Kit (New England Biolabs) was used. Similarly, the single nucleotide polymorphism (SNP) ss1367248965 mutation (G>A) in the A3A 3'-UTR was generated. Positive colonies were screened by restriction digest with EcoRV. To construct pSUPER_miR-138 hsa-miR-138 sequence was PCR amplified from HEK293T genomic DNA. The PCR amplicon and the pSUPER vector backbone (Oligoengine) were digested with BglII and HindIII and ligated using the T4 DNA ligase (New England Biolabs). PCR reactions in this section were conducted with the Q5 polymerase (New England Biolabs) and restriction reactions were done with enzymes purchased from New England Biolabs.

6.3.2 CRISPR plasmids for targeted knock-outs

Adapted from my written and experimental contribution in Faure-Dupuy*, Riedl*, *et al.* [34]: The generation of double-sgRNA containing plasmids was described elsewhere [252, 253]. Briefly, sgRNAs were selected using the CHOPCHOP version 2 web tool [254] based predicted high on-target efficiency and no or lowly scoring off-targets. These sgRNAs were included into the 5'-ends of primers targeting a 5'-sgRNA scaffold-spacer-U6 promoter-3' sequence for amplification. In a PCR reaction, the sgRNA sequences were attached to the PCR amplicon and inserted via golden gate cloning (using BsmBI and T4 ligase, both from New England Biolabs) into pUSEPR (generous gift from Darjus Tscharaganeh). For targeting only NIK or IKKβ, two sgRNAs targeting different exons were cloned into a single vector. For double knock-outs, the NIK sgRNA_forward primer was combined with the IKKβ sgRNA_reverse primer. Vectors for non-targeting control sgRNAs (sgCtrl) were generated by annealing oligos and golden-gate-assembling them into pUSEPR. Assembly was confirmed by Sanger Sequencing (performed in collaboration with the company Microsynth Seqlab).

6.3.3 HIF overexpression plasmids

Adapted from my written and experimental contribution in Riedl*, Faure-Dupuy*, et al. [4]: HIF overexpression plasmids were generated by inserting HIF ORFs into the BamHI/XhoI digested pLenti CMV/TO Hygro empty (#17484; Addgene). Wild-type HIF ORFs were obtained by BamHI/XhoI digestion of HA-HIF1alpha-pcDNA3 (#18949; Addgene), or HA-HIF2α-pcDNA3 (#18950; Addgene). The P402A/P564A double mutant HIF1α ORF was generated in the same fashion from the plasmid HA-HIF1α P402A/P564A-pcDNA3 (#18955; Addgene). The P402A/P564A mutation prevents the proline hydroxylase induced hydroxylation of HIF1α and thereby proteasomal degradation.

Restriction enzymes used in this section and the T4 ligase used in ligation reactions were purchased from New England Biolabs. All HIF vectors were a gift from William Kaelin, and pLenti CMV/TO Hygro empty (w214-1) was a gift from Eric Campeau and Paul Kaufman.

6.4   Transgenic Cell-Line Preparation

Adapted from my written and experimental contribution in Faure-Dupuy*, Riedl*, et al. [34] and Riedl*, Faure-Dupuy*, et al. [4]: HIF-overexpressing cell lines were generated from HepaRG-TR [48]. HepaRG carrying CRISPR-mediated knock-outs were generated from HepaRG-TR-Cas9 (generous gift from David Durantel), which are transgenic for the tetracycline repressor (TR) and a Cas9 coding sequence under control of a CMV promoter carrying two tetracycline operator sites (TetO sites) between the 3'-end of the promoter and the 5'-end of the coding sequence. This system, also known as the T-Rex system (commercialised by Thermo Fisher), allows inducible expression by addition of tetracycline (or derivates like doxycycline) to the medium.

Lentiviral particles and transduction of HepaRG with them was conducted according to protocols from Addgene (https://www.addgene.org/protocols/lentivirus-production/). Briefly, HEK293T cells were transfected with the respective transfer plasmids, CMV-VSV-G (generous gift from Bob Weinberg; Addgene plasmid # 8454) and psPAX2 (generous gift from Didier Trono; Addgene plasmid # 12260) using linear polyethylenimine (PEI; from Polysciences), in the presence of 25 µM chloroquine diphosphate (Sigma Aldrich). One day post transfection, cells were washed and fresh medium was added. On each of the following three days, medium was harvested and filtered through a 0.45 µM PES filter, before fresh medium was added. Aliquots containing lentiviral particles were then stored at -80°C.

For transduction of HepaRG, non-differentiated HepaRG were detached using a trypsin/EDTA solution and seeded into a T75 flask. Two to three mL lentiviral particles containing medium was added and cells were incubated for 24 hours at 37°C, 5% CO_2. Polybrene

(Hexadimethrine bromide; from Sigma Aldrich) was added to a final concentration of 8 µg/mL to facilitate efficient transduction. After 24 hours, cells were washed three times with phosphate buffered saline (PBS) and incubated with "growth medium" for 24 hours before selection was performed.

HepaRG cells were selected in "growth medium" with puromycin (10 µg/mL; from Sigma Aldrich; for CRISPR knock-out cells) or hygromycin (10 µg/mL; from Gibco; for HIF-overexpressing cells) until non-transduced control cells had fully died.

6.5 Transfections

Adapted from my written and experimental contribution in Faure-Dupuy*, Riedl*, *et al.* [34]: psiCHECK2 (20ng, the reporter vector) and pSUPER (500ng, the effector vector) constructs were co-transfected together into 150,000 HEK293T cells (293T/17; ATCC CRL-11268) with Lipofectamine 2000. NF-κB expression vectors (100 ng) and pGL3 vectors containing wild-type or mutated A3B promoter sequences (500 ng) were co-transfected with Lipofectamine 2000 into 150,000 HEK293T cells (293T/17; ATCC CRL-11268). 48 hours post transfection, cells were lysed the Dual-Glo Luciferase Assay System (Promega) was used according to the manufacturer's instructions to detect luciferase activity.

Adapted from my written and experimental contribution in Faure-Dupuy*, Riedl*, *et al.* [34] and Riedl*, Faure-Dupuy*, *et al.* [4]: 10 nM of small interfering RNAs (siRNAs) against NF-κB inducing kinase (NIK, also MAP3K14; Assay ID s17187; Ambion), hypoxia induced factor 1α (HIF1α; Assay ID: s6539; Ambion), hypoxia induced factor 2α (HIF2α; Assay ID: s4698; Ambion), aryl hydrocarbon receptor (AhR; NM_001621; Sigma-Aldrich), aryl hydrocarbon receptor nuclear translocator (ARNT; NM_001668; Sigma-Aldrich), or nontargeting control siRNAs (siCtrl; Ambion) were transfected into dHepaRG with Dharmafect 4 (1:1,000; Dharmacon). Hsa-miR-138-5p mimics (assay ID: MC11727, Ambion) or non-targeting mimic controls (Ambion) were transfected into dHepaRG at 10 nM using Dharmafect 4 (1:500; Dharmacon). Transfections were carried out according to Dharmacon's recommendations for the use of Dharmafect 4.

6.6 HBV Preparation and Inocula

Wild-type HBV and recombinant (rHBV) was generously provided by the lab of Ulrike Protzer. HBx-deficient HBV (ΔX HBV) was generously provided by Julie Lucifora and David Durantel.

Adapted from my written and experimental contribution in Faure-Dupuy*, Riedl*, *et al.* [34] and Riedl*, Faure-Dupuy*, *et al.* [4]: In brief, Heparin columns and sucrose gradient

ultracentrifugation were used to purify and concentrate HBV from the supernatant of HepAD38 cells, as described before. [255] 200 viral genome equivalents per cell were used to infect dHepaRG in the presence of 4% PEG-8000 (Sigma-Aldrich). Twenty-four hours after infection, cells were washed three times with PBS.

rHBV was purified from the supernatant of a HepG2-producer cell line concentrated as stated for HBV. This cell line was generated by the stable transfection of HepG2 with a construct expressing HBV polymerase, X-gene and surface proteins (pRR_TTR-Polymerase-LMS-IRES-Puro), as well as the 1.3 times overlength HBV genome, in which the (transthyretin) TTR promoter followed by a monomeric turbo RFP gene followed by a nuclear localization signal was inserted into the polymerase and HBsAg ORF (Wettengel and Protzer, unpublished) [256].

6.7   cccDNA clean-up and quantification

Adapted from my written and experimental contribution in Faure-Dupuy*, Riedl*, *et al.* [34] and Riedl*, Faure-Dupuy*, *et al.* [4]: The MasterPure Complete DNA and RNA Purification Kit (Epicentre; precipitation based, selective for cccDNA over rcDNA) was used to extract HBV cccDNA from infected dHepaRG. DNA was quantified by Nanodrop measurement, and 40 ng DNA were used as an input into a qPCR reaction. qPCR was performed using the Luna Universal Probe qPCR Master Mix (New England Biolabs). For detection, Carboxyfluorescein- (FAM) labelled and black hole quencher- (BHQ) quenched probes (Sigma) targeting a unique region in the HepaRG genome ([6FAM]-CAT GGA GAC CAC CGT GAA CGC CC-[BHQ1]) and the HBV genome in a way that spans the gap in the rcDNA ([6FAM]-GCT ACG CCA TCG ACA CGG TGC AGG T-[BHQ1]) were used. Primers are listed in Table 2. cccDNA levels were normalized to HepaRG gDNA and are presented as relative expression compared to non-treated controls (NT).

6.8   Southern blot

Adapted from my written and experimental contribution in Faure-Dupuy*, Riedl*, *et al.* [34] and Riedl*, Faure-Dupuy*, *et al.* [4]: Southern blot detection of HBV cccDNA was described previously [2, 257]. Briefly, the KCl protein precipitation method was used to extract episomal/mitochondrial DNA from HBV-infected dHepaRG, which was then separated through a 0.8% agarose gel. The DNA was then blotted onto a nylon membrane and a 32P HBV-DNA probe was used for detection.

6.9   Secreted HBV DNA analysis

Adapted from my written and experimental contribution in Faure-Dupuy*, Riedl*, *et al.* [34]: 25 µL cell culture supernatant from HBV infected dHepaRG was collected and digested for 30 minutes at 37°C with 0.5 µL DNaseI (New England Biolabs) and 1 µL RNaseI (Sigma Aldrich; 10 mg/mL). Afterwards, DNaseI reaction was stopped and HBV DNA was released from capsids by incubation for 10 minutes at 95°C. Then, the reactions were then diluted 1:4 with water and used in a SYBR-based qPCR reaction. The diluted DNA was diluted further 1:2.5 in the qPCR reaction. Primers were the same as for total HBV RNA. Sequences are given in Table 2.

6.10 RT-qPCR

Adapted from my written and experimental contribution in Faure-Dupuy*, Riedl*, *et al.* [34] and Riedl*, Faure-Dupuy*, *et al.* [4]: RNAs were either isolated with the Monarch Total RNA Miniprep Kit (New England Biolabs), according to the manufacturer's instructions. RNA was then measured with a nanodrop spectrometer (Thermo Fisher). For mRNA, the Quantitect Kit (Qiagen) was used for cDNA synthesis. Then, cDNA was diluted 1:10. 3 µL diluted cDNA was used as input into a qPCR reaction. The reaction further contained 6 µL FS Universal SYBR Green MasterRox (Roche), 0.12 µL reverse+forward primer mix, and 2.88 µL water (amounts given for one reaction). The qPCRs were then submitted to a run on the QuantStudio 5 light cycler (Thermo Fisher). The ΔΔCT method and the QuantStudio software (Thermo Fisher) were used for data analysis. Relative quantification was performed by comparing target genes to the housekeeping genes RHOT2 and HPRT.

Adapted from my written and experimental contribution in Faure-Dupuy*, Riedl*, *et al.* [34]: The TaqMan MicroRNA Reverse Transcription Kit (Applied Biosystems) was used for the reverse transcription of miRNAs. The manufacturer's instructions were adapted as follows: 350-1000 ng were diluted in 8 µL water. Then. 1.5 µL RT-primer for hsa-miR-138-5p and 1.5 µL RT-primer for hsa-RNU6b, 1.5 µL 10x RT buffer, 1 µL MultiScribe Reverse Transcriptase (50 U/µL), 0.19 µL RNase Inhibitor (20 U/µL), 0.15 µL 100 mM dNTPs and 1.16 µL water (all reagents from Applied Biosystems) were added. The reaction was incubated as stated in the manual. Afterwards, cDNA was then diluted 1:4 and 2.5 µL of the diluted cDNA were used in a qPCR reaction, containing in addition. 5 µL 2x TaqMan Universal PCR Master Mix II, no UNG (ThermoFisher), 0.5 µL 20x TaqMan Assays (for either hsa-miR-138-5p or for hsa-RNU6b), and 2 µL water. As for mRNA, the reactions were run on the QuantStudio 5 light cycler (Thermo Fisher). Analysis was done according to the mRNA analysis and hsa-RNU6b

was used as a housekeeping gene for relative quantification. All used primers are listed in Table 2.

6.11 RNA sequencing

Adapted from my written and experimental contribution in Faure-Dupuy*, Riedl*, *et al.* [34]: Library preparation for bulk 3'-sequencing of poly(A)-RNA was done as described previously [258]. The NextSeq 500 platform (Illumina) was used for sequencing, running with 65 cycles for the cDNA in read 1 and 16 cycles for the barcodes and unique molecular identifiers (UMIs) in read 2. Sample- and gene-wise UMI tables [259] were generated after data processing published Drop-seq pipeline (v1.0). For alignment, the human reference genome (GRCm38) was used. The ENSEMBL annotation release 75 was used to define transcripts and genes. DESeq2 was used to perform normalization and differential expression analysis [260]. Geneset enrichment analysis and pathway-based data integration and visualization were conducted using the R packages hyper [261] and Pathview [262], respectively.

6.11 Small RNA sequencing

Adapted from my written and experimental contribution in Faure-Dupuy*, Riedl*, *et al.* [34]: For small RNA sequencing, total RNA was isolated from dHepaRG as described previously and quantified using Qubit (Thermo Fisher) measurement according to manufacturer's recommendations. Library preparation was conducted with 2,000 ng total RNA as input using the TruSeq Small RNA Library Prep Kit -Set A (Illumina) and subsequently sequenced on a HiSeq 2000 v4 Single-Read 50 bp platform in the DKFZ (Deutsches Krebsforschungszentrum) Genomics and Proteomics Core Facility. Raw reads were read from fastq files and pre-processed using the mirPRo approach [263]. Briefly, sequencing adapters were removed from raw reads before alignment to the human miRbase reference (August 2019) and quantification using default analysis parameters of the mirPRo algorithm. The raw reads matrix containing only mature miRNAs was then imported into the R package DEseq2 for differential expression analysis and data visualization [260]. miRNAs displaying p-values were smaller than 0.05 and Benjamini-Hochberg false-discovery rates smaller than 10% between tested conditions were considered to be differentially expressed.

6.12 Somatic cancer genes panel sequencing

Adapted from my written and experimental contribution in Faure-Dupuy*, Riedl*, *et al.* [34]: DNA was extracted in the same fashion as described previously and DNA quantity was determined by Qubit (Thermo Fisher) measurement. Similar amounts of DNA were then used for panel sequencing by the company CeGaT in Tübingen, Germany. The CancerPrecision panel was chosen which covers 766 genes and 31 gene fusions associated with somatic mutations in tumours (see https://www.cegat.de/diagnostik/tumor-diagnostik/cancerprecision/ and Table 3). Demultiplexing of the sequencing reads was performed with Illumina bcl2fastq (2.20) after sequencing. Adapters were removed with Skewer (version 0.2.2) [264]. Quality trimming of the reads has not been performed. Trimmed raw reads were then aligned to the human reference genome (hg19-cegat) using the BurrowsWheeler Aligner (BWA-mem version 0.7.17-cegat) [265]. For local realignment of reads in target regions, ABRA (version 2.18) [266] was used to facilitate more accurate indel calling. A proprietary software was used furthermore for variant detection. Variants with low frequencies are also included in the lists (OFA down to 2% of sequenced reads). Variants were annotated based on various public databases. Copy number variations (CNVs) were detected by comparing the number of reads overlapping the genomic target regions ("coverage") with the expected number in a cohort of reference samples.

6.13 Electrophoretic mobility shift assay

Adapted from my written and experimental contribution in Faure-Dupuy*, Riedl*, *et al.* [34]: The protocol for NF-κB gel shift assays was previously reported [267]. The following complementary DNA oligonucleotides were annealed to generate the κB1 A3B probe (5'-TTG GGC CCT GGG AGG TCA CTT TAA-3' and 5'-TTG GTT AAA GTG ACC TCC CAG GGC-3') and the κB2 A3B probe (5'-TTG GAC CCC GGG GCC TCC CAC ACC-3' and 5'-TGG GGT GTG GGA GGC CCC GGG GT-3').

6.14 Chromatin immuno-precipitation

Adapted from my written and experimental contribution in Faure-Dupuy*, Riedl*, *et al.* [34] and Riedl*, Faure-Dupuy*, *et al.* [4]: Nucleic acid-protein cross-linking and immunoprecipitation for chromatin immuno-precipitation (ChIP) was previously described [268]. A QuantStudio 5 real time PCR instrument (Thermo Fisher) was used to quantify immunoprecipitated DNA in SYBR-

based qPCR reaction. Signal was normalised to the input. All primers used are listed in Table 2 and all antibodies are listed in Table 4.

Table 3: – Genes analysed for SNV by ultra-deep panel sequencing in collaboration with the company CeGaT

Genes tested										
AAK1	CALR	CYP3A5	FBXW7	HLA-DQA1	MAD2L2	NCOR1	PKHD1	RINT1	TAF1	XRCC3
ABCB1	CAMK2G	CYP4F2	FEN1	HLA-DQB1	MAF	NF1	PLCG1	RIPK1	TAF15	XRCC5
ABCG2	CARD11	DAXX	FES	HLA-DRA	MAGI1	NF2	PLCG2	RIT1	TAP1	XRCC6
ABL1	CASP8	DCC	FGF10	HLA-DRB1	MAGI2	NFE2L2	PLK1	RNASEL	TAP2	YAP1
ABL2	CBFB	DDB2	FGF14	HMGA2	MAML1	NFKB1	PML	RNF43	TAPBP	YES1
ABRAXAS1	CBL	DDR1	FGF19	HMGCR	MAP2K1	NFKB2	PREX2	ROS1	TBK1	ZFHX3
ACD	CBLB	DDR2	FGF2	HMGN1	MAP2K2	NFKBIA	PMS2	RPS20	TBL1XR1	ZNF217
ACVR1	CBLC	DDX11	FGF3	HNF1A	MAP2K3	NFKBIE	POLD1	RPS6KB1	TBX3	ZNF703
ADGRA2	CCDC6	DDX3X	FGF4	HNF1B	MAP2K4	NIN	POLE	RPS6KB2	TCF3	ZNFR3
ADRB1	CCND1	DDX41	FGF5	HOXB13	MAP2K5	NKX2-1	POLH	RPTOR	TCF4	ZRSR2
ADRB2	CCND2	DEK	FGF6	HRAS	MAP2K6	NLRC5	POLQ	RSF1	TCF7L2	
AIP	CCND3	DHFR	FGF9	HSD3B1	MAP2K7	NOTCH1	POT1	RUNX1	TCL1A	
AIRE	CCNE1	DICER1	FGFBP1	HSP90AA1	MAP3K1	NOTCH2	PPM1D	RYR1	TEK	
AJUBA	CD274	DIS3L2	FGFR1	HSP90AB1	MAP3K13	NOTCH3	PPP2R2A	SAMDH1	TENT5C	
AKT1	CD79A	DNMT1	FGFR2	HTR2A	MAP3K14	NOTCH4	PRDM1	SAV1	TERC	
AKT2	CD79B	DNMT3A	FGFR3	ID3	MAP3K3	NPM1	PREX2	SBDS	TERF2IP	
AKT3	CD82	DOTL1	FGFR4	IDH1	MAP3K4	NQO1	PRKAR2A	SCG5	TERT	
ALK	CDC73	DPYD	FH	IDH2	MAP3K6	NR1I3	PRKCA	SDHA	TET1	
ALOX12B	CDH1	E2F3	FLCN	IDO1	MAP3K8	NRAS	PRKD1	SDHAF2	TET2	
AMER1	CDH11	EBP	FLI1	IFNGR1	MAPK1	NRG1	PRKDC	SDHB	TFE3	
ANKRD26	CDH2	EED	FLT1	IFNGR2	MAPK11	NRG2	PRKN	SDHC	TCFB1	
APC	CDH5	EFL1	FLT3	IGF1R	MAPK12	NSD1	PRMT5	SDHD	TGFBR2	
APLNR	CDK1	EGFR	FLT4	IGF2	MAPK14	NSD2	PRSS1	SEC23B	TLR4	
APOBEC3A	CDK12	EGLN1	FOXA1	IGF2R	MAPK3	NSD3	PSMB1	SERPINB9	TLX1	
APOBEC3B	CDK4	EGLN2	FOXA2	IKBKB	MAX	NT5C2	PSMB10	SETBP1	TMEM127	
AR	CDK5	EIF1AX	FOXE1	IKBKE	MBCD1	NT5E	PSMB2	SETD2	TMPRSS2	
ARAF	CDK6	ELAC2	FOXL2	IKZF1	MC1R	NTHL1	PSMB5	SETDB1	TNFAIP3	
ARHGAP35	CDK8	ELF3	FOXO1	IKZF3	MCL1	NTRK1	PSMB8	SF3B1	TNFRSF11A	
ARID1A	CDKN1A	EME1	FOXO3	IL1B	MDC1	NTRK2	PSMB9	SGK1	TNFRSF13B	
ARID1B	CDKN1B	EML4	FOXP1	IL1RN	MDH2	NTRK3	PSMC3IP	SH2B1	TNFRSF14	
ARID2	CDKN1C	EMSY	FOXQ1	ING4	MDM2	NUMA1	PSME1	SH2B3	TNFRSF8	
ARID5B	CDKN2B	EP300	FRK	INPP4A	MDM4	NUP98	PSME2	SHH	TNFSF11	
ASXL1	CDKN2C	EPAS1	FRS2	INPP4B	MECOM	NUTM1	PSME3	SIK2	TNK2	
ASXL2	CEBPA	EPCAM	FUBP1	INPPL1	MED12	OPRM1	PSPH	SIN3A	TOP1	
ATM	CENPA	EPHA2	FUS	INSR	MEF2B	PAK1	PTCH1	SKP2	TOP2A	
ATP1A1	CEP57	EPHA4	FYN	IRF1	MEN1	PAK3	PTCH2	SLC19A1	TP53	
ATR	CFTR	EPHB4	G6PD	IRF2	MERTK	PAK4	PTEN	SLC26A3	T53BP1	
ATRX	CHD1	EPHB6	GALNT12	IRS1	MET	PAK5	PTGS2	SLCO1B1	TP63	
AURKA	CHD2	ERBB2	GATA1	IRS2	MGA	PALB2	PTK2	SLIT2	TPMT	
AURKB	CHD4	ERBB3	GATA2	IRS4	MGMT	PALLD	PTK6	SLX4	TPX2	
AURKC	CHEK1	ERBB4	GATA3	ITPA	MITF	PARP1	PTK7	SMAD3	TRAF2	
AXIN1	CHEK2	ERCC1	GATA4	JAK1	MLH1	PARP2	PTPN12	SMAD4	TRAF3	
AXIN2	CIC	ERCC3	GATA6	JAK2	MLH3	PARP4	PTPRC	SMARCA4	TRAF5	
AXL	CIITA	ERCC4	GGT1	JAK3	MLLT10	PAX3	PTPRD	SMARCB1	TRAF6	
B2M	CKS1B	ERCC5	GLI1	JUN	MLLT3	PAX5	PTPRS	SMARCD1	TRAF7	
BAP1	CNKSR1	ERG	GLI2	KAT6A	MN1	PAX7	PTPRT	SMARCE1	TRRAP	
BARD1	COL1A1	ERRFI1	GLI3	KDM5A	MPL	PBK	RABL3	SMC1A	TSC1	
BAX	COMT	ESR1	GNA11	KDM5C	MRE11	PBRM1	RAC1	SMC3	TSC2	
BCHE	COQ2	ESR2	GNA13	KDM6A	MS4A1	PBX1	RAC2	SMO	TSHR	
BCL10	CREB1	ETNK1	GNAQ	KDR	MSH2	PDCD1	RAD21	SOCS1	TTK	
BCL11A	CREBBP	ETS1	GNAS	KEAP1	MSH3	PDCD1LG2	RAD50	SOX11	TUBB	
BCL11B	CRKL	ETV1	GNB3	KIAA1549	MSH4	PDGFA	RAD51	SOX2	TYMS	
BCL2	CRLF2	ETV4	GPC3	KIF1B	MSH5	PDGFB	RAD51B	SOX9	U2AF1	
BCL3	CRTC1	ETV5	GPER1	KIT	MSH6	PDGFC	RAD51C	SPEN	UBE2T	
BCL6	CRTC2	ETV6	GREM1	KLF2	MSR1	PDGFD	RAD51D	SPINK1	UBR5	
BCL9	CSF1R	EWSR1	GRIN2A	KLF4	MST1R	PDGFRA	RAD54B	SPOP	UGT1A1	
BCL9L	CSF3R	EXO1	GRM3	KLHL6	MTAP	PDGFRB	RAD54L	SPRED1	UGCT2B15	
BCOR	CSMD1	EXT1	GSK3A	KLLN	MTHFR	PDIA3	RAF1	SPTA1	UGT2B7	
BCORL1	CSNK1A1	EXT2	GSK3B	KMT2A	MTOR	PDK1	RALGDS	SRC	UINC1	
BCR	CTCF	EZH1	GSPT1	KMT2B	MT-RNR1	PDPK1	RARA	SRD5A2	UNG	
BIRC2	CTLA4	EZH2	H3-3A	KMT2C	MTRR	PGR	RASA1	SRGAP1	USP34	
BIRC3	CTNNA1	FAN1	H3-3B	KMT2D	MUC1	PHF6	RASAL1	SRSF2	USP9X	
BIRC5	CTNNB1	FANCA	H3C2	KNSTRN	MUTYH	PHOX2B	RB1	SSTR1	VEGFA	
BLM	CTRC	FANCB	HABP2	KRAS	MXI1	PIGA	RBRM10	SSTR2	VEGFB	
BMI1	CUX1	FANCC	HCK	KSR1	MYB	PIK3C2A	RECQL4	SSX1	VHL	
BMPR1A	CXCR4	FANCD2	HDAC1	LATS1	MYC	PIK3C2B	RET	STAG1	VKORC1	
BRAF	CYLD	FANCE	HDAC2	LTAS2	MYCL	PIK3C2G	RFC2	STAG2	WRN	
BRCA1	CYP1A2	FANCF	HDAC6	LCK	MYCN	PIK3CA	RFWD3	STAT1	WT1	
BRCA2	CYP2A7	FANCG	HGF	LIG4	MYD88	PIK3CB	RFX5	STAT3	XIAP	
BRD3	CYP2B6	FANCI	HIF1A	LIMK2	MYH11	PIK3CD	RFXANK	STAT5A	XPA	
BRD4	CYP2C19	FANCL	HLA-A	LRP1B	MYH9	PIK3CG	RFXAP	STAT5B	XPC	
BRD7	CYP2C8	FANCM	HLA-B	LRRK2	NAT2	PIK3R1	RHBDF2	STK11	XPO1	
BRIP1	CYP2C9	FAS	HLA-C	LTK	NBN	PIK3R2	RHEB	SUFU	XRCC1	
BTK	CYP2D6	FAT1	HLA-DPA1	LYN	NCOA1	PIK3R3	RHOA	SUZ12	XRCC2	
BUB1B	CYP3A4	FBXO11	HLA-DPB1	LZTR1	NCOA3	PIM1	RICTOR	SYK	XRCC3	

6.15 Polysome analysis

Adapted from my written and experimental contribution in Faure-Dupuy*, Riedl*, *et al.* [34]: For polysome fractionation, three minutes prior to harvest, 100 μg/mL cycloheximide (Sigma Aldrich) were added to the medium. Then medium was then aspirated and ice-cold PBS containing 100 μg/ml cycloheximide was used to wash the cells. Cells were harvested with a cell scraper, then pelleted at 800x g for five minutes at 4°C and cytoplasmic RNA was obtained by mechanical lysis (20 strokes of a P1000 pipet) of the cell pellet in 1 mL of polysome buffer. This buffer contained 10 mM Tris-HCl (pH 8.0), 140 mM NaCl, 1.5 mM MgCl2, 0.5% Nonidet P-40, and 40 mM vanadyl ribonucleosides complexes, 100 μg/mL cycloheximide, 20 mM dithiothreitol, and 1 mM phenylmethanesulfonyl fluoride (all reagents obtained from Sigma). Mitochondria and membrane debris were pelleted and discarded. 250 mM EDTA (Sigma) were added to control release samples. The post-mitochondrial supernatants were loaded onto a 15-40% sucrose gradient and centrifuged at 38,000 rounds per minute (rpm) for 2 hours at 4°C in a SW41Ti rotor (Beckman Coulter). Fractions were harvested from the top of each gradient using a 240 nm UV reader-coupled fraction collector (Brandel). By interpretation of UV gradient traces, free messenger ribonucleoproteins (mRNPs), 40S and 60S subunits, monosomes as well as, polysomes were located. mRNAs were cleaned up using phenol-chlorophorm extraction and were analysed by SYBR-based RT-qPCR as given above for RT-qPCR.

6.16 Immunoblotting

Adapted from my written and experimental contribution in Faure-Dupuy*, Riedl*, *et al.* [34] and Riedl*, Faure-Dupuy*, *et al.* [4]: RIPA buffer (Cell Signalling Technologies) supplemented with Complete and PhosSTOP (both Roche) was used for cell lysis. Protein concentration was measured by bicinchoninic acid (BCA) assay. Equal amounts of protein were loaded onto an SDS-PAGE and proteins were separated by size before transfer to a 0.22 μM PVDF membrane (Fisher Scientific). 5% non-fat dry milk was used for blocking. Membranes were then incubated with primary antibodies over-night at 4°C and with secondary antibodies one hour at room temperature. All used antibodies are listed in the Table 4.

Table 4: Antibodies used for immunoblotting, ChIP, IHC, ICC and FACS

Target	Supplier	Cat. No.	concentration
Immunoblotting Antibodies			
Primary Antibodies			
AhR	Cell Singaling Technologies	83200	1:1000
APOBEC3B/G	BEI Resources	190376	1:1000
ARNT	Cell Singaling Technologies	5537	1:1000
GAPDH	Cell Singaling Technologies	2118	1:10000
HIF1a	Becton Dickinson	610959	1:500
Histone H3	Abclonal	A2348	1:1000
IkBa	Cell Signaling Technologies	9242	1:1000
IKKβ	Cell Signaling Technologies	2678	1:1000
NF-kB1	Cell Signaling Technologies	3035	1:1000
NF-kB2	Becton Dickinson	05-361	1:500
phospho-RelA	Cell Signaling Technologies	3033	1:1000
RelA	Cell Signaling Technologies	6956	1:1000
RelB	Cell Signaling Technologies	4922	1:1000
Vinculin	Sigma-Aldrich	V9131	1:1000
α-Tubulin	Sigma-Aldrich	T6074	1:5000
γ-Tubulin	Sigma-Aldrich	T6557	1:5000
Secondary Antibodies			
mouse IgG	Cell Signaling Technologies	7076	1:20000
rabbit IgG	Cell Signaling Technologies	7074	1:20000
ChIP Antibodies			
HIF1α	R and D systems	NB100-105	1:150
NF-kB1	Cell Signaling Technologies	3035	1:200
NF-kB2	Cell Signaling Technologies	37359	1:200
Polymerase II	Abcam	ab26721	1:150
RelA	Cell Signaling Technologies	8242	1:200
RelB	Cell Signaling Technologies	10544	1:200
IHC/ICC Antibodies			
HBcAg	DAKO	B0586	1:250
HIF1α (IHC)	Novus Biologicals	NB100-105	1:40
HIF1α (IHC/ISH)	Novus Biologicals	NB100-134	1:500
RelA	Novus Biologicals	NB100-2176	1:200
RelB	Cell Signaling Technologies	4922	1:200
FACS Antibodies			
Lymphotoxin beta receptor	Novus Biologicals	AF629	1:150
Goat-IgG	Invitrogen	A-11012	1:400

6.16 Cytoplasm/nucleus extraction

Adapted from my written and experimental contribution in Riedl*, Faure-Dupuy*, et al. [4]: After washing with ice-cold PBS, cells were harvested with a cell scraper and pelleted 2000 rpm for five minutes at 4°C. Cytosolic fractions were generated by lysing of the cell pellet in 1 mL Buffer (Hepes 10 mM pH7.9, KCl 10 mM, MgCl2 2 mM, EDTA 0.1 mM, Nonident P-40 0.02%, DTT 1 mM) supplemented with Complete and PhosSTOP. Lysates were incubated 10 minutes in ice, followed by centrifugation at 2,000 rpm for five minutes at 4°C. Nuclear pellets were washed (Hepes 10 mM pH7.9, KCl 20 mM, MgCl2 2 mM, EDTA 0.1 mM) then incubated on ice for 30 minutes in nuclear Buffer Lysis (Hepes 20 mM pH7.9, MgCl2 1.5 mM, EDTA 0.2 mM, NaCl 0.42 M, Glycerol 25%, DTT 0.5 mM) supplemented with Complete and PhosSTOP. Debris were removed by centrifugation.

6.17 Mass spectrometry

Adapted from my written and experimental contribution in Faure-Dupuy*, Riedl*, et al. [34] and Riedl*, Faure-Dupuy*, et al. [4]: For mass spectrometry analysis, RIPA buffer, complemented with Complete and PhosStop (both Roche) was used for cell lysis. After clearing samples via centrifugation at 15,000x g for five minutes at 4°C, protein concentration was measured by BCA assay as described for immunoblotting. Equal protein amounts were then submitted to the DKFZ Genomics and Proteomics Core Facility. Proteins were run a short distance of only around 0.5 mm on a SDS-PAGE and the whole, unfractionated sample was cut out of the gel after Coomassie blue staining. Proteins were afterwards digested with trypsin uing a slightly modified protocol of Shevchenko et al. [269] on a DigestPro MSi robotic system (INTAVIS Bioanalytical Instruments AG). Peptides from the tryptic digest were then loaded on a cartridge trap column, packed with Acclaim PepMap300 C18, 5 μm, 300 Å wide pore (Thermo Fisher) and separated in a three step, 180 minutes gradient from 3% to 40% ACN on a nanoEase MZ Peptide analytical column (300Å, 1.7 μm, 75 μm x 200 mm, Waters) carried out on a UltiMate 3000 UHPLC system. Eluting peptides were analysed by a coupled Q-Exactive-HF-X mass spectrometer (Thermo Fisher) via an online data depend acquisition mode. Here, one full scan at 120 k resolution (375-1,500 m/z, maxIT 54 ms) was performed prior to up to 35 MSMS scans at 15 k resolution of eluting peptides at an isolation window of 1.6 m/z and a collision energy of 27 NCE. Settings for the ion injection time were at a maximum of 22 ms or 1e5 ions (AGC target). Unassigned and singly charged peptides have been removed from fragmentation and dynamic exclusion set to 60 seconds was used to prevent oversampling of same peptides. An organism specific database extracted from Uniprot.org under default settings was used for data analysis by MaxQuant (version 1.6.3.3) [270]. An identification FDR

cut-offs of 0.01 on peptide level and on protein level was used. Based on accurate retention time and m/z, match between runs option was enabled for the transfer of peptide identifications across Raw files. Quantification was performed using a label free approach based on the MaxLFQ algorithm [271]. For protein quantification, ≥2 quantified peptides per protein were required. Further processing of data was performed by in-house compiled R-scripts to plot and filter data and the Perseus software package (version 1.6.7.0) using default settings for the imputation of missing values and statistical analysis [272]. Only proteins displaying three non-missing intensities in at least one condition were kept for analysis. The remaining missing values were imputed either by half of the minimum measured intensity and then log2 transformed, or after log2 transformation via the regularized expectation maximization (REM) algorithm by Schneider et al. [273], regarded as superior in a variety of settings explored in [274]. R package Limma [275] was used to generate a moderated t statistics [276] for each contrast of interest and for each imputed data-set. To control for the false discovery rate (FDR), resulting p-values for each contrast were adjusted with the Benjamini-Hochberg [277] procedure. For each contrast for plotting and pathway analysis purposes, and to enhance the robustness of the analysis, only proteins significant or non-significant at level 5% in both analyses, i.e. under each imputation approach, and the corresponding REM imputed analysis values, were retained. The Limma function mroast was applied for self-contained pathway analyses (KEGG annotation), where p-values for each pathway were obtained via the rotation test method described in [278]. The FDR was controlled via the Benjamini-Hochberg adjustment as well. The regularized expectation maximization algorithm was computed in MatLab v. R2019b, with code available at https://github.com/tapios/RegEM. The remaining analyses were performed in R, v. 3.6.1.

6.18 Human Liver Specimen

Adapted from my written and experimental contribution in Riedl*, Faure-Dupuy*, et al. [4]: The DZIF (Deutsches Zentrum für Infektionsforschung) partner site in Heidelberg/Institute of Pathology at the Medical University Heidelberg provided sections of formalin-fixed, paraffin-embedded liver resections from 15 patients chronically infected with HBV. The CHB patients all in the immune-active phase of the disease, presenting F3/F4 fibrosis grading and A3 activity (METAVIR scoring). Sections were 2 or 5 µM thick. Work with patient material was approved by the Heidelberg ethics committee under the following number: S206/2005.

6.19 Immunohistochemistry and *in-situ* hybridization

Adapted from my written and experimental contribution in Riedl*, Faure-Dupuy*, et al. [4]: Using the BOND-MAX Automated IHC/ISH (immunohistochemistry/*in-situ* hybridisation) Stainer (Leica), 2 µM slices of human liver tissue were stained with antibodies against HIF1α or HBcAg. All reagents were purchased from Leica. For detection, a secondary antibody-polymer (Leica) coupled to horseradish peroxidase was used. All used antibodies are listed in the Table 4.

For APOBEC3B ISH, 5 µM sections of human liver specimen were used. The probe, all buffers and other reagents were purchased from ACD (Catalogue number 701271). ISH was performed strictly according to the manufacturer's instructions. For double immunohistochemistry and ISH was done by first performing the ISH procedure, then IHC on the same slide. Shortly, manufacturer's instructions (ACD) were followed closely for ISH with one exception: to insure good protein detection by the subsequent IHC, the suggested incubation time with protease of 30 minutes was reduced to 15 minutes. IHC was conducted as described above and signal was detected using Opal chemistry (Akoya Biosciences). This HRP substrate emits in the FITC channel and was chosen to detect HIF1α protein (i.e. Opal520). Nuclei were stained with DAPI (Invitrogen) for 10 min.

6.19 Immunocytochemistry

Adapted from my written and experimental contribution in Riedl*, Faure-Dupuy*, et al. [4]: HepaRG were grown in 4-well chamber slides (Thermo Fisher). To stop the experiments, cells were fixed with 4% paraformaldehyde (Carl Roth) for 15 minutes at room temperature. Then, the slides were then washed with PBS twice and cells were permeabilised with 0.2% Triton X-100 (Sigma Aldrich) for 10 minutes at room temperature. Cells were rinsed with PBS, incubated 5 minutes in 70% ethanol, followed by extensive washing in PBS. Slides were then submitted to automated staining using the BOND-MAX Automated IHC/ISH Stainer (Leica). Secondary antibody-polymer (Leica) coupled to alkaline phosphatase was used for detection. All used antibodies are listed in the Table 4.

6.20 Flow cytometry

Adapted from my written and experimental contribution in Riedl*, Faure-Dupuy*, et al. [4]: Cells were detached with Versene (Lonza), then pelleted by centrifugation and immediately incubated with 4% paraformaldehyde for 5 minutes at room temperature for fixation. After

washing cells with PBS, cells were labelled with a primary antibody against LTβR and a secondary, Alexa-647-linked, antibody. Incubation each antibody was for 30 minutes at room temperature. Analysis was conducted on a Fortessa flow cytometer (Becton Dickinson). All antibodies are listed in Table 4.

6.21 Viability assays

Adapted from my written and experimental contribution in Faure-Dupuy*, Riedl*, *et al.* [34] and Riedl*, Faure-Dupuy*, *et al.* [4]: Cytotoxicity was assessed by neutral red uptake and Sulforhodamin B (both Sigma Aldrich) staining as previously described [279].

6.22 Mice

Adapted from my written and experimental contribution in Riedl*, Faure-Dupuy*, *et al.* [4]: 11 to 12 weeks old C57BL6/J mice (3 males and 3 females), were i.p. injected with 300 mg/kg of DMOG. 6 hours after injection, mice were sacrificed and livers were harvested for mRNA and protein extraction. Experiment on mice were approved by the Ethics Committee of ULiege (#1939).

6.23 Statistical Analysis

Adapted from my written and experimental contribution in Faure-Dupuy*, Riedl*, *et al.* [34] and Riedl*, Faure-Dupuy*, *et al.* [4]: One-way and two-way ANOVA, Spearman correlation, and the unpaired Student two-tailed t test were performed using Prism software (version 8; from GraphPad Software Inc). Data are shown as mean ± SD (*: $p < 0.05$; **: $p < 0.01$; ***: $p < 0.001$; ****: $p < 0.0001$; ns: not significant).

7   Results

7.1   Aim 1: Deciphering transcriptional and post-transcriptional control of APOBEC3B

7.1.1 Canonical and non-canonical NF-κB signaling induce APOBEC3B upon LTβR agonisation

Adapted from my written and experimental contribution in Faure-Dupuy*, Riedl*, *et al.* [3]: First, to validate that treatment with BS1 specifically induces A3B in the APOBEC3 family, I in collaboration with Mira Stadler and the Genomics and Proteomics Core Facility performed a short-term treatment of 24 hours with differentiated HepaRG (dHepaRG) and analysed the transcriptome and proteome of these cells via RNA sequencing and mass spectrometry. Among all members of the APOBEC3 family, A3B showed the strongest upregulation, of 2-fold on the transcriptional level and more than 45-fold on the protein level (**FIGURE 11a**), compared to non-treated (NT) cells. To further validate increased translation of A3B, polysomal fractions were analysed. As expected, A3B mRNA was found to be enriched in polysomal fractions of higher molecular weight after treatment of dHepaRG with BS1 for six days, compared to non-treated cells (**FIGURE 11b-c**). Of note, A3B mRNA was mainly found in fractions with higher molecular weight rather than disomes (i.e. two ribosomes on a single mRNA molecule). Interaction with heavy polysomes indicate a strong translational activity of A3B. EDTA release control [280] confirmed the polysomal origin of the A3B signal (**FIGURE 11d**) (adapted from Faure-Dupuy*, Riedl*, *et al.* [3]).

Whereas ligand-induced activation of the LTβR was previously identified in transformed cancer cells to induce the transcriptional activation of A3B via NF-κB [150, 151, 281], the underlying mechanisms of A3B induction in non-transformed hepatocytes remains elusive. To confirm the involvement of NF-κB in A3B transcriptional regulation, I performed *in silico* analysis of the A3B upstream genomic region to find putative NF-κB sites. Two sites could be identified (**FIGURE 12a**; called hereafter κB1 and κB2 for the more proximal and distal site, respectively). Radiolabelled probes corresponding to the 20 nt surrounding those sites were tested by EMSA (electrophoretic mobility shift assay) to assess their capacity to be bound by nuclear proteins of BS1 treated cells. Binding of the probes was confirmed in a BS1 treatment-dependent and time-dependent manner (**FIGURE 12b**). Furthermore, to analyse the NF-κB dependent activation of the A3B promoter, I together with Emmanuel Dejardin and Nicolas Gillet fused the A3B promoter (ranging from nt -230 to the nt +18 in respect to the transcription start site) to a luciferase open reading frame (ORF). Mutants of the kB1 and kB2 site were also generated by exchanging the most distal 5' GGG-tri-nucleotide to an AAA-tri-nucleotide (**FIGURE 12c**).
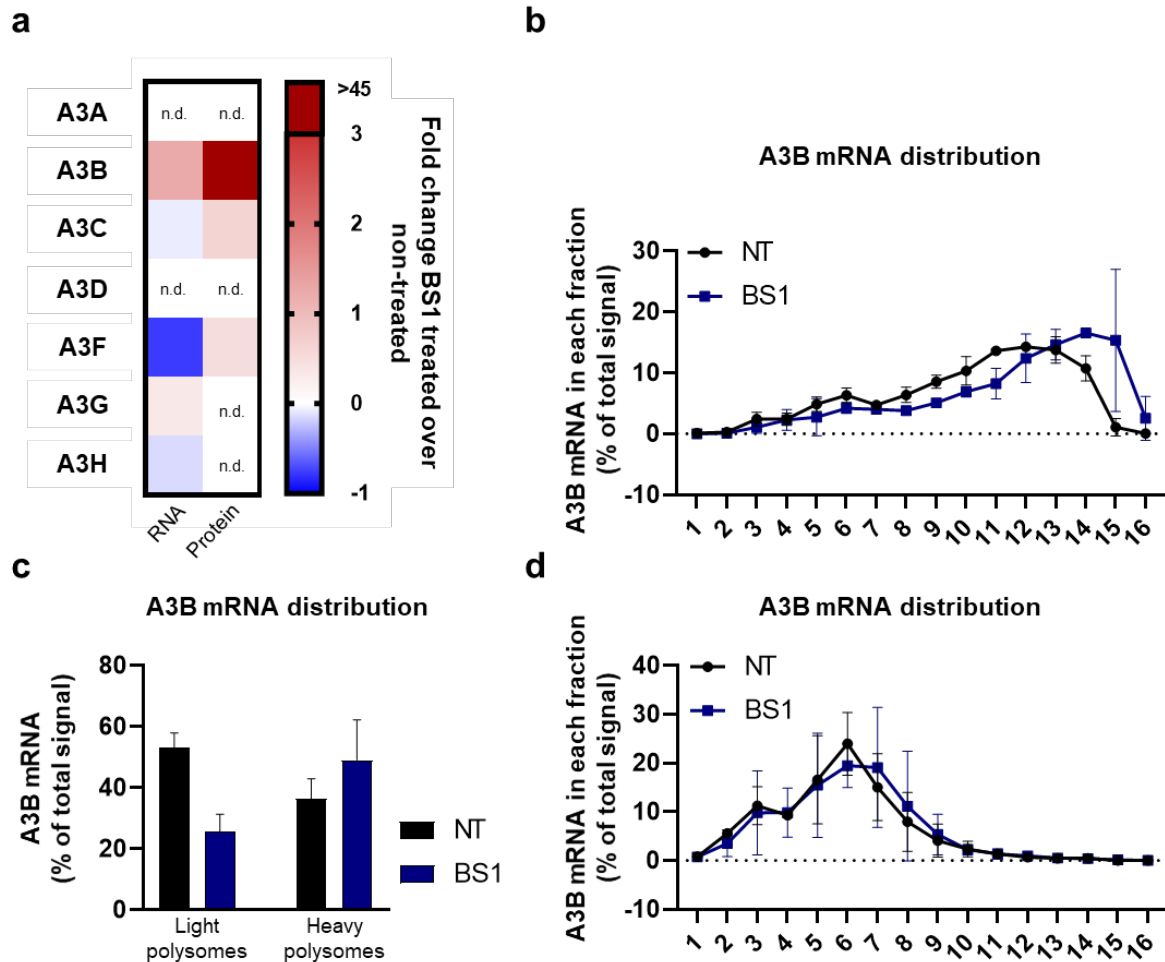
Figure 11: LTβR agonisation induces A3B expression and translation (adapted from Faure-Dupuy*, Riedl*, *et al.* [3])

Adapted from my written and experimental contribution in Faure-Dupuy*, Riedl*, *et al.* [3]: **(a)** Overnight treatment of dHepaRG was performed with BS1. RNA and proteins were extracted analysed via RNA sequencing and mass spectrometry, respectively. Relative fold change in BS1-treated over non-treated dHepaRG is shown. n.d. = not detected. **(b-d)** Six-day treatment of dHepaRG was performed with BS1. Then, cells were treated with cycloheximide, washed, scraped, and lysed, followed by **(b-c)** no treatment, or **(d)** EDTA treatment and isopycnic centrifugation. Polysome fractionation was performed afterwards with the lysates. Gradient traces (240nm) allowed for identification of polysomal fractions (as denser as 80S subunits and defined by a typical, oscillating, OD pattern). RT-qPCR was used for determination of the specific mRNA distribution in the sucrose gradient. **(b, d)** The distribution of A3B mRNA in different fractions as a percentage of total A3B mRNA is shown for **(b)** untreated and **(d)** EDTA-treated lysates. Data are based on the means of two independent experiments. **(c)** Distribution (in percent) of total A3B mRNA signal in the "light polysomes" fraction (i.e. fractions 8-12) and in the "heavy polysome" fraction (i.e. fractions 13-16) was analysed in non-treated and BS1-treated samples.

Luciferase plasmids and plasmids expressing the NF-κB transcription factors p50 (NF-κB1), p52 (NF-κB2), RelA, and RelB were transfected into HEK293T cells in different combinations and luciferase activity was measured 48 hours after plasmid transfection. Of note, p52-transfected cells displayed a higher luciferase activity, in combination with both RelA and RelB than p50-transfected cells on a wild-type promoter. Interestingly, I found that the kB1 site, if mutated, showed a severe reduction in the luciferase activity in the co-transfection with RelB

and p52, which otherwise gave the strongest signal of more than 8-fold increased over luciferase-only transfected cells (**FIGURE 12d**). In dHepaRG, ChIP experiments revealed that the promoter engagement of the A3B upstream region by RelB, p52, and p50: (I) occurred rapidly after treatment start and (II) remained fairly stable during constant treatment, contrary to RelA which showed no increase of promoter occupancy (**FIGURE 12e**). PolII, however, followed the dynamics of the previously mentioned transcription factors and bound to the A3B promoter as early as day one post treatment and onward under constant treatment (**FIGURE 12e**, right panel).

To functionally prove the involvement of NF-κB in the upregulation of A3B in non-transformed cells, I treated dHepaRG with two different IKKβ inhibitors, two distinct inhibitors TPCA-1 [282] and PHA-408 [283], as well knocked-down NIK. Expectedly, dHepaRG, either treated with inhibitor or depleted for NIK, showed impaired A3B upregulation under BS1 treatment, and effects of the combinatory treatment were stronger than with the pharmacological IKKβ inhibition or the NIK knock-down alone (**FIGURE 12f**). These results were recapitulated in dHepaRG cell lines knocked-out for different NF-κB signalling molecules (i.e. NIK, IKKβ, RelA, and/or RelB). Whereas BS1 treatment for three days upregulated A3B expression more than 6-fold in the control cell line, the effect of BS1 was severely decreased in the knock-out cell lines (**FIGURE 12g**) (adapted from Faure-Dupuy*, Riedl*, *et al.* [3]).

In summary, both NF-κB pathways (i.e. canonical and non-canonical) are involved in the transcriptional activation of A3B upon LTβR activation, notably through two NF-κB binding sites in A3B promoter region.

7.1.2 miRNA 138-5p is a post-transcriptional regulator of APOBEC3B mRNA

Adapted from my written and experimental contribution in Faure-Dupuy*, Riedl*, *et al.* [3]: To analyse expression dynamics of A3B in comparison to other NF-κB target genes, I did a time course of BS1 treated dHepaRG and analysed, besides A3B, A20 (also called TNFAIP3) and CXCL10 (also called IP10), two direct NF-κB target genes. Interestingly, while the NF-κB target genes peaked only eight hours after treatment start (A20: 6-fold and CXCL10: 25-fold increased) and then dropped again in expression levels (down to around 5-fold for both genes), A3B was not induced after eight hours and only slightly after 24 hours (**FIGURE 13a**). However, the expression level of A3B started to increase after 96 hours of treatment. Induction of NF-κB transcription factors as early as eight hours post treatment was confirmed by western blotting (**FIGURE 13b**). Furthermore, whereas protein levels of A3G were not changed by BS1 treatment, A3B protein was slightly accumulating after 24-72 hours and most prominent after 96 hours of treatment, in line with the mRNA expression data (**FIGURE 13b**). These data

highlight a peculiar "lag" phase of A3B expression from treatment start to around four days post-treatment.
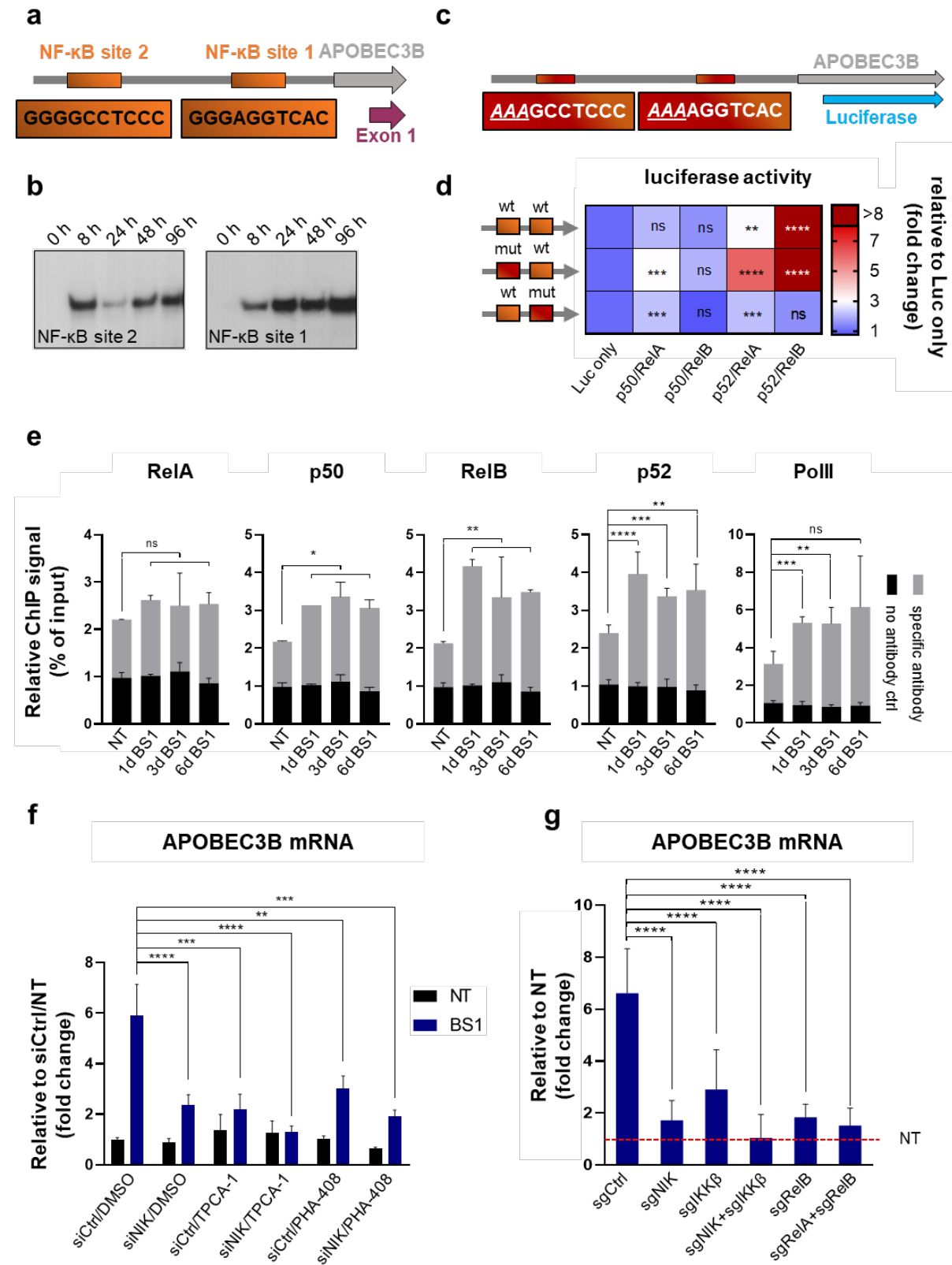
Figure 12: NF-κB engagement of the promoter induces A3B induction after LTβR agonisation (adapted from Faure-Dupuy*, Riedl*, *et al.* [3])

Adapted from my written and experimental contribution in Faure-Dupuy*, Riedl*, *et al.* [3]: **(a)** Schematic representation of the binding sites for NF-κB transcription factors in the promoter of A3B. **(b)** Nuclear lysates were extracted from dHepaRG treated for indicated times with BS1. Then, labelled probes containing the indicated NF-κB binding sites were incubated with the nuclear extracts and analysed by EMSA. **(c)** Schematic representation of the A3B upstream promoter region with the mutated NF-κB binding sites. **(d)** Luciferase constructs containing APOBEC3B promoter (-230, +18, distance to transcription start site) wild-type sequence or mutated for each NF-κB binding site were co-transfected into HEK293T cells together with NF-κB transcription factor expressing plasmids. 48 hours post-transfection, luciferase activity was measured. Heat map represents the mean of one experiment performed in triplicates. **(e)** dHepaRG were treated for different times with BS1. Binding of the indicated NF-κB transcription factors and polymerase II to the A3B promoter was analysed by ChIP, followed by qPCR. **(f)** Three-day treatment of dHepaRG was performed with BS1, TPCA-1 and/or PHA-408. One day before the treatment start, transfection of dHepaRG was carried out with control (siCtrl) or NIK-targeting (siNIK) siRNAs. RNAs were extracted and analysed by RT-qPCR. **(g)** Three-day treatment of knock-out dHepaRG lines for NIK (sgNIK), IKKβ (sgIKKβ), NIK and IKKβ (sgNIK+sgIKKβ), RelB (sgRelB), or RelA and RelB (sgRelA+sgRelB), as well as control dHepaRG (sgCtrl) was performed with BS1. mRNAs were extracted and analysed by RT-qPCR. Bars represent the mean +/- SD of **(e)** four, **(f)** two or **(g)** three independent experiments. Data were submitted to **(d-g)** one-way ANOVA. *: $p < 0.05$; **: $p < 0.01$; ***: $p < 0.001$; ****: $p < 0.001$; ns: not significant. NT: non-treated

The observed expression dynamics, which is very different to "classical" NF-κB target genes, could be explained by the time-dependent down-regulation of a repressor of A3B. I previously showed that over six days of treatment, the promoter occupancy of A3B is fairly stable (**FIGURE 12e**), both when it comes to NF-κB transcription factors and PolII. Therefore, I expected the repressor of A3B to rather act post-transcriptionally and influence the mRNA turnover as long as it is present. Micro RNAs (miRNAs) have been described to be potent mRNA destabilisers, involved in a multitude of biological processes, e.g. in regulation of immunity and response to immune stimulatory cues [284], and thus are tightly regulated themselves. I hypothesised that in the case of A3B, a rapid and efficient upregulation could be detrimental to the genome because of the mutagenic activity of the enzyme, as it was shown that A3B can be a source of somatic mutations in cancer [285]. Only in the case of a prolonged activation signal, the increased A3B levels can be beneficial (e.g. during a viral infection), and therefore, the repressor, which keeps A3B in check under homeostasis and during accidental short-term activation, is downregulated. Subsequently, A3B can be potently induced and exert its antiviral activity (schematic representation shown in **FIGURE 13c**).

To test the hypothesis, I used a combined approach of *in silico* target prediction tools (Targetfinder V5.1 [286]), RT-qPCR and, in collaboration with Kristian Unger and the DKFZ Genomics and Proteomics Core Facility, small RNA sequencing. In dHepaRG treated for two days (i.e. during the lag phase) and four days (i.e. after the lag phase) with BS1, I found three different clusters among the 50 most dysregulated miRNAs (**FIGURE 13d**). Cluster I, in which I expected our miRNA of interest, contained miRNAs that are upregulated after two days of BS1 treatment and downregulated after four days of treatment. Cluster II contained miRNAs that are downregulated after two days and upregulated after four days of BS1 treatment.

Cluster III contains miRNAs that are generally downregulated by the treatment (**FIGURE 13d**). Among the miRNAs of cluster I, I only found the hsa-miR-138-5p to have a strong predicted *in silico* binding to the 3'-UTR of A3B (**FIGURE 13e**). Hsa-miR-138-5p was repressed by approximatively 70% upon four days of BS1 treatment, whereas no change of miRNA levels were observed after two days (**FIGURE 13f**). To functionally show that hsa-miR-138-5p can repress UTRs containing the predicted binding site, I in collaboration with Emmanuel Dejardin and Nicolas Gillet used the UTRs of A3A, which contains no binding site for the miRNA, or A3B and A3G, which both contain binding sites for the miRNA, fused to a luciferase ORF. Furthermore, mutations were introduced into those UTRs to either enable miRNA binding for A3A or prevent miRNA binding for A3B and A3G (**FIGURE 14a**). These plasmids were transfected into HEK293T cells, together with expression plasmids for the hsa-miR-138-5p hairpin or a control non-targeting miRNA. Whereas hsa-miR-138-5p expression did not reduce luciferase activity in any UTR-fusion where there was no predicted binding (i.e. wild type A3A, mutated A3B, or mutated A3G), luciferase activity was 20% reduced for the A3A 3'-UTR fusion with the mutated site and the A3B 3'-UTR fusion with the wild type site and 50% for the A3G 3'-UTR fusion with the wild type site (**FIGURE 14b**) (adapted from Faure-Dupuy*, Riedl*, *et al.* [3]).

These results confirm that there is a post-transcriptional regulation of the A3B mRNA by hsa-miR-138-5p, and that also A3G and potentially mutated A3A can be regulated by this miRNA.

7.1.3 Interfering with APOBEC3B upregulation prevents antiviral effects of LTβR activation

Since others and my research group have shown that the activation of A3B by LTβR signalling is important to exert the antiviral effects on HBV [48, 287]], I aimed to investigate the effects of impaired A3B induction on cccDNA levels.

Adapted from my written and experimental contribution in Faure-Dupuy*, Riedl*, *et al.* [3]: Different NF-κB knock-out cell lines, namely NIK-, IKKβ-, and a NIK-IKKβ double knock-out cell line were generated, and were infected with HBV and treated for 12 days with BS1. Although in control cells, a 75% reduction in cccDNA level was observed, none of the knock-out cell lines was able to clear the cccDNA to significant levels (**FIGURE 15a**). Similarly, BS1-mediated decrease of HBV secreted DNA was reduced in the knock-out cells compared to control cells (**FIGURE 15b**). Of note, the different knock-outs had no effect on the efficiency of tenofovir treatment on both cccDNA (i.e. no effect) and HBV secreted DNA (i.e. strong decrease). As expected, A3B upregulation by BS1 treatment was severely impaired in knock-out cells both on mRNA (**FIGURE 15c**) and protein level (**FIGURE 15d**).
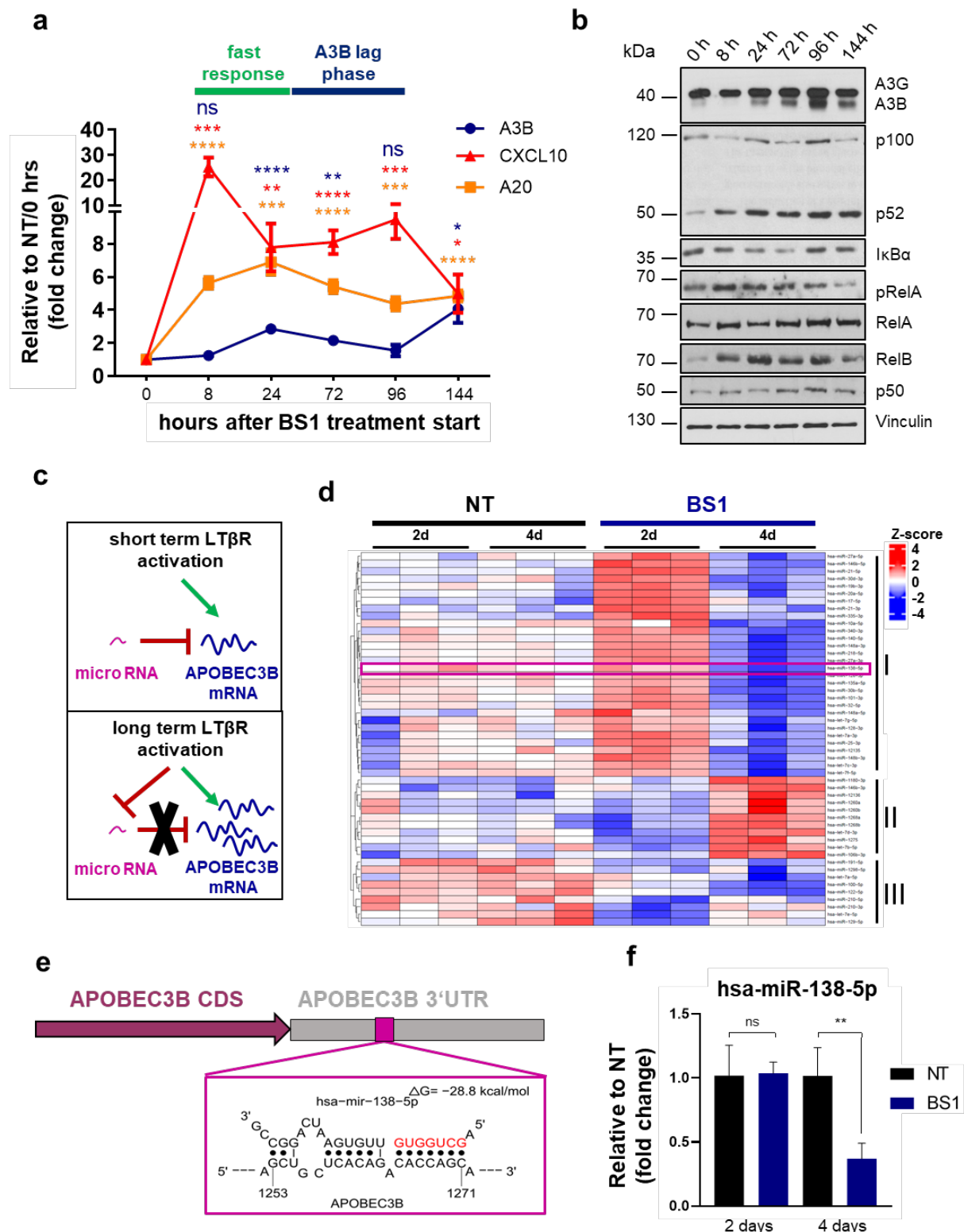
Figure 13: miRNA-138-5p is a post-transcriptional repressor of A3B (adapted from Faure-Dupuy*, Riedl*, _et al._ [3])

Adapted from my written and experimental contribution in Faure-Dupuy*, Riedl*, _et al._ [3]: **(a-b)** dHepaRG were treated for different times with BS1. **(a)** RNAs were extracted and analysed by RT-qPCR. **(b)** Proteins were extracted and analysed by immunoblotting. **(c)** Schematic representation of

the working hypothesis. Further explanation is given in the text. **(d)** Two- or four-day treatment of dHepaRG was performed with BS1. RNAs were extracted and submitted to small RNA were sequencing. Top 50 significantly dysregulated miRNAs of a combined sequencing and RT-qPCR approach were unbiased clustered and plotted. Cluster I represents highly expressed miRNAs at day two, which were lowly expressed at day four (i.e. miRNAs of interest); Cluster II represents lowly expressed miRNAs at day two, which were highly expressed at day four; Cluster III represents lowly expressed miRNAs at day two, which were also lowly expressed after day four. **(e)** Schematic representation of the miRNA-138-5p binding site on the A3B 3'-UTR. **(f)** Two or four day treatment of dHepaRG was performed with BS1. RNAs were extracted and analysed by RT-qPCR. **(a)** Points, **(f)** respectively bars, represent the mean +/- SD of **(a)** three experiments or **(f)** one experiment performed in triplicates. Data were submitted to **(a, f)** unpaired student's t-test. *: $p < 0.05$; **: $p < 0.01$; ***: $p < 0.001$; ****: $p < 0.001$; ns: not significant. NT: non-treated

Interestingly, the downregulation of hsa-miR-138-5p upon BS1 treatment, that was observed previously (**FIGURE 13f**) was recapitulated in control cells, but not observed in cells knocked-out for NF-κB upstream kinases, suggesting that hsa-miR-138-5p repression, after BS1 treatment, is regulated by NF-κB (**FIGURE 15e**).

To functionally show that hsa-miR-138-5p is involved in the control of A3B mRNA levels and in turn capable to prevent cccDNA degradation, I transfected dHepaRG with miRNA-mimics or control-mimics. Indeed, A3B expression levels were reduced in miRNA-mimics transfected cells, both on steady-state levels and after induction with BS1. Importantly, whereas BS1 treatment induced A3B expression around 8-fold in control-mimics-transfected cells, in miR-138-5p-mimic-transfected cells the induction was only around 2-fold (**FIGURE 15f**).
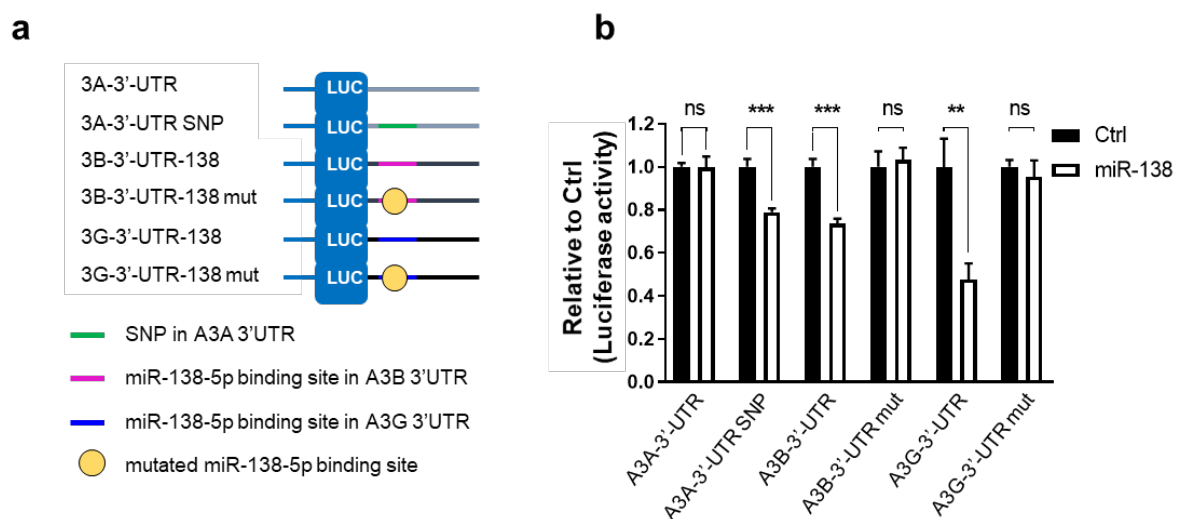
Figure 14: The hsa-miR-138-5p binding site in the A3B and the A3G 3'-UTR is functional (adapted from Faure-Dupuy*, Riedl*, *et al.* [3])

(a-b) Luciferase-3'-UTR fusion constructs containing the wild-type or mutated A3A, A3B and A3G 3'-UTRs were co-transfected into HEK293T cells with and either control miR-expressing plasmids (Ctrl) or miR-138-5p-expressing plasmids (miR-138). **(a)** Schematic representations of luciferase-3'-UTR fusions used. **(b)** 48 hours post-transfection, luciferase activity was measured. Bars represent the mean +/- SD of one experiment performed in triplicates. Data were submitted to unpaired student's t-test. **: $p < 0.01$; ***: $p < 0.001$; ns: not significant.
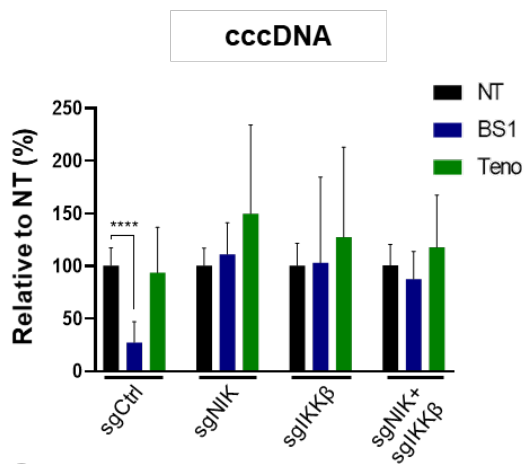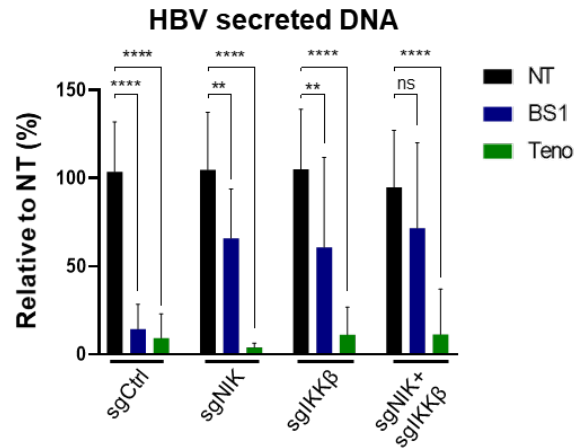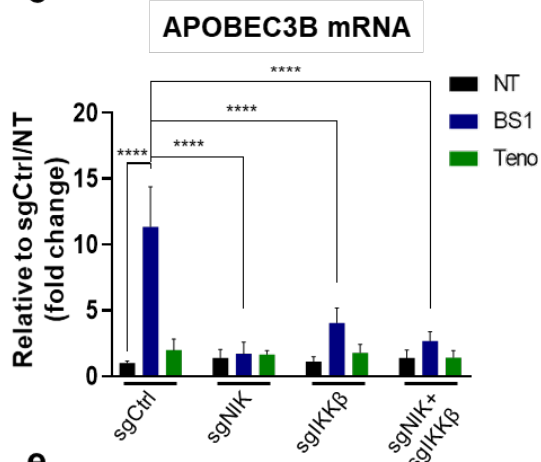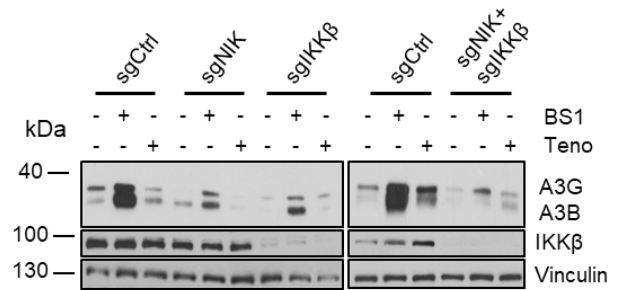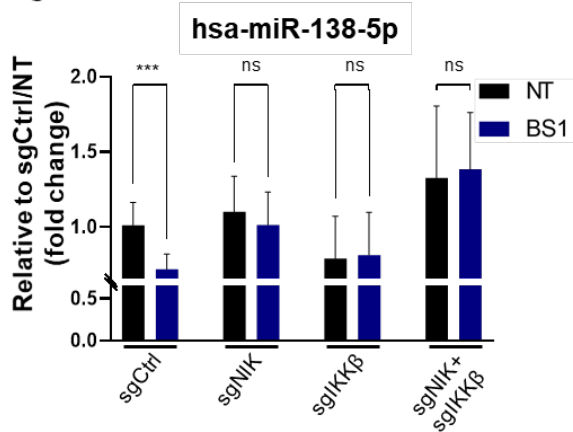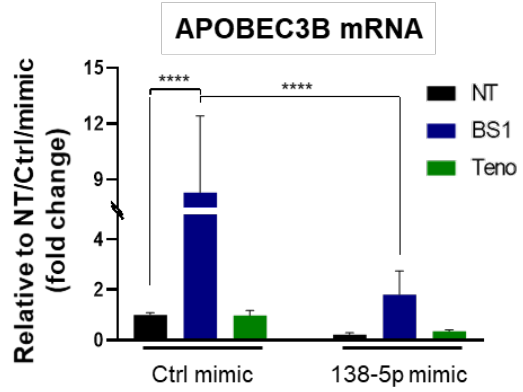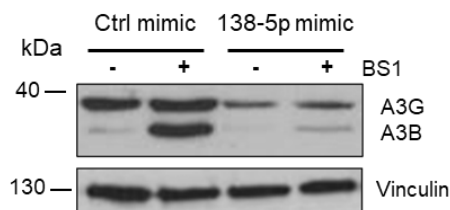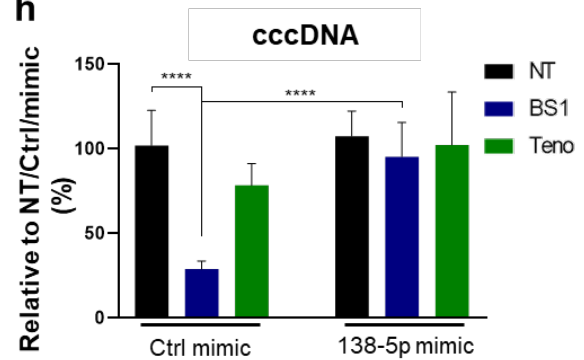
Figure 15: Blocking A3B upregulation by disruption of NF-κB signalling or mi-RNA 138-5p prevent the antiviral effect (adapted from Faure-Dupuy*, Riedl*, *et al.* [3])

Adapted from my written and experimental contribution in Faure-Dupuy*, Riedl*, *et al.* [3]: **(a-e)** dHepaRG, knocked out for NIK (sgNIK), IKKβ (sgIKKβ), or NIK and IKKβ (sgNIK+sgIKKβ), as well as control dHepaRG (sgCtrl) were infected with HBV. Twelve-day treatment of dHepaRG was performed with BS1 or tenofovir (Teno), starting seven days post infection (d.p.i). **(a)** DNA, **(c, e)** RNAs and **(d)** proteins were extracted and analysed by qPCR RT-qPCR or immunoblotting, respectively. **(b)** Secreted HBV DNA levels were determined directly from supernatant by qPCR. **(f-h)** dHepaRG were infected with HBV. Six-day treatment of dHepaRG was performed with BS1 or tenofovir (Teno) starting 13 d.p.i. Four days and one the day before treatment start, cells were transfected with miR-138-5p or control mimics. Then, **(f)** RNAs, **(g)** proteins and **(h)** DNA were isolated and analysed by RT-qPCR, immunoblotting and qPCR, respectively. Bars represent the mean +/- SD of **(a-c, e)** three or **(f, h)** six independent experiments. Data were submitted to **(a-c, e-f, h)** one-way ANOVA. *: $p < 0.05$; **: $p < 0.01$; ***: $p < 0.001$; ****: $p < 0.001$; ns: not significant. NT: non-treated

Furthermore, A3B protein levels were strongly reduced by the transfection of miR-138-5p-mimics (**FIGURE 15g**). Interestingly, also A3G protein levels were reduced by the mimics, strongly suggesting that the predicted hsa-miR-138-5p binding site in the A3G 3'-UTR is functional, as the one in the A3B 3'-UTR (**FIGURE 15g**).Similarly to the NF-κB knock-outs, the mimicked overexpression of the hsa-miR-138-5p inhibited the anti-cccDNA effects of the LTβR activation (**FIGURE 15h**) (adapted from Faure-Dupuy*, Riedl*, *et al.* [3]). Altogether, blocking the efficient upregulation of A3B by (I) interfering with NF-κB signalling or (II) aberrantly expressing the hsa-miR-138-5p, prevents cccDNA degradation.

7.1.4 Hepatitis B virus can suppress APOBEC3B induction via epigenetic relgulation

Adapted from my written and experimental contribution in Faure-Dupuy*, Riedl*, *et al.* [3]: Surprisingly, I in collaboration with Julie Lucifora and David Durantel found that HBV infection itself could block efficient A3B upregulation. Cells were infected with HBV or were left non-infected (mock) and subsequently treated with BS1 for six consecutive days, starting one day post infection. qPCR analysis revealed that A3B expression levels were 50% and 75% reduced in HepaRG (**FIGURE 16a**) and PHH (**FIGURE 16b**), respectively, compared to non-infected cells. As previously shown (**FIGURE 12f**), hsa-miR-138-5p expression levels were reduced by BS1 treatment, but were not significantly higher in cells additionally infected with HBV compared to mock (**FIGURE 16c-d**), which suggests a different mechanism by which HBV counteracts efficient A3B upregulation. In fact, I show that the activating epigenetic mark H3K4Me3 (tri-methylation of histone H3 at the position lysine 4 [288, 289]) is increased in non-infected BS1-treated cells, but not in HBV-infected BS1-treated cells (**FIGURE 16e**). Importantly, neither in non-infected nor in HBV-infected cells BS1 treatment induced cell death (**FIGURE 16f**) (adapted from Faure-Dupuy*, Riedl*, *et al.* [3]).
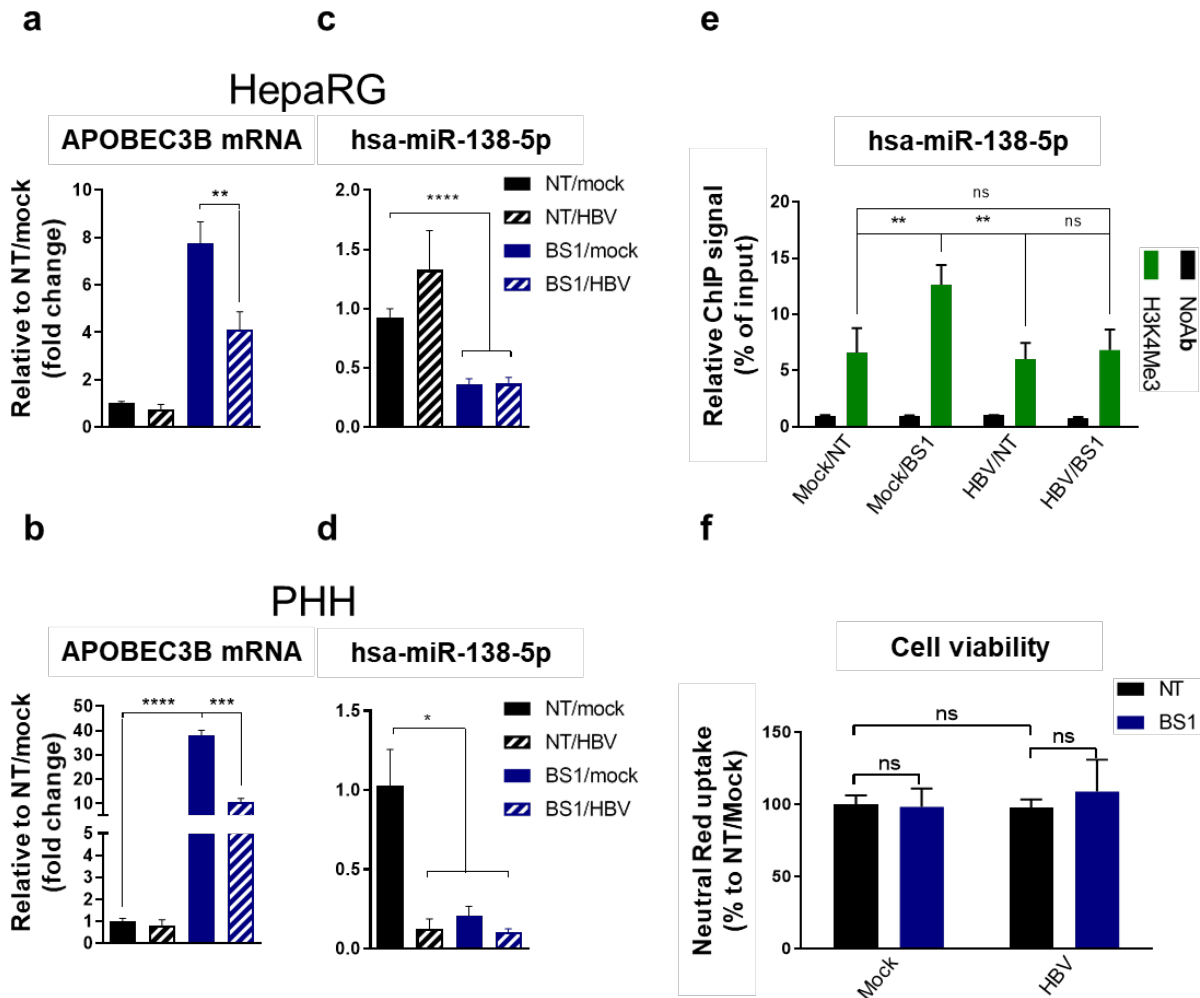
Figure 16: HBV counteracts A3B induction by epigenetic modulation of the A3B promoter (adapted from Faure-Dupuy*, Riedl*, et al. [3])

Adapted from my written and experimental contribution in Faure-Dupuy*, Riedl*, et al. [3]: Six-day treatment of **(a, c, e)** dHepaRG or **(b, d)** PHH was performed with BS1, starting one d.p.i. with HBV. Non-infected (mock) cells were treated in the same fashion. **(a-d)** RNAs were extracted and analysed by RT-qPCR. **(e)** Association of the H3K4Me3 mark on the A3B promoter was analysed by ChIP followed by qPCR. **(f)** dHepaRG were infected with HBV. Twelve-day treatment of dHepaRG was performed with BS1, starting ten d.p.i. Non-infected cells were treated in the same fashion. Viability was determined by neutral Red uptake. Bars represents the mean +/- SD of **(a, c, e-f)** three or **(b, d)** one independent experiments performed in triplicates. Data were submitted to **(a-e)** one-way ANOVA. *: p < 0.05; **: p < 0.01; ***: p < 0.001; ****: p < 0.001; ns: not significant. NT: non-treated

7.1.5 BS1 treatment does not induce detectable somatic mutational load

As previously mentioned, A3B, as a cytidine deaminase, potentially can exert its mutational activity also towards the host genome, which can lead to somatic mutations and ultimately lead to cancer development [285].

Adapted from my written and experimental contribution in Faure-Dupuy*, Riedl*, et al. [3]: To assess if treating patients with LTβR agonists to eliminate HBV could be a therapeutic option, effect of A3B induction on the genomic DNA needed to be assessed. To this end, together with the company CeGaT in Tübingen, I analysed in dHepaRG if somatic mutations on pre-selected genomic loci associated with cancer development are increased in number by BS1 treatment. In an ultra-deep panel sequencing approach, 766 cancer related-genes were analysed for point mutations with an average sequencing depth of over 1,000 x coverage. Interestingly, although strong anti-cccDNA effects were observed after treatment of 12 days with BS1 (**FIGURE 15a**), no detrimental effects on the genome were observed. 2,868 SNPs, compared to the human reference genome hg19, were detected in total; but only 12 were shared exclusively by non-treated cells and 13 were shared exclusively between BS1 treated cells above the threshold level. 2,404 of all detected SNPs were shared between groups, representing the SNP profile of HepaRG against the reference genome (**FIGURE 17a**). When closer analysing the occurrence of SNPs in all possible tri-nucleotide contexts, it became obvious that the frequency of SNPs was not significantly different between the BS1 treated and the non-treated groups with median frequencies of 0.344% and 0.319% (p=0.299) (**FIGURE 17b**) (adapted from Faure-Dupuy*, Riedl*, et al. [3]).

Taken together, my data indicate that the time-restricted administration of the LTβR agonist BS1 and subsequent upregulation of A3B, while providing a strong antiviral effect, does not lead to detectable detrimental effects on the human genome.
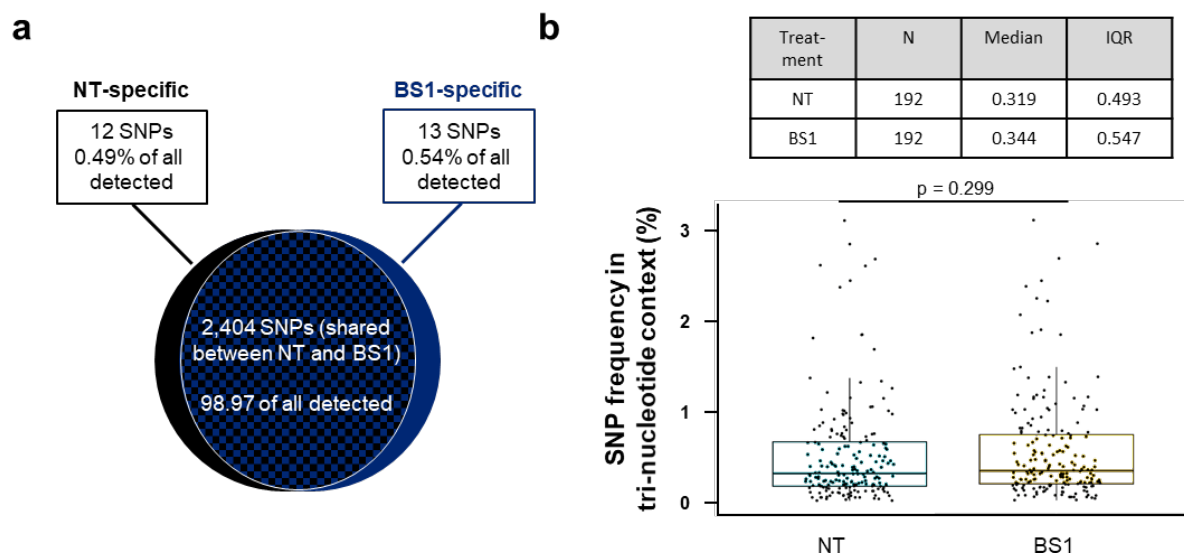
Figure 17: LTβR agonisation does not lead to somatic mutations in cancer related genes (adapted from Faure-Dupuy*, Riedl*, et al. [3])
Adapted from my written and experimental contribution in Faure-Dupuy*, Riedl*, et al. [3]: **(a-b)** dHepaRG were infected with HBV. Twelve-day treatment of dHepaRG was performed with BS1, starting ten d.p.i. DNA was extracted and a panel sequencing of a panel containing 766 genes (CeGaT CancerPrecision panel) was carried out. 2,868 SNVs (single nucleotide variants) were detected in total. **(a)** Detected SNVs were filtered to identify SNVs occurring in all samples with a number of alleles (novel

allele frequency, NAF) > 5% and a coverage > 30 (2,404), only in all treated samples (13 SNVs) and only in all 'not-treated' samples (Twelve SNVs). 439 SNVs were not specific to either of the two groups. Close evaluation of the 13 genes containing SNVs in the BS1-treated group and the twelve genes containing SNVs in the non-treated group revealed NAFs close to the cut-off of 5% but are detected in the other samples as well. **(b)** SNVs in every possible trinucleotide context were analysed for their frequency. Comparison of the frequency of SNVs between non-treated and BS1-treated samples. Median frequency and the interquartile range (IQR) of SNVs are presented in the table. In the box plot, every data point represents a SNV in a trinucleotide context. Data were submitted to Wilcoxon-signed Rank Sum test. NT: non-treated

7.1.6 APOBEC3B can exert its antiviral activity independently of transcriptionally active cccDNA and a full replication cycle

Although the LTβR activation, followed by A3B upregulation, can efficiently reduce cccDNA levels *in vitro*, some limitations for the use as an antiviral strategy in a clinical context are to be considered. Firstly, during late phases of a chronic HBV infection (i.e. during occult infection), cccDNA molecules might become silenced and therefore display tightly packed chromatin state [48, 290]. Given that A3B was suggested in literature to only act on ssDNA, as shown for other A3 family members [291], the remaining cccDNA molecules that were not targeted by A3B could then reactivate the infection. Secondly, it was reported in the literature, that the A3B deaminating activity only acts on the ssDNA during reverse transcription [292, 293]. A3B would therefore not be able to act on nuclear cccDNA, contradictory to what I have previously shown.

Adapted from my written and experimental contribution in Faure-Dupuy*, Riedl*, *et al.* [3]: To address, if LTβR activation can overcome those potential limitations, I used two different models of HBV. The first model, generously provided by Julie Lucifora and David Durantel, lacks a transcriptionally active cccDNA (HBV ΔX, which does not express a functional X protein for transactivation), which can infect cells but will not produce mRNAs [48, 290]. The second model I used is called rHBV and was designed and produced by Jochen Wettengel and Ulrike Protzer. It is a recombinant HBV that had large parts of the HBsAg and polymerase ORF disrupted to insert a TTR promoter driven expression of RFP (red fluorescent protein). This virus will infect dHepaRG and establish a cccDNA, but cannot complete the whole life cycle, since the pre-genomic RNA (pgRNA) would not be reverse transcribed due to the lack of the viral polymerase gene.

To evaluate the effects of LTβR activation on transcriptionally silent cccDNA, dHepaRG were infected with HBV ΔX or wild-type HBV, and treated with BS1 for 12 days. Interestingly, the cccDNA levels of both viruses were reduced significantly to similar extent by more than 60%, as measured by qPCR and Southern Blot analysis (**FIGURE 18a and 18b**, respectively).
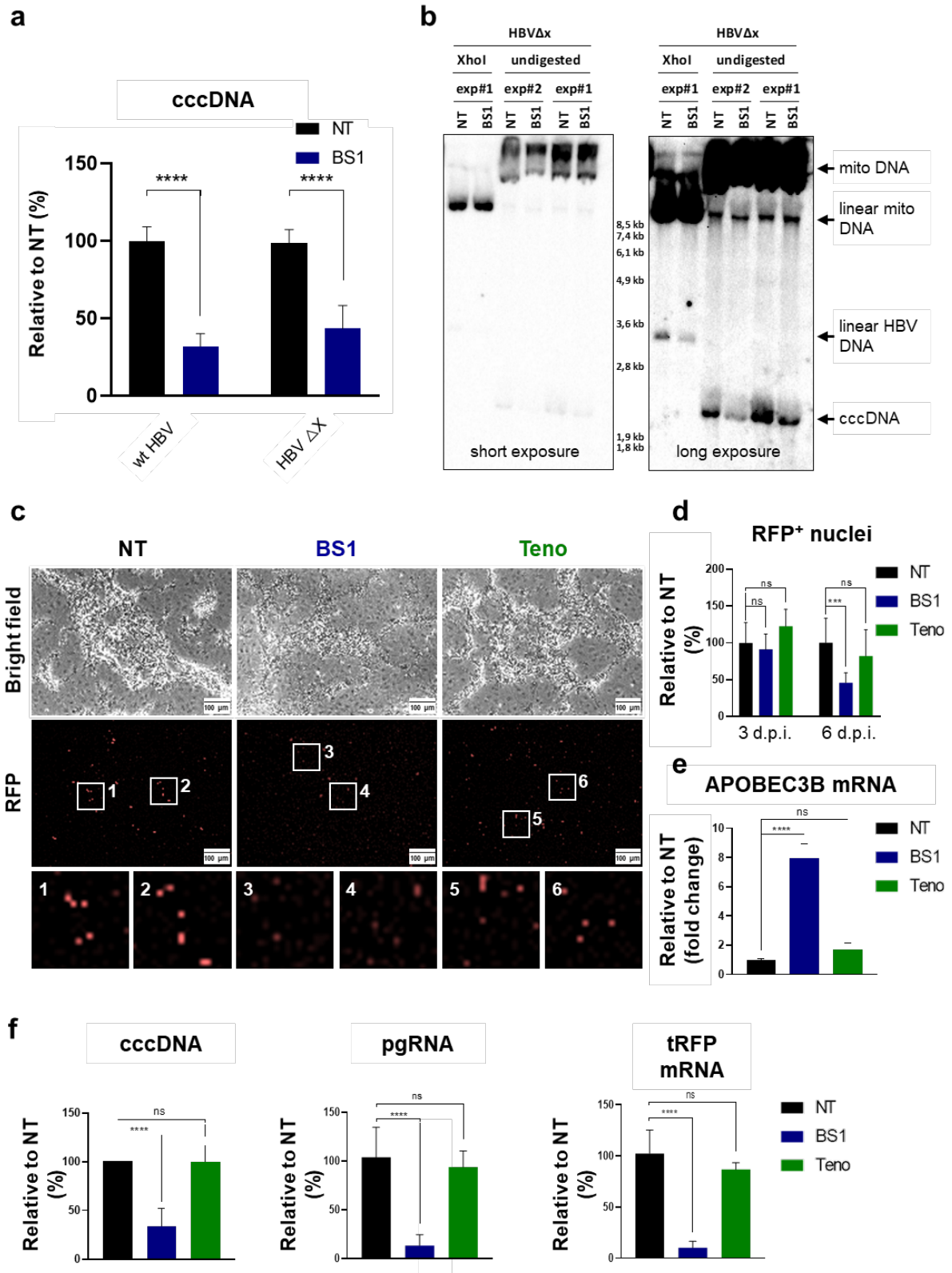
Figure 18: APOBEC3B effect on cccDNA is independent of transcription or a full replication cycle (Adapted from Faure-Dupuy*, Riedl*, et al. [3])

Adapted from my written and experimental contribution in Faure-Dupuy*, Riedl*, et al. [3]: **(a-b)** dHepaRG were infected with wild-type (wt) HBV or HBx-deficient (ΔX) HBV. Ten-day treatment of dHepaRG was performed with BS1, starting seven d.p.i. DNA was extracted and analysed by **(a)** qPCR and **(b)** Southern blot. **(c-f)** dHepaRG were infected with recombinant tRFP-rHBV. Nine-day treatment

of dHepaRG was performed with BS or tenofovir (Teno), starting seven d.p.i. **(c)** Representative bright field and fluorescent images of the different treatments at six d.p.i. **(d)** Quantification of tRFP positive nuclei per view field (VF). **(e-f)** RNAs and DNA were extracted and quantified by RT-qPCR and qPCR, respectively. Bars represent the mean +/- SD of **(a)** four or **(e-f)** two independent experiments performed in triplicates. Data were submitted to **(a)** unpaired student's t-test or **(e-f)** one-way ANOVA. ***: $p < 0.001$; ****: $p < 0.001$; ns: not significant. NT: non-treated

To address whether A3B was only acting on ssDNA during reverse transcription, as suggested by others [294, 295], dHepaRG were infected with rHBV and treated with BS1 or with tenofovir as control. Infected cells were positive for red fluorescence (**FIGURE 18c**) and BS1 treatment, but not tenofovir treatment reduced the amount of positive nuclei after 6 days of treatment by around 50% (**FIGURE 17d**). A3B expression was upregulated in BS1 treated cells (**FIGURE 18e**) and cccDNA levels were significantly reduced, as well as the pre-genomic RNA and the RFP mRNA (**Figure 18f**), indicative of a strong antiviral effect of BS1 treatment (adapted from Faure-Dupuy*, Riedl*, *et al.* [3]).

Taken together, these results strongly suggest that LTβR activation can even efficiently target transcriptionally inactive cccDNA. Furthermore, I show that A3B can directly act on the cccDNA. Moreover, the A3B-induced cccDNA reduction is independent of (I) the whole life cycle of the virus (i.e. not due to prevention of capsid recycling in the cytoplasm) and (II) the occurrence of ssDNA during reverse transcription. This observation is contradictory to reports in literature, stating that A3B mainly works on the relaxed circular DNA (rcDNA) during reverse transcription [292]. Importantly, by ruling out these two possible limitations to the use of LTβR activation as a possible treatment option against HBV, I showed that the treatment could be efficient for patients at different stages of HBV pathogenesis.

7.2 Aim 2: Hypoxia reduces antiviral effects of LTβR activation and offers a niche for HBV to avoid immune responses

7.2.1 "HIF1α high" areas in patients offer a reservoir for HBV in immune active patients

Hypoxia is an important microenvironmental cue, that was described to both positively and negatively influence immune responses, depending on cells and mode of action of the immune responses involved [296]. Our research group, our collaborators and others have shown that the activation of the immune system or of immune responses by receptor activation can efficiently restrict HBV [279, 297, 298]. I wanted to understand the effect of hypoxia and HIF1α stabilisation, an early step in hypoxia responses, on LTβR activation and if hypoxia might be involved in HBV persistence by reducing antiviral immune responses in chronically infected patients.
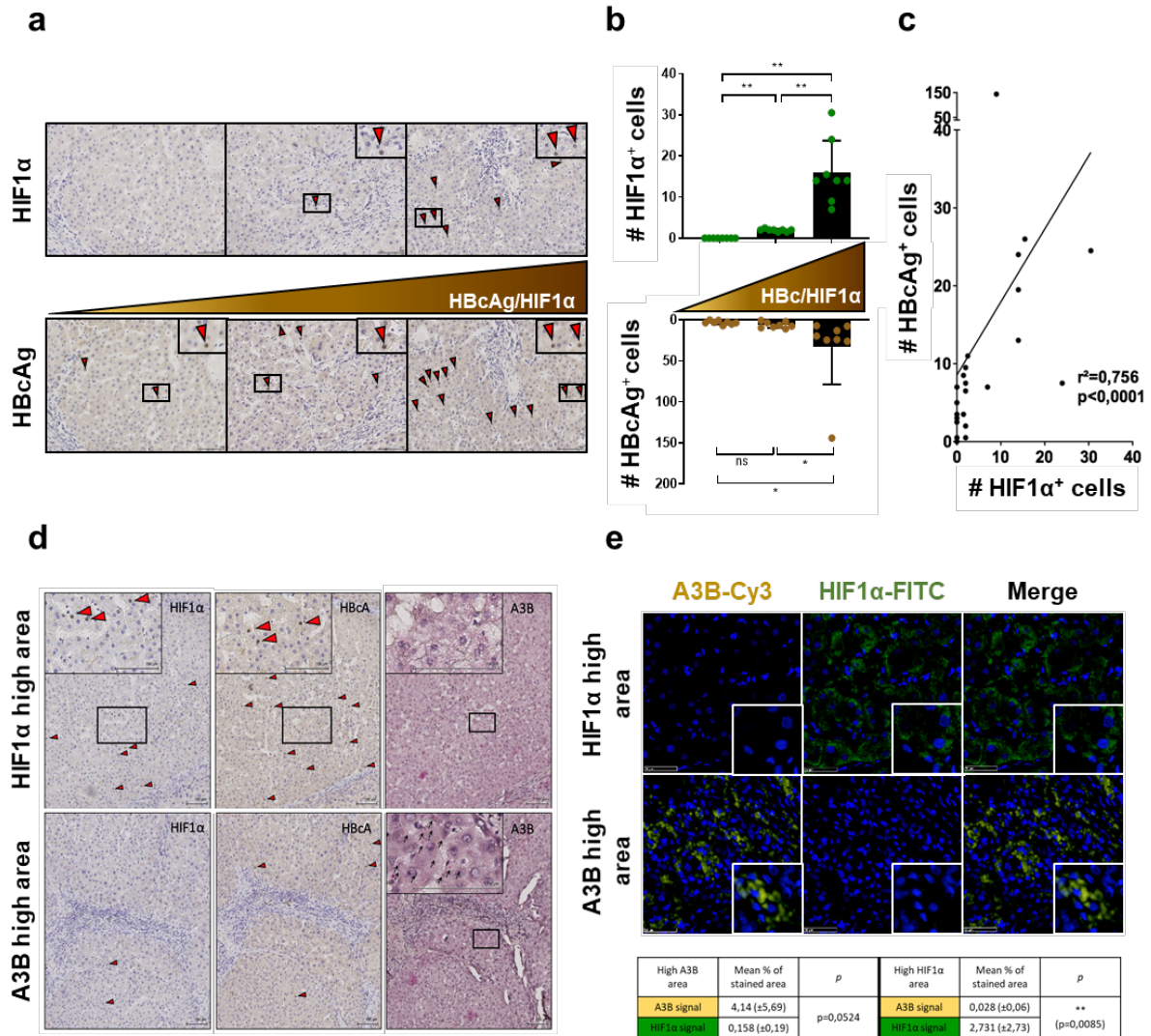
Figure 19: HIF1α stabilisation allows HBV persistence in vivo (adapted from Riedl*, Faure-Dupuy*, et al. [4])

Adapted from my written and experimental contribution in Riedl*, Faure-Dupuy*, et al. [4]: **(a-e)** Formalin fixed, paraffin embedded liver tissues of chronic HBV patients were consecutively sectioned and stained for HIF1α and HBcAg protein by immunohistochemistry (IHC), or APOBEC3B mRNA by in situ hybridisation (ISH); or co-stained for HIF1α protein and APOBEC3B mRNA in a double fluorescent IHC/ISH. (a-c) Three different zones were distinguished, based on HIF1α staining: (i) no HIF1α positive nuclei per view field (VF); (ii) 1-5 HIF1α positive nuclei per VF; (iii) >5 HIF1α positive cells per VF. Arrowheads show positive nuclei. **(a)** Representative images of the three zones of HIF1α (upper panels) and HBcAg (lower panels) from the same specimen. **(b)** Quantification of HIF1α and HBcAg positive nuclei in the 3 different zones. Every point represents the mean of two VF and the bars show the mean +/- SD of eight patients. **(c)** Pearson's correlation analysis was performed for HIF1α- and HBcAg-positivity per VF. **(d)** Representative pictures of patients stained for HIF1α and HBcAg protein and A3B mRNA. Upper three pictures show a representative "HIF1α high" area, lower three pictures show "A3B high" area of the same patient sample. **(e)** Representative images of one slide stained for both HIF1α protein and A3B mRNA. Upper three pictures show a representative "HIF1α high" area, lower three pictures show a representative "A3B high" area of the same patient sample. Percentage of stained area for A3B and HIF1α was quantified and is presented in the table +/- SD of nine different patients. Data were submitted to **(b, e)** one-way ANOVA. *: $p < 0.05$; **: $p < 0.01$; ns: not significant.

(Adapted from my written and experimental contribution in Riedl*, Faure-Dupuy*, et al. [4]):

Therefore, consecutive liver sections of patients that underwent liver resection and suffered

from end stage CHB ("HBeAg-positive chronic hepatitis B", also considered as the immune active phase of the infection) were obtained from the DZIF partner site in Heidelberg/Institute of Pathology of the Medical University Heidelberg. These sections were stained for HIF1α and the HBcAg. I found that in corresponding areas of the two consecutive sections, high numbers of HIF1α positive cells appeared in conjunction with high numbers of HBcAg positive cells and, reciprocally, that decreased numbers of HIF1α positive cells came along with decreased numbers of HBcAg positive cells (**FIGURE 19a and 19b**). The numbers of positive cells for HIF1α and HBcAg in the corresponding areas correlated significantly (**FIGURE 19c**).

I showed that LTβR activation leads to A3B upregulation, which can drive cccDNA degradation, and my research group previously published that lymphotoxin alpha and beta (LTα/β) are upregulated in CHB patients [299]. It could be expected that in patients, LTβR activation is happening, inducing antiviral activity in activated hepatocytes, leading to eradication of the virus. However, CHB patients do not manage to clear the infection. I assessed if the correlation of HIF1α and HBcAg in patients within "HIF1α/HBcAg high areas" went together with a decreased induction of antiviral mediators, in this case A3B. In fact, staining of consecutive cuts for HBcAg, HIF1α, and A3B mRNA suggested that A3B is "depleted" from the areas that stain strongly for HIF1α and HBcAg (**FIGURE 19d**). To further evaluate the interplay of HIF1α and A3B expression, sections were co-stained with a probe against A3B mRNA for fluorescence *in situ* hybridisation and with an antibody against HIF1α for immunofluorescence. I found that "HIF1α high" areas were depleted of A3B mRNA and *vice versa*, that areas enriched for A3B mRNA showed low HIF1α signal (**FIGURE 19e**) (adapted from Riedl*, Faure-Dupuy*, et al. [4]).

Taken together, these data highlight that in patients, efficient induction of A3B is only happening in liver areas low for HIF1α, even though these livers are inflamed. This process allows viral persistence and potentially offer HBV a reservoir in which it is protected from efficient eradication.

7.2.2 Stabilisation of HIF1α impairs antiviral effects of LTβR activation

(Adapted from my written and experimental contribution in Riedl*, Faure-Dupuy*, et al. [4]): To confirm the observations made with patients samples and test my hypothesis that HIF1α stabilisation protects HBV from eradication by A3B, I deployed three different methods to stabilise HIF1α *in vitro*: (I) hypoxia (1% O_2), which is the canonical stabiliser and inducer of HIF1α, (II) DMOG, and (III) FG-4592. The latter two are small molecules inhibiting the proline hydroxylases PHD1-3 and therefore block HIF1α degradation even in the presence of oxygen. HBV infected dHepaRG were treated with BS1 in the presence or absence of any of the HIF1α stabilising conditions. Under conditions not stabilising HIF1α (normoxia, NO, 20% O_2; or

DMSO) A3B expression was upregulated by BS1 (**FIGURE 20a, c, e**; siCtrl/BS1) and cccDNA degradation was observed (**FIGURE 20b, d, f**; siCtrl/BS1). Interestingly, under HIF1α stabilising conditions (hypoxia, HO, 1% O_2; or DMOG and FG-4592), A3B induction was strongly impaired (**FIGURE 20a, c, e**; siCtrl/BS1), as well as the anti-cccDNA effect of the treatment (**FIGURE 20b, d, f**; siCtrl/BS1). Surprisingly, the knock-down of HIF1α by siRNA transfection was able to rescue A3B induction by BS1 under HIF1α stabilising conditions (**FIGURE 20a, c, e**; siHIF1α/BS1) and restored anti-cccDNA effects (**FIGURE 20b, d, f**; siHIF1α/BS1). Together with Julie Lucifora, I confirmed BS1-induced cccDNA reduction and inhibition thereof by DMOG treatment by Southern Blot analysis (**FIGURE 20g**).

Of note, HIF1α knock-down under normoxia was sufficient to slightly increase A3B levels under steady state levels and this effect was even more pronounced under BS1 treatment (**FIGURE 20a**, siHIF1α/BS1). Immuno-precipitation experiments showed that BS1 treatment under normoxia induced the production of HIF1α, which can be the explanation that the induction of A3B is further improved after HIF1α knock-down, considering that HIF1α impairs efficient A3B upregulation (**FIGURE 20h**) (adapted from Riedl*, Faure-Dupuy*, et al. [4]).

Besides BS1, other immune stimulatory molecules were described to induce cccDNA degradation, namely IFNα2A (Roferon) [2], IFNγ and TNFα, [299]. I aimed to elucidate if HIF1α stabilisation might as well affect the antiviral effects of those cytokines. To this end, dHepaRG, infected with HBV were treated with mentioned cytokines in either presence or absence of DMOG. cccDNA degradation was observed at various rates for all three molecules (30% reduction for both interferons and 50% for TNFα) (**FIGURE 21a**; DMSO). Surprisingly, this effect was blocked under HIF1α stabilisation with DMOG (**FIGURE 21a**; DMOG). Similarly, treatment with different immune-stimulatory molecules highlighted a strong reduction of NF-κB activation in dHepaRG under hypoxia. While BS1, TNFα, IL-17A and LPS, under 20% oxygen, lead to an upregulation of A3B, NIK, and NF-κB2 to different extends, under 1% oxygen this induction was dampened (**FIGURE 21b-d**) (adapted from Riedl*, Faure-Dupuy*, et al. [4]).

In summary, these data suggest that HIF1α is directly involved in the suppression of anti-cccDNA effects by BS1, but also other antiviral molecules. HIF1α depletion alone was sufficient to rescue the reduced A3B induction under HIF1α stabilisation and restored cccDNA degradation.
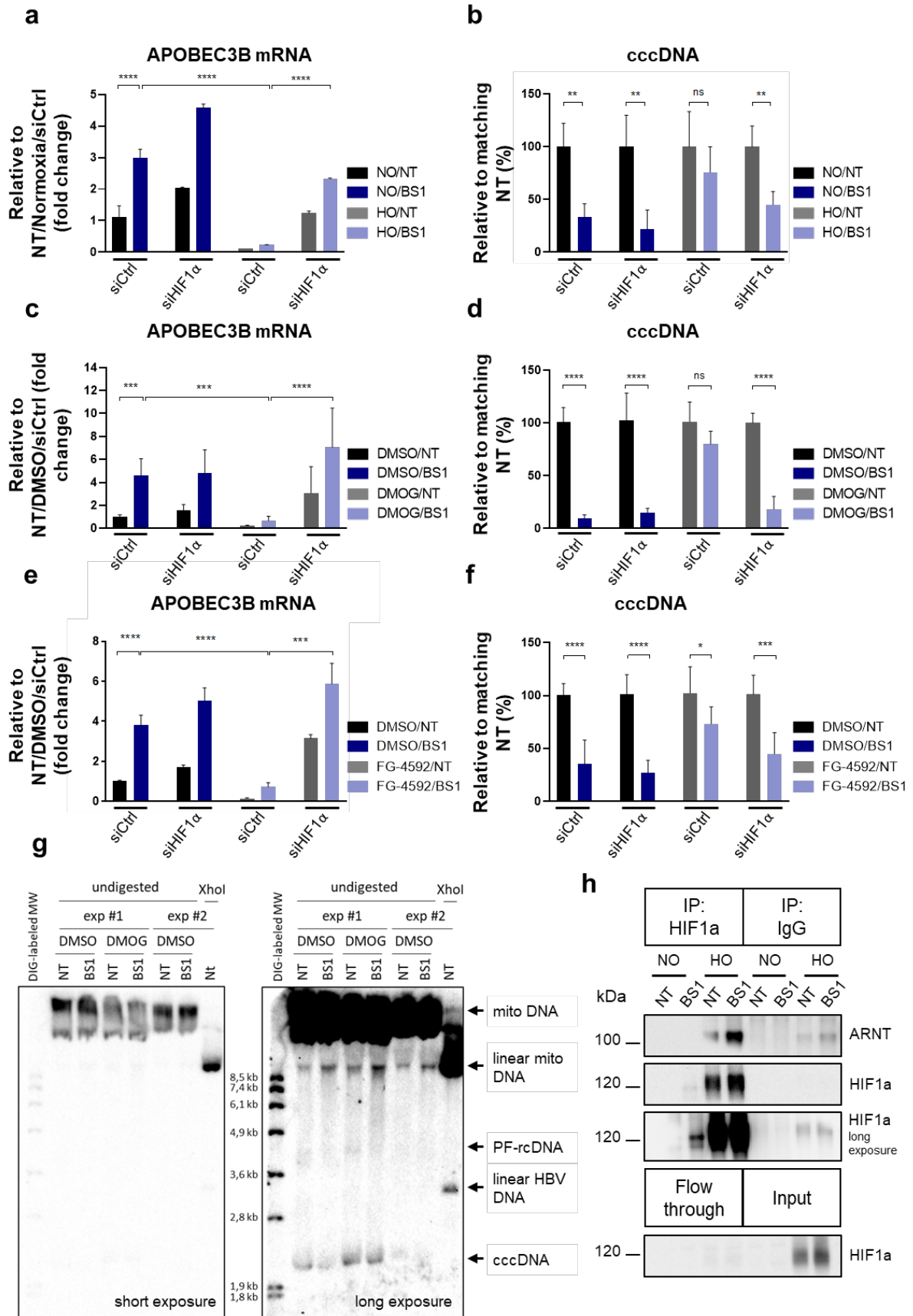
Figure 20: HIF1α stabilisation prevents the anti-viral effects of APOBEC3B in vitro (adapted from Riedl*, Faure-Dupuy*, et al. [4])

Adapted from my written and experimental contribution in Riedl*, Faure-Dupuy*, et al. [4]: **(a-b)** dHepaRG were infected with HBV. Six-day treatment of dHepaRG was performed under either 20% oxygen ("Normoxia", NO) or 1% oxygen ("Hypoxia", HO) with BS1, starting six d.p.i. Before treatment start and after the first three days of treatment, cells were transfected with HIF1α-targeting (siHIF1α) or control siRNAs (siCtrl). **(c-f)** dHepaRG were infected with HBV. Six-day treatment of dHepaRG was performed with BS1 **(c-d)** and/or DMOG **(e-f)** and/or FG-4592, starting 13 days post infection with HBV. Four days and on the day before treatment start, cells were transfected with HIF1α-targeting or control siRNAs. **(a, c, e)** RNAs and **(b, d, d)** DNA were extracted and analysed by RT-qPCR and qPCR, respectively. Bars represent the mean +/- SD of **(a-b)** one, or **(c-f)** three independent experiments performed in quadruplicates. Data were submitted to **(a, c, e)** one-way ANOVA or **(b, d, f)** unpaired student's t-test. **(g)** dHepaRG were infected with HBV. Twelve-day treatment of differentiated HepaRG (dHepaRG) was performed with BS1 and/or DMOG starting ten d.p.i. Episomal DNA was extracted and analysed by Southern blot. **(h)** Three-day treatment dHepaRG was performed under either 20% oxygen or 1% oxygen with BS1. Proteins were pulled down with the indicated antibody and analysed by immunoblotting. *: $p < 0.05$; **: $p < 0.01$; ***: $p < 0.005$; ****: $p < 0.0001$; ns: not significant. NT: non-treated
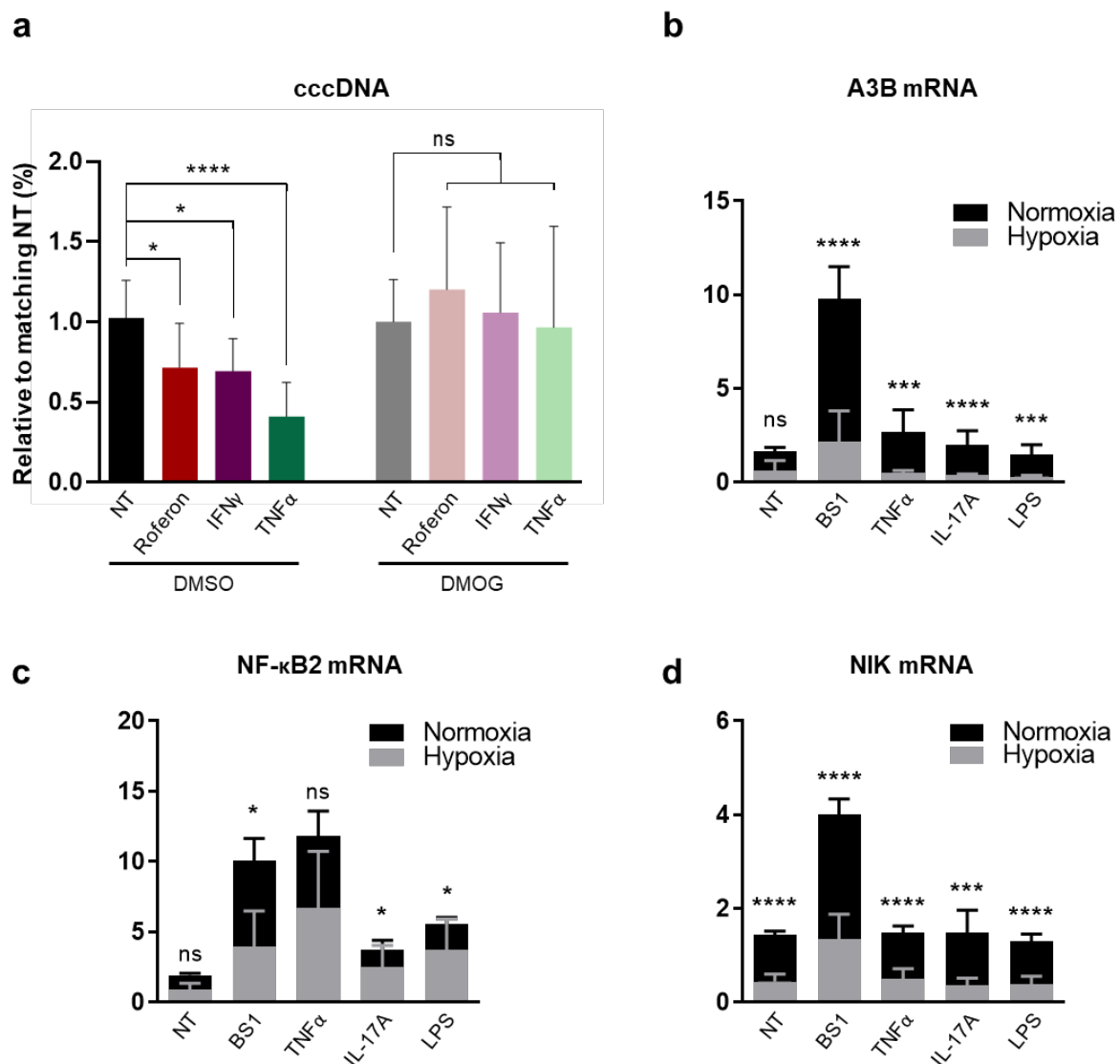
Figure 21: HIF1α stabilisation impairs the response to a multitude of immune stimulatory molecules (adapted from Riedl*, Faure-Dupuy*, et al. [4])

Adapted from my written and experimental contribution in Riedl*, Faure-Dupuy*, et al. [4]: **(a)** dHepaRG were infected with HBV. Twelve-day treatment of dHepaRG was performed with Roferon (i.e. interferon

α 2A), IFNγ, TNFα and/or DMOG starting seven d.p.i. DNA was extracted and cccDNA levels were analysed by qPCR. **(b-d)** Six-day treatment of dHepaRG was performed under either normoxia or hypoxia with BS1, TNFα, IL-17A, or LPS. RNAs were extracted and analysed via RT-qPCR. Bars represent the mean +/- SD of **(a-d)** three independent experiments performed in triplicates. *: p < 0.05; ***: p < 0.005; ****: p < 0.0001; ns: not significant. NT: non-treated

7.2.3 HIF1α, but not HIF2α is involved in the repression of A3B induction

(Adapted from my written and experimental contribution in Riedl*, Faure-Dupuy*, *et al.* [4]): My data so far showed a strong involvement of HIF1α in the repression of A3B. To rule out that HIF2α, another hypoxia induced transcription factor with the same destabilising features in the presence of oxygen [300], is involved in this process, I set up both gain-of-function and loss-of-function experiments. First, cell lines inducible for the overexpression of either wild-type HIF1α, wild-type HIF2α or degradation resistant HIF1α (dr-HIF1α) were produced based on the tetracycline repressor expressing cell line HepaRG-TR. In dr-HIF1α, two prolines (P402 and P564) were substituted by alanines, which prevents hydroxylation of HIF1α and therefore blocks proteasomal degradation, even under high oxygen levels. Under doxycycline treatment, cells expressed the respective proteins, however, the wild type HIF1α was not detectable under normoxia, probably due to the fast turn-over of the protein. Only dr-HIF1α and HIF2α were detected on western blot (**FIGURE 22a**) and were therefore used for further experiments. Carbonic anhydrase IX (CAIX), as a functional read-out of HIF1α transcriptional activity, was strongly overexpressed in the dr-HIF1α cell line under treatment with 0.1 μg/mL doxycycline, as well as HIF2α in the HIF2α expressing cell line (**FIGURE 22b**). While in the empty vector control cell line, no effect on A3B expression was observed, I could detect a dose dependent effect of A3B repression when cells were treated with BS1 in addition to doxycycline (**FIGURE 22c**). Although this effect was slightly weaker in the HIF2α cell line than in the dr-HIF1α cell line, these data suggested that both proteins might be involved in the repression of A3B under HIF stabilising conditions.

To functionally test this hypothesis once more, I transfected dHepaRG with siRNAs targeting either HIF1α or HIF2α or transfected both siRNAs at once. Only the transfection with HIF1α-targeting, but not with HIF2α-targeting siRNAs was able to rescue the reduced A3B expression under hypoxia (**FIGURE 22d**), although knock-down efficiencies were strong for both genes in the single and double knock-down cells (**FIGURE 22e**). Interestingly, while no rescue was observed in the single HIF2α knock-down cells, also no additional effect of the HIF2α knock-down in the double knock-down cells was present (**FIGURE 22d**, siHIF1α+siHIF2α).

Of important note, hypoxia neither induced a downregulation of the LTβR on the cell surface (**FIGURE 22f-g**), nor cell death (**FIGURE 22h**), indicating that the observed effects are no bystander effects of reduced sensing of the ligands or response to cell death (adapted from Riedl*, Faure-Dupuy*, *et al.* [4]).
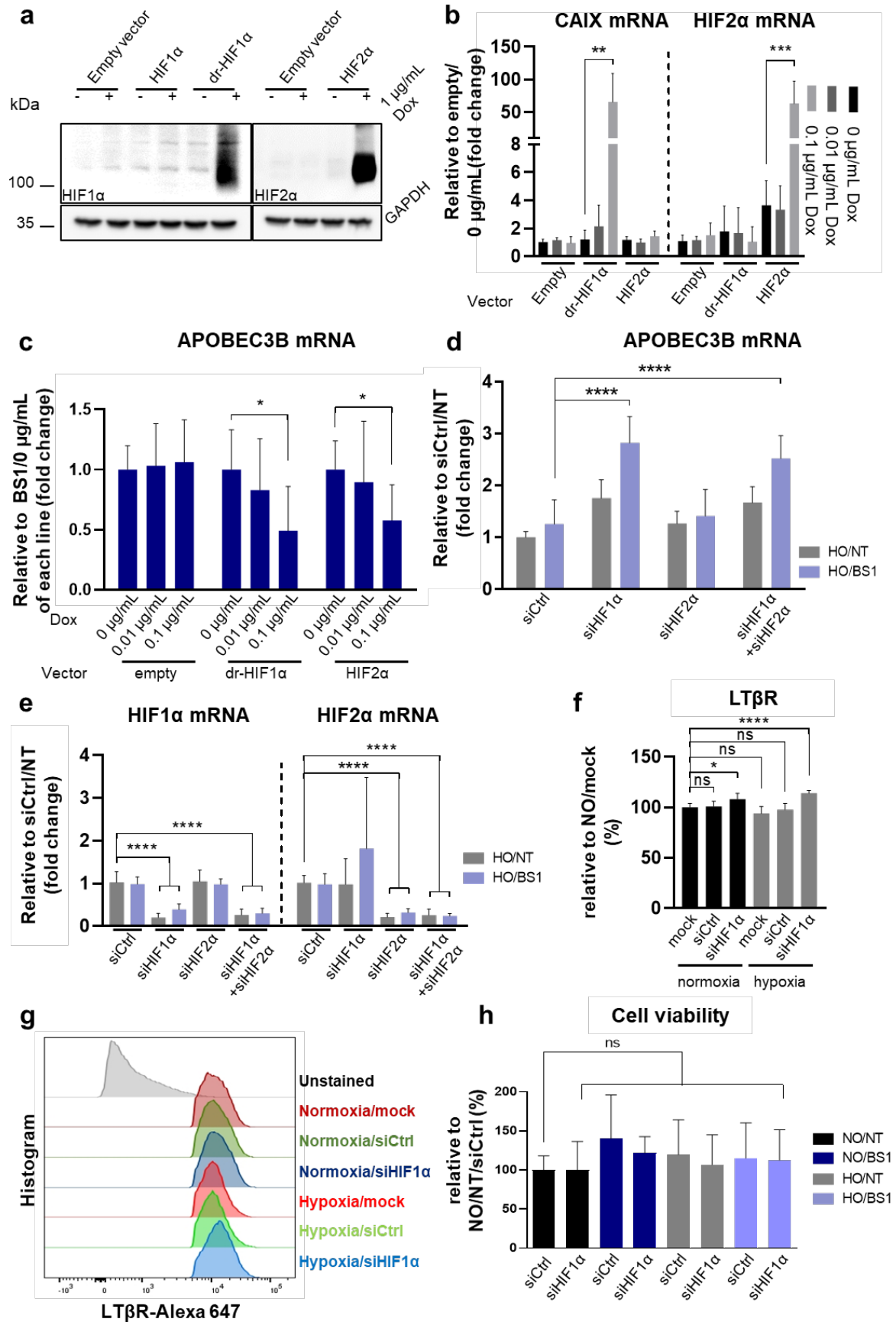
Figure 22: HIF1α, but not HIF2α is involved in the repression of APOBEC3B upregulation under physiologic conditions (adapted from Riedl*, Faure-Dupuy*, *et al.* [4])

Adapted from my written and experimental contribution in Riedl*, Faure-Dupuy*, et al. [4]: **(a)** Wild-type HIF1α expressing, a degradation resistant mutated HIF1α (P402A/P564A, "dr-HIF1α") expressing, or wild-type HIF2α expressing dHepaRG were exposed to 1 µg/mL doxycycline (Dox) for the induction of the transgene for three days. Proteins were extracted and analysed via immunoblotting. **(b)** dHepaRG were treated with indicated doses of doxycycline. mRNAs were extracted and analysed by RT-qPCR. **(c)** Three-day treatment of dHepaRG expressing either inducible dr-HIF1α, HIF2α or containing an empty vector was performed with BS1 and indicated concentrations of doxycycline. RNAs were extracted and A3B expression was analysed by RT-qPCR. **(d-e)** Three-day treatment of dHepaRG was performed under hypoxia in the presence or absence of BS1. One day before treatment start, cells were transfected with either HIF1α-targeting (siHIF1α), HIF2α-targeting (siHIF2α), both siRNAs (siHIF1α+siHIF2α), or control siRNAs (siCtrl). RNAs were extracted and **(d)** A3B expression or **(e)** HIF1α and HIF2α expression was analysed by RT-qPCR. **(f-g)** dHepaRG were incubated under hypoxia or normoxia for three days. One day before, cells were transfected with either HIF1α-targeting or control siRNAs or left untransfected. LTβR surface expression was analysed by flow cytometry. **(f)** Bars represent the geometric mean of two independent experiments with three or four biological replicates in percent to non-transfected cells incubated under NO. **(g)** Histograms of representative samples. **(h)** Six-day treatment of dHepaRG was performed under either normoxia or hypoxia with BS1. One day before treatment start, cells were transfected with either HIF1α-targeting or control siRNAs. Viability was assessed by sulforhodamine B assay. Data represent the mean +/- SD of **(b-c)** four or **(d-f, h)** three independent experiments performed in triplicates. Data were subjected **(b)** to unpaired Student's t-test or **(c-f, h)** to one-way ANOVA. *: p < 0.05; **: p < 0.01; ***: p < 0.001; ****: p < 0.0001; ns: not significant. NT: non-treated

In summary, the data I present here indicate that HIF1α is the main driver of the observed repression of A3B induction under low oxygen or other HIF stabilising conditions. HIF2α, if specifically overexpressed, might also play a role in this setting, but under physiological conditions, the removal of HIF1α is both necessary and sufficient for the rescue of A3B induction. Furthermore, the observed reduction in A3B overexpression by BS1 treatment is not due to a downregulation of the LTβR on the cell surface.

7.2.4 HIF1α stabilisation prevents RelB accumulation under LTβR activation, blocking A3B induction

As demonstrated extensively for my work on aim 1, NF-κB, downstream of LTβR activation, is the signalling pathway involved in A3B upregulation. When investigating, for example, promoter occupancy of the A3B promoter (**FIGURE 12e**) or conducting promoter-luciferase fusion experiments (**FIGURE 12d**), it became obvious that RelB is highly important in this process.

RelB itself is an interesting candidate for being under control of HIF1α stabilisation, since it is at a crossroad between the canonical and the alternative NF-κB signalling pathway. Whereas its mRNA is induced by the IKK complex- and RelA-dependent canonical NF-κB pathway, it is the major transcription factor in the heterodimer p52/RelB downstream of NIK-dependent alternative NF-κB signalling [281].

(Adapted from my written and experimental contribution in Riedl*, Faure-Dupuy*, et al. [4]): Comparison of nuclear and cytosolic extracts of dHepaRG incubated with DMOG showed that

RelB protein levels, especially in the nucleus, but also in the cytoplasm were severely reduced in DMOG treated cells (**FIGURE 23a**). Interestingly, effects on RelA were not obvious in cytosolic fractions and only minor in nuclear fractions (**FIGURE 23a**). Furthermore, similar to the rescue of A3B induction, RelB protein levels were restored under DMOG treatment when HIF1α was knocked-down with siRNAs (**FIGURE 23b**). Importantly, the RelB mRNA levels under DMOG treatment were not reduced compared to control cells but rather slightly increased (**FIGURE 23c**). In collaboration with Maude Rolland and Emmanuel Dejardin, I confirmed these observations *in vivo*. Mice were injected with DMOG and sacrificed six hours later. In the liver of all animals, RelB protein levels were reduced when DMOG, but not the vehicle, was injected (**FIGURE 23d**). HIF1α levels were elevated under DMOG treatment and RelA and p50 protein levels were unchanged. Surprisingly, RelB mRNA levels were unchanged between the vehicle and the DMOG injected group (**FIGURE 23e**), implicating again that HIF1α stabilisation directly leads to a RelB protein destabilisation without further effects on the RelB mRNA expression. Of note, the most important binding partner of RelB, p52, was not found on the A3B promoter under hypoxia under BS1 treatment, whereas its occupancy of the promoter was 3-fold increased in BS1 treated cells under normoxia (**FIGURE 23f**). This shows that the repression of RelB is directly linked to reduced A3B induction by diminished promoter engagement of the NF-κB heterodimer RelB/p52.

I could further observe a "dosage effect" of HIF1α stabilisation on RelB protein levels, as RelB levels under 3% oxygen (i.e. "mild hypoxia"), showed an intermediate level when compared to 20% and 1% oxygen (**FIGURE 23g**). A3B induction, however, was not affected by 3% oxygen, whereas it was strongly reduced by 1% oxygen (**FIGURE 23h**) (adapted from Riedl*, Faure-Dupuy*, *et al.* [4]).

In line with the previous results, RelB protein was strongly induced under BS1 treatment, which was prevented under hypoxia, as shown by ICC (**FIGURE 24a**). However, RelA translocation was induced by BS1 regardless of the oxygen levels (**FIGURE 24b**) (adapted from Riedl*, Faure-Dupuy*, *et al.* [4]).

7.2.5 HIF1α represses RelB protein accumulation independently of its transcriptional activity

HIF1α belongs to a large family of DNA binding proteins, the basic helix-loop-helix (bHLH) family. Within this group, it more specifically belongs to the PAS domain proteins (PAS: the protein domain shared by Per, ARNT and Sim). In the same group is found ARNT (aryl hydrocarbon receptor nuclear translocator), sometimes called HIF1β. ARNT is the interacting partner of HIF1α, and under HIF1α stabilising conditions, HIF1α translocates to the nucleus to bind together with ARNT to hypoxia responsive elements (HREs) in the DNA to induce

transcription of hypoxia induced genes [301]. However, ARNT can also bind different transcription factors among which AhR (aryl hydrocarbon receptor), a protein induced as a response to xenobiotics, e.g. dioxin.
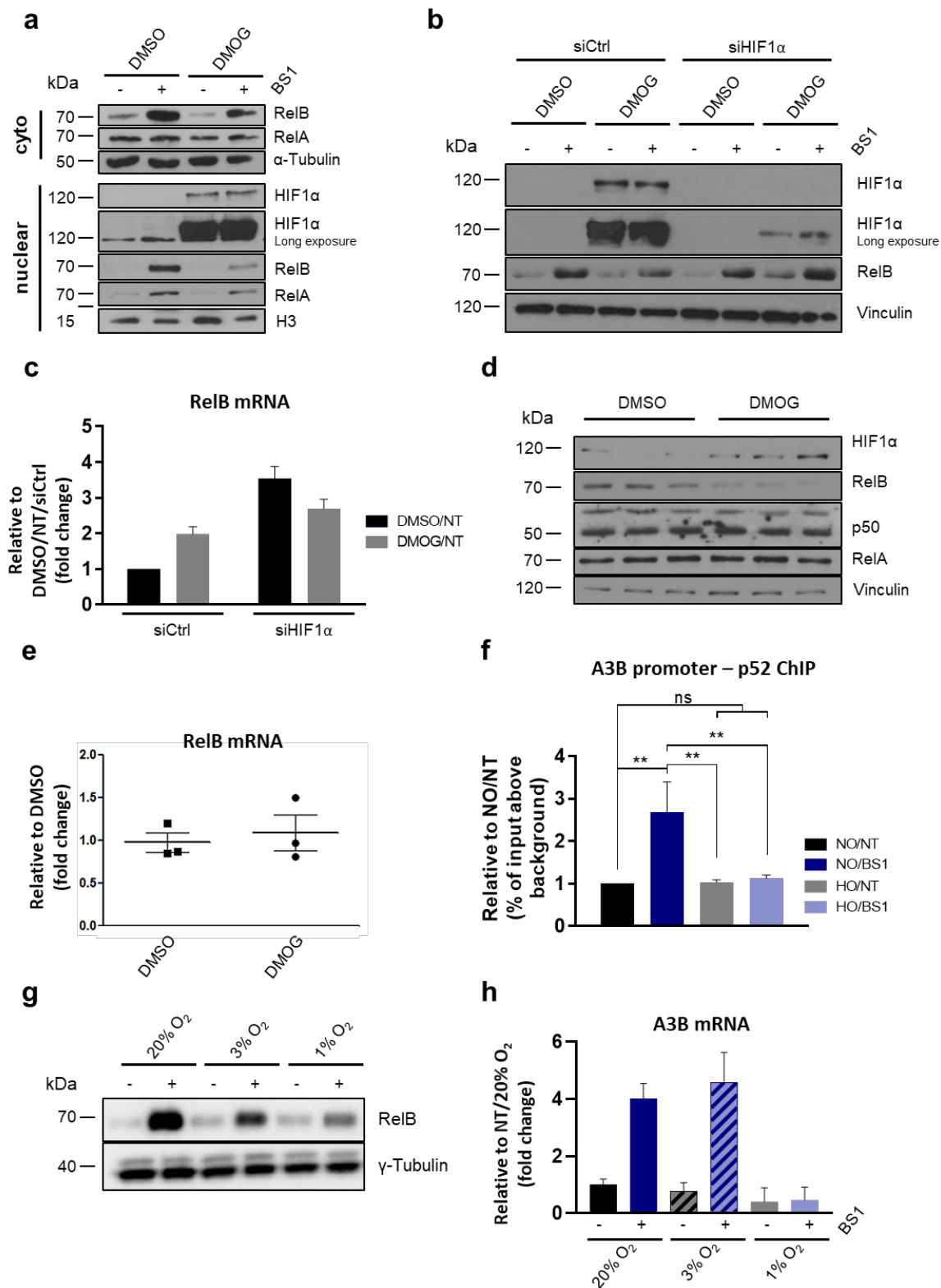
Figure 23: RelB protein levels are reduced under HIF1α stabilising conditions (adapted from Riedl*, Faure-Dupuy*, et al. [4])

Adapted from my written and experimental contribution in Riedl*, Faure-Dupuy*, et al. [4]: **(a-c)** Overnight treatment of dHepaRG was performed with BS1 and/or DMOG. **(a)** Nuclei were separated from the cytoplasm and proteins were analysed by immunoblotting. **(b-c)** Two days before treatment start, cells were transfected with either HIF1α-targeting (siHIF1α) or control siRNAs (siCtrl). **(b)** Proteins and **(c)** RNAs were extracted and analysed by immunoblotting and RT-qPCR, respectively. **(d-e)** Mice were injected intraperitoneal with DMOG or the equal amount of DMSO. Six hours post injection, mice were sacrificed and **(d)** proteins and **(e)** RNAs were isolated from liver tissue. **(f)** Six-day treatment of dHepaRG was performed under either normoxia or hypoxia with BS1. Then, nucleic acids were cross-linked with proteins and submitted to ChIP. p52 binding to A3B promoter was quantified by qPCR. **(g-h)** Three-day treatment of dHepaRG was performed under either 20%, 3% or 1% oxygen with BS1. **(a-b, d, g)** Proteins were isolated and analysed by immunobloting using indicated antibodies. **(c, e, h)** RNAs were extracted and analysed by RT-qPCR. Data represent the mean +/- SD of **(c, f, h)** three or **(e)** one and independent experiments performed in triplicates. Data were subjected **(f)** to one-way ANOVA. *: $p < 0.05$; **: $p < 0.01$; ***: $p < 0.001$; ****: $p < 0.0001$; ns: not significant. NT: non-treated
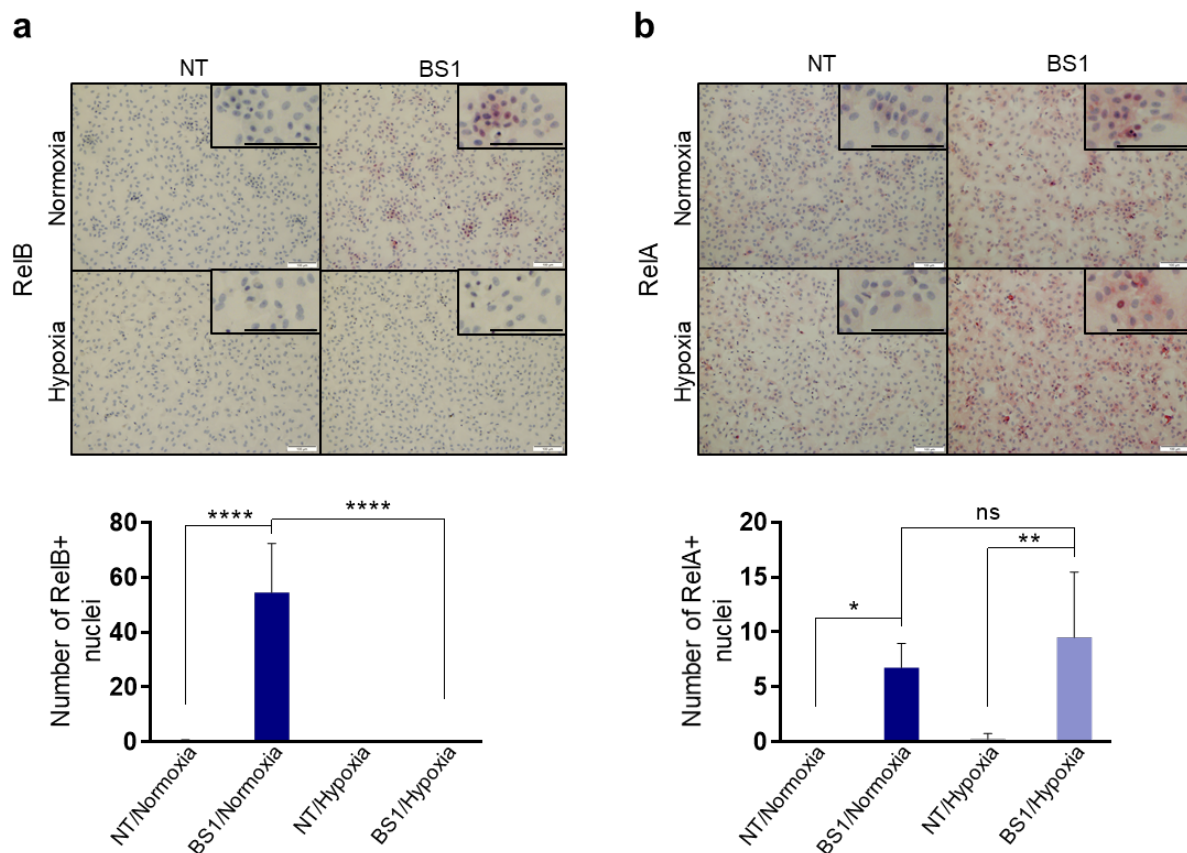
Figure 24: RelB, but not RelA, is reduced by HIF1α stabilisation in vitro and in vivo (adapted from Riedl*, Faure-Dupuy*, et al. [4])

(Adapted from my written and experimental contribution in Riedl*, Faure-Dupuy*, et al. [4]): **(a-b)** dHepaRG were seeded into 4-well chamber slides. Three-day treatment of dHepaRG was performed under either normoxia or hypoxia with BS1. Cells were then and stained for **(a)** RelB and **(b)** RelA. Upper panels show representative pictures and lower panels show quantification of positive nuclei. Data represent the mean of five pictures per condition of two independent experiments. Data were subjected to one-way ANOVA. *: $p < 0.05$; **: $p < 0.01$; ****: $p < 0.0001$; ns: not significant. NT: non-treated

Literature on these relationships showed that competition between interacting proteins might occur (e.g. competition for common partners, HIF1α/ARNT and AhR/ARNT [302]). Furthermore, there are reports that RelB can interact with ARNT to regulate CD30 signalling

[303] and with AhR to regulate the expression of cytokines [304], which can also control RelB stability and/or its transcriptional activity [305]. The possible interactions are presented in **FIGURE 25**.
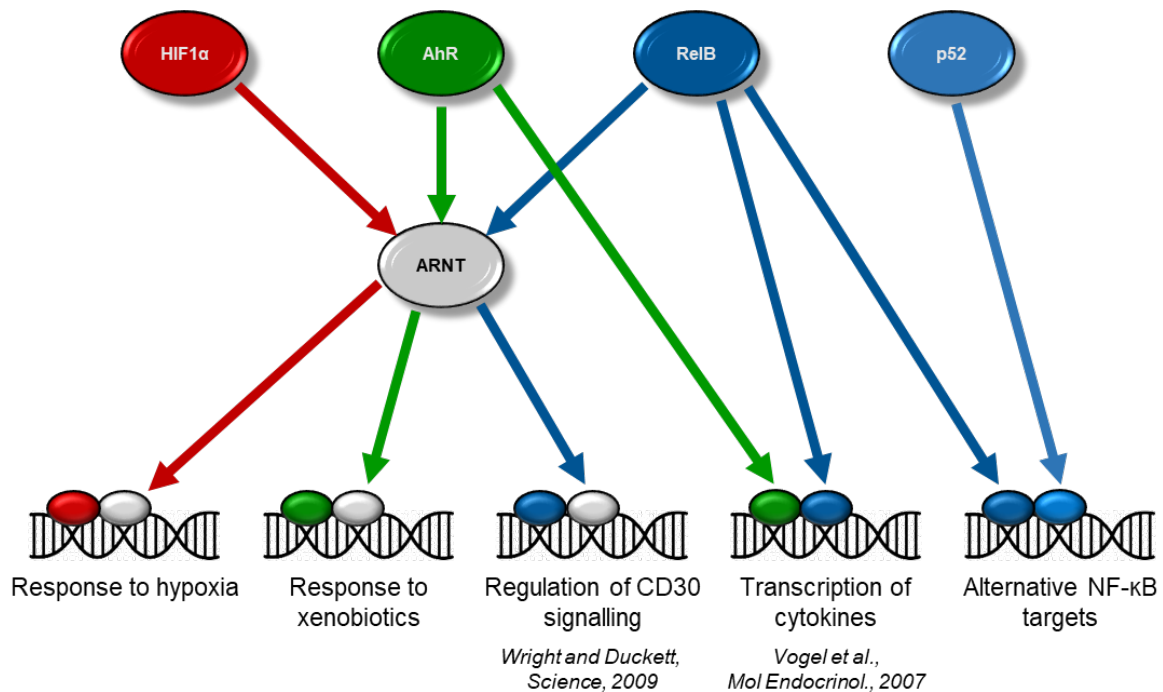
Figure 25: ARNT, RelB, and HIF1α are part of a multi-functional network of transcription factors
Schematic representation of intersections and crossroads of HIF1α, AhR, RelB, p52, and ARNT. ARNT is the canonical binding partner of HIF1α and AhR to activate specific genes in response to hypoxia and xenobiotics, respectively. A competition for ARNT between HIF1α and AhR can be expected if limited amounts of ARNT are present in cells. Furthermore, RelB can bind both AhR and ARNT, besides its canonical binding partner p52, suggesting even more competition for common factors.

Based on all these possible connections, I first wanted to know if removing AhR from the equation would increase RelB protein levels. For instance, with less AhR being present in the cell, more ARNT protein might be available for a binding of HIF1α, preventing high HIF1α level from interfering with RelB protein levels.

(Adapted from my written and experimental contribution in Riedl*, Faure-Dupuy*, et al. [4]): To this end, I knocked-down AhR in cells treated with DMOG. Although AhR protein levels were strongly reduced, the decreased RelB protein levels were not restored under DMOG treatment (**FIGURE 26a**). Concomitant, A3B mRNA levels were not restored (**FIGURE 26b**) as previously shown for HIF1α knock-down (**FIGURE 20c**).

Interestingly, RelB levels (**FIGURE 26c**), as well as A3B expression (**FIGURE 26d**) were not rescued either in cells knocked-down for ARNT. RelB mRNA expression was also not altered upon ARNT knock-down (**FIGURE 26e**), as shown previously under HIF1α knock-down (**FIGURE 23c**). Of important note, ARNT knock-down prevented efficient induction of the HIF1α target gene VEGFα (**FIGURE 26f**), indicating that transcriptional activity of HIF1α is

blocked by removal of ARNT (adapted from Riedl*, Faure-Dupuy*, *et al.* [4]). This is of special interest as the canonical function of HIF1α is to sense oxygen levels and to subsequently activate the transcription of genes that set the cell to a "hypoxic state" to cope with these conditions. My data suggest another a non-canonical, function of HIF1α leading to direct regulation of RelB protein levels (I) without affecting RelB mRNA levels and (II) independently of ARNT and therefore of HIF1α transcriptional activity.
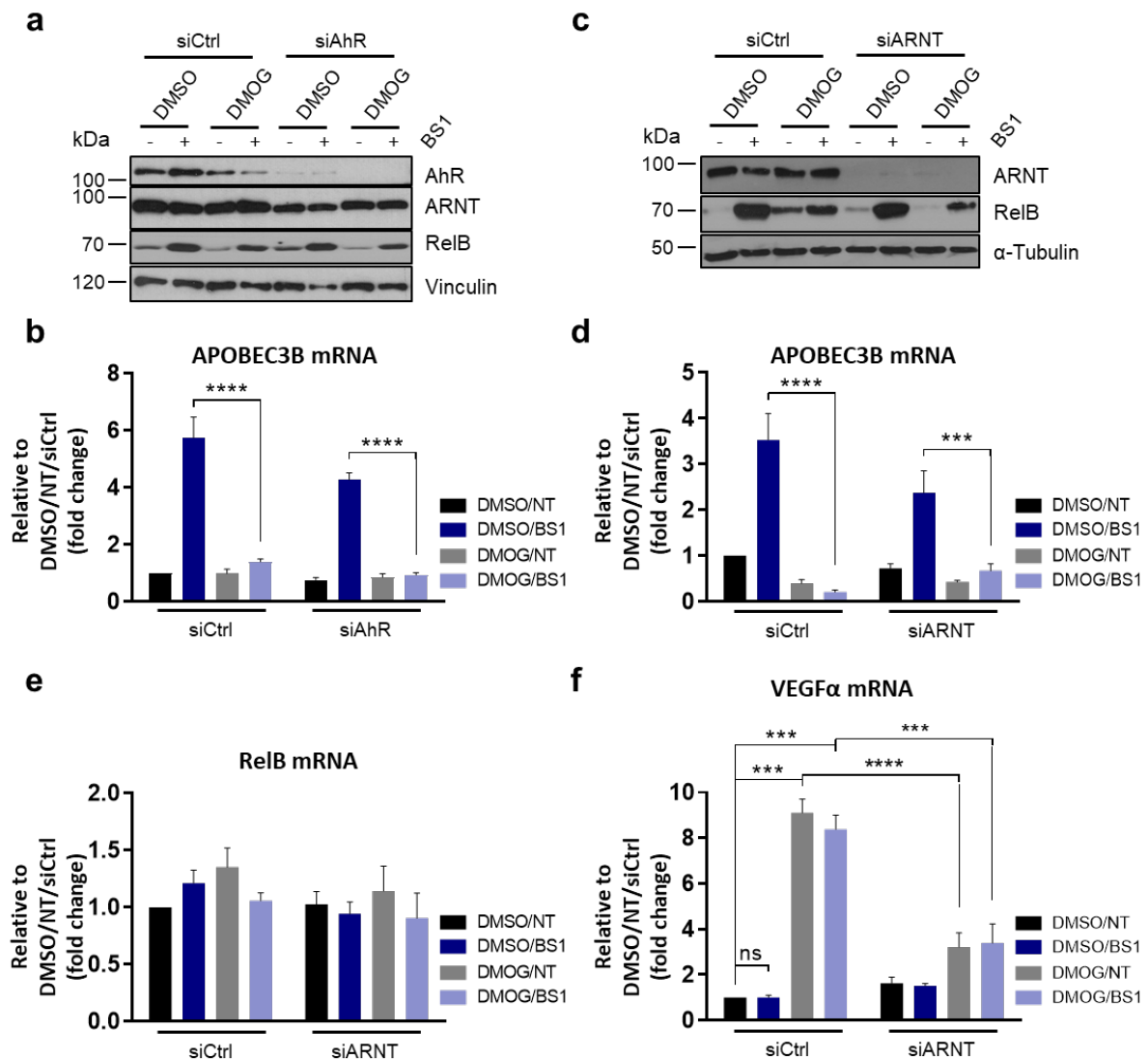
Figure 26: RelB protein levels are independent of AhR and HIF1α transcriptional activity (adapted from Riedl*, Faure-Dupuy*, *et al.* [4])
(Adapted from my written and experimental contribution in Riedl*, Faure-Dupuy*, *et al.* [4]): **(a-f)** Overnight treatment of dHepaRG was performed with BS1 and/or DMOG. Two days before treatment start, cells were transfected with **(a-b)** AhR-targeting (siAhR), **(c-f)** ARNT-targeting (siARNT) or control siRNAs (siCtrl). **(a, c)** Proteins and **(b, d-f)** RNAs were extracted and analysed by immunoblotting and RT-qPCR, respectively. Bars represent the mean +/-SD of **(b, d-f)** three independent experiments. Data were submitted to **(b, d, f)** one-way ANOVA. ***: $p < 0.001$; ****: $p < 0.0001$; ns: not significant. NT: non-treated

7.2.6 Cellular pathways important for execution of immune stimuli-induced signalling are repressed under hypoxia, independently of HIF1α

(Adapted from my written and experimental contribution in Riedl*, Faure-Dupuy*, et al. [4]): Next, I wanted to investigate the global effect of hypoxia on the HepaRG proteome. To this end, dHepaRG, treated or not with BS1, transfected or not with HIF1α targeting siRNAs and cultured under 20% (normoxia, NO) or 1% (hypoxia, HO) oxygen were analysed by mass spectrometry with support of Silvia Calderazzo and Martin Schneider from the DKFZ Biostatistics Core Facility and the genomics and proteomics core facility, respectively. Surprisingly, whereas 418 proteins were significantly dysregulated when comparing BS1-treated to non-treated cells under normoxia, there were only two dysregulated proteins found for the same comparison under hypoxia (**FIGURE 27a**). This suggested that under hypoxia, cells were generally less activatable by LTβR activation with BS1. When analysing the regulation of pathways, I separated pre-selected pathways into four clusters: I - transcription and translation; II - signal transduction and immune response; III - metabolism; and IV - DNA replication and repair. BS1 treatment very prominently induced upregulation of all pathways of cluster I and cluster IV, while repressing metabolic pathways of cluster III (**FIGURE 27b**). Of cluster II, most pathways were not significantly dysregulated, except from "antigen processing and presentation" and "NF-κB signalling" pathway, which were upregulated and "PPAR (peroxisome proliferator-activated receptor) signalling pathway", which was downregulated, which goes in line with the downregulation observed for fatty acid metabolism (**FIGURE 27b**).

To find out how HIF1α affects the response to hypoxia, I used the following pairwise comparisons of samples: (1): non-treated, normoxia, control siRNA transfected versus BS1-treated, normoxia, control siRNA transfected (NO/NT/siCtrl vs. NO/BS1/siCtrl); (2): non-treated, normoxia, control siRNA transfected versus BS1-treated, hypoxia, control siRNA transfected (NO/NT/siCtrl vs. HO/BS1/siCtrl) and (3) non-treated, hypoxia, control siRNA transfected versus BS1-treated, hypoxia, HIF1α-targeting siRNA transfected (NO/NT/siCtrl vs. HO/BS1/siHIF1α). With the first comparison, I wanted to confirm that siRNA transfected cells react the same way as the non-transfected cells from **FIGURE 27b**. Indeed, the same pathways were significantly dysregulated as in the previous experiment with non-transfected cells (**FIGURE 27c**). With the comparison (2), I aimed to investigate whether BS1 treated cells under hypoxia would upregulate the pathways similarly as under normoxia. Surprisingly, the effect of hypoxia on the cells was much stronger than the effect of BS1 treatment. Precisely, of cluster I, II, and III, nearly all pathways showed a significant repression under hypoxia, although cells were treated with BS1, and cluster IV was not significantly upregulated anymore (**FIGURE 27d**).
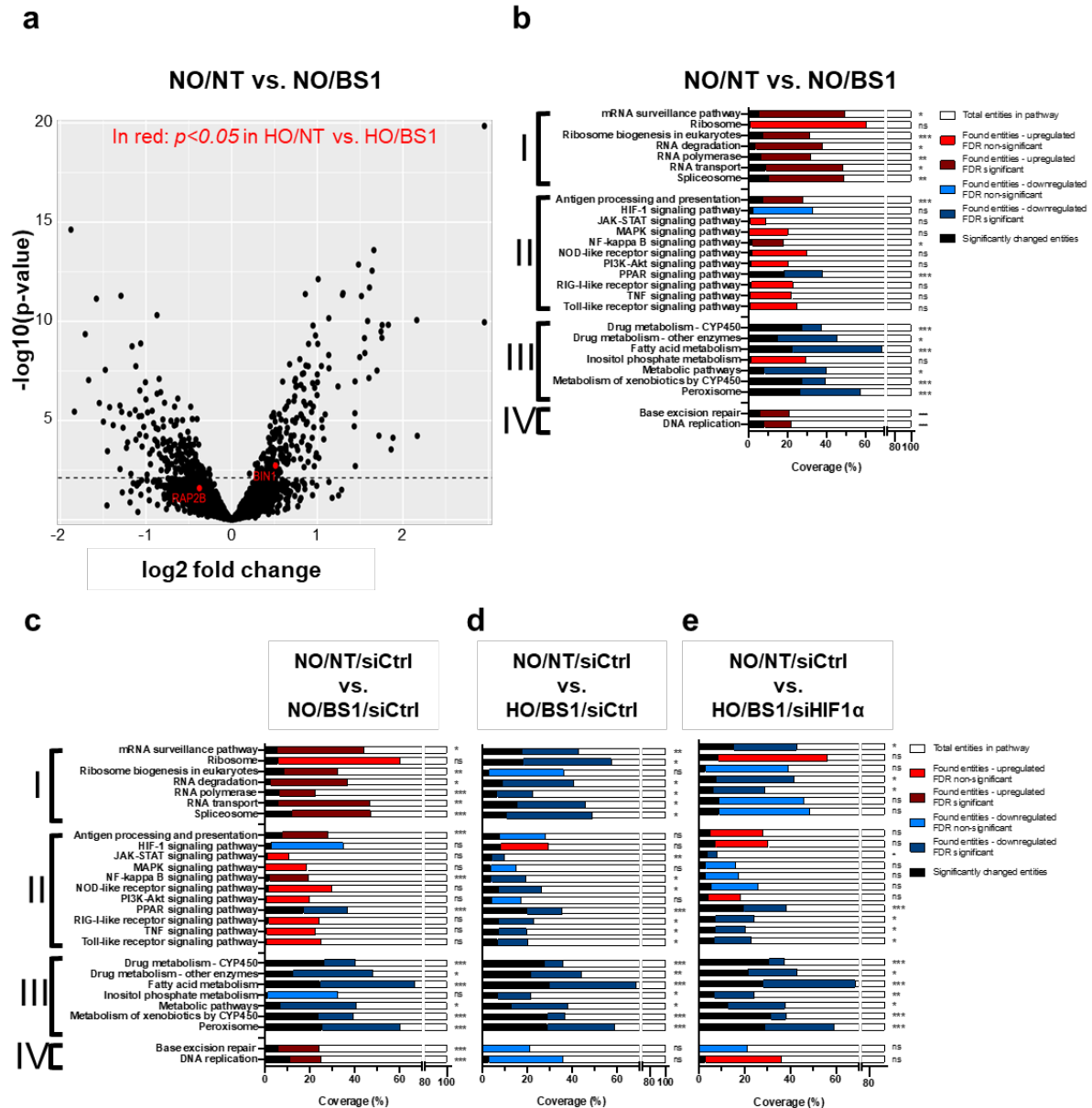
Figure 27: HIF1α knock-down rescues "mRNA processing" and "ribosomes" pathways. (adapted from Riedl*, Faure-Dupuy*, et al. [4])

Adapted from my written and experimental contribution in Riedl*, Faure-Dupuy*, et al. [4]: **(a-e)** Three-day treatment of differentiated HepaRG (dHepaRG) was performed under either normoxia or hypoxia with BS1. dHepaRG were either **(a-b)** left untransfected or **(c-e)** one day before treatment start, transfected with either HIF1α-targeting (siHIF1α) or control siRNAs (siCtrl). Proteins were extracted and submitted to unbiased mass spectrometry analysis. **(a)** Volcano plot represents proteins of normoxia non-treated (NO/NT) vs. normoxia BS1-treated (NO/BS1) comparison. Dotted line represents the limit of significance (adjusted p-value < 0.05). Red dots represent the only two proteins, which are significantly dysregulated (i.e. adjusted p-value < 0.05) in similar comparison under hypoxia (HO/NT vs. HO/BS1). **(b-e)** Cellular pathways of significantly changed proteins were analysed for pre-selected KEGG pathways using the ROAST algorithm. Pathway analysis is shown for the following comparisons: **(b)** NO/NT vs. NO/BS1, **(c)** NO/NT/siCtrl vs. NO/BS1/siCtrl, **(d)** NO/BS1/siCtrl vs. HO/BS1/siCtrl, and **(e)** HO/BS1/siCtrl vs. HO/BS1/siHIF1α. The significantly (respectively, non-significant) upregulated (dark red bar; respectively, light red bar) or downregulated (dark blue bar; respectively, light blue bar) pathways are presented as the percentage of proteins analysed in the pathways. Of note, black bars represent the number of significantly dysregulated proteins in the pathway. Data were submitted to LIMMA algorithm for selection of significantly changed proteins. *: p < 0.05; **: p < 0.01; ***: p < 0.001; ****: p < 0.0001; ns: not significant. NT: non-treated

Of special interest was that the machinery for the transcription and translation was severely downregulated, which points towards the direction that even if immune stimulatory cues would be sensed by the cells, effectors would be very inefficiently produced. Finally, the comparison (3) served to elucidate, if HIF1α on its own is the driver of this hypoxic state that strongly impairs previously mentioned pathways, especially of the cluster I. Interestingly, some pathways of cluster I were rescued from being significantly downregulated by HIF1α knock-down; the "ribosome" pathway even showed a tendency to upregulation, albeit not significantly (**FIGURE 27e**). Also the "NF-κB signalling pathway" was changed from being significantly downregulated in comparison (2), it was not significantly changed in comparison (3) (**FIGURE 27d and 27e**, respectively) (adapted from Riedl*, Faure-Dupuy*, *et al.* [4]).

In summary, when considering the comparison (1), it was obvious that although differences between comparison (2) and (3) were detected, there was no complete reversal of the "hypoxic state" of the cells only by the knock-down of HIF1α. However, as presented previously, I showed that the knock-down of HIF1α was sufficient to (I) rescue RelB protein levels (**FIGURE 23b**), which results in (II) restored A3B expression under BS1 treatment, which eventually leads to (III) a rescued antiviral effect under HIF1α stabilising conditions (**FIGURE 20a-f**). In line with previously shown data, HIF1α stabilisation can prevent the response to NF-κB triggers, as well as the degradation of HBV cccDNA (**FIGURE 21a-d**), potentially by the prevention of efficient upregulation of antiviral effector molecules. However, the effect of increased HIF1α levels on A3B and RelB seems to be more direct. If other antiviral treatments involving different triggers, e.g. type I and type III interferons, are impaired by a similar mechanism of HIF1α or by the downregulation of genes of the cluster I remains elusive and should be under investigation; especially considering that IFNα2A is of clinical relevance. Understanding underlying mechanisms can be of high importance for the treatment of CHB patients with immune stimulatory drugs.

8   Discussion

8.1   Aim 1: Deciphering transcriptional and post-transcriptional control of APOBEC3B

Adapted from my written and experimental contribution in Faure-Dupuy*, Riedl* et al [3]: In the frame of the first aim of my PhD thesis, I report several findings to help decipher the role of LTβR-mediated NF-κB signalling and a specific miRNA in regulating A3B in the context of HBV infection and cccDNA degradation. Furthermore, I elucidated the efficiency of A3B-induced antiviral effects in a transcriptionally repressed and a replication-deficient engineered strain of HBV. A graphical illustration of my findings is presented in **Figure 27** (adapted from Faure-Dupuy*, Riedl*, *et al.* [3]).
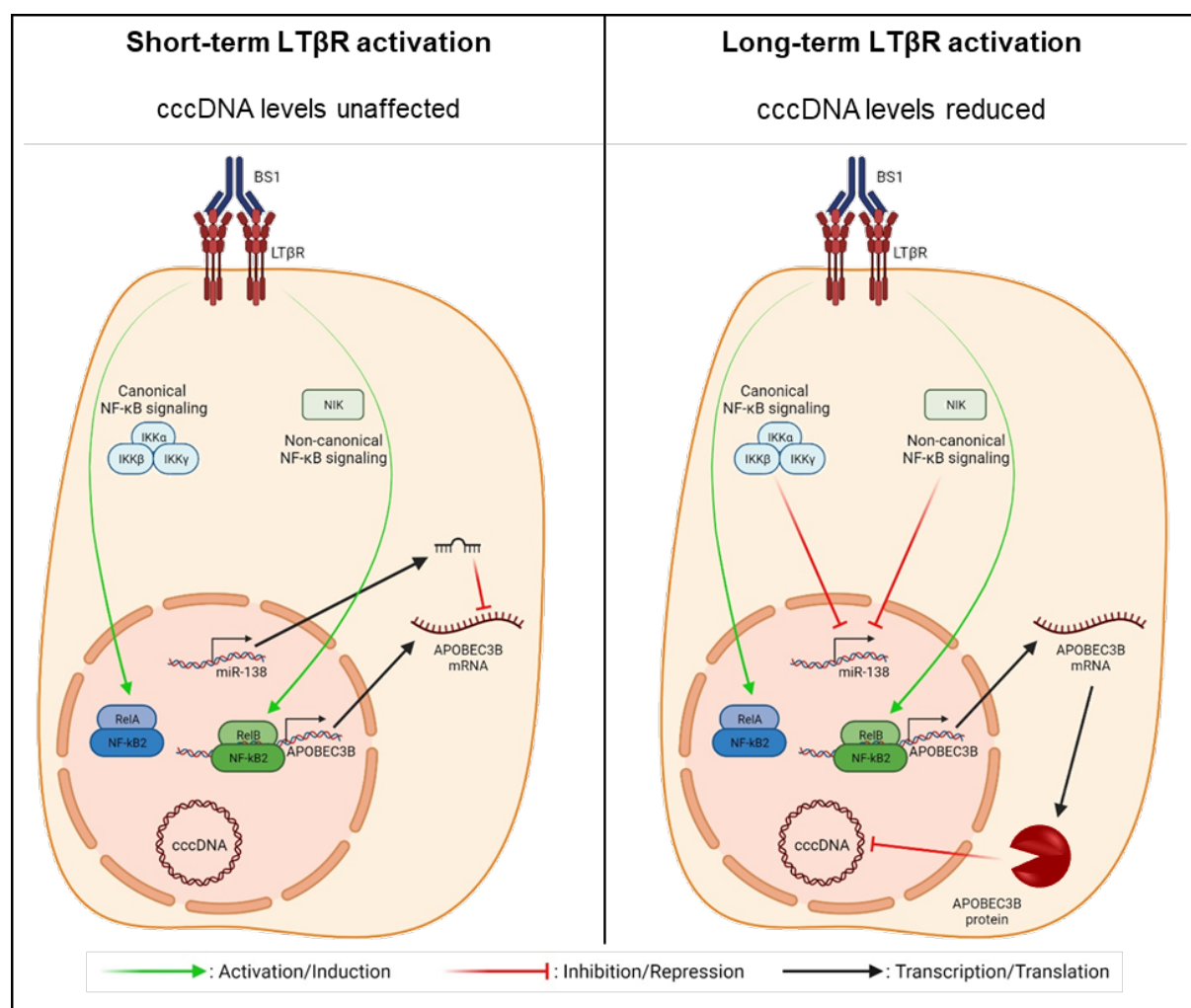
Figure 28 NF-κB and hsa-miR-138-5p control APOBEC3B-mediated cccDNA degradation (adapted from Faure-Dupuy*, Riedl*, *et al.* [3])

Adapted from my written and experimental contribution in Faure-Dupuy*, Riedl*, *et al.* [3]: Schematic representation of the key findings of aim 1 of my PhD thesis. Short-term lymphotoxin beta receptor (LTβR) activation, here depicted is the agonisation of the receptor by BS1, induces NF-κB signalling. This leads to binding of RelB/p52 dimers to the APOBEC3B promoter and the transcriptional activation of the gene. However, the micro RNA hsa-miR-138-5p (miR-138) targets APOBEC3B mRNA and prevents high levels thereof, which results in low anti-cccDNA (covalently closed circular DNA) activity

(left panel). Under long-term stimulation, expression of miR-138 is repressed in an NF-κB-dependent manner, allowing for high A3B mRNA levels and strong antiviral effects (right panel).

Cytidine deaminases of the APOBEC3 family have been under investigation for their antiviral activities for several years. For a long time, the research focus was on A3G, which is best known for its strong activity against Vif-deficient HIV [306]. In recent years, other A3 enzymes have raised more and more interest. A3B was under investigation as an enzyme targeting a wide spectrum of DNA viruses, including *inter alia* HIV as well [307] or human papilloma viruses [308]. That A3B can target HBV was first suggested in 2005 [309], but it took nice years until it was first shown that the natural induction of A3B, mediated by immune cell-related agonisation of the LTβR, can induce damage in the cccDNA, leading to its degradation [2]. While said results were obtained by using recombinant, specific LTβR activating antibodies (one of which is BS1 that I extensively used during my PhD thesis), another research group reported that natural LTβR ligands on the membrane of activated T-cells can induce similar effects *in vitro* [287]. Of important note, both studies point out that the antiviral effect comes with no cytotoxicity.

Considering the unbroken need for novel antiviral strategies, as discussed *in extenso* previously, the idea of utilising an intracellular antiviral machinery to attack HBV is an interesting approach. Understanding underlying mechanisms of this process is of outstanding importance to further consider LTβR activation as an anti-HBV strategy in clinical settings.

A3B was previously described to be regulated by NF-κB in cancer cell lines [151], but not much was known about molecular mechanisms of A3B induction in non-transformed hepatocytes. I describe here that both arms of NF-κB signalling, the canonical (or classical) and the non-canonical (or alternative) pathway, are involved in the LTβR-activation-mediated A3B induction in dHepaRG. My *in silico* analysis revealed two putative NF-κB binding sites in the A3B promoter region. Electrophoretic mobility shift assays and chromatin immunoprecipitation confirmed a binding of NF-κB transcription factors to this genomic region. Of note, RelA, which is the main transcription factor involved in the canonical NF-κB signalling, was not found enriched at the A3B promoter, whereas RelB and p52, which are part of non-canonical NF-κB signalling. I in collaboration with Emmanuel Dejardin and Nicolas Gillet confirmed a more profound involvement of non-canonical NF-κB signalling in the A3B promoter engagement in luciferase-fusion assays, showing that in fact, the combination of RelB and p52 induced the strongest promoter activity. Pharmacological inhibition, combined with genetic loss of function methods revealed the involvement of both arms of NF-κB in A3B induction. I hypothesise that canonical NF-κB, while not being the main driver of A3B induction, increases the expression of the main components of non-canonical NF-κB, namely NIK, NF-κB2, and RelB. Therefore, it is involved in driving the expression of A3B by fuelling the

alternative arm of NF-κB. Further studies will try to unravel the exact interplay and involvement of NF-κB pathways in this process. Of note, naturally occurring SNPs in genes involved in NF-κB signaling were described to be linked to several diseases like type II diabetes [310], breast cancer [311], Non-Hodgkin Lymphoma [312] or inflammatory bowel disease [313]. It will be interesting to evaluate the effects of common SNPs in regard to the response to LTβR activation and downstream antiviral effects and the status of individual patients should be evaluated in clinical settings. SNPs leading to reduced function of NF-κB proteins might require higher doses of LTβR agonists, while SNPs promoting the protein function might need lower doses for strong antiviral effects or even confer an *a priori* resistance to HBV through elevated A3B expression levels.

Time course experiments revealed a "lag phase" in A3B mRNA induction, which was different to classical NF-κB target genes described so far. These observations were contradicting to the ChIP results, which showed an A3B promoter engagement already one day after treatment start not only by NF-κB transcription factors, but also by PolII. This suggested a possible post-transcriptional control of A3B mRNA stability. Thus, I looked into the small RNA transcriptome to find miRNAs that might confer a repression of A3B. In collaboration with Kristian Unger and the DKFZ Genomics and Proteomics Core Facility, I used small RNA sequencing, combined with RT-qPCR and *in silico* analysis, which resulted in one interesting hit: hsa-miR-138-5p. This miRNA was found to be slightly upregulated two days after BS1 treatment, when A3B mRNA was still in the "lag" phase, but was downregulated after four days of BS1 treatment, when A3B expression increased to higher levels. Expression analysis of this miRNA showed that the downregulation by BS1 treatment was dependent on both classical and alternative NF-κB signalling [3]. I speculate that NF-κB signalling could induce the expression of a repressor of hsa-miR-138-5p, or alternatively, that the p52 homodimer could directly bind and repress the hsa-miR-138-50 promoter [314].

The peculiar regulation of A3B could potentially represent a conserved mechanism to prevent somatic mutations of genomic DNA by A3B activity. Numerous studies linked A3B expression to a specific mutational pattern in cancer [315]. Additionally, hsa-miR-138-5p was described to be a tumour suppressor that controls several cellular processes linked to cancer development [316]. It is possible that hsa-miR-138-5p also controls A3B, which is a potential harm for genome integrity, as an additional level of its tumour suppressor function – thus being naturally selected and conserved besides it's here characterized role in the context of A3B biology. As such, it would prevent high A3B levels upon a short-term activation, which could happen often during local and transient inflammation, but long-term stimulation would then downregulate the miRNA, allowing high A3B levels, which are needed to efficiently fight persistent viruses like HBV. Concerning cancer, it will be interesting to see if a link between

hsa-miR-138-5p expression, A3B expression, and somatic mutations with A3B signatures can be found.

HBV cccDNA levels can efficiently be reduced by prolonged BS1 treatment [2] (**Figure 27, step 5**). However, interfering with the transcriptional activation or increasing levels of hsa-miR-138-5p will strongly inhibit A3B upregulation and anti-cccDNA effects. dHepaRG depleted for NF-κB kinases IKKβ and NIK display no reduction of cccDNA levels after long-term treatment. Furthermore, mimicking the overexpression of hsa-miR-138-5p leads to strongly reduced A3B levels and no detectable cccDNA reduction as well. My results raise important implications for novel therapeutic tools using LTβR agonists for the treatment of patients chronically infected with HBV. Important to mention, it was demonstrated that long-term activation of the LTβR in hepatocytes is tumorigenic [317]. Thus, long-term treatment (e.g. >8 weeks) of patients should be avoided to prevent unlikely, but possible adverse effects and should be only given for a limited period. Another therapeutic option to reach elevated A3B expression levels might be to reduce hsa-miR-138-5p levels or interfere with its transcription. Circular RNAs can act as "miRNA sponges" to sequester miRNAs and prevent them from binding to their targets [318] and "antagomirs" were described in literature to inhibit miRNA function *in vitro* [319] and *in vivo* [320]. These approaches might present useful strategies to transiently inhibit hsa-miR-138-5p to induce A3B, if save delivery methods (e.g. tissue restricted nanoparticles) are available and efficient in the context of CHB. Nonetheless, as constant LTβR activation, this approach might turn out to be a two-edged sword, since it is repressing a tumour-suppressor and adverse effects of time-restricted anti-miRNA treatments need to be ruled out first *in vivo*.

To assess if a time-restricted treatment of cells in culture would lead to an increased mutational load, I in collaboration with the company CeGaT, used ultra-deep sequencing (average sequencing depth of >1,000x) of 766 cancer-related genes. No differences were found between BS1-treated and untreated cells. These findings indicate that a time-restricted administration of BS1, while providing strong antiviral effects, had no obvious adverse effects on the genome. Nevertheless, more in-depth assessment of the effects on genomic DNA, especially also in *in vivo* studies, should be done to provide a high level of safety.

Interestingly, I found that A3B expression is in part controlled by HBV, which was previously described in the context of interferon β [321]. Non-infected cells upregulated A3B after BS1 to a higher extent than HBV infected cells. ChIP analysis revealed that the activating histone mark H3K4me3, which is increased at the A3B promoter after treatment in non-infected, was not observed anymore in HBV infected cells. Further studies will be necessary to shine a light on exact mechanisms and the relevance of those observations in the context of clinical settings

As a member of the APOBEC3 family, A3B was suggested to deaminate exclusively ssDNA [291, 293], which for instance occurs during reverse transcription of the HBV pgRNA [292]. However, I here show that both an X-deficient HBV (i.e. transcriptionally inactive) and a replication-deficient recombinant HBV (i.e. lacking the reverse transcriptase), were sensitive to LTβR-activation-mediated cccDNA degradation. On the one hand, my findings indicate that the anti-cccDNA effect observed are not due to a reimport of mutated or damaged rcDNAs or other replicative intermediates as suggested by others [292]. On the other hand, the observation that X-deficient HBV can also be degraded as a consequence of BS1-treatment is enigmatic. HBV lacking HBx was shown to be transcriptionally inactive [48] and considering that A3B only has ssDNA deaminase activity, a special mechanism behind the cccDNA degradation of X-deficient HBV should be discussed. Actively transcribing HBV could offer a target ssDNA to A3B for deamination, but this is not expected to happen in this system. Thus, it remains to be determined, if A3B (I) possesses an unknown DNA helicase activity to unwind cccDNA, (II) can act on ssDNA that occurs naturally in a transcription-independent manner (e.g. "breathing" of DNA [322-324]), (III) can act on dsDNA, or (IV) acts on ssDNA downstream of a protein actively unwinding cccDNA, which might also be induced by LTβR activity. However, my findings indicate that a treatment aiming to induce A3B against HBV could be effective in patients with lowly active or non-active cccDNA (i.e. chronic carriers). Therefore, this treatment could be used before any reactivation of HBV.

Finally, it will be interesting to address the effect of A3B induction on integrated cccDNA and how this is involved in the subsequent degradation of cccDNA. The integration event, as discussed previously, might happen early and is involved in liver pathogenesis [80]. In addition, the probability of integration events increases over time, therefore it is of high importance to diagnose patients early after infection and start the treatment as soon as possible. I speculate that if patients are treated before or early after integration events occur, the cccDNA degradation, together with a natural turnover of hepatocytes in the liver could lead to an eradication of the viral infection, especially if the spread of the virus is prevented by the additional administration of e.g. tenofovir.

In summary, I here presented that NF-κB signalling, downstream of the activation of the LTβR, leads to A3B induction. Beyond that, I describe hsa-miR-138-5p as a potent negative regulator of A3B mRNA. Dysfunctional NF-κB and aberrant expression of hsa-miR-138-5p prevent an increase in A3B levels and cccDNA degradation. I believe that inhibiting hsa-miR-138-5p function in general or more specifically binding to A3B as a therapeutic approach, could, in a time-restricted setting, ensure high A3B expression and therefore increase the effectiveness of LTβR agonist-based treatments.

8.2 Aim 2: Hypoxia reduces antiviral effects of LTβR activation and offers a niche for HBV to avoid immune responses

Adapted from my written and experimental contribution in Riedl*, Faure-Dupuy* [4]: In the frame of the second aim of my PhD thesis, I describe how hypoxia, and even more generally HIF1α stabilisation, can promote HBV persistence by blocking antiviral cellular responses. In patients, areas with strong positivity for HBcAg are associated with "HIF1α-high" areas, whereas A3B is reduced in those. *In vitro*, cellular responses to BS1 treatment are reduced under HIF1α stabilisation, preventing efficient cccDNA reduction. This process is independent of HIF1α transcriptional activity and involves reduction of RelB protein. A graphical illustration of my findings is presented in **Figure 28** (adapted from Riedl*, Faure-Dupuy*, *et al.* [4]).
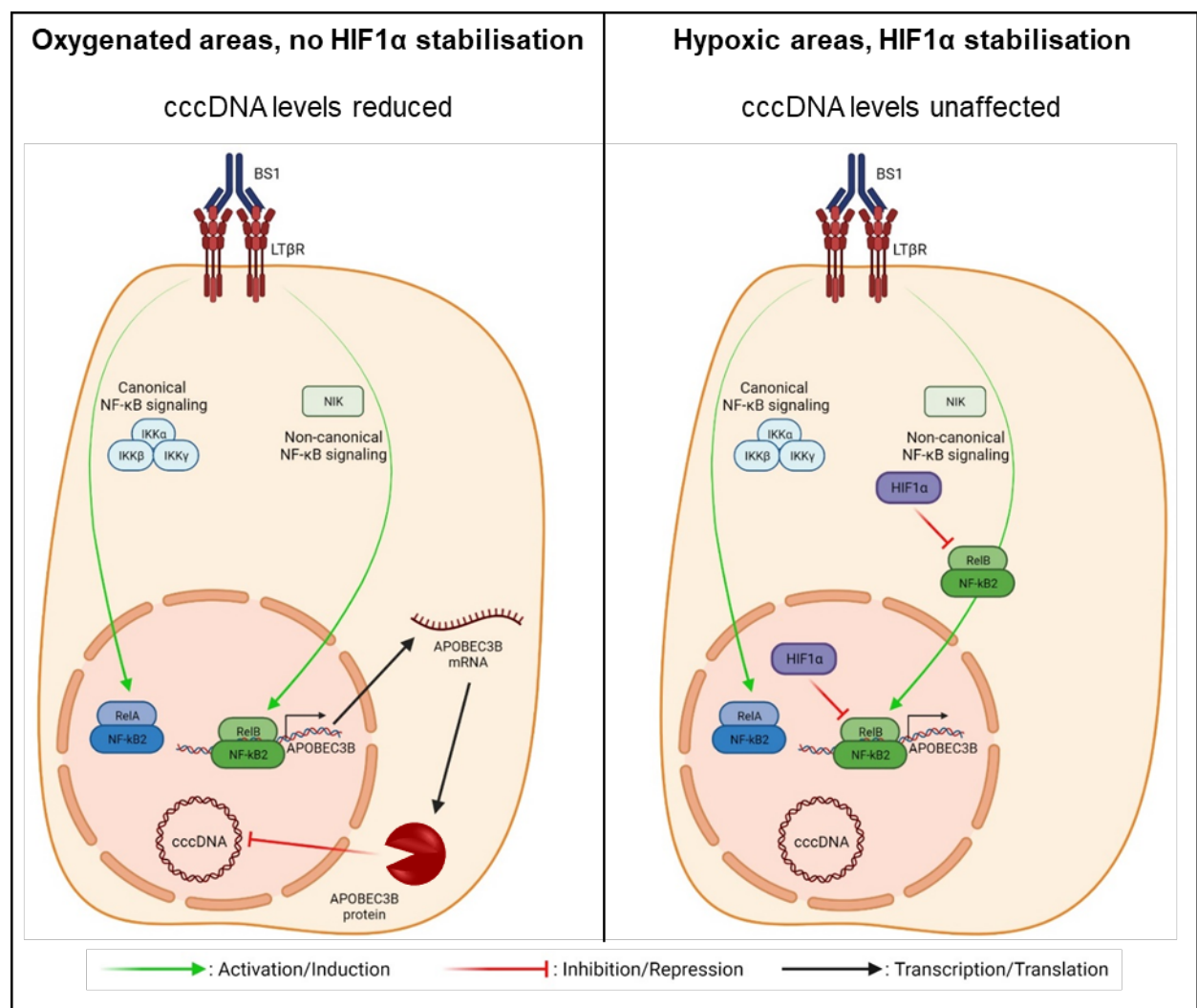
Figure 29: NF-κB and hsa-miR-138-5p control APOBEC3B-mediated cccDNA degradation (Adapted from Riedl*, Faure-Dupuy*, *et al.* [4])

(Adapted from my written and experimental contribution in Riedl*, Faure-Dupuy*, *et al.* [140]): Schematic representation of the key findings of aim 2 of my PhD thesis. In well-oxygenated areas of the liver, where HIF1α stabilisation is not present, lymphotoxin beta receptor (LTβR) activation, here depicted is the agonisation of the receptor by BS1, leads to the induction of APOBEC3B mRNA in a RelB/p52-dependent manner. The upregulation of APOBEC3B eventually leads to a degradation of covalently closed circular DNA (cccDNA) (left panel). If HIF1α is stabilised, for example by hypoxia,

RelB protein levels are reduced, preventing efficient APOBEC3B induction and thereby cccDNA degradation (right panel). Since the exact mechanism of RelB protein reduction remains elusive, HIF1α is shown to repress RelB both in the nucleus and in the cytoplasm.

Current treatments against HBV suffer from two major problems: NAs are efficiently in suppressing HBV, but have to be administered life-long to prevent a relapse; IFNα treatment increase rates of seroconversion, leading to a "functional cure", but response rates can be low [15] and side effects can be severe [325, 326]. To overcome the limitations in treatment options for patients suffering from a chronic hepatitis B, numerous novel treatments are under development. These novel treatments include substances targeting HBV (e.g. the entry receptor burlevitide, or capsid assembly modulators), and substances activating the immune system. The latter have shown promising results both *in vitro* and *in vivo* [297, 327-330] and are of special interest, since the virus can hardly develop resistance against drugs targeting the host. Among immune-stimulatory treatments with diverse cellular targets (e.g. TLRs), the activation of the LTβR showed promising results in directly targeting the cccDNA and leading to its non-cytolytic degradation [2, 287], providing a relapse-free treatment option. Activation of the LTβR leads to the induction of the antiviral cytidine deaminase A3B, which is the source of the mutational damage to the cccDNA. Note wise, the natural source of LTβR ligands (i.e. LTα1β2 trimers) are membrane bound protein complexes on activated specific T-cells. Engineered HBV-specific chimeric antigen receptor T-cell cells were even successfully used to induce A3B induction and non-cytopathic purging of cccDNA [287]. The LTβR activation and subsequent A3B induction might play an important role in the control of an acute HBV infection. High levels of A3B mRNA were detected in acute HBV infected patients, whereas in CHB patients, only little A3B expression was detected [299], and in those patients usually HBV-specific T-cells are highly reduced in number [132]. The effectiveness of LTβR-mediated HBV clearance therefore not only is important to understand in the context of treatments with LTβR agonists but also in regard to the natural antiviral response mediated by the immune system.

A cross-talk between NF-κB and HIF1α signalling was described in literature by several research groups. HIF1α was shown to be upregulated transcriptionally by NF-κB signalling [243, 247] and to promote [242, 331, 332] or inhibit [239, 333] NF-κB signalling. The peculiar interplay between NF-κB and HIF1α might be a result of the different models and cell types used by different research groups and could indeed also be context-specific. Noteworthy, I was able to confirm that inflammatory LTβR signalling induced HIF1α on the protein level, even in the absence of hypoxia. Chronic infection with HBV, especially if left untreated, results in progressing fibrosis, which by itself can influence the perfusion of the liver with oxygenated blood, thus disrupting the natural oxygen gradient and promote the emergence of hypoxic zones [221, 334]. Furthermore, as mentioned before, inflammatory signalling can induce

HIF1α in inflammatory liver disease, and HBV itself has also been described to induce HIF1α [335, 336]. In liver sections of patients suffering from a chronic hepatitis B in the immune-active phase, I describe here a positive correlation between HIF1α and HBcAg positive nuclei, indicating that HBV is predominantly found in areas of HIF1α stabilising conditions. Interestingly, A3B mRNA expression was found to be low in those areas and high in areas of reduced HIF1α protein levels, suggesting that, *in vivo*, anti-HBV immune responses relying *inter alia* on A3B are dampened in "HIF1α-high" areas. Importantly, those areas potentially offer HBV a niche to escape immune-mediated eradication by the induction of intracellular effector molecules like A3B. The reservoir of HBV in "HIF1α-high" zones could then give rise to a new wave of infections if the immune environment in the liver changes (e.g. by immune-suppressive treatment or the natural course of the HBV infection). Furthermore, I speculate that the prevention of HIF1α stabilisation or the inhibition of HIF1α transcriptional activation during immune-active phases of a CHB infection, or during immune-activating treatments, could allow more efficient responses against HBV and probably induce an immune-mediated eradication of HBV.

My observations in patients were confirmed *in vitro*: HIF1α stabilisation, mediated either by low oxygen content or different HIF1α stabilising small molecules, strongly impaired the BS1-treatment induced A3B induction and cccDNA degradation. Moreover, in cells overexpressing HIF1α in an inducible manner, A3B showed decreased expression levels dependently on the dose of doxycycline used to induce HIF1α. Taken together, these results confirm that HIF1α is a negative regulator of A3B expression. Furthermore, I could provide evidence that not only LTβR-mediated antiviral responses are impaired by HIF1α stabilisation, but also that the response to other antiviral molecules, namely IFNα [2], IFNγ, and TNFα [299] show decreased anti-cccDNA activity. Additionally, cells were responding less to different NF-κB inducing molecules. These data suggest that HIF1α stabilisation impairs the induction of immune mediators, highlighting that liver regions enriched for HIF1α signalling might offer a niche for HBV and allow persistence.

I in collaboration with Emmanuel Dejardin and Nicolas Gillet have previously shown that RelB is one of the main transcription factors involved in A3B induction. Together with Maude Rolland and Emmanuel Dejardin, I could demonstrate that RelB was reduced on the protein level under HIF1α stabilising conditions *in vitro* and *in vivo*, but not on mRNA level. While RelA was nearly unaffected by HIF1α stabilisation on protein level and nuclear translocation upon BS1 treatment, RelB was reduced both in the cytosolic fraction and in the nuclear faction. Considering the unchanged mRNA levels of RelB, several hypothesis can be made: HIF1α stabilisation leads to (I) reduced nuclear export of RelB mRNA, (II) reduced translation rate, or (III) reduced post-translational stability of the RelB protein. Further studies are necessary to find the exact mechanisms of HIF1α-mediated RelB decrease.

Here I also report that hypoxia completely blocks the effects of LTβR-activation proteome-wide. For instance, many pathways (e.g. KEGG pathways for mRNA processing and ribosome) involved in transcription and translation were downregulated in BS1-treated cells cultured under hypoxia, whereas they were strongly induced in BS1-treated cells cultured under normoxic conditions. HIF1α knock-down, although sufficient to rescue RelB protein levels, A3B mRNA levels and anti-cccDNA effects of BS1 treatment under hypoxia, was not sufficient to rescue this proteome-wide "hypoxic state" of the cells, indicating a direct effect of HIF1α onto RelB. This hypothesis is supported by the fact that I found that ARNT, which is the main interaction partner for HIF1α to exert its activity as a transcription factor, was dispensable for the observed reduction of RelB protein and A3B mRNA levels under HIF1α stabilising conditions. This suggested a "non-canonical" role of HIF1α in this process, independent of its function as a transcription factor. Notably, I could not find any indication that HIF2α, another important transcription factor involved in responses to low oxygen levels, plays a significant role in this process.

Taken together, the cell-intrinsic (antiviral) response to immune-stimulatory treatments with different ligands was blocked under HIF1α stabilising conditions. In the case of BS1 treatment, RelB protein is strongly reduced, which prevents upregulation of A3B; in the case of other treatments, I speculate that the lack of response to and the ineffectiveness against HBV of the treatment might be a result of a general downregulation of pathways executing the response to the immune-stimulatory molecules, such as pathways involved in transcription and translation. This finding has clear indications for immune-stimulatory treatment in patients, either for existing (IFNα) or experimental (e.g. TLR ligands) drugs. Modulation of HIF1α signalling, especially in patients with progressed liver fibrosis, should be considered to (I) increase effectiveness of the treatment, (II) overcome HIF1α-mediated immune-suppressive niches, and thereby (III) be able to lower the dose and/or the duration of the treatment to avoid overshooting side effects, which might prevent adherence of patients to the treatment. Recently developed HIF1α inhibitors [337] might be promising candidates for combinatory treatments with immune-activating drugs [297, 328] that stimulate the intra-cellular, but also immune-cell mediated antiviral response in the whole liver.

In summary, I here present that HIF1α is both necessary and sufficient to prevent LTβR-mediated A3B induction and subsequent cccDNA degradation in a RelB dependent manner. I consider the inhibitory role of HIF1α on RelB protein levels an interesting pharmacological target in the case of LTβR activating therapeutic approaches, which could be extrinsic (e.g. agonising antibodies like BS1) or intrinsic by activating or generating HBV-specific T-cells. Preventing HIF1α with inhibitors from reducing RelB protein levels could ensure increased efficiency of such treatments.

9   References

1.   Tsukuda, S., et al., *Hepatitis B virus biology and life cycle.* 2020. **182**.
2.   Lucifora, J., et al., *Specific and Nonhepatotoxic Degradation of Nuclear Hepatitis B Virus cccDNA.* 2014. **343**.
3.   Faure-Dupuy, S., et al., *Control of APOBEC3B induction and cccDNA decay by NF-κB and miR-138-5p.* 2021. **3**.
4.   Riedl, T., et al., *Hypoxia-Inducible Factor 1 Alpha–Mediated RelB/APOBEC3B Down-regulation Allows Hepatitis B Virus Persistence.* 2021. **74**.
5.   James, S.L., et al., *Global, regional, and national incidence, prevalence, and years lived with disability for 354 diseases and injuries for 195 countries and territories, 1990–2017: a systematic analysis for the Global Burden of Disease Study 2017.* 2018. **392**.
6.   Razavi-Shearer, D., et al., *Global prevalence, treatment, and prevention of hepatitis B virus infection in 2016: a modelling study.* 2018. **3**.
7.   Schweitzer, A., et al., *Estimations of worldwide prevalence of chronic hepatitis B virus infection: a systematic review of data published between 1965 and 2013.* 2015. **386**.
8.   Chang, M.S., et al., *Epidemiology of hepatitis B and the role of vaccination.* 2017. **31**.
9.   Schmit, N., et al., *The global burden of chronic hepatitis B virus infection: comparison of country-level prevalence estimates from four research groups.* 2021. **50**.
10.   Thuy, P.T.B., et al., *Genotype X/C recombinant (putative genotype I) of hepatitis B virus is rare in Hanoi, Vietnam-genotypes B4 and C1 predominate.* 2010. **82**.
11.   Olinger, C.M., et al., *Possible New Hepatitis B Virus Genotype, Southeast Asia.* 2008. **14**.
12.   Tatematsu, K., et al., *A Genetic Variant of Hepatitis B Virus Divergent from Known Human and Ape Genotypes Isolated from a Japanese Patient and Provisionally Assigned to New Genotype J.* 2009. **83**.
13.   Dény, P., et al., *Hepatitis B virus: From diagnosis to treatment.* 2010. **58**.
14.   Locarnini, S., et al., *Possible origins and evolution of the hepatitis B virus (HBV).* 2013. **23**.
15.   Kao, J.-H., et al., *Hepatitis B genotypes and the response to interferon therapy.* 2000. **33**.
16.   Kao, J.-H., et al., *Hepatitis B genotypes correlate with clinical outcomes in patients with chronic hepatitis B.* 2000. **118**.
17.   Liu, L. and *Fields Virology, 6th Edition.* 2014. **59**.
18.   Velkov, S., et al., *The Global Hepatitis B Virus Genotype Distribution Approximated from Available Genotyping Data.* 2018. **9**.
19.   Kidd-Ljunggren, K., et al., *High levels of hepatitis B virus DNA in body fluids from chronic carriers.* 2006. **64**.
20.   Neuveut, C., et al., *Mechanisms of HBV-related hepatocarcinogenesis.* 2010. **52**.
21.   Chang, M.-H. and *Natural history and clinical management of chronic hepatitis B virus infection in children.* 2008. **2**.
22.   Rajoriya, N., et al., *How viral genetic variants and genotypes influence disease and treatment outcome of chronic hepatitis B. Time for an individualised approach?* 2017. **67**.
23.   Lin, C.-L., et al., *The clinical implications of hepatitis B virus genotype: Recent advances.* 2011. **26**.
24.   Liang, T.J. and *Hepatitis B: The virus and disease.* 2009. **49**.
25.   Moolla, N., et al., *Regulatory elements of hepatitis B virus transcription.* 2002. **9**.
26.   Seeger, C., et al., *Molecular biology of hepatitis B virus infection.* 2015. **479-480**.
27.   Soussan, P., et al., *The expression of hepatitis B spliced protein (HBSP) encoded by a spliced hepatitis B virus RNA is associated with viral replication and liver fibrosis.* 2003. **38**.
28.   Murray, P.R.R.K.S.P.M.A., *Medical microbiology.* 2021.
29.   Mabit, H.l.n., et al., *Intracellular Hepadnavirus Nucleocapsids Are Selected for Secretion by Envelope Protein-Independent Membrane Binding.* 2000. **74**.

30.   Perlman, D.H., et al., *Reverse transcription-associated dephosphorylation of hepadnavirus nucleocapsids.* 2005. **102**.

31.   Yeh, C.T., et al., *The arginine-rich domain of hepatitis B virus precore and core proteins contains a signal for nuclear transport.* 1990. **64**.

32.   Standring, D.N., et al., *A signal peptide encoded within the precore region of hepatitis B virus directs the secretion of a heterogeneous population of e antigens in Xenopus oocytes.* 1988. **85**.

33.   Parekh, S., et al., *Genome Replication, Virion Secretion, and e Antigen Expression of Naturally Occurring Hepatitis B Virus Core Promoter Mutants.* 2003. **77**.

34.   Nassal, M. and *Hepatitis B viruses: Reverse transcription a different way.* 2008. **134**.

35.   Okamoto, H., et al., *Point mutation in the S gene of hepatitis B virus for a d/y or w/r subtypic change in two blood donors carrying a surface antigen of compound subtype adyr or adwr.* 1987. **61**.

36.   Wei, X., et al., *Expression, Purification, and Characterization of an Active RNase H Domain of the Hepatitis B Viral Polymerase.* 1996. **271**.

37.   Bruss, V., et al., *The role of envelope proteins in hepatitis B virus assembly.* 1991. **88**.

38.   Wunderlich, G., et al., *Characterization of early hepatitis B virus surface protein oligomers.* 1996. **141**.

39.   Persing, D.H., et al., *The preS1 protein of hepatitis B virus is acylated at its amino terminus with myristic acid.* 1987. **61**.

40.   Meier, A., et al., *Myristoylated PreS1-domain of the hepatitis B virus L-protein mediates specific binding to differentiated hepatocytes.* 2013. **58**.

41.   Yan, H., et al., *Sodium taurocholate cotransporting polypeptide is a functional receptor for human hepatitis B and D virus.* 2012. **1**.

42.   Gilbert, R.J.C., et al., *Hepatitis B small surface antigen particles are octahedral.* 2005. **102**.

43.   Heermann, K.H., et al., *Large surface proteins of hepatitis B virus containing the pre-s sequence.* 1984. **52**.

44.   Patient, R., et al., *Morphogenesis of hepatitis B virus and its subviral envelope particles.* 2009. **11**.

45.   Ganem, D., et al., *Hepatitis B Virus Infection — Natural History and Clinical Consequences.* 2004. **350**.

46.   Bruss, V. and *Hepatitis B virus morphogenesis.* 2007. **13**.

47.   Herrscher, C., P. Roingeard, and E. Blanchard, *Hepatitis B Virus Entry into Cells.* Cells, 2020. **9**(6).

48.   Lucifora, J., et al., *Hepatitis B virus X protein is essential to initiate and maintain virus replication after infection.* 2011. **55**.

49.   Zoulim, F., et al., *Woodchuck hepatitis virus X protein is required for viral infection in vivo.* 1994. **68**.

50.   Decorsière, A., et al., *Hepatitis B virus X protein identifies the Smc5/6 complex as a host restriction factor.* 2016. **531**.

51.   Murphy, Christopher M., et al., *Hepatitis B Virus X Protein Promotes Degradation of SMC5/6 to Enhance HBV Replication.* 2016. **16**.

52.   Melegari, M., et al., *Hepatitis B Virus DNA Replication Is Coordinated by Core Protein Serine Phosphorylation and HBx Expression.* 2005. **79**.

53.   Lara-Pezzi, E., et al., *The hepatitis B virus X protein up-regulates tumor necrosis factor α gene expression in hepatocytes.* 1998. **28**.

54.   Tian, Y., et al., *HBV regulated RhoC expression in HepG2.2.15 cells by enhancing its promoter activity.* 2013. **53**.

55.   Wei, C., et al., *The Hepatitis B Virus X Protein Disrupts Innate Immunity by Downregulating Mitochondrial Antiviral Signaling Protein.* 2010. **185**.

56.   Wei, Y., et al., *Molecular biology of the hepatitis B virus and role of the X gene.* 2010. **58**.

57.   Fallot, G., et al., *Diverse roles of hepatitis B virus in liver cancer.* 2012. **2**.

58.   Schulze, A., et al., *Hepatitis B virus infection initiates with a large surface protein-dependent binding to heparan sulfate proteoglycans.* 2007. **46**.

59.   Leistner, C.M., et al., *Role of glycosaminoglycans for binding and infection of hepatitis B virus.* 2007. **0**.

60.   Sun, Y., et al., *The Hepatitis B Surface Antigen Binding Protein: An Immunoglobulin G Constant Region-Like Protein That Interacts With HBV Envelop Proteins and Mediates HBV Entry.* 2018. **8**.

61.   Iwamoto, M., et al., *Epidermal growth factor receptor is a host-entry cofactor triggering hepatitis B virus internalization.* 2019. **116**.

62.   Hao, X., et al., *Single-Particle Tracking of Hepatitis B Virus-like Vesicle Entry into Cells.* 2011. **7**.

63.   Huang, H.-C., et al., *Entry of Hepatitis B Virus into Immortalized Human Primary Hepatocytes by Clathrin-Dependent Endocytosis.* 2012. **86**.

64.   Macovei, A., et al., *Hepatitis B Virus Requires Intact Caveolin-1 Function for Productive Infection in HepaRG Cells.* 2010. **84**.

65.   Chen, S.-W., et al., *Modulation of hepatitis B virus infection by epidermal growth factor secreted from liver sinusoidal endothelial cells.* 2020. **10**.

66.   Rabe, B., et al., *Lipid-Mediated Introduction of Hepatitis B Virus Capsids into Nonsusceptible Cells Allows Highly Efficient Replication and Facilitates the Study of Early Infection Events.* 2006. **80**.

67.   Kann, M., et al., *Phosphorylation-dependent Binding of Hepatitis B Virus Core Particles to the Nuclear Pore Complex.* 1999. **145**.

68.   Rabe, B., et al., *Nuclear import of hepatitis B virus capsids and release of the viral genome.* 2003. **100**.

69.   Wang, G.-H., et al., *The reverse transcriptase of hepatitis B virus acts as a protein primer for viral DNA synthesis.* 1992. **71**.

70.   Gerlich, W. and *Hepatitis B virus contains protein attached to the 5' terminus of its complete DNA strand.* 1980. **21**.

71.   Guo, H., et al., *Characterization of the Intracellular Deproteinized Relaxed Circular DNA of Hepatitis B Virus: an Intermediate of Covalently Closed Circular DNA Formation.* 2007. **81**.

72.   Boyd, A., et al., *Decay of ccc-DNA marks persistence of intrahepatic viral DNA synthesis under tenofovir in HIV-HBV co-infected patients.* 2016. **65**.

73.   Bock, C.T., et al., *Structural organization of the hepatitis B virus minichromosome.* 2001. **307**.

74.   Pollicino, T., et al., *Hepatitis B Virus Replication Is Regulated by the Acetylation Status of Hepatitis B Virus cccDNA-Bound H3 and H4 Histones.* 2006. **130**.

75.   Zoulim, F. and *New insight on hepatitis B virus persistence from the study of intrahepatic viral cccDNA.* 2005. **42**.

76.   Yang, H.-C., et al., *Persistence of hepatitis B virus covalently closed circular DNA in hepatocytes: molecular mechanisms and clinical significance.* 2014. **3**.

77.   Mason, A.L., et al., *Molecular basis for persistent hepatitis B virus infection in the liver after clearance of serum hepatitis B surface antigen.* 1998. **27**.

78.   Marusawa, H., et al., *Latent hepatitis B virus infection in healthy individuals with antibodies to hepatitis B core antigen.* 2000. **31**.

79.   Werle–Lapostolle, B., et al., *Persistence of cccDNA during the natural history of chronic hepatitis B and decline during adefovir dipivoxil therapy1 ☆*2004. **126**.

80.   Tu, T., et al., *HBV DNA Integration: Molecular Mechanisms and Clinical Implications.* 2017. **9**.

81.   Ryu, D.-K., et al., *Proximity between the cap and 5' ε stem–loop structure is critical for the suppression of pgRNA translation by the hepatitis B viral polymerase.* 2010. **406**.

82.   Pollack, J.R., et al., *Site-specific RNA binding by a hepatitis B virus reverse transcriptase initiates two distinct reactions: RNA packaging and DNA synthesis.* 1994. **68**.

83.   Loeb, D.D., et al., *Sequence-independent RNA cleavages generate the primers for plus strand DNA synthesis in hepatitis B viruses: implications for other reverse transcribing elements.* 1991. **10**.

84.   Haines, K.M., et al., *The Sequence of the RNA Primer and the DNA Template Influence the Initiation of Plus-strand DNA Synthesis in Hepatitis B Virus.* 2007. **370**.

85.   Watanabe, T., et al., *Involvement of host cellular multivesicular body functions in hepatitis B virus budding.* 2007. **104**.

86.   Patient, R., et al., *Hepatitis B Virus Subviral Envelope Particle Morphogenesis and Intracellular Trafficking.* 2007. **81**.

87.   Wang, J., et al., *HBV Genome and Life Cycle*, in *Hepatitis B Virus Infection: Molecular Virology to Antiviral Drugs*, H. Tang, Editor. 2020, Springer Singapore: Singapore. p. 17-37.

88.   Locarnini, S., et al., *Strategies to control hepatitis B: Public policy, epidemiology, vaccine and drugs.* 2015. **62**.

89.   Fanning, G.C., et al., *Therapeutic strategies for hepatitis B virus infection: towards a cure.* Nat Rev Drug Discov, 2019. **18**(11): p. 827-844.

90.   Bertoletti, A., et al., *The immune tolerant phase of chronic HBV infection: new perspectives on an old concept.* 2015. **12**.

91.   Bertoletti, A., et al., *HBV infection and HCC: the 'dangerous liaisons'.* 2018. **67**.

92.   Kennedy, P., et al., *Immune Tolerant Chronic Hepatitis B: The Unrecognized Risks.* 2017. **9**.

93.   Mason, W.S., et al., *HBV DNA Integration and Clonal Hepatocyte Expansion in Chronic Hepatitis B Patients Considered Immune Tolerant.* 2016. **151**.

94.   Lampertico, P., et al., *EASL 2017 Clinical Practice Guidelines on the management of hepatitis B virus infection.* 2017. **67**.

95.   Volz, T., et al., *Impaired Intrahepatic Hepatitis B Virus Productivity Contributes to Low Viremia in Most HBeAg-Negative Patients.* 2007. **133**.

96.   Kwak, M.-S. and *Occult hepatitis B virus infection.* 2014. **6**.

97.   Levrero, M., et al., *Control of cccDNA function in hepatitis B virus infection.* 2009. **51**.

98.   Lavanchy, D. and *Hepatitis B virus epidemiology, disease burden, treatment, and current and emerging prevention and control measures.* 2004. **11**.

99.   Chen, H.-L. and *Seroepidemiology of Hepatitis B Virus Infection in Children.* 1996. **276**.

100.   CHEN, C.-J., et al., *Epidemiological characteristics and risk factors of hepatocellular carcinoma.* 1997. **12**.

101.   Flink, H.J., et al., *Relapse after treatment with peginterferon -2b alone or in combination with lamivudine in HBeAg positive chronic hepatitis B.* 2007. **56**.

102.   Kaymakoglu, S., et al., *Pegylated Interferon Alfa-2b Monotherapy and Pegylated Interferon Alfa-2b plus Lamivudine Combination Therapy for Patients with Hepatitis B Virus E Antigen-Negative Chronic Hepatitis B.* 2007. **51**.

103.   Papatheodoridis, G.V., et al., *The long-term outcome of interferon-α treated and untreated patients with HBeAg-negative chronic hepatitis B.* 2001. **34**.

104.   Janssen, H.L., et al., *Pegylated interferon alfa-2b alone or in combination with lamivudine for HBeAg-positive chronic hepatitis B: a randomised trial.* 2005. **365**.

105.   Lau, G.K.K., et al., *Peginterferon Alfa-2a, Lamivudine, and the Combination for HBeAg-Positive Chronic Hepatitis B.* 2005. **352**.

106.   Marcellin, P., et al., *Peginterferon Alfa-2a Alone, Lamivudine Alone, and the Two in Combination in Patients with HBeAg-Negative Chronic Hepatitis B.* 2004. **351**.

107.   Marzio, D.H.-D. and *Then and now: The progress in hepatitis B treatment over the past 20 years.* 2014. **20**.

108.   Belloni, L., et al., *IFN-α inhibits HBV transcription and replication in cell culture and in humanized mice by targeting the epigenetic regulation of the nuclear cccDNA minichromosome.* 2012. **122**.

109. Liu, F., et al., *Alpha-Interferon Suppresses Hepadnavirus Transcription by Altering Epigenetic Modification of cccDNA Minichromosomes.* 2013. **9**.

110. Liu, S., et al., *The effect of peginterferon alpha-2a vs. interferon alpha-2a on intrahepatic covalently closed circular DNA in HBeAg-positive chronic hepatitis B patients.* 2016. **40**.

111. De Ridder, R.J.J., et al., *Effect of long-term lamivudine therapy on histological outcome in chronic hepatitis b.* 2003. **125**.

112. Eun, J.R., et al., *Risk assessment for the development of hepatocellular carcinoma: According to on-treatment viral response during long-term lamivudine therapy in hepatitis B virus-related liver disease.* 2010. **53**.

113. Liaw, Y.-F., et al., *Lamivudine for Patients with Chronic Hepatitis B and Advanced Liver Disease.* 2004. **351**.

114. Hann, H.-W., et al., *A review of the one-year incidence of resistance to lamivudine in the treatment of chronic hepatitis B.* 2008. **2**.

115. Kim, K.M., et al., *Adefovir Dipivoxil Alone or in Combination with Ongoing Lamivudine in Patients with Decompensated Liver Disease and Lamivudine-resistant Hepatitis B Virus.* 2005. **20**.

116. Peters, M.G., et al., *Adefovir dipivoxil alone or in combination with lamivudine in patients with lamivudine-resistant chronic hepatitis B.* 2004. **126**.

117. Viganò, M., et al., *Drug safety evaluation of adefovir in HBV infection.* 2011. **10**.

118. Chang, T.-T., et al., *A Comparison of Entecavir and Lamivudine for HBeAg-Positive Chronic Hepatitis B.* 2006. **354**.

119. Leung, N., et al., *Early hepatitis B virus DNA reduction in hepatitis B e antigen-positive patients with chronic hepatitis B: A randomized international study of entecavir versus adefovir.* 2009. **49**.

120. Tenney, D.J., et al., *Long-term monitoring shows hepatitis B virus resistance to entecavir in nucleoside-naïve patients is rare through 5 years of therapy.* 2009. **49**.

121. Lai, C.-L., et al., *Telbivudine versus Lamivudine in Patients with Chronic Hepatitis B.* 2007. **357**.

122. Zeisel, M.B., et al., *Towards an HBV cure: state-of-the-art and unresolved questions—report of the ANRS workshop on HBV cure.* 2015. **64**.

123. Auyeung, Vincent C., et al., *Beyond Secondary Structure: Primary-Sequence Determinants License Pri-miRNA Hairpins for Processing.* 2013. **152**.

124. Bogomolov, P., et al., *Treatment of chronic hepatitis D with the entry inhibitor myrcludex B: First results of a phase Ib/IIa study.* 2016. **65**.

125. Kawamata, T., et al., *Structural determinants of miRNAs for RISC loading and slicer-independent unwinding.* 2009. **16**.

126. Aizarani, N., et al., *A human liver cell atlas reveals heterogeneity and epithelial progenitors.* 2019. **572**.

127. Bazinet, M., et al., *Safety and Efficacy of 48 Weeks REP 2139 or REP 2165, Tenofovir Disoproxil, and Pegylated Interferon Alfa-2a in Patients With Chronic HBV Infection Naïve to Nucleos(t)ide Therapy.* 2020. **158**.

128. Bazinet, M., et al., *Safety and efficacy of REP 2139 and pegylated interferon alfa-2a for treatment-naive patients with chronic hepatitis B virus and hepatitis D virus co-infection (REP 301 and REP 301-LTF): a non-randomised, open-label, phase 2 trial.* 2017. **2**.

129. Bandarra, D., et al., *HIF-1α restricts NF-κB dependent gene expression to control innate immunity signals.* 2014.

130. Adolph, M.B., et al., *Biochemical Basis of APOBEC3 Deoxycytidine Deaminase Activity on Diverse DNA Substrates.* 2018. **4**.

131. Acharya, P., et al., *Cellular Mechanisms of Liver Fibrosis.* 2021. **12**.

132. Ye, B., et al., *T-cell exhaustion in chronic hepatitis B infection: current knowledge and clinical significance.* Cell Death & Disease, 2015. **6**(3): p. e1694-e1694.

133. Refsland, E.W., et al., *The APOBEC3 Family of Retroelement Restriction Factors.* 2013.
134. Vasudevan, A.A.J., et al., *Structural features of antiviral DNA cytidine deaminases.* 2013. **394**.
135. Chiu, Y.-L., et al., *The APOBEC3 Cytidine Deaminases: An Innate Defensive Network Opposing Exogenous Retroviruses and Endogenous Retroelements.* 2008. **26**.
136. Sadeghpour, S., et al., *Human APOBEC3 Variations and Viral Infection.* 2021. **13**.
137. Maiti, A., et al., *Interactions of APOBEC3s with DNA and RNA.* Curr Opin Struct Biol, 2021. **67**: p. 195-204.
138. Milewska, A., et al., *APOBEC3-mediated restriction of RNA virus replication.* Sci Rep, 2018. **8**(1): p. 5960.
139. Zharkov, D.O. and *Base excision DNA repair.* 2008. **65**.
140. Yang, B., et al., *Virion-associated uracil DNA glycosylase-2 and apurinic/apyrimidinic endonuclease are involved in the degradation of APOBEC3G-edited nascent HIV-1 DNA.* J Biol Chem, 2007. **282**(16): p. 11667-75.
141. Jarmuz, A., et al., *An Anthropoid-Specific Locus of Orphan C to U RNA-Editing Enzymes on Chromosome 22.* 2002. **79**.
142. Conticello, S.G., et al., *Evolution of the AID/APOBEC Family of Polynucleotide (Deoxy)cytidine Deaminases.* 2005. **22**.
143. OhAinle, M., et al., *Adaptive Evolution and Antiviral Activity of the Conserved Mammalian Cytidine Deaminase <i>APOBEC3H</i>.* 2006. **80**.
144. Dang, Y., et al., *Identification of APOBEC3DE as Another Antiretroviral Factor from the Human APOBEC Family.* 2006. **80**.
145. Harris, R.S., et al., *APOBECs and virus restriction.* 2015. **479-480**.
146. Sawyer, S.L., et al., *Ancient Adaptive Evolution of the Primate Antiviral DNA-Editing Enzyme APOBEC3G.* 2004. **2**.
147. Zhang, J. and *Rapid evolution of primate antiviral enzyme APOBEC3G.* 2004. **13**.
148. Peng, G., et al., *Induction of APOBEC3 family proteins, a defensive maneuver underlying interferon-induced anti–HIV-1 activity.* 2006. **203**.
149. Bonvin, M., et al., *Interferon-inducible expression of APOBEC3 editing enzymes in human hepatocytes and inhibition of hepatitis B virus replication.* 2006. **43**.
150. Leonard, B., et al., *The PKC/NF-κB Signaling Pathway Induces APOBEC3B Expression in Multiple Human Cancers.* 2015. **75**.
151. Maruyama, W., et al., *Classical NF-κB pathway is responsible for APOBEC3B expression in cancer cells.* 2016. **478**.
152. Periyasamy, M., et al., *Induction of APOBEC3B expression by chemotherapy drugs is mediated by DNA-PK-directed activation of NF-κB.* 2021. **40**.
153. Kopp, E.B., et al., *NF-κB and Rel Proteins in Innate Immunity.* 1995.
154. Williams, L.M., et al., *Looking Down on NF-κB.* 2020. **40**.
155. Sun, S.-C., et al., *Regulation of nuclear factor-κB in autoimmunity.* 2013. **34**.
156. Hayden, M.S. and *Signaling to NF- B.* 2004. **18**.
157. Sun, S.-C. and *Non-canonical NF-κB signaling pathway.* 2011. **21**.
158. BEINKE, S., et al., *Functions of NF-κB1 and NF-κB2 in immune cell biology.* 2004. **382**.
159. Zhang, H., et al., *NF-κB in inflammation and renal diseases.* 2015. **5**.
160. Karin, M., et al., *NF-κB: linking inflammation and immunity to cancer development and progression.* 2005. **5**.
161. Takaesu, G., et al., *TAK1 is Critical for IκB Kinase-mediated Activation of the NF-κB Pathway.* 2003. **326**.
162. Liu, T., et al., *NF-κB signaling in inflammation.* 2017. **2**.
163. Liao, G., et al., *Regulation of the NF-κB-inducing Kinase by Tumor Necrosis Factor Receptor-associated Factor 3-induced Degradation.* 2004. **279**.

164.   Zarnegar, B.J., et al., *Noncanonical NF-κB activation requires coordinated assembly of a regulatory complex of the adaptors cIAP1, cIAP2, TRAF2 and TRAF3 and the kinase NIK.* 2008. **9**.

165.   Xiao, G., et al., *Induction of p100 Processing by NF-κB-inducing Kinase Involves Docking IκB Kinase α (IKKα) to p100 and IKKα-mediated Phosphorylation.* 2004. **279**.

166.   Xiao, G., et al., *NF-κB-Inducing Kinase Regulates the Processing of NF-κB2 p100.* 2001. **7**.

167.   Shehata, M.F., *Rel/Nuclear factor-kappa B apoptosis pathways in human cervical cancer cells.* Cancer Cell Int, 2005. **5**(1): p. 10.

168.   Jost, P.J., et al., *Aberrant NF-κB signaling in lymphoma: mechanisms, consequences, and therapeutic implications.* 2007. **109**.

169.   O'Brien, J., et al., *Overview of MicroRNA Biogenesis, Mechanisms of Actions, and Circulation.* 2018. **9**.

170.   Lee, R.C., et al., *The C. elegans heterochronic gene lin-4 encodes small RNAs with antisense complementarity to lin-14.* 1993. **75**.

171.   Ha, M., et al., *Regulation of microRNA biogenesis.* 2014. **15**.

172.   Lee, Y., et al., *MicroRNA genes are transcribed by RNA polymerase II.* 2004. **23**.

173.   CAI, X. and *Human microRNAs are processed from capped, polyadenylated transcripts that can also function as mRNAs.* 2004. **10**.

174.   Lee, Y. and *MicroRNA maturation: stepwise processing and subcellular localization.* 2002. **21**.

175.   Kim, V.N., et al., *Biogenesis of small RNAs in animals.* 2009. **10**.

176.   Krol, J., et al., *The widespread regulation of microRNA biogenesis, function and decay.* 2010. **11**.

177.   Davis, B.N., et al., *Mechanisms of control of microRNA biogenesis.* 2010.

178.   Lee, Y., et al., *The nuclear RNase III Drosha initiates microRNA processing.* 2003. **425**.

179.   Gregory, R.I., et al., *The Microprocessor complex mediates the genesis of microRNAs.* 2004. **432**.

180.   Ma, H., et al., *Lower and upper stem-single-stranded RNA junctions together determine the Drosha cleavage site.* 2013. **110**.

181.   Zeng, Y., et al., *Recognition and cleavage of primary microRNA precursors by the nuclear processing enzyme Drosha.* 2005. **24**.

182.   Yi, R. and *Exportin-5 mediates the nuclear export of pre-microRNAs and short hairpin RNAs.* 2003. **17**.

183.   Okada, C., et al., *A High-Resolution Structure of the Pre-microRNA Nuclear Export Machinery.* 2009. **326**.

184.   Bernstein, E., et al., *Role for a bidentate ribonuclease in the initiation step of RNA interference.* 2001. **409**.

185.   Grishok, A., et al., *Genes and Mechanisms Related to RNA Interference Regulate Expression of the Small Temporal RNAs that Control C. elegans Developmental Timing.* 2001. **106**.

186.   Hutvágner, G.r., et al., *A Cellular Function for the RNA-Interference Enzyme Dicer in the Maturation of the <i>let-7</i> Small Temporal RNA.* 2001. **293**.

187.   Zhang, H., et al., *Single Processing Center Models for Human Dicer and Bacterial RNase III.* 2004. **118**.

188.   Fukunaga, R., et al., *Dicer Partner Proteins Tune the Length of Mature miRNAs in Flies and Mammals.* 2012. **151**.

189.   Lee, H.Y., et al., *TRBP alters human precursor microRNA processing in vitro.* 2012. **18**.

190.   Azuma-Mukai, A., et al., *Characterization of endogenous human Argonautes and their miRNA partners in RNA silencing.* 2008. **105**.

191.   Dueck, A., et al., *microRNAs associated with the different human Argonaute proteins.* 2012. **40**.

192.   Liu, J., et al., *Argonaute2 Is the Catalytic Engine of Mammalian RNAi.* 2004. **305**.

193. Su, H., et al., *Essential and overlapping functions for mammalian Argonautes in microRNA silencing.* 2009. **23**.

194. Huntzinger, E., et al., *Gene silencing by microRNAs: contributions of translational repression and mRNA decay.* 2011. **12**.

195. Meister, G., et al., *Human Argonaute2 Mediates RNA Cleavage Targeted by miRNAs and siRNAs.* 2004. **15**.

196. Yoda, M., et al., *ATP-dependent human RISC assembly pathways.* 2010. **17**.

197. Khvorova, A., et al., *Functional siRNAs and miRNAs Exhibit Strand Bias.* 2003. **115**.

198. Schwarz, D.S., et al., *Asymmetry in the Assembly of the RNAi Enzyme Complex.* 2003. **115**.

199. Winter, J., et al., *Many roads to maturity: microRNA biogenesis pathways and their regulation.* Nat Cell Biol, 2009. **11**(3): p. 228-34.

200. Liep, J., et al., *Feedback networks between microRNAs and epigenetic modifications in urological tumors.* 2012. **7**.

201. Vrba, L., et al., *miRNA Gene Promoters Are Frequent Targets of Aberrant DNA Methylation in Human Breast Cancer.* 2013. **8**.

202. García-Cruz, R., et al., *The role of p19 and p21 H-Ras proteins and mutants in miRNA expression in cancer and a Costello syndrome cell model.* 2015. **16**.

203. Li, J., et al., *Species-specific mutual regulation of p53 and miR-138 between human, rat and mouse.* 2016. **6**.

204. Hu, Z., et al., *Hormonal Regulation of MicroRNA Expression in Steroid Producing Cells of the Ovary, Testis and Adrenal Gland.* 2013. **8**.

205. Ma, F., et al., *MiR-138 Suppresses Cell Proliferation by Targeting Bag-1 in Gallbladder Carcinoma.* 2015. **10**.

206. Mitomo, S., et al., *Downregulation of miR-138 is associated with overexpression of human telomerase reverse transcriptase protein in human anaplastic thyroid carcinoma cell lines.* 2008. **99**.

207. Zhang, H., et al., *MiR-138 Inhibits Tumor Growth Through Repression of EZH2 in Non-Small Cell Lung Cancer.* 2013. **31**.

208. XU, R., et al., *miR-138 suppresses the proliferation of oral squamous cell carcinoma cells by targeting Yes-associated protein 1.* 2015. **34**.

209. Li, B., et al., *MicroRNA-138 inhibits proliferation of cervical cancer cells by targeting c-Met.* 2016. **20**.

210. Cao, Q., et al., *Repression of E-cadherin by the polycomb group protein EZH2 in cancer.* 2008. **27**.

211. Sun, D.-K., et al., *MicroRNA-138 Regulates Metastatic Potential of Bladder Cancer Through ZEB2.* 2015. **37**.

212. Gao, S., et al., *Role of miR-138 in the regulation of larynx carcinoma cell metastases.* 2016. **37**.

213. You, C., et al., *Expression of miR-21 and miR-138 in colon cancer and its effect on cell proliferation and prognosis.* 2018.

214. Zheng, S., et al., *Downregulation of miR-138 predicts poor prognosis in patients with esophageal squamous cell carcinoma.* 2017. **20**.

215. Long, L., et al., *Down-regulation of miR-138 promotes colorectal cancer metastasis via directly targeting TWIST2.* 2013. **11**.

216. Yeh, Y.M., et al., *MicroRNA-138 suppresses ovarian cancer cell invasion and metastasis by targeting SOX4 and HIF-1α.* Int J Cancer, 2013. **133**(4): p. 867-78.

217. Jungermann, K., et al., *Oxygen: Modulator of metabolic zonation and disease of the liver.* 2000. **31**.

218. Kietzmann, T. and *Liver Zonation in Health and Disease: Hypoxia and Hypoxia-Inducible Transcription Factors as Concert Masters.* 2019. **20**.

219. Kisseleva, T., et al., *Molecular and cellular mechanisms of liver fibrosis and its regression.* 2021. **18**.
220. Ringelhan, M., et al., *The immunology of hepatocellular carcinoma.* 2018. **19**.
221. Foglia, B., et al., *Hypoxia, Hypoxia-Inducible Factors and Liver Fibrosis.* 2021. **10**.
222. Fukuda, R., et al., *HIF-1 Regulates Cytochrome Oxidase Subunits to Optimize Efficiency of Respiration in Hypoxic Cells.* 2007. **129**.
223. Giorgi, R.B., et al., *Severe Cushing Syndrome Due to Ectopic ACTH Secretion by Pheochromocytoma.* 2021. **5**.
224. Semenza, G.L. and *Oxygen Sensing, Homeostasis, and Disease.* 2011. **365**.
225. Semenza, Gregg L. and *Hypoxia-Inducible Factors in Physiology and Medicine.* 2012. **148**.
226. Bertout, J.A., et al., *The impact of O2 availability on human cancer.* 2008. **8**.
227. Kietzmann, T., *Metabolic zonation of the liver: The oxygen gradient revisited.* Redox Biol, 2017. **11**: p. 622-630.
228. Kaelin, W.G., et al., *Oxygen Sensing by Metazoans: The Central Role of the HIF Hydroxylase Pathway.* 2008. **30**.
229. Jaakkola, P., et al., *Targeting of HIF-α to the von Hippel-Lindau Ubiquitylation Complex by O$_2$-Regulated Prolyl Hydroxylation.* 2001. **292**.
230. Masson, N., et al., *Independent function of two destruction domains in hypoxia-inducible factor-α chains activated by prolyl hydroxylation.* 2001. **20**.
231. Maxwell, P.H., et al., *The tumour suppressor protein VHL targets hypoxia-inducible factors for oxygen-dependent proteolysis.* 1999. **399**.
232. Cockman, M.E., et al., *Hypoxia Inducible Factor-α Binding and Ubiquitylation by the von Hippel-Lindau Tumor Suppressor Protein.* 2000. **275**.
233. Kamura, T., et al., *Activation of HIF1alpha ubiquitination by a reconstituted von Hippel-Lindau (VHL) tumor suppressor complex.* 2000. **97**.
234. Lando, D. and *FIH-1 is an asparaginyl hydroxylase enzyme that regulates the transcriptional activity of hypoxia-inducible factor.* 2002. **16**.
235. Hirsilä, M., et al., *Characterization of the Human Prolyl 4-Hydroxylases That Modify the Hypoxia-inducible Factor.* 2003. **278**.
236. Ehrismann, D., et al., *Studies on the activity of the hypoxia-inducible-factor hydroxylases using an oxygen consumption assay.* 2007. **401**.
237. Multhoff, G., et al., *Hypoxia Compromises Anti-Cancer Immune Responses.* 2020.
238. Kumar, V., et al., *Hypoxia-inducible factors in regulation of immune responses in tumour microenvironment.* 2014. **143**.
239. D'Ignazio, L., et al., *NF-κB and HIF crosstalk in immune responses.* 2016. **283**.
240. Bandarra, D., et al., *A tale of two transcription factors: NF-kB and HIF crosstalk.* 2013. **1**.
241. Koong, A.C., et al., *Hypoxia causes the activation of nuclear factor kappa B through the phosphorylation of I kappa B alpha on tyrosine residues.* 1994. **54**.
242. Cummins, E.P., et al., *Prolyl hydroxylase-1 negatively regulates I B kinase-beta, giving insight into hypoxia-induced NF B activity.* 2006. **103**.
243. Rius, J., et al., *NF-κB links innate immunity to the hypoxic response through transcriptional regulation of HIF-1α.* 2008. **453**.
244. Cramer, T., et al., *HIF-1α Is Essential for Myeloid Cell-Mediated Inflammation.* 2003. **112**.
245. Karhausen, J., et al., *Epithelial hypoxia-inducible factor-1 is protective in murine experimental colitis.* 2004. **114**.
246. Wright, C.W., et al., *The Aryl Hydrocarbon Nuclear Translocator Alters CD30-Mediated NF-κB–Dependent Transcription.* 2009. **323**.
247. van Uden, P., et al., *Regulation of hypoxia-inducible factor-1α by NF-κB.* 2008. **412**.
248. Saint Martin, A., C. Castañeda, and M. Robles-Flores, *The Role of Hypoxia-Inducible Factors in Cancer Resistance.* Journal of Cell Signaling, 2017. **2**.

249. Gripon, P., et al., *Infection of a human hepatoma cell line by hepatitis B virus.* Proc Natl Acad Sci U S A, 2002. **99**(24): p. 15655-60.

250. Schulze-Bergkamen, H., et al., *Primary human hepatocytes--a valuable tool for investigation of apoptosis and hepatitis B virus infection.* J Hepatol, 2003. **38**(6): p. 736-44.

251. Dejardin, E., et al., *Regulation of major histocompatibility complex class I expression by NF-kappaB-related proteins in breast cancer cells.* Oncogene, 1998. **16**(25): p. 3299-307.

252. Cao, J., et al., *An easy and efficient inducible CRISPR/Cas9 platform with improved specificity for multiple gene targeting.* Nucleic Acids Res, 2016. **44**(19): p. e149.

253. Namineni, S., et al., *A dual role for hepatocyte-intrinsic canonical NF-κB signaling in virus control.* 2020. **72**.

254. Labun, K., et al., *CHOPCHOP v2: a web tool for the next generation of CRISPR genome engineering.* Nucleic Acids Res, 2016. **44**(W1): p. W272-6.

255. Seitz, S., et al., *A Slow Maturation Process Renders Hepatitis B Virus Infectious.* Cell Host Microbe, 2016. **20**(1): p. 25-35.

256. Rad, R., et al., *PiggyBac transposon mutagenesis: a tool for cancer gene discovery in mice.* Science, 2010. **330**(6007): p. 1104-7.

257. Gao, W. and J. Hu, *Formation of hepatitis B virus covalently closed circular DNA: removal of genome-linked protein.* J Virol, 2007. **81**(12): p. 6164-74.

258. Parekh, S., et al., *The impact of amplification on differential expression analyses by RNA-seq.* Sci Rep, 2016. **6**: p. 25533.

259. Macosko, E.Z., et al., *Highly Parallel Genome-wide Expression Profiling of Individual Cells Using Nanoliter Droplets.* Cell, 2015. **161**(5): p. 1202-1214.

260. Love, M.I., W. Huber, and S. Anders, *Moderated estimation of fold change and dispersion for RNA-seq data with DESeq2.* Genome Biol, 2014. **15**(12): p. 550.

261. Federico, A. and S. Monti, *hypeR: an R package for geneset enrichment workflows.* Bioinformatics, 2020. **36**(4): p. 1307-1308.

262. Luo, W. and C. Brouwer, *Pathview: an R/Bioconductor package for pathway-based data integration and visualization.* Bioinformatics, 2013. **29**(14): p. 1830-1.

263. Shi, J., et al., *mirPRo-a novel standalone program for differential expression and variation analysis of miRNAs.* Sci Rep, 2015. **5**: p. 14617.

264. Jiang, H., et al., *Skewer: a fast and accurate adapter trimmer for next-generation sequencing paired-end reads.* BMC Bioinformatics, 2014. **15**: p. 182.

265. Li, H. and R. Durbin, *Fast and accurate short read alignment with Burrows-Wheeler transform.* Bioinformatics, 2009. **25**(14): p. 1754-60.

266. Mose, L.E., et al., *ABRA: improved coding indel detection via assembly-based realignment.* Bioinformatics, 2014. **30**(19): p. 2813-5.

267. Dejardin, E., et al., *The lymphotoxin-beta receptor induces different patterns of gene expression via two NF-kappaB pathways.* Immunity, 2002. **17**(4): p. 525-35.

268. Testoni, B., et al., *Ribavirin restores IFNα responsiveness in HCV-infected livers by epigenetic remodelling at interferon stimulated genes.* Gut, 2016. **65**(4): p. 672-82.

269. Shevchenko, A., et al., *In-gel digestion for mass spectrometric characterization of proteins and proteomes.* Nat Protoc, 2006. **1**(6): p. 2856-60.

270. Tyanova, S., T. Temu, and J. Cox, *The MaxQuant computational platform for mass spectrometry-based shotgun proteomics.* Nat Protoc, 2016. **11**(12): p. 2301-2319.

271. Cox, J., et al., *Accurate proteome-wide label-free quantification by delayed normalization and maximal peptide ratio extraction, termed MaxLFQ.* Mol Cell Proteomics, 2014. **13**(9): p. 2513-26.

272. Tyanova, S. and J. Cox, *Perseus: A Bioinformatics Platform for Integrative Analysis of Proteomics Data in Cancer Research.* Methods Mol Biol, 2018. **1711**: p. 133-148.

273.   Schneider, T., *Analysis of Incomplete Climate Data: Estimation of Mean Values and Covariance Matrices and Imputation of Missing Values %J Journal of Climate.* 2001. **14**(5): p. 853-871.

274.   Webb-Robertson, B.J., et al., *Review, evaluation, and discussion of the challenges of missing value imputation for mass spectrometry-based label-free global proteomics.* J Proteome Res, 2015. **14**(5): p. 1993-2001.

275.   Ritchie, M.E., et al., *limma powers differential expression analyses for RNA-sequencing and microarray studies.* Nucleic Acids Res, 2015. **43**(7): p. e47.

276.   Smyth, G.K., *Linear models and empirical bayes methods for assessing differential expression in microarray experiments.* Stat Appl Genet Mol Biol, 2004. **3**: p. Article3.

277.   Benjamini, Y. and Y. Hochberg, *Controlling the False Discovery Rate: A Practical and Powerful Approach to Multiple Testing.* 1995. **57**(1): p. 289-300.

278.   Wu, D., et al., *ROAST: rotation gene set tests for complex microarray experiments.* Bioinformatics, 2010. **26**(17): p. 2176-82.

279.   Isorce, N., et al., *Antiviral activity of various interferons and pro-inflammatory cytokines in non-transformed cultured hepatocytes infected with hepatitis B virus.* 2016. **130**.

280.   Chernokalskaya, E., R. Dompenciel, and D.R. Schoenberg, *Cleavage properties of an estrogen-regulated polysomal ribonuclease involved in the destabilization of albumin mRNA.* Nucleic Acids Res, 1997. **25**(4): p. 735-42.

281.   Dejardin, E., *The alternative NF-kappaB pathway from biochemistry to biology: pitfalls and promises for future drug development.* Biochem Pharmacol, 2006. **72**(9): p. 1161-79.

282.   Podolin, P.L., et al., *Attenuation of murine collagen-induced arthritis by a novel, potent, selective small molecule inhibitor of IkappaB Kinase 2, TPCA-1 (2-[(aminocarbonyl)amino]-5-(4-fluorophenyl)-3-thiophenecarboxamide), occurs via reduction of proinflammatory cytokines and antigen-induced T cell Proliferation.* J Pharmacol Exp Ther, 2005. **312**(1): p. 373-81.

283.   Sommers, C.D., et al., *Novel tight-binding inhibitory factor-kappaB kinase (IKK-2) inhibitors demonstrate target-specific anti-inflammatory activities in cellular assays and following oral and local delivery in an in vivo model of airway inflammation.* J Pharmacol Exp Ther, 2009. **330**(2): p. 377-88.

284.   Wu, C.J. and L.F. Lu, *MicroRNA in Immune Regulation.* Curr Top Microbiol Immunol, 2017. **410**: p. 249-267.

285.   Burns, M.B., et al., *APOBEC3B is an enzymatic source of mutation in breast cancer.* Nature, 2013. **494**(7437): p. 366-70.

286.   Agarwal, V., et al., *Predicting effective microRNA target sites in mammalian mRNAs.* Elife, 2015. **4**.

287.   Koh, S., et al., *Nonlytic Lymphocytes Engineered to Express Virus-Specific T-Cell Receptors Limit HBV Infection by Activating APOBEC3.* 2018. **155**.

288.   Barski, A., et al., *High-resolution profiling of histone methylations in the human genome.* Cell, 2007. **129**(4): p. 823-37.

289.   Heintzman, N.D., et al., *Distinct and predictive chromatin signatures of transcriptional promoters and enhancers in the human genome.* Nat Genet, 2007. **39**(3): p. 311-8.

290.   Belloni, L., et al., *Nuclear HBx binds the HBV minichromosome and modifies the epigenetic regulation of cccDNA function.* Proc Natl Acad Sci U S A, 2009. **106**(47): p. 19975-9.

291.   Siriwardena, S.U., K. Chen, and A.S. Bhagwat, *Functions and Malfunctions of Mammalian DNA-Cytosine Deaminases.* Chem Rev, 2016. **116**(20): p. 12688-12710.

292.   Chen, Y., et al., *APOBEC3B edits HBV DNA and inhibits HBV replication during reverse transcription.* Antiviral Res, 2018. **149**: p. 16-25.

293.   Liu, M., et al., *Evaluation of APOBEC3B Recognition Motifs by NMR Reveals Preferred Substrates.* ACS Chem Biol, 2018. **13**(9): p. 2427-2432.

294.   Kvach, M.V., et al., *Inhibiting APOBEC3 Activity with Single-Stranded DNA Containing 2'-Deoxyzebularine Analogues.* Biochemistry, 2019. **58**(5): p. 391-400.

295.   Janahi, E.M. and M.J. McGarvey, *The inhibition of hepatitis B virus by APOBEC cytidine deaminases.* J Viral Hepat, 2013. **20**(12): p. 821-8.

296.   Balamurugan, K., *HIF-1 at the crossroads of hypoxia, inflammation, and cancer.* Int J Cancer, 2016. **138**(5): p. 1058-66.

297.   Lucifora, J., et al., *Direct antiviral properties of TLR ligands against HBV replication in immune-competent hepatocytes.* 2018. **8**.

298.   Faure-Dupuy, S., et al., *Hepatitis B virus-induced modulation of liver macrophage function promotes hepatocyte infection.* J Hepatol, 2019. **71**(6): p. 1086-1098.

299.   Xia, Y., et al., *Interferon-γ and Tumor Necrosis Factor-α Produced by T Cells Reduce the HBV Persistence Form, cccDNA, Without Cytolysis.* 2016. **150**.

300.   Lee, J.W., et al., *Hypoxia signaling in human diseases and therapeutic targets.* Exp Mol Med, 2019. **51**(6): p. 1-13.

301.   Bersten, D.C., et al., *bHLH-PAS proteins in cancer.* Nat Rev Cancer, 2013. **13**(12): p. 827-41.

302.   Gradin, K., et al., *Functional interference between hypoxia and dioxin signal transduction pathways: competition for recruitment of the Arnt transcription factor.* Mol Cell Biol, 1996. **16**(10): p. 5221-31.

303.   Wright, C.W. and C.S. Duckett, *The aryl hydrocarbon nuclear translocator alters CD30-mediated NF-kappaB-dependent transcription.* Science, 2009. **323**(5911): p. 251-5.

304.   Vogel, C.F., et al., *RelB, a new partner of aryl hydrocarbon receptor-mediated transcription.* Mol Endocrinol, 2007. **21**(12): p. 2941-55.

305.   Millet, P., C. McCall, and B. Yoza, *RelB: an outlier in leukocyte biology.* J Leukoc Biol, 2013. **94**(5): p. 941-51.

306.   Farrow, M.A. and A.M. Sheehy, *Vif and Apobec3G in the innate immune response to HIV: a tale of two proteins.* Future Microbiol, 2008. **3**(2): p. 145-54.

307.   Doehle, B.P., A. Schäfer, and B.R. Cullen, *Human APOBEC3B is a potent inhibitor of HIV-1 infectivity and is resistant to HIV-1 Vif.* Virology, 2005. **339**(2): p. 281-8.

308.   Warren, C.J., et al., *Roles of APOBEC3A and APOBEC3B in Human Papillomavirus Infection and Disease Progression.* Viruses, 2017. **9**(8).

309.   Suspène, R., et al., *Extensive editing of both hepatitis B virus DNA strands by APOBEC3 cytidine deaminases in vitro and in vivo.* Proc Natl Acad Sci U S A, 2005. **102**(23): p. 8321-6.

310.   Coto, E., et al., *Gene variants in the NF-KB pathway (NFKB1, NFKBIA, NFKBIZ) and their association with type 2 diabetes and impaired renal function.* Hum Immunol, 2018. **79**(6): p. 494-498.

311.   Ghali, R.M., et al., *Association of Genetic Variants in NF-kB with Susceptibility to Breast Cancer: a Case Control Study.* Pathol Oncol Res, 2019. **25**(4): p. 1395-1400.

312.   Wang, S.S., et al., *Common gene variants in the tumor necrosis factor (TNF) and TNF receptor superfamilies and NF-kB transcription factors and non-Hodgkin lymphoma risk.* PLoS One, 2009. **4**(4): p. e5360.

313.   Bank, S., et al., *Polymorphisms in the NFkB, TNF-alpha, IL-1beta, and IL-18 pathways are associated with response to anti-TNF therapy in Danish patients with inflammatory bowel disease.* Aliment Pharmacol Ther, 2019. **49**(7): p. 890-903.

314.   Smale, S.T., *Dimer-specific regulatory mechanisms within the NF-κB family of transcription factors.* Immunol Rev, 2012. **246**(1): p. 193-204.

315.   Kuong, K.J. and L.A. Loeb, *APOBEC3B mutagenesis in cancer.* Nat Genet, 2013. **45**(9): p. 964-5.

316.   Yeh, M., et al., *Pivotal role of microRNA-138 in human cancers.* Am J Cancer Res, 2019. **9**(6): p. 1118-1126.

317.   Haybaeck, J., et al., *A lymphotoxin-driven pathway to hepatocellular carcinoma.* Cancer Cell, 2009. **16**(4): p. 295-308.

318. Panda, A.C., *Circular RNAs Act as miRNA Sponges.* Adv Exp Med Biol, 2018. **1087**: p. 67-79.

319. Meister, G., et al., *Sequence-specific inhibition of microRNA- and siRNA-induced RNA silencing.* Rna, 2004. **10**(3): p. 544-50.

320. Krützfeldt, J., et al., *Silencing of microRNAs in vivo with 'antagomirs'.* Nature, 2005. **438**(7068): p. 685-9.

321. Luangsay, S., et al., *Early inhibition of hepatocyte innate responses by hepatitis B virus.* J Hepatol, 2015. **63**(6): p. 1314-22.

322. Peyrard, M., S. Cuesta-López, and G. James, *Nonlinear analysis of the dynamics of DNA breathing.* J Biol Phys, 2009. **35**(1): p. 73-89.

323. Jose, D., S.E. Weitzel, and P.H. von Hippel, *Breathing fluctuations in position-specific DNA base pairs are involved in regulating helicase movement into the replication fork.* Proc Natl Acad Sci U S A, 2012. **109**(36): p. 14428-33.

324. von Hippel, P.H., N.P. Johnson, and A.H. Marcus, *Fifty years of DNA "breathing": Reflections on old and new approaches.* Biopolymers, 2013. **99**(12): p. 923-54.

325. Renault, P.F. and J.H. Hoofnagle, *Side effects of alpha interferon.* Semin Liver Dis, 1989. **9**(4): p. 273-7.

326. Sleijfer, S., et al., *Side effects of interferon-alpha therapy.* Pharm World Sci, 2005. **27**(6): p. 423-31.

327. Du, K., et al., *Recent advances in the discovery and development of TLR ligands as novel therapeutics for chronic HBV and HIV infections.* Expert Opin Drug Discov, 2018. **13**(7): p. 661-670.

328. Niu, C., et al., *Toll-like receptor 7 agonist GS-9620 induces prolonged inhibition of HBV via a type I interferon-dependent mechanism.* J Hepatol, 2018. **68**(5): p. 922-931.

329. Hu, Y., et al., *A novel TLR7 agonist as adjuvant to stimulate high quality HBsAg-specific immune responses in an HBV mouse model.* J Transl Med, 2020. **18**(1): p. 112.

330. Zhang, E. and M. Lu, *Toll-like receptor (TLR)-mediated innate immune responses in the control of hepatitis B virus (HBV) infection.* Med Microbiol Immunol, 2015. **204**(1): p. 11-20.

331. Scortegagna, M., et al., *HIF-1alpha regulates epithelial inflammation by cell autonomous NFkappaB activation and paracrine stromal remodeling.* Blood, 2008. **111**(7): p. 3343-54.

332. Walmsley, S.R., et al., *Hypoxia-induced neutrophil survival is mediated by HIF-1alpha-dependent NF-kappaB activity.* J Exp Med, 2005. **201**(1): p. 105-15.

333. Palazon, A., et al., *HIF transcription factors, inflammation, and immunity.* Immunity, 2014. **41**(4): p. 518-28.

334. Medina, J., et al., *Angiogenesis in chronic inflammatory liver disease.* Hepatology, 2004. **39**(5): p. 1185-95.

335. Lee, S.W., et al., *Human hepatitis B virus X protein is a possible mediator of hypoxia-induced angiogenesis in hepatocarcinogenesis.* Biochem Biophys Res Commun, 2000. **268**(2): p. 456-61.

336. Wilson, G.K., D.A. Tennant, and J.A. McKeating, *Hypoxia inducible factors in liver disease and hepatocellular carcinoma: current understanding and future directions.* J Hepatol, 2014. **61**(6): p. 1397-406.

337. Fallah, J. and B.I. Rini, *HIF Inhibitors: Status of Current Clinical Development.* Curr Oncol Rep, 2019. **21**(1): p. 6.

10   Acknowledgements

"Doing a PhD is a marathon, not a sprint" is something probably every PhD student heard at some point. It is true, although it might feel like running a marathon at the pace of a sprint from time to time. This work represents years of doing experiments and months of writing, times that brought out the best and probably the worst in me. Nevertheless, my colleagues, my family and my friends were always there to support me, on the one hand to catch me and lift me up when I was falling and on the other hand to celebrate my achievements with me and share my excitement and my happiness. In this last part of my thesis, I want to thank the people that have guided me through the last years and were going on this journey with me: My grateful thanks go to:

- Mathias Heikenwälder, who already believed in me to be able to carry a whole project when I was still doing my Master studies in Vienna and never stopped in seeing my potential. I want to thank you, Mathias, for giving me the opportunity to work on these interesting projects, for helping me visualise my goals and that you were always there for support, even if I sometimes had hard times seeing it. I really appreciate the way you manage this lab, keeping an inspiring environment, closely connected with efficiency and state-of-the-art techniques; yours is a kind of lab, people wish they would work in. I might not have been your easiest student, therefore I would especially thank you for staying patient with me and making me the researcher I am today.

- My first thesis supervisor and examiner, Ralf Bartenschlager. Dear Ralf, I have always appreciated your calm and thoughtful way of communication; I really want to thank you for your support as member of my thesis advisory committee and your suggestions for the project throughout the years. I always had the feeling, that you had an open door for me if needed.

- My third thesis advisory committee member, Ulrike Protzer. Thank you Ulla for your tireless supply with HBV that made all my studies presented here even possible. Also, thank you for always having a critical view on my data, both during the thesis advisory committee meetings and during conferences. I really appreciated our discussions and I am convinced it helped me and my projects become better.

- My fourth thesis advisory committee member, Julie Lucifora, who was probably the first "outside-our-group"-researcher I was in contact with, back in 2016. Thank you Julie for always lending me an ear when I had one of my numerous requests, thank you for your amazing support on all my projects. Also, I want to say that I never had the feeling you were looking down to me, even some years back when data I presented was at best "questionable" regarding its informational value. Lastly, I can only say that it has

always been a pleasure to meet you and I hope that we see each other again some time.

- My PhD thesis examiners, Nina Papavasiliou and Richard Harbottle, for their support and their time.

- My supervisor in the lab, Suzanne Faure-Dupuy. Thank you Susu for taking me by the hand and revisiting with me everything I had done in the years before you came, and shape it to two wonderful papers. Thank you for being always there when I needed support, be it hands-on support in the lab, support on discussions and brainstorming, or mental support in hard times. You are the ultimate "lab mommy", you are a friend and you are an inspiration. Thank you for just existing, for being there and for going a part of my way with me. I know, I could probably not even write half of what I would like to say to you, but that is fine, others also need some space. Just be aware that I appreciate everything you have done for me, you were the best thing that could possibly happen to a PhD student. I hope you are doing fine now in Paris and that we can see each other soon again and stay in touch.

- My "lab sister", Svenja Schühle. Thank you Svenja for keeping me together, now that Suzanne is gone. I know that I could always come to you if there are problems and I want to thank you for supporting me whenever I need it. I am trying to do the same for you.

- My "adopted lab brother" Enrico. Thanks for all the times you agreed to share with me and supported my bad habits. Also thank you for your mental support and sharing your clear view on things, it is always a pleasure to take a break with you and do a small recap of what is going on.

- My Austrian ex-colleague Mira. We started nearly at the same time in 2016 and we both had problems getting used to the new environment. Thank you for helping me adjust here in Heidelberg, thank you for the fun times listening to Backstreet Boys and Justin Bieber, thank you for the support in difficult times and for sharing some of the struggles.

- The technical team of my lab. Without your constant work and tireless assistance, where would I be now? My special thanks go to Sandra, who was the first supervisor in the lab that I had and who showed me how things are done here in Heidelberg. It was such a pleasure working with you, you made my start here, back in 2016, a very joyful experience. I also want to mention my gratefulness to Danijela. Thank you for being there to help with my and my collaborator's crazy requests for stainings. I highly appreciate that there was never a "no, we cannot do it" but always a "let's see how we can succeed". The same goes also to Jenny, thank you for your efforts in the lab and

your good mood. Thank you also, Corinna and Flo, without your support I would not have been able to perform even slightly as good as I did, thank you for having my back and making things run smoothly. Thank you Tim for your friendliness and your positive vibes and thank you Anna-Lena for making sure that I can always rock the cell culture by fulfilling all those invisible tasks.

- My so far unmentioned lab members. Thank you Mirian for all the fun we have, if you do not make me smile at least a bit every day, who would. Thank you José for spreading positivity, even in the absence of significant data. Thank you Phil for helping me out and cheering me up. Thank you Jakob for always helping to organize the necessary consumable for our lab-internal "Happy Hours" with me. Thank you, Jan, for your thoughts on different cloning strategies and molecular biology protocols; in a lab mainly consisting of immunologists and cancer researchers, a true molecular biologist to discuss with is a true hero. Thank you Katie for all our conversations, you are one of the most positive people I know and being able to count on you means a lot to me. I also want to warmly thank all my other lab members for your input on lab meetings, for sharing thoughts and protocols, for the open discussion culture you bring to this lab and the positive energy you bring to me and the other colleagues.

- My collaboration partners who were not mentioned already. I am very glad and thankful for the many fruitful and inspiring collaborations I could be part of. Not only do I want to thank many people who supported me on my projects and helped me generate some of the data presented in this thesis and in my publications, but also those researchers who I was able to help push their projects. I want to thank every single person I was allowed to work with and I am proud to be part in several projects more or less related to my core interests. I have learned a lot from you and your projects and it helped me to broaden my own horizon.

- My family, especially to my parents. Thank you Gabi and Claus for always having my back, for supporting me throughout the years. You were always aware of what I can do and saw that I would make my way even when I struggled or lost track. Not many people at the end of their 30s would describe a great holiday as spending two weeks with their parents, but I really enjoy time at home with you. I would also like to thank my brothers, Beni and Neli, I am proud of you and I will always be there for you if you need me. I also want to thank my stepparents, Karin and Klemens, for being there for me, for all the fun and the heartiness. Thank you also for making my mom and my dad happy. Thank you Marianne, Edelgard and Helmut, not only for helping my parents raise me, but also for your support (and all the amazing meals and family gatherings) along the way. Grandparents make a family complete. I also want to thank my "parents-

in-law", Kirsten and Rolf, for taking me up in their family and giving me a second home here in Germany, so many kilometres apart from my actual home.

- My friends, the old and the new ones. Thank you Lukas for all the fun times, the parties and that you brought me back to (the very time-intense game) Magic. Thank you Chris for the great celebrations, your jokes and just for being in my close circle for like 20 years; you are an evergreen. Thank you Jasmin, Lilly, Lari, Isi, Jakob, David and Gregi; it is crazy how close people can still be over 10 years after high school graduation. I do not think this is usual and I am definitely not taking this for granted. Thank you Reggy for the amazing times with you, you were always there for a good party and lots of fun. Thank you Amina and Dani, Jaqui and Mo, Steffi and Alex, we do not meet often, but when we do, it is like having met the last time was just a week ago. Beni, I cannot thank you enough for the one time you just sent me the 3D printed HBV virion. You would probably never understand how much this meant to me, it just arrived at my place at a very rough time for me and was really lifting me up. Thank you Ossi for the legendary parties at your (parent's) house and the delicious, home-smoked meat you always prepare. Thank you Agi, my partner in "after-work beer drinking". We know each other since years, lost a bit track of each other, but since you moved to Heidelberg, we became closer than ever. The conversations with you are just filled with fun and even if we discuss problems or unpleasant situations, I feel like we can lift each other up. Thank you Linda for the fun times we had together and for bringing me to the volleyball team, I would really have missed out on something great there. Thank you Domi, Maxi and Flo, it is really amazing to have a boy-group here in Heidelberg to sit together and drink some beer with, forgetting about the world for a bit and discussing our DKFZ lives from different perspectives. Thank you Max for all our inspiring conversations. It is amazing how you make your way and I really enjoy talking to you, there is so much I can learn from you and I hope I will have the opportunity also often in the future. Thank you Laurin and Robert for not forgetting to invite me to your parties even if you know I would probably not be able to come. I love that we stayed in touch after our studies and how we can have so much fun talking about our (similar, but different) paths to our PhDs. I also want to thank all partners of my friends, who also have become friends to me as well, for making my friends happy. I am really glad that my "self-chosen" family is growing, and there are only people who are truly wonderful.

- Last, but not least, my wonderful girlfriend Kim. There is so much I would like to tell you, but first of all, thank you for taking me as I am; a man with all kind of weird flaws, often emotional, often chaotic and all over the place. I want to thank you for all the understanding you manage to bring up for me even after a long and tough week of

your own, that you listen to me and try to understand my worries. Thank you for having my back, thank you for sharing your time with me and for bringing a lot of joy and sunshine in my life. You bring out the best in me, making myself grow a little bit every day, having me become the man I am today. I really enjoy spending my time with you, and I would not want to imagine how it would be without you. In the end, I just want to thank you for being who you are and being with me. You are amazing.

Sincerely,
Tobias Riedl

11 Appendix

Within this appendix, I include the following two articles I published as a co-first author during my time as a PhD student.

Control of APOBEC3B induction and cccDNA decay by NF-κB and miR-138-5p

Suzanne Faure-Dupuy*, **Tobias Riedl***, Maude Rolland*, Zoheir Hizir, Florian Reisinger, Katharina Neuhaus, Svenja Schuehle, Caroline Remouchamps, Nicolas Gillet, Maximilian Schönung, Mira Stadler, Jochen Wettengel, Romain Barnault, Romain Parent, Linda C. Schuster, Rayan Farhat, Sandra Prokosch, Corinna Leuchtenberger, Rupert Öllinger, Thomas Engleitner, Karsten Rippe, Roland Rad, Kristian Unger, Darjus Tscharahganeh, Daniel B. Lipka, Ulrike Protzer, David Durantel, Julie Lucifora, Emmanuel Dejardin[#], Mathias Heikenwälder[#]

*, [#]: Contributed equally

Hypoxia-Inducible Factor 1 Alpha-Mediated RelB/APOBEC3B Down-regulation Allows Hepatitis B Virus Persistence

Tobias Riedl*, Suzanne Faure-Dupuy*, Maude Rolland*, Svenja Schuehle, Zohier Hizir, Silvia Calderazzo, Xiaodong Zhuang, Jochen Wettengel, Martin A. Lopez, Romain Barnault, Valbona Mirakaj, Sandra Prokosch, Danijela Heide, Corinna Leuchtenberger, Martin Schneider, Bernd Heßling, Benjamin Stottmeier, Isabel M. Wessbecher, Peter Schirmacher, Jane A. McKeating, Ulrike Protzer, David Durantel, Julie Lucifora, Emmanuel Dejardin[#], Mathias Heikenwalder[#]

*, [#]: Contributed equally

11.1 Control of APOBEC3B induction and cccDNA decay by NF-κB and miR-138-5p

Suzanne Faure-Dupuy*, **Tobias Riedl***, Maude Rolland*, Zoheir Hizir, Florian Reisinger, Katharina Neuhaus, Svenja Schuehle, Caroline Remouchamps, Nicolas Gillet, Maximilian Schönung, Mira Stadler, Jochen Wettengel, Romain Barnault, Romain Parent, Linda C. Schuster, Rayan Farhat, Sandra Prokosch, Corinna Leuchtenberger, Rupert Öllinger, Thomas Engleitner, Karsten Rippe, Roland Rad, Kristian Unger, Darjus Tscharahganeh, Daniel B. Lipka, Ulrike Protzer, David Durantel, Julie Lucifora, Emmanuel Dejardin[#], Mathias Heikenwälder[#]

*, [#]: Contributed equally

Control of APOBEC3B induction and cccDNA decay by NF-κB and miR-138-5p

Authors

Suzanne Faure-Dupuy, Tobias Riedl, Maude Rolland, Zoheir Hizir, Florian Reisinger, Katharina Neuhaus, Svenja Schuehle, Caroline Remouchamps, Nicolas Gillet, Maximilian Schönung, Mira Stadler, Jochen Wettengel, Romain Barnault, Romain Parent, Linda Christina Schuster, Rayan Farhat, Sandra Prokosch, Corinna Leuchtenberger, Rupert Öllinger, Thomas Engleitner, Karsten Rippe, Roland Rad, Kristian Unger, Darjus Tscharahganeh, Daniel B. Lipka, Ulrike Protzer, David Durantel, Julie Lucifora, Emmanuel Dejardin, Mathias Heikenwälder

Correspondence

e.dejardin@uliege.be (E. Dejardin), m.heikenwaelder@dkfz.de (M. Heikenwälder).

Graphical abstract
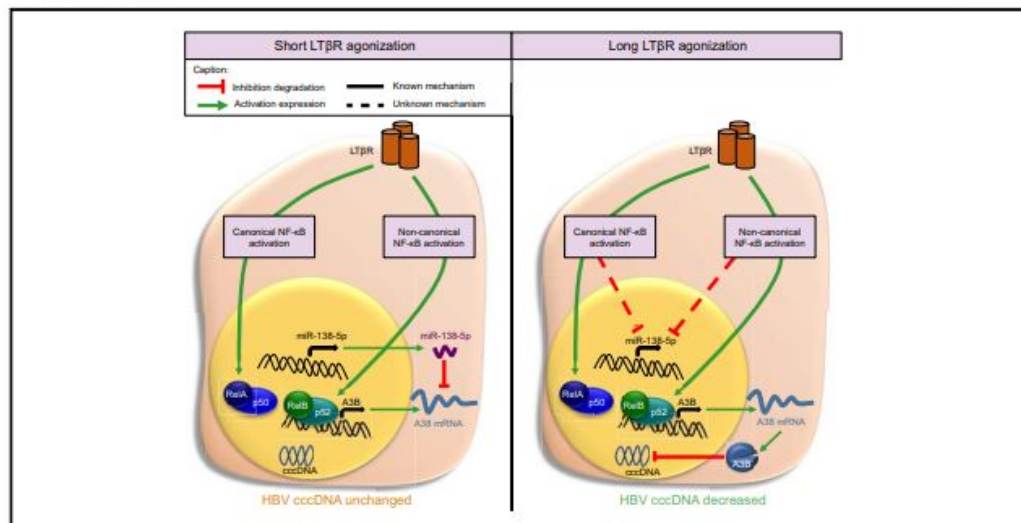
Highlights

- Impairment of NF-κB signalling prevents APOBEC3B induction and cccDNA decay.

- APOBEC3B is post-transcriptionally regulated by the hsa-miR-138-5p.

- Over-expression of the hsa-miR-138-5p inhibits APOBEC3B expression and cccDNA decay.

- A3B timely induces cccDNA decay without damage to cancer-related genes.

- APOBEC3B-mediated cccDNA decay is independent of cccDNA transcriptional activity.

Lay summary

Immune-mediated induction of cytidine deaminase APOBEC3B is transcriptionally regulated by NF-κB signalling and post-transcriptionally downregulated by hsa-miR-138-5p expression, leading to cccDNA decay. Timely controlled APOBEC3B-mediated cccDNA decay occurs independently of cccDNA transcriptional activity and without damage to a subset of cancer-related genes. Thus, APOBEC3B-mediated cccDNA decay could offer an efficient therapeutic alternative to target hepatitis B virus chronic infection.

Control of APOBEC3B induction and cccDNA decay by NF-κB and miR-138-5p

Suzanne Faure-Dupuy,[1,2,†] Tobias Riedl,[1,3,†] Maude Rolland,[4,†] Zoheir Hizir,[4] Florian Reisinger,[1,5]
Katharina Neuhaus,[1] Svenja Schuehle,[1,3] Caroline Remouchamps,[4] Nicolas Gillet,[6] Maximilian Schönung,[3,7]
Mira Stadler,[1,3] Jochen Wettengel,[5] Romain Barnault,[8] Romain Parent,[8] Linda Christina Schuster,[9] Rayan Farhat,[8]
Sandra Prokosch,[1] Corinna Leuchtenberger,[1] Rupert Öllinger,[10] Thomas Engleitner,[10] Karsten Rippe,[9] Roland Rad,[10]
Kristian Unger,[11] Darjus Tscharahganeh,[12] Daniel B. Lipka,[7,13] Ulrike Protzer,[5] David Durantel,[8] Julie Lucifora,[8]
Emmanuel Dejardin,[4,*,‡] Mathias Heikenwälder[1,2,*,‡]

[1]Division of Chronic Inflammation and Cancer, German Cancer Research Center (DKFZ), Heidelberg, Germany; [2]Department of Infectious Diseases,
Molecular Virology, Heidelberg University, Heidelberg, Germany; [3]Faculty of Biosciences, Heidelberg University, Heidelberg, Germany; [4]Laboratory of
Molecular Immunology and Signal Transduction, GIGA-Institute, University of Liège, Liège, Belgium; [5]Institute of Virology, Helmholtz Zentrum München,
Munich, Germany; [6]Integrated Veterinary Research Unit, Namur Research Institute for Life Sciences, Namur, Belgium; [7]Section Translational Cancer
Epigenomics, Division of Translational Medical Oncology, German Cancer Research Center (DKFZ) and National Center for Tumor Diseases (NCT),
Heidelberg, Germany; [8]INSERM, U1052, Cancer Research Center of Lyon (CRCL), University of Lyon (UCBL1), CNRS UMR_5286, Centre Léon Bérard (CLB),
Lyon, France; [9]Division of Chromatin Networks, German Cancer Research Center (DKFZ) and Bioquant, Heidelberg, Germany; [10]Institute of Molecular
Oncology and Functional Genomics, Rechts der Isar University Hospital, Munich, Germany; [11]Research Unit of Radiation Cytogenetics, Helmholtz Zentrum
München, Neuherberg, Germany; [12]Helmholtz-University Group 'Cell Plasticity and Epigenetic Remodeling', German Cancer Research Center (DKFZ) and
Institute of Pathology University Hospital, Heidelberg, Germany; [13]Faculty of Medicine, Otto-von-Guericke-University, Magdeburg, Germany

Background & Aims: Immune-mediated induction of cytidine deaminase APOBEC3B (A3B) expression leads to HBV covalently closed circular DNA (cccDNA) decay. Here, we aimed to decipher the signalling pathway(s) and regulatory mechanism(s) involved in A3B induction and related HBV control.

Methods: Differentiated HepaRG cells (dHepaRG) knocked-down for NF-κB signalling components, transfected with siRNA or micro RNAs (miRNA), and primary human hepatocytes ± HBV or HBVΔX or HBV-RFP, were treated with lymphotoxin beta receptor (LTβR)-agonist (BS1). The biological outcomes were analysed by reverse transcriptase-qPCR, immunoblotting, luciferase activity, chromatin immune precipitation, electrophoretic mobility-shift assay, targeted-bisulfite-, miRNA-, RNA-, genome-sequencing, and mass-spectrometry.

Results: We found that canonical and non-canonical NF-κB signalling pathways are mandatory for A3B induction and anti-HBV effects. The degree of immune-mediated A3B production is independent of A3B promoter demethylation but is controlled post-transcriptionally by the miRNA 138-5p expression (hsa-miR-138-5p), promoting A3B mRNA decay. Hsa-miR-138-5p over-expression reduced A3B levels and its antiviral effects. Of note, established infection inhibited BS1-induced A3B expression through epigenetic modulation of A3B promoter. Twelve days of treatment with a LTβR-specific agonist BS1 is sufficient to reduce the cccDNA pool by 80% without inducing significant damages to a subset of cancer-related host genes. Interestingly, the A3B-mediated effect on HBV is independent of the transcriptional activity of cccDNA as well as on rcDNA synthesis.

Conclusions: Altogether, A3B represents the only described enzyme to target both transcriptionally active and inactive cccDNA. Thus, inhibiting hsa-miR-138-5p expression should be considered in the combinatorial design of new therapies against HBV, especially in the context of immune-mediated A3B induction.

Lay summary: Immune-mediated induction of cytidine deaminase APOBEC3B is transcriptionally regulated by NF-κB signalling and post-transcriptionally downregulated by hsa-miR-138-5p expression, leading to cccDNA decay. Timely controlled APOBEC3B-mediated cccDNA decay occurs independently of cccDNA transcriptional activity and without damage to a subset

ELSEVIER

EASL
The Home of Hepatology

of cancer-related genes. Thus, APOBEC3B-mediated cccDNA decay could offer an efficient therapeutic alternative to target hepatitis B virus chronic infection.

Introduction

HBV is a major global health burden with more than 250 million people chronically infected and about 900,000 related deaths per year (WHO, 2017). Patients with chronic hepatitis B (CHB) are at high risk of developing end-stage liver disease and hepatocellular carcinoma (WHO, 2017). Current treatments (e.g. nucleos(t) ides analogues such as tenofovir or pegylated-interferon alpha) allow the control of the infection but not its complete eradication owing to the persistence of the viral minichromosome, called covalently closed circular DNA (cccDNA).[1] Upon stopping treatment the infection can relapse, as a result of side effects or development of resistance.[1] Therefore, new treatments are urgently needed to cure chronic HBV infection.

We and others previously showed that the cytidine deaminase apolipoprotein B mRNA editing enzyme catalytic subunit 3B (APOBEC3B, A3B) is upregulated upon immune-mediated lymphotoxin-β receptor (LTβR) agonisation.[2,3] A3B induction subsequently leads to cccDNA hypermutation and viral decrease in a non-hepatotoxic manner in vitro.[2] Notably, it is the extent and quality of hepatic inflammation that can contribute to HBV elimination (e.g. in the setting of an acute HBV infection).[3,4] These results opened the door for new R&D strategies to improve functional cure in CHB.[2] LTβR is expressed on different hepatic cells (e.g. hepatocytes, endothelial cells, hepatic stellate cells)[5] and direct, chronic agonisation in CHB patients with the current tools available (e.g. BS1 — an LTβR agonist with non-hepatocyte-specific targeting) might affect liver biology. Thus, understanding the mechanisms of A3B regulation in hepatocytes is an important first step towards the targeted development of new therapies aiming at hepatocyte-specific cccDNA decay.

In distinct cancer types, A3B induction has been shown to be mediated by the nuclear factor-kappa B (NF-κB) pathways.[6] However, whether NF-κB signalling is mandatory for A3B induction in non-cancerous hepatocytes or in the context of a chronic HBV infection has remained unknown. The NF-κB-signalling pathway can be divided into 2 arms: the classical/canonical and the alternative/non-canonical pathways.[7] The canonical pathway, commonly activated by tumour necrosis factor (TNF) family members, signals through the IKK complex (inhibitor of NF-κB kinase complex, consisting of NEMO/IKKα/IKKβ), triggering the phosphorylation and ubiquitination of nuclear factor of kappa light polypeptide gene enhancer in B-cells inhibitor alpha (IκBα) and the release of p50/RelA heterodimer.[7] In addition to the canonical pathway, LTβR agonisation signals through the non-canonical pathway by activating the NF-κB inducing kinase (NIK). This leads to phosphorylation of IKKα and p100 and its processing into p52 forming p52/RelB heterodimers which translocate to the nucleus to activate target genes such as immune mediators.[8]

The liver displays an overall immunosuppressive environment.[9] To regulate the immunosuppressive state, and to prevent inappropriate and/or chronic inflammation induced by pathogen recognition, a large number of immune factors can additionally be regulated at the post-transcriptional level by micro RNAs (miRNAs).[10] miRNAs are small non-coding RNAs involved in mRNA silencing and post-transcriptional regulation through base-pairing with complementary RNA sequences.[10] Protein synthesis of mRNAs targeted by miRNAs is then reduced, either because of the cleavage of the mRNA strand, destabilisation of mRNAs by shortening of the poly(A) tail, or reduced translation of the mRNA.[10]

Here we describe the regulatory mechanisms of A3B induction upon immune-mediated LTβR agonisation at the transcriptional and post-transcriptional level, and identify the regulation of hsa-miR-138-5p as a novel antiviral strategy against HBV.

Materials and methods

Cell culture

HepaRG, a non-transformed progenitor cell line that can be differentiated into hepatocytes, were cultured as described previously.[11] HEK293T cells (ATCC® CRL-1573™, for lentivirus production) and HEK293T/17 cells (293T/17; ATCC CRL-11268, for luciferase assays) were cultured in DMEM (Gibco, Paisley, United-Kingdom) supplemented with 10% foetal calf serum (Gibco) and 50 U/ml penicillin/streptomycin (Gibco). Primary human hepatocytes (PHHs) were isolated were isolated and cultured as previously described.[12] Work with primary cells was approved by the local ethics committee (French ministerial authorisations [AC 2013-1871, DC 2013–1870, AFNOR NF 96 900 Sept 2011]). Written consent was obtained from all patients. HBV, HDV, or HIV chronically infected specimens were excluded.

Transgenic cell line preparation

Knockout HepaRG cell lines were generated by lentiviral transduction of a double-sgRNA containing construct into HepaRG-iCas9-TR (David Durantel, unpublished). Briefly, HepaRG cells were transduced with pLenti6-TR to introduce the tetracyclin repressor (TetR), and subsequently with pLenti4/TO/V5 (Invitrogen, Carlsbad, United-States), in which the coding sequence of an N-terminally 3× FLAG-tagged Cas9 was inserted between the EcoRI and XhoI sites of the vector. The generation of double-sgRNA containing vectors for the knockout cell line generation was described previously.[13] In short, sgRNAs were chosen based on high scoring and no high scoring off-targets using the CHOPCHOP version 2 web tool.[14] These sgRNAs were inserted into pUSEPR (generous gift from Dr. Tscharaganeh, DKFZ, Heidelberg, unpublished) based on methods as described elsewhere.[15]

Preparation of lentiviral particles and transduction of HepaRG cells were performed based on protocols from Addgene. After each transduction step, HepaRG were selected with blasticidin (Invitrogen; 5 μg/ml; TetR), Zeocin (Invitrogen; 300 μg/ml; Cas9) and puromycin (Sigma Aldrich, Taufkirchen, Germany; 10 μg/ml; sgRNAs) until non-transduced cells have died.

Additional material and methods can be found in the supplementary material.

Results

Canonical and non-canonical NF-κB signalling induces APOBEC3B upon LTβR agonisation

We and others have shown that agonisation of LTβR triggers A3B transcription.[8] However, in non-transformed hepatocytes, the signalling pathways activated remain to be identified. First, we confirmed that of among APOBEC3 family members, A3B displayed the strongest upregulation (2-fold increase by mRNA sequencing and 3-fold increase by mass spectrometry [MS], respectively) at 1 day post-treatment with BS1, an antibody agonising LTβR (Fig. S1A,B). In addition to the MS results, we also observed an enrichment of A3B mRNA in the polysomes fractions of BS1-treated dHepaRG cells compared with untreated cells (Fig. S1C,D). Of note, this increase was mostly based on signals located in heavy polysomes, indicative of strong translational activity (Fig. S1E). EDTA release control[16] confirmed that the A3B transcript signal was of polysomal origin (Fig. S1F).

To decipher the pathway activated by BS1, RNA sequencing was performed and highlighted that constant BS1 treatment up to 40 days downregulated metabolic pathways (e.g. cytochrome P450 mediated detoxification of drugs and xenobiotics) and 'complement and coagulation cascades', whereas pathways usually activated during virus-infection were upregulated (Fig. S2A). In-depth analysis of specific pathways highlighted a strong induction of many of the NF-κB signalling proteins by LTβR agonisation (Fig. S2B), and upregulation of many transcripts of proteins involved in MAPK, NOD-like receptor, IL17, and TNF-signalling pathways (Fig. S2C–F).

Because LTβR activates the 2 NF-κB signalling pathways (canonical and non-canonical),[8] we performed in silico analyses of the proximal A3B promoter region to find putative NF-κB binding sites (Fig. 1A). Two κB sites (κB1 and κB2) were identified and tested in electrophoretic mobility shift assays with nuclear extracts of BS1-treated dHepaRG cells (Figs. 1A and S3A). Both κB probes displayed NF-κB binding activities, although with different patterns. In addition, the contribution of both κB sites to the A3B transcriptional activity was monitored with a luciferase vector containing the proximal A3B promoter with wild-type and/or mutated κB1/2 sites. We observed that all NF-κB heterodimers tested were able to induce a luciferase activity with varying efficacy, but p50/RelA and p50/RelB showed the poorest activity (Fig. 1B). Our mutagenesis analysis of each κB site revealed that the κB1 site was the major active site, as its mutation strongly decreased luciferase activity (Fig. 1B). Chromatin immunoprecipitation of the A3B proximal promoter in HepaRG cells highlighted an increase of binding for RelB, p52, and p50 but not RelA, upon BS1 treatment (Figs. 1C and S3B). Of note, binding of p52 as well as polymerase II (a marker of active transcription) was constant from Day 1 to 6 post treatment (Fig. 1C,D).

Furthermore, siRNAs against NIK, or specific IKKβ inhibitors,[17,18] or a combination of both, blocked BS1-induced A3B upregulation at the mRNA and protein level (Figs. 1E and S3C). Results were confirmed using other NF-κB inducing agents (Fig. S3D,E). In addition, HepaRG knockout lines of genes involved in canonical (i.e. IKKβ, RelA) and non-canonical (i.e. NIK, RelB) NF-κB pathways were generated (Fig. S3F–H). A significant impairment of BS1-induced A3B upregulation was observed in all tested cell lines (Figs. 1F and S3I). Knockdown of NIK in combination with IKKβ was most efficient to prevent A3B upregulation.

Taken together, these data highlight that both arms of NF-κB signalling play an important role in the induction of immune-mediated APOBEC3B expression, and confirmed our previous findings on the crucial role of RelB for A3B promoter activation.[19]

APOBEC3B is as an atypical NF-κB target

Unlike prototypic C-X-C motif chemokine 10 (CXCL10) or A20 (typical NF-κB target genes), which have an induction peak shortly after treatment start, A3B mRNA was significantly, but only weakly induced at 24 h after BS1 exposure (Figs. 2A and S4A). Whereas continued BS1 treatment led to decreased CXCL10 and A20 expression, A3B mRNA levels remained low during a 4-day 'lag phase' followed by a constant rise after 4 days of constant or pulse-chase BS1 treatments (Figs. 2A and S4A, respectively). Similarly, A3B protein level remained low during a 4-day lag phase and increased after 4 days of BS1 treatment (Fig. 2B). RelA phosphorylation, p100 processing to p52, and RelB protein levels were elevated from 18 h post-treatment (Fig. 2B). Notably, similar results for A3B expression were obtained with other NF-κB inducing cytokines (Fig. S4B). The lag phase was not linked to delayed A3B transcription because a constant binding of p52 and polymerase II on A3B promoter were detected from 1 day post treatment onwards (Fig. 1C,D). As promoter demethylation is a key factor of gene expression and could play a role in the observed lag phase, targeted bisulfite sequencing was performed.[20] Over a 12-day period of constant BS1 treatment, no change in A3B promoter methylation was detected (Fig. S4C).

These data highlighted that A3B is an atypical NF-κB target which displays a lag phase profile upon NF-κB activation.

Hsa-miR-138-5p post-transcriptionally regulates APOBEC3B mRNA

Our results suggest that A3B lag phase induction might be a result of post-transcriptional regulation by miRNAs. Therefore, we hypothesised that miRNAs might be negative regulators of A3B mRNA to buffer A3B induction upon short-time LTβR stimulation, which potentially leads to genomic DNA damage.[21] However, a sustained stimulation would lead to a repression of the miRNAs leading to high A3B mRNA levels, needed for an efficient antiviral effect (Fig. 2C).

Combined unbiased small RNA sequencing, RT-qPCR, and in silico target prediction algorithms[22] revealed 3 clusters of dysregulated miRNAs in untreated compared with BS1-treated HepaRG cells (Fig. 2D): (i) miRNAs highly expressed at Day 2 post-treatment (when A3B mRNA is low) but downregulated at Day 4 (when A3B mRNA is higher). This group includes the candidates of interest; (ii) miRNAs lowly expressed at Day 2 but with increased expression at Day 4; (iii) miRNAs downregulated under BS1 treatment.

Our in-silico analysis revealed that among the 30 miRNAs identified in cluster I, only hsa-miR-138-5p was predicted to have a high binding affinity within the 3′-UTR of A3B (Fig. 2E). Next, we confirmed by RT-qPCR the reduced expression of hsa-

miR-138-5p between Day 2 (*i.e.* during the lag phase) and Day 4 (*i.e.* after the lag phase) post BS1-treatment (Fig. 2F).

To assess the functional activity of miR-138-5p on A3B, we fused the luciferase gene upstream of the 3′-UTR of A3B and co-transfected the plasmid together with, either a miRNA ctrl or a miRNA-138-5p expression vector. We observed that expression of miRNA-138-5p decreased luciferase activity whereas expression of miRNA control did not (Fig. 2G,H; 3B-3′-UTR-138). Conversely, insertion of point mutations within the miRNA-138-5p binding site of the 3′-UTR of A3B abrogated the sensitivity to the miRNA-138-5p (Fig. 2G,H; 3B-3′-UTR-138 mut). We next extended our *in-silico* analysis for the presence of miR-138 binding site in the 3′-UTR of other APOBEC3 family members. We found that APOBEC3G (A3G) displays 1 single site whereas APOBEC3A (A3A) contains a pseudo-miR-138-5p binding site with a single point mutation. Interestingly, an A3A variant with a matching miR-138-5p binding site in its 3′-UTR has been identified in a low percentage of the population (single nucleotide polymorphism [SNP] rs1367248965). We confirmed that A3G (3G-3′-UTR-138) and A3A (3A-3′-UTR SNP) variant containing of intact miR-138 binding site were responsive to the expression of miR-138 as opposed to their mutant counterpart (3G-3′-UTR-138 mut and 3A-3′-UTR) (Fig. 2G,H). The sensitivity of these APOBEC mRNAs to miRNA-138 were similar when the full coding sequences (CDS) of the APOBEC3 genes (Fig. S5A,B) or the minimal miRNA-138-5p binding site was cloned downstream of the luciferase gene (Fig. S5C,D).

Noteworthy, in the human genome, two different loci encode hsa-miR-138-5p genes (Fig. S5E,F). However, dHepaRG cells mainly express the hsa-miR-138-1 located on chromosome 3 (Fig. S5G). We observed that BS1-mediated hsa-miR-138-5p repression was prevented either by inhibiting IKK kinase activities (*i.e.* by using TPCA, an IKK inhibitor) or by depleting NIK in HepaRG cells (Fig. S5H,I). Altogether, these results suggest that activation of NF-κB acts as a positive regulator of A3B transcription while inhibiting hsa-miR-138-5p transcription.

Inhibition of NF-κB signalling or forced expression of hsa-miR-138-5p mimics abolish A3B-mediated anti-HBV activity

We next investigated how NF-κB and miRNA-138-5p modulate HBV viraemia. HepaRG control and knockout for different NF-κB signalling proteins were treated with BS1 or tenofovir (Teno) for either 6 or 12 days and cccDNA and viraemia were monitored (Fig. 3A). We observed that BS1-mediated anti-HBV effects (on cccDNA and viraemia) was significantly reduced (Figs. 3B and S6A). Teno, a nucleoside analogue that reduces secreted DNA but not the cccDNA content, was used as control. These results

correlate with the absence of BS1-mediated A3B induction and hsa-miR138-5p repression in NIK or IKKβ-deficient cells (Figs. 3C and S6B,C) and was not the consequence of induced cell death (Fig. S6D).

These results were also phenocopied using a miRNA mimic approach (see experimental timeline Fig. 3D). Indeed, transfection of hsa-miR-138-5p mimics reduced A3B levels (Fig. 3E,F) and prevented antiviral effects on cccDNA (Fig. 3G). These results further validate our observations in Fig. 2H showing the effect of the miR-138 binding site in the 3′-UTR of A3B and A3G.

Of note, from the 704 hsa-miR-138-5p predicted targets genes (Table S3), only 6 genes were related to NF-κB signalling or hepatocyte function (HIF1α, HNF4α, JMJD8, MAPKBP1, RelA, UBE2V1). None of the latter was significantly affected by hsa-miR-138-5p mimics or BS1 treatment (Fig. S6E; UBE2V1 could not be detected in dHepaRG), highlighting that the effect of the 138-5p-mimic was most probably limited to A3B.

Interestingly, 7 days post infection, even though both non-infected and infected cells (HepaRG or PHH) showed a significant upregulation of A3B mRNA upon BS1 treatment, HBV-infected cells displayed a 50% reduction of A3B mRNA expression as compared with the non-infected counterpart, which was (i) independent of an increase of hsa-miR-138-5p expression levels and (ii) not sufficient to prevent the antiviral effect on HBV secreted protein (Fig. 4A–E). Chromatin immune precipitation on the activating epigenetic mark H3K4Me3 highlighted that the increase of H3K4Me3 on the A3B promoter induced by BS1 treatment was lost when the cells were infected with HBV (Fig. S6F).

In summary, disrupting A3B induction prevents the immune-mediated effect on HBV cccDNA levels. Moreover, HBV infection itself partially counteracts A3B upregulation during persistent infection.

Transient APOBEC3B induction triggers cccDNA decay without inducing damage to cancer-related genes

One of the major risks in the induction of A3B to eliminate cccDNA might possibly be a DNA-modifying effect. Indeed, A3B expression has been described to be associated with cancer development.[21] As we have previously described that A3B-induced cccDNA decay does not lead to rebounds of HBV infection *in vitro*,[2] we hypothesised that short-term A3B induction could be sufficient to ensure viral decay without affecting genomic DNA, in line with the observation that high A3B levels are present in acute, self-limiting HBV infection in patients.[4]

Whereas 12 days of BS1-treatment led to an ∼80% decrease of cccDNA (Figs. 3A,B and 5A), no significant mutational load was observed on a subset of genes related to cancer development, as

Fig. 2. APOBEC3B is post-transcriptionally regulated by the miRNA-138-5p. (A,B) Treatment of dHepaRG with 0.5 µg/ml BS1 was started sequentially and stopped altogether at the indicated time points. (A) Upper panel: schematic representation of the experiment. Lower panel: mRNAs of interest were extracted and analysed by RT-qPCR. (B) Proteins were analysed by immunoblotting. (C) Schematic representation of the working hypothesis. (D) dHepaRG were treated for 2 or 4 days with 0.5 µg/ml of BS1. Upper panel: schematic representation of the experiment. Lower panel: RNAs were extracted and small RNA were sequenced. Top 50 significantly dysregulated miRNAs of combined sequencing and RT-qPCR data was unbiased clustered and plotted. Cluster I represents miRNAs highly expressed at Day 2 and lowly expressed at Day 4 (*i.e.* miRNAs of interest); Cluster II represents miRNAs lowly expressed at Day 2 and highly expressed at Day 4; Cluster III
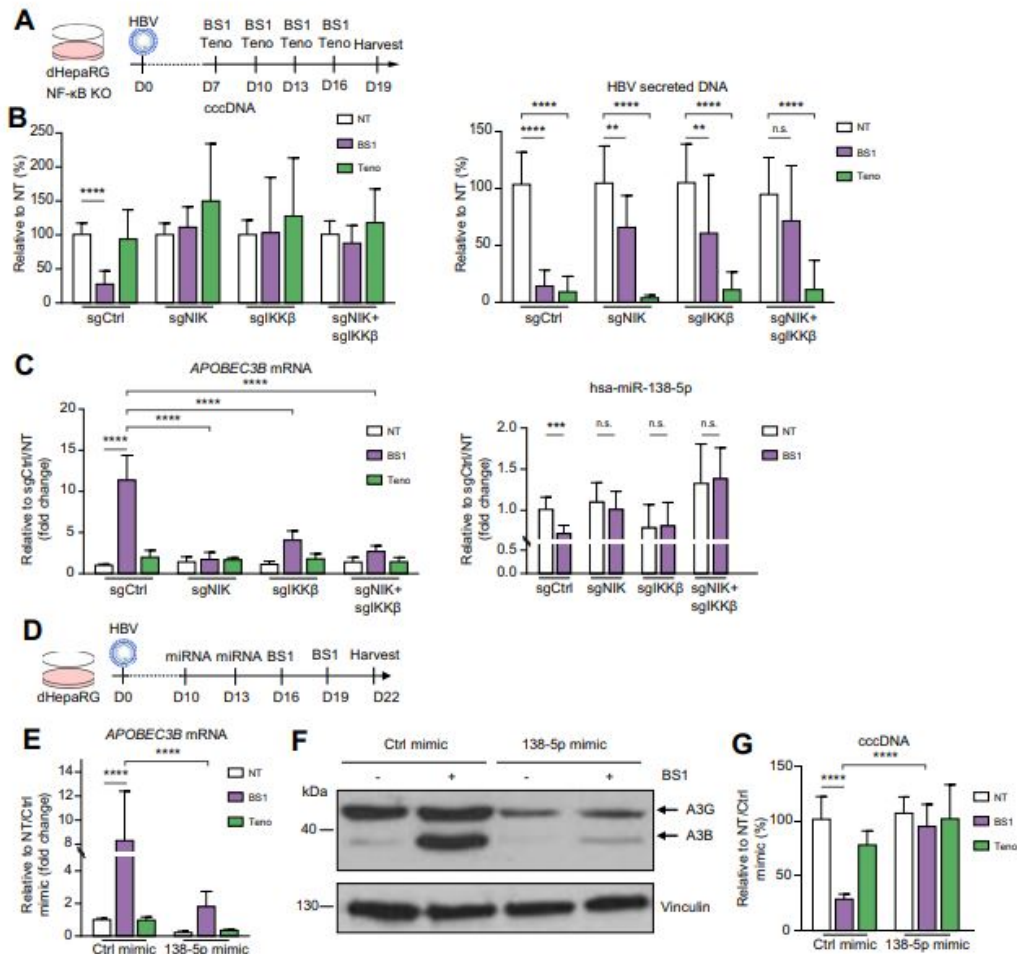
Fig. 3. Dysregulation of APOBEC3B expression by disruption of NF-κB signalling and mi-RNA 138-5p prevent the antiviral effect. (A) Schematic representation of the experiment presented in panels B and C. (B,C) Knockout dHepaRG lines for NIK (sgNIK), IKKβ (sgIKKβ), or NIK and IKKβ (sgNIK + sgIKKβ), as well as control dHepaRG (sgCtrl) were infected with HBV. Seven-d.p.i. cells were left untreated (NT) or treated with 0.5 μg/ml of BS1 or 0.5 μM of tenofovir for 12 days. (B) DNA and (C) RNAs were isolated and analysed using RT-qPCR or qPCR. (D–G) dHepaRG were infected with HBV and 10 and 13 d.p.i. transfected with 10 nM microRNA (miR)-138-5p or control mimics. Cells were then left untreated (NT) or treated for 6 days with 0.5 μg/ml of BS1 or 0.5 μM of tenofovir. (D) Schematic representation of the experiment presented in panels E–G. (E) RNAs, (F) proteins, and (G) DNA were isolated and analysed using RT-qPCR, immunoblotting, and qPCR, respectively. Bars represent the mean ± SD of (B,C) 3 or (E, G) 6 independent experiments. Data were submitted to (B, C, E, G) 1-way ANOVA. *p <0.05; **p <0.01; ***p <0.001; ****p <0.001. APOBEC3B, apolipoprotein B mRNA editing catalytic polypeptide-like A; d.p.i., days post infection; IKKβ: inhibitor of nuclear factor kappa B kinase subunit beta; NF-κB, nuclear factor kappa B; NIK, NF-κB inducing kinase; n.s., not significant.

represents miRNA lowly expressed at Day 2 and Day 4. (E) Schematic illustration of the miRNA-138-5p binding site on the APOBEC3B 3'-UTR. (F) dHepaRG were left untreated (NT) or treated with 0.5 μg/ml of BS1 for 2 or 4 days (see schematic representation of the experiment in D). miRNAs were extracted and analysed by RT-qPCR. (G,H) HEK293T cells were co-transfected with luciferase-3'-UTR fusion constructs and either miR-138-5p-expressing plasmids or control miR-expressing plasmids. (G) Schematic representations of luciferase-3'-UTR fusions used. (H) Upper panel: schematic representation of the experiment. Lower panel: luciferase activity was assayed 48 h post transfection. Bars, respectively points, represent the mean ± SD of (F, H) 1 experiment, or (A) 3 experiments performed in triplicate. Data were submitted to (A, F, H) unpaired Student's t test. *p <0.05; **p <0.01; ***p <0.001; ****p <0.001. APOBEC3B, apolipoprotein B mRNA editing catalytic polypeptide-like A; n.s., not significant; UTR, untranslated transcribed region.
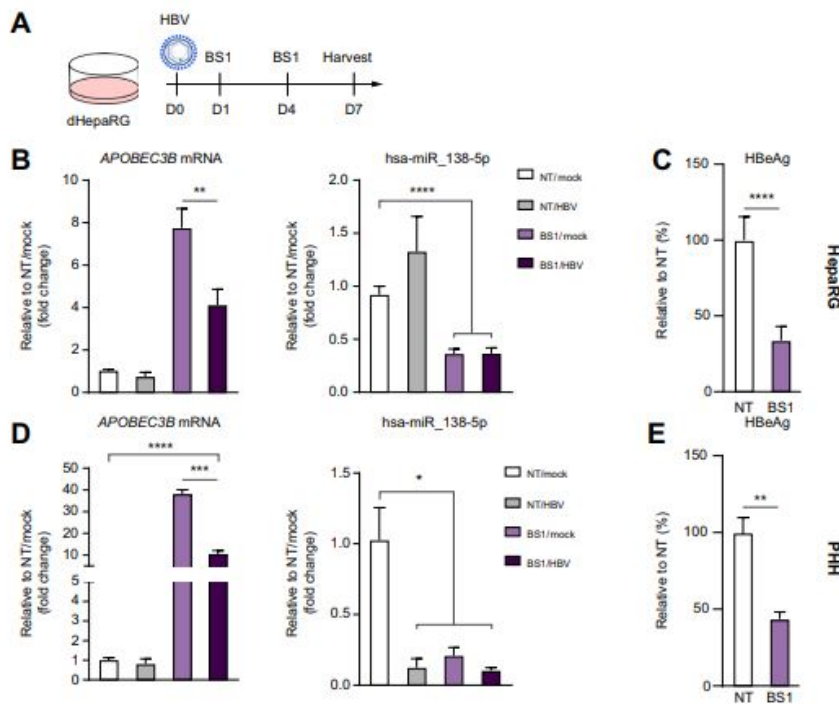
Fig. 4. HBV-mediated inhibition of APOBEC3B expression is not sufficient to prevent the antiviral effect. (A) Schematic representation of the experiment presented in panels B–E. (B,C) dHepaRG or (D,E) PHH were infected with HBV and left untreated (NT) or treated with 0.5 μg/ml of BS1 starting 1 d.p.i, for 6 days. (B,D) RNAs were isolated and analysed using RT-qPCR or qPCR. (C,E) Levels of HBeAg were detected in the cell culture supernatant via ELISA. Bars represent the mean ± SD of (D,E) 1 experiment, or (B,C) 3 independent experiments. Data were submitted to (B-E) unpaired Student's t test. *p <0.05; **p <0.01; ***p <0.001; ****p <0.001. d.p.i., day post infection; n.s., not significant; PHH, primary human hepatocytes.

analysed by targeted deep-sequencing of 766 genes associated with somatic mutations in tumours (*e.g.* tumour suppressors; oncogenes) (Table S4). Of 2,868 detected SNPs (compared with the human reference genome hg19), only 13 were shared by all BS1-treated cells, whereas 12 were also shared in non-treated cells above the cut-off level (Fig. 5B). Closer analyses of SNPs in the tri-nucleotide context revealed no significant differences in SNP frequencies between non-treated and BS1-treated cells (Fig. 5C–E).

Altogether, transient upregulation of A3B in hepatocytes is sufficient to eliminate cccDNA without inducing a detrimental mutational load to a subset of cancer-related genes *in vitro*.

The antiviral effects of APOBEC3B expression are independent of cccDNA transcriptional activity and can occur on double-stranded DNA

Finally, two of the suggested limitations of A3B-induced cccDNA decay are that: (i) transcriptionally inactive cccDNA (*i.e.* during

occult infection), might escape deamination and lead to HBV relapses further on; (ii) like other members of the APOBEC3 family (*e.g.* A3G), A3B might act only on single-stranded DNA during HBV reverse transcription.[23,24]

X-protein deficient HBV (HBV ΔX) cccDNA has been shown to be transcriptionally inactive and have a condensed chromatin state.[25,26] To address if A3B can target transcriptionally inactive cccDNA, dHepaRG were infected with HBV wild-type (wt) or HBV ΔX (Fig. 6A). In both HBV wt- and HBV ΔX-infected cells, a similar reduction of cccDNA levels was observed upon BS1-treatment (Fig. 6B). The decrease of cccDNA levels in BS1-treated HBV ΔX-infected dHepaRG cells was confirmed by Southern-blot analysis (Fig. 6C).

Moreover, we infected dHepaRG with a tRFP-NLS recombinant strain of HBV (tRFP-rHBV), in which the Pol/HBsAg ORF was disrupted by the insertion of a TTR promoter driving a tRFP-NLS reporter (*i.e.* there is no reverse transcription, and no produced relaxed circular DNA or rcDNA) (Fig. 6D). Infected cells were
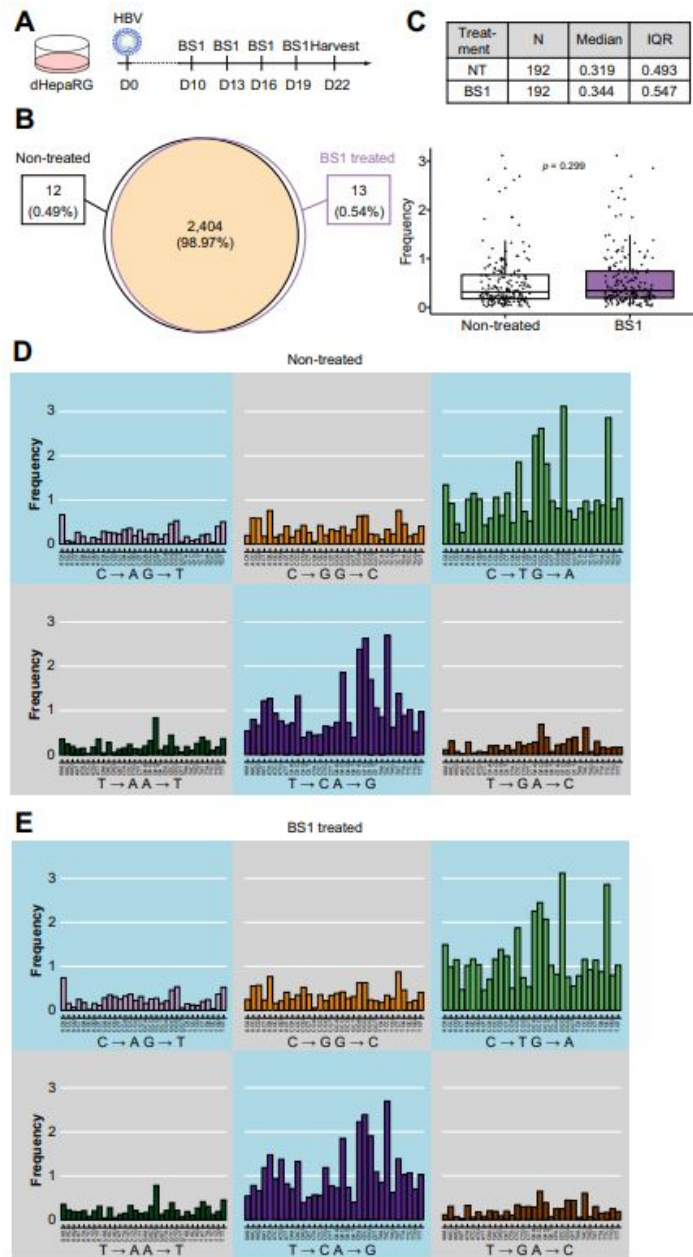
Fig. 5. APOBEC3B induction does not induce *de novo* mutations in a subset of genes related to cancer development. (A–E) dHepaRG were infected and 10 d.p.i. were left untreated (NT) or treated with 0.5 μg/ml BS1 for 12 days. DNA was extracted and subjected to panel sequencing of a panel containing 766 genes (CeGaT CancerPrecision panel). A total of 2,868 single nucleotide variants (SNVs) were detected. (A) Schematic representation of the experiment. (B) These SNVs were then filtered to identify SNVs, that occur in all samples with a number of alleles (NAF) >5% and a coverage >30 (2,404), only in all treated samples (13) and

positive for RFP (Fig. 6E). BS1 treatment decreased the number RFP-positive cells (Fig. 6F), induced A3B (Fig. 6G), and reduced cccDNA levels (Fig. 6H), as well as pregenomic RNA (pgRNA) and RFP mRNA (Fig. 6I). As no rcDNA can be formed in these cells, the reduction of HBV DNA observed was specific of cccDNA.

Thus, A3B acted directly on inactive cccDNA in a reverse transcription-independent manner.

Discussion

APOBEC3B (A3B) has been proposed to be an antiviral enzyme, targeting a multitude of DNA viruses.[2,27,28] We have previously shown that induction of A3B by LTβR agonisation leads to non-cytolytic degradation of nuclear HBV cccDNA, enabling long-term inhibition of HBV-replication without rebound, even after treatment cessation.[2] These findings were also independently confirmed in vivo by T cell-mediated LTβR activation.[3]

Previous studies identified A3B as a NF-κB target gene in cancer cell lines.[29] Here, we describe that both NF-κB pathways (canonical and non-canonical) are involved in LTβR-induced A3B in non-transformed human hepatocytes (dHepaRG). In silico analysis identified 2 putative NF-κB binding sites in the proximal promoter of A3B. These sites were bound by NF-κB complexes in mobility shift and chromatin immunoprecipitation assays, as well as activated in luciferase assays. Chemical based-approaches combined with genetic loss of function of IKKβ and NIK further highlighted the involvement of both NF-κB pathways for A3B induction. A time course analysis of NF-κB (p52 and RelB) and polymerase II recruitment to the A3B promoter and the level of A3B transcript highlighted a post-transcriptional mechanism involving the hsa-miR-138-5p. Amongst the miRNAs previously identified to repress A3B in silico,[30] only hsa-miR-138-5p was detected in our miRNA analysis. An IKKβ- and NIK-dependent inverse correlation between the expression of hsa-miR-138-5p and A3B was observed in BS1-stimulated cells. These results suggest that NF-κB pathways regulate the expression of a repressor of hsa-miR-138-5p expression. Alternatively, generation of p52/p52 dimers could compete out transcriptionally active NF-κB dimers on the hsa-miR-138-5p promoter region.

The peculiar regulation of A3B might be a conserved evolutionary mechanism to avoid a detrimental A3B-mediated genome editing.[21] Several studies have demonstrated a link between hsa-miR-138-5p and tumour development suggesting a tumour suppressor activity for hsa-miR-138-5p.[31] Thus, it will be interesting to assess whether the hsa-miR-138-5p is downregulated in cancer harbouring an A3B signature or high A3B expression.

We observed that interfering with A3B transcriptionally or post-transcriptionally severely impaired BS1-mediated cccDNA decay. Thus, these findings raise important considerations concerning new therapeutic tools involving LTβR activation for the treatment of patients with CHB. As chronic inflammation and tumour development might develop with long-lasting BS1 treatment, a time-restricted administration (e.g. 4 weeks) would be mandatory. Indeed, we confirmed in vitro that 12 days BS1-treatment was sufficient to strongly decrease cccDNA levels without inducing mutations within a subset of cancer-related genes.

A repression of A3B was observed in infected cells, upon BS1 treatment and independently of hsa-miR-138-5p. We showed that HBV infection inhibited A3B transcription activation at the epigenetic level, as previously described for interferon β.[32] Thus, understanding the full repertoire of HBV-inhibitory mechanisms on hepatic immune responses might reveal promising targets to enable full A3B induction and other immune mediators. Understanding the HBV-mediated A3B expression, the mechanisms of downregulation of the hsa-miR-138-5p, and — as recently published — the inhibition of HIF1α stabilisation, could ensure effective immune-mediated control of the viral infection.[19]

Although A3B has been proposed to deaminate only ssDNA,[23,33] as described for A3A and A3G,[34] we have shown that an X-deficient HBV with a transcriptionally inactive cccDNA and a replication-deficient virus (i.e. no reverse transcription) were still susceptible to cccDNA degradation. These results ruled out that the antiviral effects are due to the editing of replicative intermediate of HBV, i.e. the relaxed circular DNA, in the cytoplasm, and the nuclear re-import of dysfunctional, mutated HBV genomes. Whether A3B can either induce unwinding of the cccDNA via yet to be described helicase activity, act on ssDNA that naturally occurs in a transcription-independent manner, or act on dsDNA, remains to be determined. Thus, we propose that A3B induction could possibly be used in the treatment of patients with poorly active cccDNA (i.e. inactive carrier), to eliminate the virus before any reactivation.

It will be also important to assess the effect of A3B on integrated HBV genomes, as it is a recurrent event which has been described to be involved in liver pathogenesis.[35] Moreover, as integrations risks increase over time, it is important to diagnose and treat the patients early on. Indeed, if patients are treated before or soon after integrations, we could hypothesise that both the elimination of HBV cccDNA by A3B, and the natural renewal of hepatocytes within the liver, might lead to elimination of hepatocytes in which the HBV genome has been integrated.

In summary, we have shown that LTβR agonisation and activated NF-κB signalling pathways lead to APOBEC3B induction (Fig. 7). Moreover, hsa-miR-138-5p negatively regulates APOBEC3B expression and aberrant hsa-miR-138-5p expression inhibits A3B-mediated cccDNA decay, as measured by qPCR and Southern-blot analyses. We believe that blocking hsa-miR-138-5p expression or preventing hsa-miR-138-5p binding to A3B

---

only in all 'not treated' samples (12). Four hundred and thirty-nine SNVs were not found in all samples but they were not specific to either of the 2 groups. Inspection of the 13 and 12 genes showed that they have NAFs close to the cut-off of 5% but are detected in the other samples also. (C–E) SNVs in every possible trinucleotide context were analysed for their frequency. (C) Comparison of the frequency of SNVs between non-treated and BS1 treated samples. In the table, the median frequency and the IQR of SNVs are presented. In the box plot, every data point represents a SNV in a trinucleotide context. Data were submitted to the Wilcoxon-signed Rank Sum test. (D) Frequency for all SNVs in a trinucleotide context of non-treated samples. (E) Frequency for all SNVs in a trinucleotide context of non-treated samples. APOBEC3B, apolipoprotein B mRNA editing catalytic polypeptide-like A; d.p.i., days post infection.
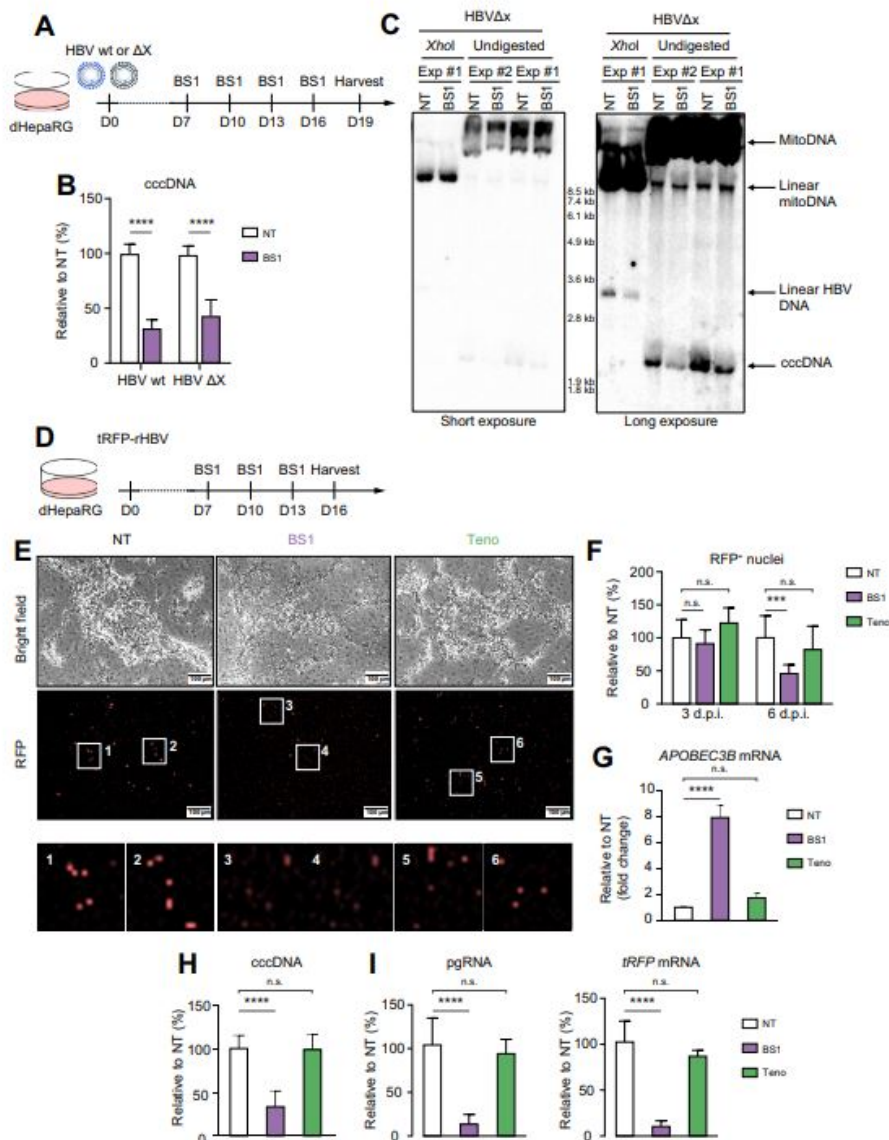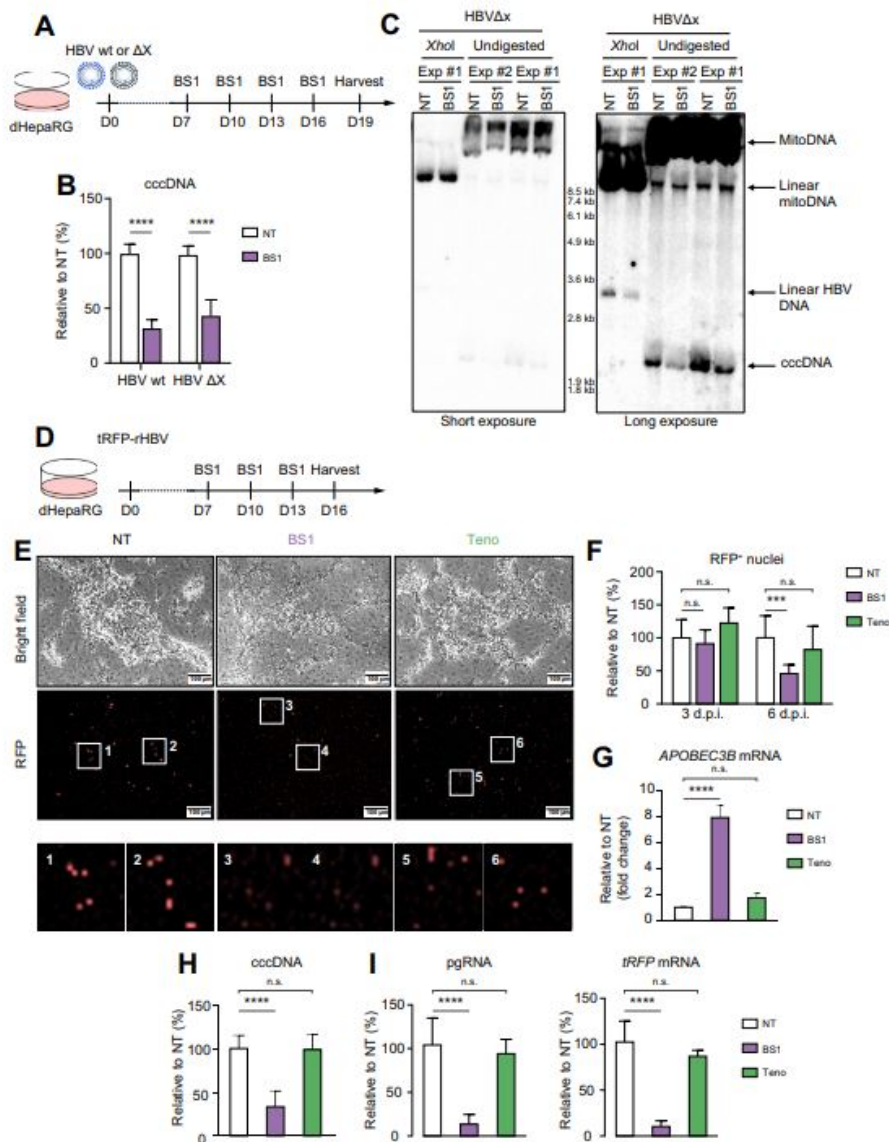
Fig. 6. APOBEC3B effect on double-stranded DNA is independent of transcription. (A–C) dHepaRG were infected with wild-type (wt) HBV or HBx deficient (ΔX) HBV. Seven d.p.i, cells were left untreated (NT) or treated with 0.5 μg/ml BS1 for 11 days. (A) Schematic representation of the experiment. (B,C) DNA were extracted and analysed using (B) qPCR and (C) Southern-blotting. (D–I) dHepaRG were infected with a recombinant tRFP-rHBV virus. Seven d.p.i., cells were left untreated (NT) or treated with 0.5 μg/ml BS1 or 0.5 μM of tenofovir for 9 days. (D) Schematic representation of the experiments presented in panels E–I. (E) Representative photos of bright field and fluorescent microscopy of the different treatments at 6 d.p.i. (F) Quantification of the number of RFP positive cells per view field. (G,I) RNA and (H) DNA were extracted and quantified by RT-qPCR and qPCR. Bars represent the mean ± SD of (F–I) 2 or (B) 4 independent experiments performed in triplicate. Data were submitted to (B) unpaired Student's t test or (F–I) 1-way ANOVA. ***p <0.001; ****p <0.001. APOBEC3B, apolipoprotein B mRNA editing catalytic polypeptide-like A; d.p.i., days post infection; n.s., not significant.

Fig. 6. APOBEC3B effect on double-stranded DNA is independent of transcription. (A–C) dHepaRG were infected with wild-type (wt) HBV or HBx deficient (ΔX) HBV. Seven d.p.i, cells were left untreated (NT) or treated with 0.5 µg/ml BS1 for 11 days. (A) Schematic representation of the experiment. (B,C) DNA were extracted and analysed using (B) qPCR and (C) Southern-blotting. (D–I) dHepaRG were infected with a recombinant tRFP-rHBV virus. Seven d.p.i., cells were left untreated (NT) or treated with 0.5 µg/ml BS1 or 0.5 µM of tenofovir for 9 days. (D) Schematic representation of the experiments presented in panels E–I. (E) Representative photos of bright field and fluorescent microscopy of the different treatments at 6 d.p.i. (F) Quantification of the number of RFP positive cells per view field. (G,I) RNA and (H) DNA were extracted and quantified by RT-qPCR and qPCR. Bars represent the mean ± SD of (F–I) 2 or (B) 4 independent experiments performed in triplicate. Data were submitted to (B) unpaired Student's t test or (F–I) 1-way ANOVA. ***p <0.001; ****p <0.001. APOBEC3B, apolipoprotein B mRNA editing catalytic polypeptide-like A; d.p.i., days post infection; n.s., not significant.

Fig. 7. APOBEC3B induction and subsequent cccDNA decay depend on NF-κB signalling and miR-138-5p decrease. Graphical representation of the main proposed mechanism(s). Upon short-time agonisation of the LTβR, NF-κB signalling induces weak APOBEC3B mRNA expression because of the inhibitory activity of miR-138-5p, thereby preventing cccDNA decay. Upon a prolonged agonisation of LTβR, the miR-138-5p levels is decreased allowing potent induction of APOBEC3B mRNA, and subsequently cccDNA decay that is independent of cccDNA transcriptional activity. APOBEC3B, apolipoprotein B mRNA editing catalytic polypeptide-like A; cccDNA, covalently closed circular DNA; NF-κB, nuclear factor kappa B.

might represent a new therapeutic approach (e.g. in a combinatorial regiment with other treatments) that should be considered to ensure the full functionality of LTβR agonists-based treatments.

Conflicts of interest

The authors declare no conflicts of interest that pertain to this work.

Please refer to the accompanying ICMJE disclosure forms for further details.

Authors' contributions

Conceptualisation: SFD, TR, MR, FR, DD, JL, ED, MH. Methodology: SFD, TR, MR, FR, DD, JL, ED, MH. Formal analysis: SFD, TR, MR, ZH. Investigation: SFD, TR, MR, ZH, FR, KN, SS, CR, NG, MS, MSt, JW, RB, RP, LCS, RF, SP, CL, RO, TE, KR, RR, KU, DT, JL, DBL. Resources: KU, UP, DD, JL, ED, MH. Data curation: SFD, TR, MR, ZH. Writing-original draft: SFD, TR, DD, JL, ED, MH. Visualisation: SFD, TR, MR, ED, MH. Supervision: ED, MH. Project administration: ED, MH. Funding acquisition: DD, JL, ED, MH.

Data availability statement

The data that support the findings of this study are available from the corresponding author, MH, upon reasonable request.

Supplementary data

Supplementary data to this article can be found online at https://doi.org/1 0.1016/j.jhep.2021.100354.

References

Author names in bold designate shared co-first authorship

[1] Fanning GC, Zoulim F, Hou J, Bertoletti A. Therapeutic strategies for hepatitis B virus infection: towards a cure. Nat Rev Drug Discov 2019;18:827–844. https://doi.org/10.1038/s41573-019-0037-0.

[2] **Lucifora J**, **Xia Y**, Reisinger F, Zhang K, Stadler D, Cheng X, et al. Specific and nonhepatotoxic degradation of nuclear hepatitis B virus cccDNA. Science 2014;343:1221–1228. https://doi.org/10.1126/science.1243462.

[3] Koh S, Kah J, Tham CYL, Yang N, Ceccarello E, Chia A, et al. Nonlytic Lymphocytes Engineered to Express Virus-Specific T-Cell Receptors Limit HBV Infection by Activating APOBEC3. Gastroenterology 2018;155:180–193.e6. https://doi.org/10.1053/j.gastro.2018.03.027.

[4] Xia Y, Stadler D, Lucifora J, Reisinger F, Webb D, Hösel M, et al. Interferon-γ and Tumor Necrosis Factor-α Produced by T Cells Reduce the HBV Persistence Form, cccDNA, Without Cytolysis. Gastroenterology 2016;150:194–205. https://doi.org/10.1053/j.gastro.2015.09.026.

[5] McCarthy DD, Summers-Deluca L, Vu F, Chiu S, Gao Y, Gommerman JL. The lymphotoxin pathway: beyond lymph node development. Immunol Res 2006;35:41–54. https://doi.org/10.1385/IR:35:1:41.

[6] Covino DA, Gauzzi MC, Fantuzzi L. Understanding the regulation of APOBEC3 expression: Current evidence and much to learn. J Leukoc Biol 2018;103:433–444. https://doi.org/10.1002/JLB.2MR0717-310R.

[7] Dejardin E. The alternative NF-kappaB pathway from biochemistry to biology: pitfalls and promises for future drug development. Biochem Pharmacol 2006;72:1161–1179. https://doi.org/10.1016/j.bcp.2006.08.007.

[8] Dejardin E, Droin NM, Delhase M, Haas E, Cao Y, Makris C, et al. The Lymphotoxin-β Receptor Induces Different Patterns of Gene Expression via Two NF-κB Pathways. Immunity 2002;17:525–535. https://doi.org/10. 1016/S1074-7613(02)00423-5.

[9] Crispe IN. The liver as a lymphoid organ. Annu Rev Immunol 2009;27:147–163. https://doi.org/10.1146/annurev.immunol.021908. 132629.

[10] Wu C-J, Lu L-F. MicroRNA in Immune Regulation. Curr Top Microbiol Immunol 2017;410:249–267. https://doi.org/10.1007/82_2017_65.

[11] Gripon P, Rumin S, Urban S, Le Seyec J, Glaise D, Cannie I, et al. Infection of a human hepatoma cell line by hepatitis B virus. Proc Natl Acad Sci U S A 2002;99:15655–15660. https://doi.org/10.1073/pnas.232137699.

[12] Schulze-Bergkamen H, Untergasser A, Dax A, Vogel H, Büchler P, Klar E, et al. Primary human hepatocytes–a valuable tool for investigation of apoptosis and hepatitis B virus infection. J Hepatol 2003;38:736–744. https://doi.org/10.1016/s0168-8278(03)00120-x.

[13] Namineni S, O'Connor T, Faure-Dupuy S, Johansen P, Riedl T, Liu K, et al. A dual role for hepatocyte-intrinsic canonical NF-κB signaling in virus control. J Hepatol 2020. https://doi.org/10.1016/j.jhep.2019.12.019.

[14] **Labun K**, **Montague TG**, Gagnon JA, Thyme SB, Valen E. CHOPCHOP v2: a web tool for the next generation of CRISPR genome engineering. Nucleic Acids Res 2016;44:W272–W276. https://doi.org/10.1093/nar/gkw398.

[15] easy and efficient inducible CRISPR/Cas9 platform with improved speci-ficity for multiple gene targeting | Nucleic Acids Research | Oxford Academic n.d. https://academic.oup.com/nar/article/44/19/e149/2468398 (accessed March 19, 2020).

[16] Chernokalskaya E, Dompenciel R, Schoenberg DR. Cleavage properties of an estrogen-regulated polysomal ribonuclease involved in the destabili-zation of albumin mRNA. Nucleic Acids Res 1997;25:735–742. https://doi. org/10.1093/nar/25.4.735.

[17] Sommers CD, Thompson JM, Guzova JA, Bonar SL, Rader RK, Mathialagan S, et al. Novel tight-binding inhibitory factor-kappaB kinase (IKK-2) inhibitors demonstrate target-specific anti-inflammatory activ-ities in cellular assays and following oral and local delivery in an in vivo model of airway inflammation. J Pharmacol Exp Ther 2009;330:377–388. https://doi.org/10.1124/jpet.108.147538.

[18] Podolin PL, Callahan JF, Bolognese BJ, Li YH, Carlson K, Davis TG, et al. Attenuation of Murine Collagen-Induced Arthritis by a Novel, Potent, Selective Small Molecule Inhibitor of IκB Kinase 2, TPCA-1 (2-[(Amino-carbonyl)amino]-5-(4-fluorophenyl)-3-thiophenecarboxamide), Occurs via Reduction of Proinflammatory Cytokines and Antigen-Induced T Cell Proliferation. J Pharmacol Exp Ther 2005;312:373–381. https://doi.org/10. 1124/jpet.104.074484.

[19] **Riedl T**, **Faure-Dupuy S**, **Rolland M**, Schuehle S, Hizir Z, Calderazzo S, et al. HIF1α-mediated RelB/APOBEC3B downregulation allows Hepatitis B Virus persistence. Hepatol Baltim Md 2021 oct;74(4):1766–1781. https:// doi.org/10.1002/hep.31902. Epub 2021 Aug 15.

[20] Schönung M, Hess J, Bawidamann P, Stäble S, Hey J, Langstein J, et al. AmpliconDesign – an interactive web server for the design of high-throughput targeted DNA methylation assays. Epigenetics 2021 Sep;16(9):933–939. https://doi.org/10.1080/15592294.2020.1834921. Epub 2020 Oct 24.

[21] **Burns MB**, **Lackey L**, Carpenter MA, Rathore A, Land AM, Leonard B, et al. APOBEC3B is an enzymatic source of mutation in breast cancer. Nature 2013;494:366–370. https://doi.org/10.1038/nature11881.

[22] Agarwal V, Bell GW, Nam J-W, Bartel DP. Predicting effective microRNA target sites in mammalian mRNAs. ELife 2015;4. https://doi.org/10.7554/ eLife.05005.

[23] **Chen Y**, **Hu J**, Cai X, Huang Y, Zhou X, Tu Z, et al. APOBEC3B edits HBV DNA and inhibits HBV replication during reverse transcription. Antiviral Res 2018;149:16–25. https://doi.org/10.1016/j.antiviral.2017.11.006.

[24] **McDaniel YZ**, **Wang D**, Love RP, Adolph MB, Mohammadzadeh N, Chelico L, et al. Deamination hotspots among APOBEC3 family members are defined by both target site sequence context and ssDNA secondary structure. Nucleic Acids Res 2020;48:1353–1371. https://doi.org/10.1093/ nar/gkz1164.

[25] **Lucifora J**, **Arzberger S**, Durantel D, Belloni L, Strubin M, Levrero M, et al. Hepatitis B virus X protein is essential to initiate and maintain virus replication after infection. J Hepatol 2011;55:996–1003. https://doi.org/ 10.1016/j.jhep.2011.02.015.

[26] Belloni L, Pollicino T, De Nicola F, Guerrieri F, Raffa G, Fanciulli M, et al. Nuclear HBx binds the HBV minichromosome and modifies the epigenetic

regulation of cccDNA function. Proc Natl Acad Sci U S A 2009;106:19975–19979. https://doi.org/10.1073/pnas.0908365106.

[27] Doehle BP, Schäfer A, Cullen BR. Human APOBEC3B is a potent inhibitor of HIV-1 infectivity and is resistant to HIV-1 Vif. Virology 2005;339:281–288. https://doi.org/10.1016/j.virol.2005.06.005.

[28] Warren CJ, Westrich JA, Van Doorslaer K, Pyeon D. Roles of APOBEC3A and APOBEC3B in Human Papillomavirus Infection and Disease Progression. Viruses 2017;9. https://doi.org/10.3390/v9080233.

[29] Maruyama W, Shirakawa K, Matsui H, Matsumoto T, Yamazaki H, Sarca AD, et al. Classical NF-κB pathway is responsible for APOBEC3B expression in cancer cells. Biochem Biophys Res Commun 2016;478:1466–1471. https://doi.org/10.1016/j.bbrc.2016.08.148.

[30] Cao W, Wu W. MicroRNAs regulate APOBEC gene expression. Histol Histopathol 2018;33:117–120. https://doi.org/10.14670/HH-11-912.

[31] Yeh M, Oh CS, Yoo JY, Kaur B, Lee TJ. Pivotal role of microRNA-138 in human cancers. Am J Cancer Res 2019;9:1118–1126.

[32] Luangsay S, Gruffaz M, Isorce N, Testoni B, Michelet M, Faure-Dupuy S, et al. Early inhibition of hepatocyte innate responses by hepatitis B virus. J Hepatol 2015;63:1314–1322. https://doi.org/10.1016/j.jhep.2015.07.014.

[33] Liu M, Mallinger A, Tortorici M, Newbatt Y, Richards M, Mirza A, et al. Evaluation of APOBEC3B Recognition Motifs by NMR Reveals Preferred Substrates. ACS Chem Biol 2018;13:2427–2432. https://doi.org/10.1021/acschembio.8b00639.

[34] Siriwardena SU, Chen K, Bhagwat AS. Functions and Malfunctions of Mammalian DNA-Cytosine Deaminases. Chem Rev 2016;116:12688–12710. https://doi.org/10.1021/acs.chemrev.6b00296.

[35] Tu T, Budzinska MA, Shackel NA, Urban S. HBV DNA Integration: Molecular Mechanisms and Clinical Implications. Viruses 2017;9. https://doi.org/10.3390/v9040075.

135

11.2 Hypoxia-Inducible Factor 1 Alpha-Mediated RelB/APOBEC3B Down-regulation Allows Hepatitis B Virus Persistence

Tobias Riedl*, Suzanne Faure-Dupuy*, Maude Rolland*, Svenja Schuehle, Zohier Hizir, Silvia Calderazzo, Xiaodong Zhuang, Jochen Wettengel, Martin A. Lopez, Romain Barnault, Valbona Mirakaj, Sandra Prokosch, Danijela Heide, Corinna Leuchtenberger, Martin Schneider, Bernd Heßling, Benjamin Stottmeier, Isabel M. Wessbecher, Peter Schirmacher, Jane A. McKeating, Ulrike Protzer, David Durantel, Julie Lucifora, Emmanuel Dejardin[#], Mathias Heikenwalder[#]

*, [#]: Contributed equally

Hypoxia-Inducible Factor 1 Alpha–Mediated RelB/APOBEC3B Down-regulation Allows Hepatitis B Virus Persistence

Tobias Riedl [ID] ,[1,2*] Suzanne Faure-Dupuy [ID] ,[1,3*] Maude Rolland [ID] ,[4*] Svenja Schuehle,[1,2] Zohier Hizir,[4] Silvia Calderazzo,[5] Xiaodong Zhuang,[6,7] Jochen Wettengel,[8] Martin Alexander Lopez,[4] Romain Barnault,[9] Valbona Mirakaj,[9] Sandra Prokosch,[1] Danijela Heide,[1] Corinna Leuchtenberger,[1] Martin Schneider,[10] Bernd Heßling,[10] Benjamin Stottmeier,[11,12] Isabel M. Wessbecher [ID] ,[11,13] Peter Schirmacher,[11,13] Jane A McKeating,[6,7] Ulrike Protzer [ID] ,[8] David Durantel [ID] ,[14] Julie Lucifora [ID] ,[14] Emmanuel Dejardin [ID] ,[4**] and Mathias Heikenwalder [ID] [1,3**]

BACKGROUND AND AIMS: Therapeutic strategies against HBV focus, among others, on the activation of the immune system to enable the infected host to eliminate HBV. Hypoxia-inducible factor 1 alpha (HIF1α) stabilization has been associated with impaired immune responses. HBV pathogenesis triggers chronic hepatitis-related scaring, leading *inter alia* to modulation of liver oxygenation and transient immune activation, both factors playing a role in HIF1α stabilization.

APPROACH AND RESULTS: We addressed whether HIF1α interferes with immune-mediated induction of the cytidine deaminase, apolipoprotein B mRNA editing enzyme catalytic subunit 3B (APOBEC3B; A3B), and subsequent covalently closed circular DNA (cccDNA) decay. Liver biopsies of chronic HBV (CHB) patients were analyzed by immunohistochemistry and *in situ* hybridization. The effect of HIF1α induction/stabilization on differentiated HepaRG or mice ± HBV ± LTβR-agonist (BS1) was assessed *in vitro* and *in vivo*. Induction of A3B and subsequent effects were analyzed by RT-qPCR, immunoblotting, chromatin immunoprecipitation, immunocytochemistry, and mass spectrometry. Analyzing CHB highlighted that areas with high HIF1α levels and low A3B expression correlated with high HBcAg, potentially representing a reservoir for HBV survival in immune-active patients. *In vitro*, HIF1α stabilization strongly impaired A3B expression and anti-HBV effect. Interestingly, HIF1α knockdown was sufficient to rescue the inhibition of A3B up-regulation and -mediated antiviral effects, whereas HIF2α knockdown had no effect. HIF1α stabilization decreased the level of v-rel reticuloendotheliosis viral oncogene homolog B protein, but not its mRNA, which was confirmed *in vivo*. Noteworthy, this function of HIF1α was independent of its partner, aryl hydrocarbon receptor nuclear translocator.

CONCLUSIONS: In conclusion, inhibiting HIF1α expression or stabilization represents an anti-HBV strategy in the context of immune-mediated A3B induction. High HIF1α, mediated by hypoxia or inflammation, offers a reservoir for HBV survival *in vivo* and should be considered as a restricting factor in the development of immune therapies. (HEPATOLOGY 2021;74:1766-1781).

H BV chronically infects >250 million persons worldwide who are at high risk of developing end-stage liver disease and HCC.[1] Current treatments allow control of the infection, but

1766

not its complete eradication because of the persistence of the viral DNA matrix, called covalently closed circular DNA (cccDNA).[2] Upon treatment arrest, the infection can relapse.[2] Therefore, treatments are urgently needed to progress toward a cure for chronic HBV infection.

Therapeutics developed for the treatment of HBV focus on activation of the adaptive and innate immune system. Several Toll-like receptor agonists have offered promising results both *in vitro* and *in vivo*.[3-5] Among these treatments, we and others have shown that induction of the cytidine deaminase, apolipoprotein B mRNA editing enzyme catalytic subunit 3B (APOBEC3B; A3B), upon immune-mediated

lymphotoxin-β receptor (LTβR) agonization (e.g., by T cells) leads to cccDNA decay.[6,7]

Most immune receptors such as LTβR are described to signal through the nuclear factor-kappa B (NF-κB) pathways.[8,9] NF-κB signaling is divided into two arms: the classical/canonical and the alternative/noncanonical pathway.[10] The canonical pathway signals through the IκB kinase (IKK) complex (inhibitor of nuclear factor κB kinase complex, consisting of NF-κB essential modulator/IKKα/IKKβ), triggering the phosphorylation and ubiquitination of nuclear factor of kappa light polypeptide gene enhancer in B-cells inhibitor alpha and the release of p50/RelA (NF-κB p65 subunit) heterodimer.[10]

ARTICLE INFORMATION:

From the [1]Division of Chronic Inflammation and Cancer, German Cancer Research Center (DKFZ), Heidelberg, Germany; [2]Faculty of Biosciences, Heidelberg University, Heidelberg, Germany; [3]Department of Infectious Diseases, Molecular Virology, Heidelberg University, Heidelberg, Germany; [4]Laboratory of Molecular Immunology and Signal Transduction, GIGA-Institute, University of Liège, Liège, Belgium; [5]Division of Biostatistics, German Cancer Research Center (DKFZ), Heidelberg, Germany; [6]Nuffield Department of Medicine, University of Oxford, Oxford, United Kingdom; [7]Chinese Academy of Medical Sciences (CAMS) Oxford Institute (COI), University of Oxford, Oxford, United Kingdom; [8]Institute of Virology, Helmholtz Zentrum München, Munich, Germany; [9]Departement of Anesthesiology and Intensive Care Medicine, Molecular Intensive Care Medicine, University Hospital Tübingen, Eberhard-Karls-University, Tuebingen, Germany; [10]Mass Spectrometry Based Protein Analysis Unit, German Cancer Research Center (DKFZ), Heidelberg, Germany; [11]Institute of Pathology, University Hospital Heidelberg, Heidelberg, Germany; [12]German Center for Infection Research (DZIF), partner site Heidelberg, Heidelberg, Germany; [13]Tissue Bank of the German Center for Infection Research (DZIF), Institute of Pathology, Heidelberg University Hospital, Heidelberg, Germany; [14]INSERM, U1052, Cancer Research Center of Lyon (CRCL), University of Lyon (UCBL1), CNRS UMR_5286, Centre Léon Bérard (CLB), Lyon, France.

ADDRESS CORRESPONDENCE AND REPRINT REQUESTS TO:

Mathias Heikenwälder, Ph.D.
Division Chronic Inflammation and Cancer (F180)
German Cancer Research Center (DKFZ)
Im Neuenheimer Feld 242
69120 Heidelberg, Germany
E-mail: m.heikenwaelder@dkfz-heidelberg.de
Tel.: +49 6221 42-3891
or

Dejardin Emmanuel, Ph.D.
Laboratory of Molecular Immunology and Signal Transduction,
University of Liège, GIGA-Institute
Avenue de l'Hôpital, 1
CHU, B34
4000 Liege, Belgium
E-mail: e.dejardin@uliege.be
Tel.: +32 4 3664472

1767

The noncanonical pathway signals through NF-κB-inducing kinase (NIK), leading to the phosphorylation of IKKα and p100, which is subjected to processing into p52 forming p52/RelB (v-rel reticuloendotheliosis viral oncogene homolog B) heterodimers that activate target genes such as immune mediators.[11]

To reduce the extent of chronic inflammation and its deleterious effects, NF-κB signaling has to be tightly regulated.[12] Among the factors involved in this regulation, hypoxia-inducible factor 1 alpha (HIF1α) has been shown to (1) be stabilized or induced by and (2) regulate NF-κB signaling,[13] in addition to its canonical induction by low oxygen levels.[14] HIF1α is constantly produced and is targeted to the proteasome in the absence of stabilizing conditions.[14]

Here, we identify HIF1α stabilization and the concomitant decrease of RelB protein level as a restricting factor for immune-mediated antiviral strategies against HBV.

Materials and Methods

CELL CULTURE

HepaRG, a nontransformed progenitor cell line that can be differentiated into hepatocytes, was cultured as described.[15] Cells under hypoxia were cultured under 1% or 3% oxygen (InVivO2; Baker Ruskinn, Sanford, ME), 5% CO_2, in a humidified atmosphere.

TRANSGENIC CELL-LINE PREPARATION

HIF-overexpressing cell lines were generated from HepaRG-TR.[16] HIF open reading frames (ORFs) were excised from HA-HIF1α P402A/P564A-pcDNA3 (#18955; Addgene, Teddington, United-Kingdom), or HA-HIF2α-pcDNA3 (#18950; Addgene), using BamHI and XbaI (New England Biolabs, Ipswich, MA). The P402A/P564A double mutation prevents HIF1α hydroxylation and degradation. ORFs were then inserted into the BamHI/XhoI digested pLenti CMV/TO Hygro empty (w214-1; #17484; Addgene) using T4 DNA ligase (New England Biolabs). All HIF vectors were a gift from William Kaelin, and pLenti CMV/TO Hygro empty (w214-1) was a gift from Eric Campeau and Paul Kaufman.

Preparation of lentiviral particles and transduction of HepaRG cells were performed based on protocols from Addgene. After each transduction step, HepaRG cells were selected with blasticidin (5 µg/mL; TetR; Invitrogen, Waltham, MA) and puromycin (10 µg/mL; single-guide RNA; Sigma-Aldrich, Saint-Louis, MO) until nontransduced cells had fully died.

TREATMENTS AND TRANSFECTIONS

dHepaRG cells were treated with 0.5 µg/mL of BS1 (generous gift from Dr. Jeffrey Browning, Biogen/Idec, Cambridge, MA). Additionally, dHepaRG cells, not infected with HBV, were stimulated either with 10 ng/mL of TNFα, 50 ng/mL of IL-17, or 100 ng/mL of lipopolysaccharide (LPS), or left untreated. dHepaRG cells infected with HBV were treated with 1,000 IU of interferon alpha (IFNα) 2A (Roferon; Roche, Mannheim, Germany), 800 IU of TNFα (210-TA; R&D Systems, Abingdon, United-Kingdom), or 200 IU of interferon gamma (IFNγ; 285-IF; R&D Systems). All inhibitors and molecules used are presented in Supporting Table S1. dHepaRG cells were transfected with 10 nM of small interfering RNAs (siRNAs) against HIF1α (Assay ID: s6539; Ambion, Oberursel, Germany), hypoxia-inducible factor 2 alpha (HIF2α; Assay ID: s4698; Ambion), aryl hydrocarbon receptor (AhR; Sigma-Aldrich), aryl hydrocarbon receptor nuclear translocator (ARNT; Sigma-Aldrich), v-rel reticuloendotheliosis viral oncogene homolog B (RelB; Dharmacon, Lafayette, CO), or nontargeting control siRNAs (siCtrl; 4390843; Ambion), using Dharmafect 4 (1:1,000; Dharmacon; Supporting Table S2).

HBV PREPARATION AND INOCULA

HBV was purified and concentrated from the culture medium of HepAD38 cells by heparin columns and sucrose gradient ultracentrifugation as described.[17] dHepaRG cells were infected with 200 viral genome equivalents per cell, in medium supplemented with 4% PEG-8000 (Sigma-Aldrich). Twenty-four hours after infection, cells were washed three times with PBS.

HUMAN LIVER SPECIMEN

Sections of formalin-fixed, paraffin-embedded liver resections of 15 patients chronically infected with

1768

HBV were obtained from the DZIF partner site in Heidelberg/Institute of Pathology of the Medical University Heidelberg. Chronic hepatitis B (CHB) patients were all in the immune-active phase of the disease and presented F3/F4 fibrosis grading and A3 activity (METAVIR scoring). Sections were cut to be 2 or 5 μM thick. Work with patient material was approved by the Heidelberg ethics committee under the following number: S206/2005. We confirmed that informed consent was collected from all co authors for the manuscript.

STATISTICAL ANALYSIS

Two-way ANOVA, Spearman correlation, and the unpaired Student two-tailed t test were performed using Prism software (version 8; GraphPad Software Inc., La Jolla, CA). Data are shown as mean ± SD ($*P < 0.05$; $**P < 0.01$; $***P < 0.001$; $****P < 0.001$).

Additional materials and methods information can be found in the Supporting Information.

Results

HIF1α STABILIZATION OFFERS A RESERVOIR FOR HBV IN IMMUNE-ACTIVE PATIENTS

Hypoxia has been shown to strongly modulate immune responses, both positively and negatively, depending on the cells and the immune mechanisms involved.[14] Inflammatory cytokines and/or ligands have been shown to efficiently inhibit HBV infection.[3,18,19] Thus, we wanted to decipher whether HIF1α might be involved in HBV persistence in chronically infected patients by preventing immune activation. Consecutive cuts of livers from CHB patients with end-stage CHB, also considered as an immune-active phase, were stained for HIF1α and HBcAg. Highly oxygenated/low inflammation zones, highlighted by an absence of HIF1α staining, were also low for HBcAg staining in these CHB patients (Fig. 1A,B). In contrast, zones with low oxygen level or with inflammation (i.e., strong HIF1α staining) presented an increased number of HBcAg-positive nuclei. A correlation was found between the numbers of HIF1α- and HBcAg-positive cells (Fig. 1C).

We have previously shown that, on the one hand, LTβR agonization by an agonistic antibody (BS1)

leads to cccDNA decay and HBV clearance, whereas, on the other hand, LTα/β are up-regulated in CHB patients.[6,20] Therefore, induction of LTβ in CHB patients should clear the infection given its antiviral effect. To assess whether the correlation of HIF1α and HBc observed *in vivo* (Fig. 1C) could be attributable to lower immune response in this area, liver of CHB patients were either stained for HIF1α and A3B by *in situ* mRNA hybridization on consecutive slides, or by costaining of mRNA and protein. High HIF1α staining was found in areas with low A3B expression, whereas low HIF1α staining was found in areas with strong A3B expression (Fig. 1D,E and Supporting Fig. S1).

Altogether, these data highlight that in areas with high HIF1α stabilization, A3B expression is impaired, allowing viral persistence even during liver inflammation. Therefore, high HIF1α areas provide a reservoir for HBV persistence *in vivo*.

HIF1α STABILIZATION DECREASES ANTI-cccDNA PROPERTIES OF LTβR AGONISATION

To confirm our findings *in vitro*, we used several HIF1α stabilizing conditions, namely hypoxia (canonical HIF1α stabilizer and inducer; i.e., 1% oxygen), dimethyloxallyl glycin (DMOG), or roxadustat (FG-4592; two molecules described to stabilize HIF1α through the inhibition of proline hydroxylases, enzymes that, if active, hydroxylate HIF-αs in the presence of oxygen to address it for degradation). A schematic representation of the experiment timeline is presented in Fig. 2A. Treatment with BS1 induced A3B, leading to cccDNA decrease, as described (Fig. 2B-G, siCtrl NO/BS1 or siCtrl DMSO/BS1). Upon HIF1α stabilization, A3B induction was decreased, impairing its antiviral effects on cccDNA (Fig. 2B-G, siCtrl HO/BS1, siCtrl DMOG/BS1, or siCtrl FG-4592/BS1). A3B induction and anti-cccDNA activity was partially rescued by HIF1α knockdown (Fig. 2B-G, siRNA HIF1α [siHIF1α] HO/BS1, siHIF1α DMOG/BS1, or siHIF1α FG-4592/BS1). BS1-induced decrease of cccDNA quantity and impairment thereof by DMOG treatment was also confirmed by Southern blotting analysis (Fig. 2H). Of note, HIF1α knockdown under normoxia was sufficient to (1) increase A3B mRNA levels and (2) decrease cccDNA levels as compared to siCtrl (Fig. 2A,B). This effect was attributable
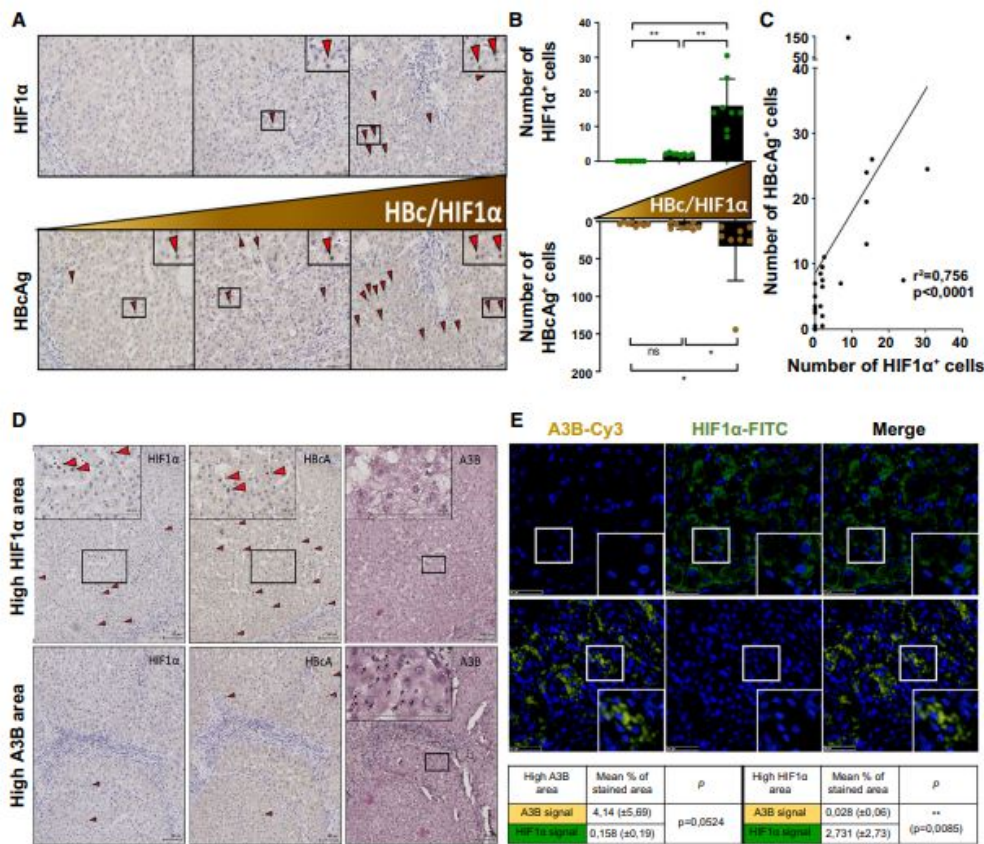
1769

FIG. 1. HIF1α stabilization allows HBV persistence *in vivo*. (A-E) Paraffin sections of CHB patients were consecutively cut and stained for HIF1α, HBcAg, or APOBEC3B mRNA *in situ* or costained for HIF1α and APOBEC3B mRNA *in situ*. (A,B) Regions were classified in three types: (1) no HIF1α-positive cells; (2) one to five HIF1α-positive cells; and (iii) greater than five HIF1α-positive cells. Arrowheads show positive nuclei. (A) Representative pictures of the three zones of HIF1α (upper panels) and HBcAg (lower panels) from the same patient. (B) Quantification of the number of HIF1α- and HBcAg-positive cells in the three different zones. Every data point represents the mean of two view fields, and the bars represent the mean ± SD of 8 patients. (C) Correlation between HIF1α and HBcAg positivity per view field. (D) Representative pictures of patients stained for A3B. Upper three pictures show a representative HIF1α-high area, and the lower three pictures show an A3B-high area of the same patient sample. (E) Representative images of a patient stained for HIF1α and A3B. Upper three pictures show a representative HIF1α-high area, and the lower three pictures show an A3B-high area of the same patient sample. Percentage of stained area for A3B and HIF1α was quantified and is presented in the table ± SD of 9 different patients. Data were submitted to (A) Pearson's correlation analysis and (E) one-way ANOVA. *P < 0.05; **P < 0.01. Abbreviations: Cy3, cyanine 3; FITC, fluorescein isothiocyanate.

to BS1-induced HIF1α stabilization, as confirmed by immunoprecipitation of HIF1α under normoxia-BS1 conditions (Supporting Fig. S2A). Like A3B, the up-regulation of nuclear factor kappa B subunit 2 (NF-κB2), a NF-κB target gene, was attenuated in cells upon HIF1α stabilization, which was rescued by HIF1α knockdown (Supporting Fig. S2B-D). Carbonic anhydrase IX, a direct target gene of HIF1α, was up-regulated upon HIF1α stabilization and showed a strong reduction when HIF1α was depleted
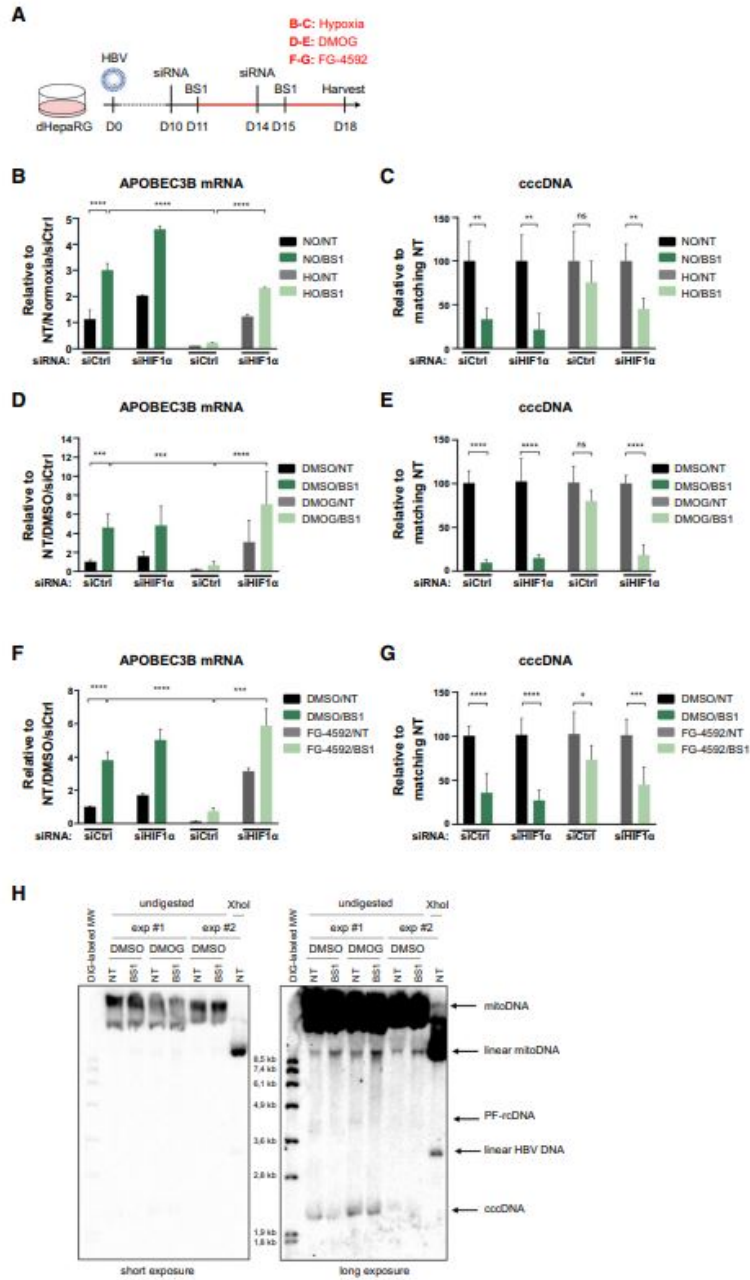
FIG. 2. HIF1α stabilization prevents the antiviral effects of APOBEC3B *in vitro*. (A) Schematic representation of the experiments. (B,C) dHepaRG cells were infected with HBV. Six d.p.i., cells were transfected with either 10 nM of HIF1α-targeting or control siRNAs. On the next day, cells were subjected to 1% or 20% oxygen for 3 days and treated with ±0.5 μg/mL of BS1. Transfection and treatments were repeated once. (D,E) dHepaRG cells were infected with HBV. At 10 and 13 d.p.i., cells were transfected with either 10 nM of HIF1α-targeting or control siRNAs. Cells were then treated with ±0.5 μg/mL of BS1 and with ±100 μM of DMOG. (F,G) dHepaRG cells were infected with HBV. At 10 and 13 d.p.i., cells were transfected with either 10 nM of HIF1α-targeting or control siRNAs. One day after the second transfection, cells were treated or not with 0.5 μg/mL of BS1, either under the presence of 30 μM of FG-4592 or DMSO. Six days later, (B,D,F) mRNAs and (C,E,G) DNA were extracted and analyzed by RT-qPCR and qPCR. Bars represent the mean ± SD of (B,C) one or (D-G) three independent experiments performed in quadruplicates. Data were submitted to (C,E,G) an unpaired Student *t* test or (B,D,F) one-way ANOVA. *$P < 0.05$; **$P < 0.01$; ***$P < 0.005$; ****$P < 0.0001$. (H) dHepaRG cells were infected with HBV. At 10 d.p.i., cells were treated with ±0.5 μg/mL of BS1 and with ±100 μM of DMOG for 12 days. Episomal DNA was extracted and analyzed by Southern blotting. Abbreviations: DIG, digoxigenin; d.p.i., days postinfection; mitoDNA, mitochondrial DNA; MW, molecular weight; NT, nontreated; PF, protein-free; rcDNA, relaxed circular DNA.

(Supporting Fig. S2B-D). LTβR mRNA expression was slightly reduced under hypoxia, which could be rescued by HIF1α knockdown and was unchanged by DMOG or FG-4592 treatments (Supporting Fig. S2B-D). Of note, HIF1α knockdown was confirmed by immunoblotting (Supporting Fig. S2B-D). Notably, cccDNA degradation induced by other treatments (e.g., IFNα [Roferon], IFNγ, or TNFα) was also prevented by HIF1α stabilization induced by DMOG (Supporting Fig. S2E).

Altogether, these data highlight that HIF1α stabilization impairs the up-regulation of A3B and anti-cccDNA activity of BS1 treatment, which can be efficiently rescued by HIF1α depletion.

HIF1α, BUT NOT HIF2α, IS INVOLVED IN HYPOXIA-MEDIATED APOBEC3B REPRESSION

Hypoxia can induce the stabilization of both HIF1α and HIF2α. Although we show that HIF1α knockdown can rescue A3B expression and antiviral effects of BS1 under HIF-stabilizing conditions (Fig. 2), we aimed to investigate a potential additional role of HIF2α. Therefore, cell lines doxycycline inducible for the overexpression of wild-type HIF1α, degradation-resistant HIF1α, or wild-type HIF2α were generated. Of note, only a degradation-resistant HIF1α (carrying a P402A and a P564A mutation, eliminating the sites that, when hydroxylated, target HIF1α for degradation) was detected in the overexpressing cell line (Supporting Fig. S3A). Consequently, subsequent experiments were only performed with the degradation-resistant HIF1α. Transcriptional activity and expression of mutated HIF1α and HIF2α were

confirmed by RT-qPCR and immunoblotting, respectively (Supporting Fig. S3A-D). Overexpression of HIF1α or HIF2α alone inhibited A3B up-regulation induced by BS1 (Fig. 3A). However, under hypoxia, only siRNAs against HIF1α, but not HIF2α, rescued A3B up-regulation, and no cumulative effect was observed when knocking down both HIF1α and HIF2α, highlighting that HIF2α only plays a minor role in A3B inhibition under hypoxic conditions (Fig. 3B). HIF1α and HIF2α knock-down efficiencies were confirmed by RT-qPCR (Supporting Fig. S3E). Moreover, inhibition of A3B by HIF1α and rescue by HIF1α knockdown were confirmed using different HIF1α stabilizers (DMOG, CoCl$_2$, and VH298; Fig. 3C,D and Supporting S3F). Of note, LTβR surface expression remained unchanged under hypoxia, with a mild increase after HIF1α knockdown, highlighting that the effect of HIF1α stabilization was not attributable to a decreased receptor expression (Supporting Fig. S4G,H). Moreover, A3B repression was not attributable to cell death under hypoxia (Supporting Fig. S3I).

Altogether, these data show that under hypoxic conditions, HIF1α—but not HIF2α—impairs the induction of A3B.

HIF1α STABILIZATION INHIBITS NF-κB-INDUCED A3B TRANSCRIPTION BY DECREASING RelB PROTEIN EXPRESSION LEVEL

The main signaling pathways activated upon LTβR agonization are related to NF-κB, suggesting that A3B is an NF-κB target gene. To confirm this hypothesis, we used two kinase inhibitors ([N-(6-chloro-7-methoxy-9H-β-carbolin-8-yl)-2-methylnicotinamide]
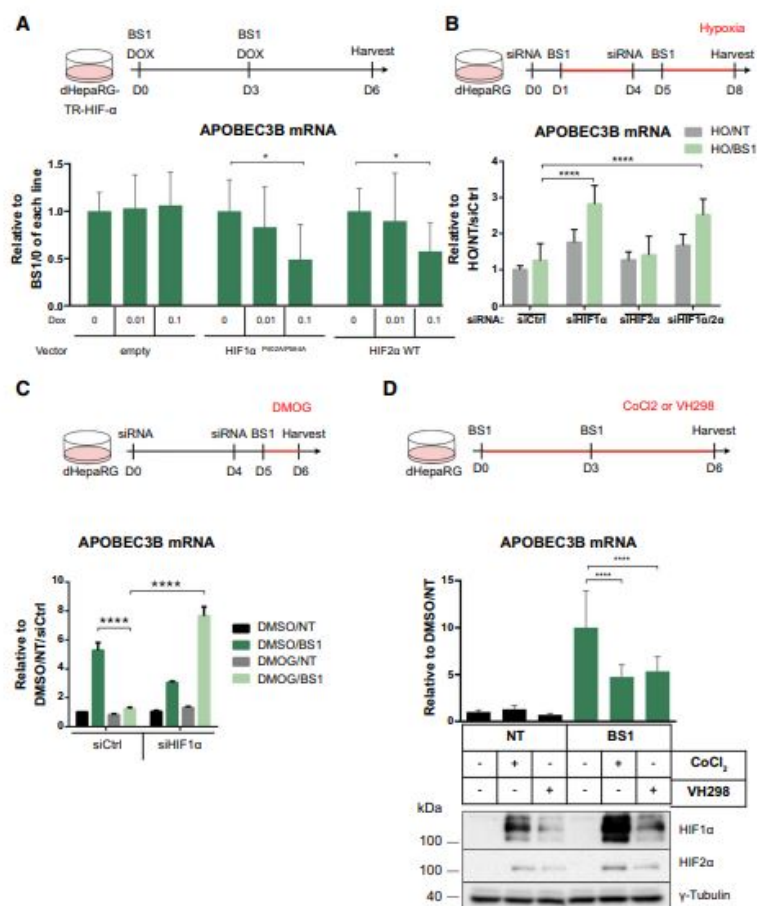
FIG. 3. HIF1α, but not HIF2α, stabilization inhibits APOBEC3s. (A-D) Schematic representation of the experiments. (A) Inducible dHepaRG cells overexpressing the HIF1α degradation-resistant mutant, P402A/P564A, or HIF2α treated for 3 days with an increasing dose of doxycycline in the presence of 0.5 μg/mL of BS1. (B) dHepaRG cells were transfected with 10 nM of either HIF1α-targeting, HIF2α-targeting, or both siRNAs or control siRNAs. The next day, cells were treated with ±0.5 μg/mL of BS1 under 1% oxygen. mRNAs were extracted and analyzed by RT-qPCR. (C) dHepaRG cells were transfected with either 10 nM of HIF1α-targeting or control siRNAs. One day after the second transfection, cells were treated or not, for 24 hours, with 0.5 μg/mL of BS1, either under the presence of 100 μM of DMOG or DMSO. mRNAs were analyzed by RT-qPCR. Bars represent the mean ± SD of three independent experiments performed in triplicates. (D) dHepaRG cells were incubated for 3 days with ±100 μM of CoCl₂ or VH298 in the presence or absence of 0.5 μg/mL of BS1. mRNAs and proteins were extracted and analyzed by RT-qPCR and immunoblotting with the indicated antibodies, respectively. (A-D) Data represent the mean ± SD of three independent experiments performed in triplicates. Data were submitted to one-way ANOVA. *$P < 0.05$; **$P < 0.01$; ***$P < 0.001$; ****$P < 0.0001$. Abbreviations: DOX, doxycycline; NT, nontreated.

and [5-(p-fluorophenyl)-2-ureido] thiophene-3-carboxamide) that target the IKK complex (IKKα/β). We observed that inhibition of IKKα/β reduces

BS1-induced A3B in dHepaRG cells (Supporting Fig. S4A). Given that we showed that HIF1α stabilization prevents BS1-induced A3B, we anticipated that

1773

HIF1α would inhibit NF-κB target genes. Indeed, the induction of the well-known NF-κB target genes, *nfkb2* and *nik*, upon BS1 treatment in normoxia is highly reduced in hypoxic conditions, and this effect was confirmed for A3B (Supporting Fig. S4B-D). We also extended our analysis with other activators of NF-κB (TNFα, IL-17, and LPS) and observed the same trend on the tested NF-κB target genes.

Therefore, our results indicate a hypoxia-related impairment of the NF-κB signaling pathways. Interestingly, RelB is at the crossroad of both NF-κB pathways; *relb* transcription is dependent on the canonical, whereas RelB protein is part of the noncanonical, NF-κB dimer, p52/RelB.[10] We confirmed that, whereas BS1 increased RelB protein expression and A3B transcription, depletion of RelB drastically reduces BS1-induced A3B expression (Supporting Fig. S5B,C). Therefore, we addressed whether the inhibitory effect of HIF1α stabilization on BS1-induced A3B up-regulation was a consequence of RelB inactivation.

Cell fractionation highlighted that DMOG strongly reduces BS1-induced RelB protein in both the cytosolic and the nuclear compartments, whereas RelA expression and nuclear translocation were not strongly affected (Fig. 4A). More important, the decrease of RelB protein levels in the DMOG/BS1 condition was completely rescued in HIF1α-depleted cells (Fig. 4B). HIF1α stabilization did not repress BS1-induced RelB mRNA up-regulation (Fig. 4C). These results were confirmed using longer DMOG treatment, a different level of hypoxia, and other HIF1α stabilizers (Supporting Fig. S5D-G). By immunostaining, we also confirmed that RelA nuclear translocation remained unchanged under hypoxia (Supporting Fig. S5H,I), whereas hypoxia impaired RelB induction (Fig. 4D). Interestingly, hypoxia also prevented BS1-induced p52 (the main binding partner of RelB) recruitment to the A3B promoter (Fig. 4E).

To investigate whether our *in vitro* findings would also be of relevance *in vivo*, C57BL6/J mice were injected either with DMSO or DMOG and euthanized 6 hours postinjection. *In vivo*, DMOG triggered HIF1α stabilization and a strong reduction of RelB protein expression in the liver, without affecting RelB mRNA. No change was observed for RelA or p50 (Fig. 4F).

Altogether, our *in vitro* and *in vivo* results identified a strong reduction of RelB protein, but not mRNA expression, as the main driver of HIF1α-induced impairment of A3B expression.

HIF1α-MEDIATED INHIBITION OF RelB/A3B EXPRESSION IS INDEPENDENT OF ITS TRANSCRIPTIONAL ACTIVITY

HIF1α belongs to a large family of proteins, including ARNT and AhR.[21] It has been reported that RelB can dimerize with AhR or ARNT (RelB/AhR or RelB/ARNT), either controlling RelB protein stability and/or RelB transcriptional activity.[22,23] Moreover, crosstalks between these proteins can occur through competition for common partners (e.g., HIF1α/ARNT vs. AhR/ARNT).[24] Thus, we investigated whether such processes could control RelB activity in our model. A schematic timeline of the experiments is depicted in Fig. 5A.

In dHepaRG cells, AhR knockdown did not interfere with BS1-induced RelB expression, highlighting that AhR was dispensable for RelB stability (Fig. 5B). Interestingly, contrary to HIF1α knockdown, RelB protein levels were not rescued in ARNT-depleted cells treated with DMOG/BS1 (Fig. 5C). It was reported that ARNT represses the transcription of particular NF-κB target genes,[23] as confirmed by the elevated expression of C-X-C motif chemokine ligand 10 in ARNT-depleted cells (Supporting Fig. S6A). However, ARNT knockdown had no impact on RelB mRNA expression, whereas vascular endothelial growth factor alpha expression (a target gene of the HIF1α/ARNT heterodimer) was reduced (Supporting Fig. S6B,C). In addition, neither AhR nor ARNT knockdown rescued A3B levels in DMOG-treated cells (Fig. 5D,E). These results indicate that HIF1α/ARNT dimerization, which is necessary for the canonical function of HIF1α as a transcription factor, is not the cause of decreased RelB protein and A3B mRNA expression.

In summary, our results demonstrate that HIF1α/RelB crosstalk prevents BS1-mediated A3B expression through an unconventional HIF1α-dependent mechanism.

HYPOXIA PREVENTS IMMUNE INDUCTION BY DYSREGULATING EXECUTING PATHWAYS

To investigate the global effect of hypoxia, mass spectrometry was performed on control or HIF1α-targeting siRNA-transfected dHepaRG cells treated
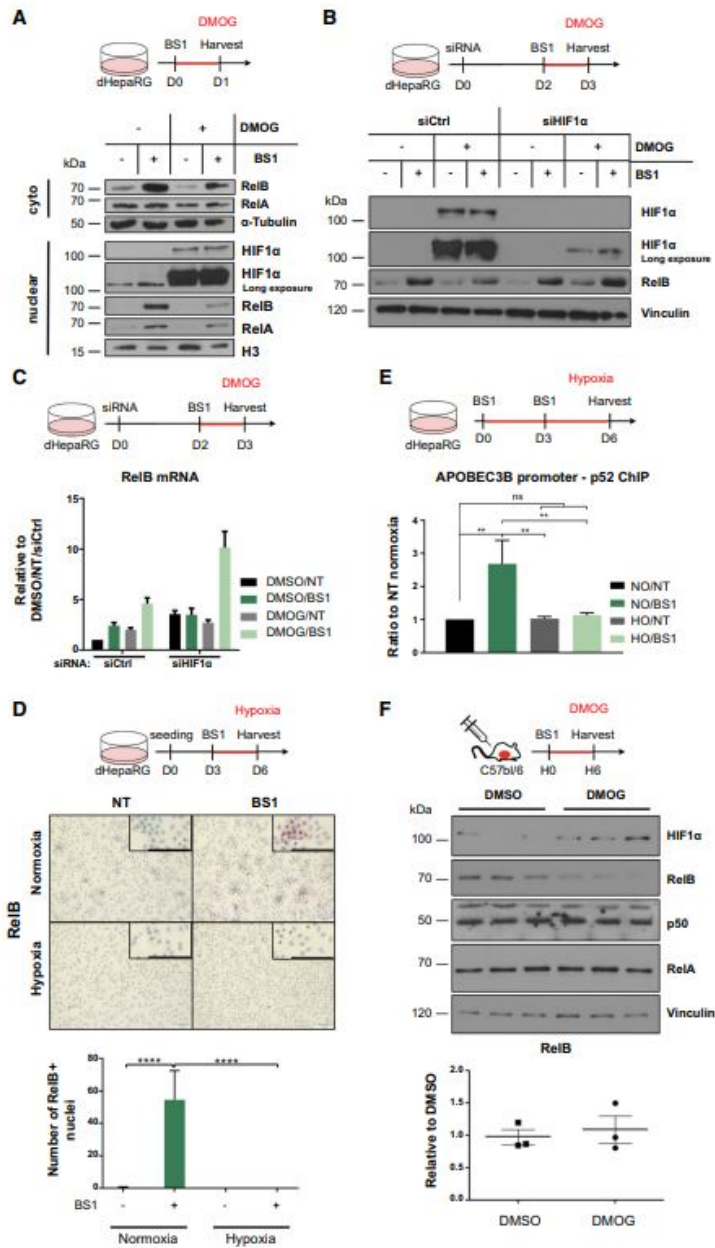
FIG. 4. HIF1α stabilization decreases RelB level *in vitro* and *in vivo*. (A-F) Schematic representation of the experiments. (A) dHepaRG cells were treated for 24 hours with DMSO or 100 μM of DMOG ± 0.5 μg/mL of BS1. Cytoplasm and nuclei were separated. (B,C) dHepaRG cells transfected with either 10 nM of HIF1α-targeting siRNAs or control siRNAs. Two days after transfection, cells were treated for 24 hours with DMSO or 100 μM of DMOG ± 0.5 μg/mL of BS1 for 24 hours. (D) dHepaRG cells were seeded into four-well chamber slides. Three days after seeding, cells were cultured under either 1% (Hypoxia) or 20% (Normoxia) oxygen for 3 days, either in the presence or absence of 0.5 μg/mL of BS1. Cells were then prepared for immunocytochemistry and stained for RelB. Representative pictures and quantification of RelB-positive nuclei. Data represent the mean of five pictures per condition of two experiments. (E) dHepaRG cells were cultured under 1% or 20% oxygen ± 0.5 μg/mL of BS1. Six days posttreatment, protein and nucleic acids were cross-linked and submitted to ChIP. DNA was extracted, and binding of p52 to APOBEC3B promoter was analyzed by qPCR. (F) Mice were injected i.p. with 300 mg/kg of DMOG or the equal amount of DMSO for 6 hours. (A,B,F) Proteins were analyzed by immunoblotting. (C,F) mRNAs were analyzed by RT-qPCR. Bars represent the mean ± SD of (C,R) three independent experiments. Data were submitted to (D,E) one-way ANOVA. *$P < 0.05$; **$P < 0.01$; ****$P < 0.0001$. Abbreviations: ChIP, chromatin immunoprecipitation; NT, nontreated.
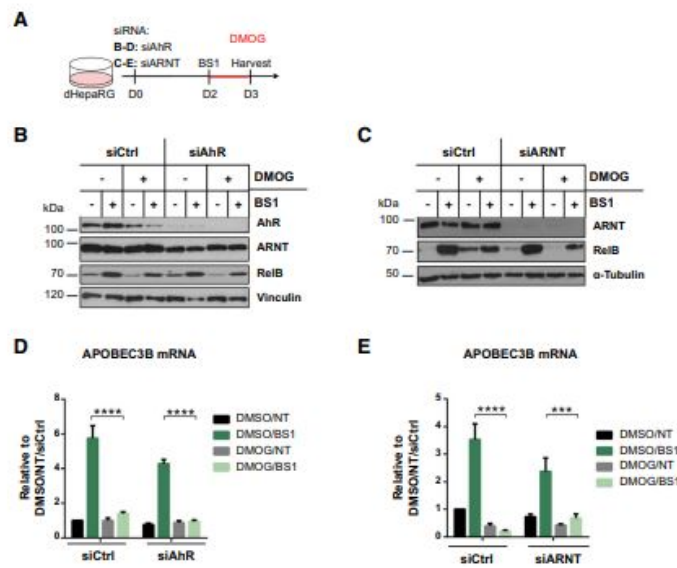

FIG. 5. ARNT knockdown does not rescue RelB and A3B level. (A) Schematic representation of the experiment. (B-E) dHepaRG cells were transfected with either 10 nM of AhR-targeting (siAhR), ARNT-targeting (siARNT), or control siRNAs (siCtrl). Two days after transfection, cells were treated for 24 hours with DMSO or 100 μM of DMOG ± 0.5 μg/mL of BS1. (B,C) Proteins were analysed by immunoblotting. (D, E) mRNAs were analysed by RT-qPCR. Bars represent the mean ± SD of (D, E) three independent experiments. Data were submitted to (D, E) one-way ANOVA. ***$P < 0.001$; ****$P < 0.0001$. Abbreviation: NT, nontreated.

with or without BS1 under normoxia (NO) or hypoxia (HO). A schematic timeline of the experiment is depicted in Fig. 6A. Interestingly, whereas 418 proteins were significantly dysregulated in BS1-treated versus nontreated cells under normoxia (NO/NT vs. NO/BS1), only two proteins were found to be dysregulated when comparing the same treatments under hypoxia (HO/NT vs. HO/BS1), indicating a global inhibition of responses to BS1 treatment (Fig. 6B). Pathways were grouped into four different clusters: I, transcription and translation; II, signal transduction and immune response; III, metabolism; and IV, DNA replication and repair. Results highlighted that BS1 treatment impaired the metabolism (e.g., drug and fatty acid metabolism) of dHepaRG cells and cellular transcriptional and translational machinery were among the most up-regulated pathways, leading to production of immune response pathway effectors (Fig. 6C).

1776

Additional pathway analyses were conducted for the following comparisons: nontreated normoxia, siRNA control-transfected versus BS1-treated normoxia, siRNA control-transfected (NO/NT/siCtrl vs. NO/BS1/siCtrl); nontreated normoxia, siRNA control-transfected versus BS1-treated hypoxia, siRNA control-transfected (NO/NT/siCtrl vs. HO/BS1/siCtrl); nontreated hypoxia, siRNA control-transfected versus BS1-treated hypoxia, siHIF1α-transfected (NO/NT/siCtrl vs. HO/BS1/siHIF1α).
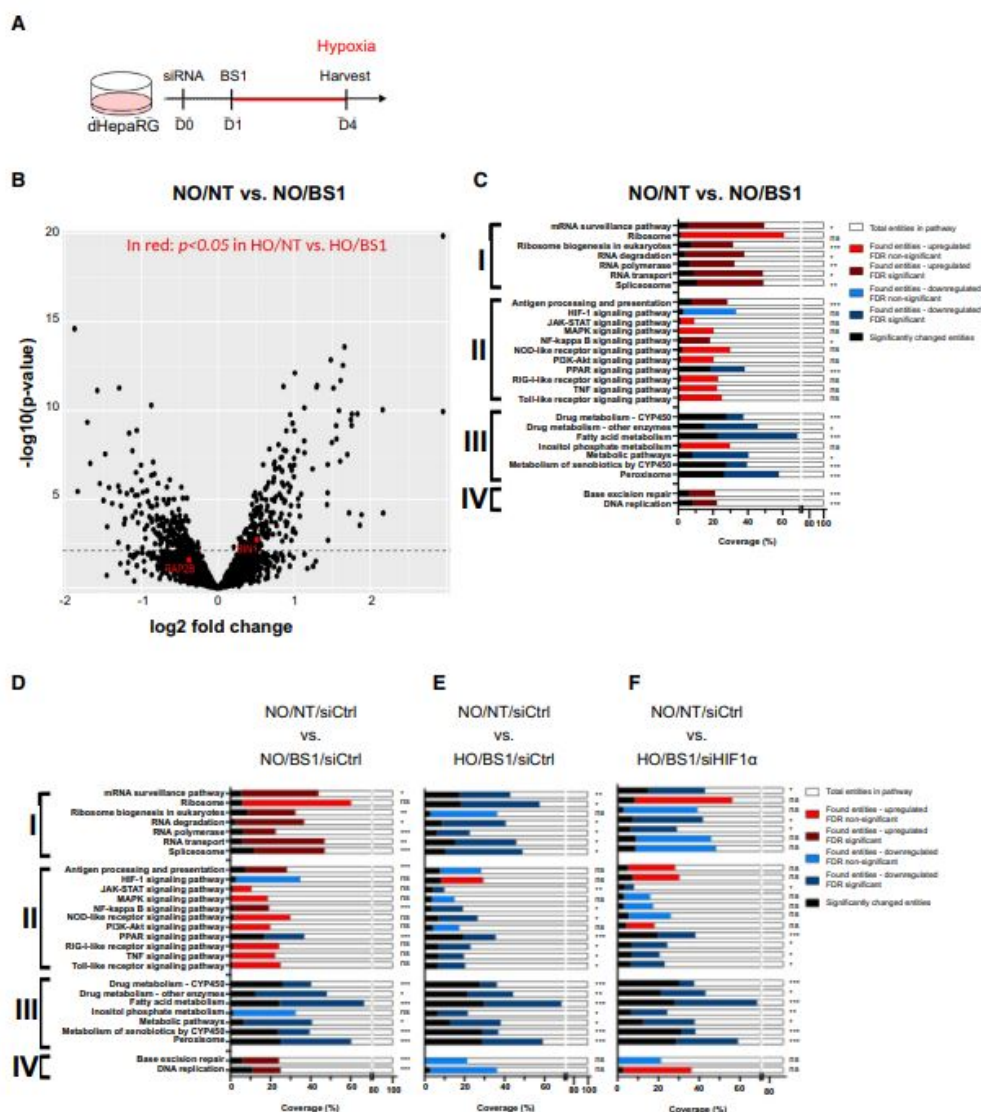
FIG. 6. HIF1α knockdown rescues mRNA-processing and ribosomes pathways. (A) Schematic representation of the experiment. (B-F) dHepaRG were (B,C) either left untransfected or (D-F) transfected with either 10 nM of HIF1α-targeting or control siRNAs. On the next day, cells were subjected to 1% (Hypoxia) or 20% (Normoxia) oxygen for 3 days ± 0.5 μg/mL of BS1. Proteins were submitted to unbiased mass spectrometry analysis. (B) Data are presented as volcano plot of normoxia nontreated (NO/NT) versus normoxia BS1-treated (NO/BS1) comparison. Dotted line represents the limit of significance (adjusted P value, <0.05). Red dots represent the only two proteins that are still significantly dysregulated (i.e., adjusted P value, <0.05) in similar comparison under hypoxia (HO/NT vs. HO/BS1). (C-F) Pathway analysis of significantly changed proteins was conducted with preselected KEGG pathways using the ROAST algorithm. The pathways are represented for (C) NO/NT versus NO/BS1, (D) NO/NT/siCtrl versus NO/BS1/siCtrl, (E) NO/BS1/siCtrl versus HO/BS1/siCtrl, and (F) HO/BS1/siCtrl versus HO/BS1/siHIF1α. The significantly (respectively, nonsignificant) up-regulated (dark red bar; respectively, light red bar) or down-regulated (dark blue bar; respectively, light blue bar) pathways are presented as the percentage of proteins analyzed in the pathways. Of note, black bars represent the number of significantly dysregulated proteins in the pathway. Data were submitted to a LIMMA algorithm for selection of significantly changed proteins. *$P < 0.05$; **$P < 0.01$; ***$P < 0.001$; ****$P < 0.0001$. Abbreviations: Akt, protein kinase B; CYP450, cytochrome P450; FDR, false discovery rate; JAK, Janus kinase; KEGG, Kyoto Encyclopedia of Genes and Genomes; MAPK, mitogen-activated protein kinase; NT, nontreated; PI3K, phosphoinositide 3-kinase; PPAR, peroxisome proliferator-activated receptor; RIG-I, retinoic-acid–inducible gene I; ROAST, rotation gene set testing; STAT, signal transducer and activator of transcription.

NO/NT/siCtrl versus NO/BS1/siCtrl comparison confirmed the results obtained in nontransfected conditions (Fig. 6D). However, the NO/NT/siCtrl versus HO/BS1/siCtrl comparison highlighted a significant down-regulation of pathways implicated in RNA transcription and translation (e.g., ribosome, mRNA surveillance), preventing the increase of immune response pathway effectors (Fig. 6E). While being up-regulated under NO/BS1 conditions (Fig. 6D), the NF-kB signaling pathway was down-regulated under hypoxia (Fig. 6E). Interestingly, NO/NT/siCtrl versus HO/BS1/siHIF1α comparison showed a partial rescue of some of these pathways upon HIF1α knockdown, namely RNA processing (i.e., Spliceosome) and transport, as well as NF-κB- and NOD-like receptor-signaling pathways (Fig. 6F). Importantly, the ribosome pathway returned to a level similar to normoxia upon HIF1α knockdown (Fig. 6F). Surprisingly, several metabolisms (i.e., drug, fatty acid, and xenobiotics metabolism) were similarly impaired by BS1 treatment under hypoxia and normoxia.

Altogether, these data showed that hypoxia globally impaired immune responses by inhibiting cellular pathways implicated in RNA processing and surveillance, as well as protein production, independently of the target gene or the stimulus. Interestingly, HIF1α knockdown rescued A3B induction, most probably by rescuing RNA processing and ribosome pathways, although it was not sufficient to completely revert the hypoxic state of the cells.

Discussion

Development of new therapeutics against HBV have largely focused on the use of immune mediators,

given that they have shown promising results both *in vitro* and *in vivo*.[3-5] We and others have previously shown that immune-mediated induction of A3B by LTβR agonization (i.e., with the LTβR agonist, BS1, or LTα$_1$β$_2$-expressing T cells) leads to noncytolytic degradation of nuclear HBV cccDNA, enabling long-term inhibition of HBV replication without rebound, even after treatment arrest.[6,7]

HIF1α has been shown to impair immune responses.[13,25] Inflammatory signaling has been shown to induce HIF1α, which we confirmed in our current study. Moreover, HBV pathogenesis and resulting fibrotic scaring processes will influence liver oxygenation, therefore modulation of HIF1α induction and stabilization. In the liver of CHB patients in immune-active (i.e., patients who potentially could clear the infection given that they likely express high levels of cytokines), we found a positive correlation between HIF1α expression and HBcAg-positive areas. Given that A3B mRNA was low in areas with high HIF1α, it can be expected that, *in vivo*, HBV might escape the immune responses in areas with elevated HIF1α staining.

We hypothesized that the correlation observed between HIF1α, HBcAg, and A3B mRNA highlights that low immune responses in HIF1α-high areas allow viral persistence, creating a viral reservoir. Therefore, we can hypothesize that blocking HIF1α stabilization during the immune-active phase of CHB patients could indeed be sufficient to allow more-potent immune responses, among which is induction of A3B, and viral elimination.

In vitro, we confirmed, using 1% oxygen, DMOG, and a number of other molecules inducing HIF1α stabilization, as well as HIF1α-overexpressing cell
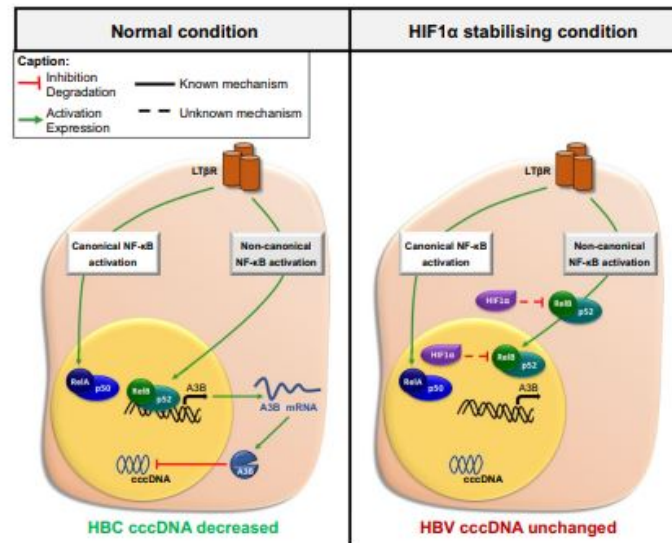
1778

FIG. 7. HIF1α stabilization prevents APOBEC3B-mediated anti-cccDNA effect by decreasing RelB protein. Graphical representation of the main proposed mechanism. Briefly, HIF1α stabilization under hypoxia or stabilizing molecule treatment decreases RelB protein levels, but not its mRNA. The decrease of RelB protein prevents the induction of APOBEC3B by LTβR agonization and, subsequently, cccDNA decay.

lines, that HIF1α stabilization mediates a strong impairment of LTβR-dependent A3B induction. However, impairment of immune responses was not limited to A3B as an NF-κB target gene, neither to BS1 as an NF-κB inducer, highlighting that HIF1α modulated NF-κB and other immune-signaling pathways (e.g., IFNα/γ-induced cccDNA degradation) to prevent the induction of immune mediators. Indeed, we identified that HIF1α impairs RelB protein, but not RelB mRNA level, *in vitro* and *in vivo*. This suggests that either RelB mRNA is not properly exported from the nucleus and/or is not efficiently translated, as confirmed by our proteomic data, which showed an impairment of RNA-processing and ribosome pathways under hypoxia. Alternatively, RelB stability is subjected to posttranslational modifications associated with pro-teasomal/lysosomal protein degradation.[26] We also found that the inhibitory activity of HIF1α toward RelB was independent of its partner, ARNT. An

ARNT-independent function of HIF1α starts to emerge,[27] and the HIF1α/RelB crosstalk we discovered could bring more insights into the immune metabolism of the liver.

The global inhibition of immune responses observed under HIF1α stabilization, with different ligands and on several targets, suggests the need to modulate HIF1α to obtain optimal immune activation and thus an antiviral response during immune therapies administration. However, it will be important to confirm the effect of HIF1α on other immune therapies and antiviral targets, as well as *in vivo*, in a therapeutic setup. Mass spectrometry revealed that even though HIF1α knockdown partially rescued pathways implicated in RNA and protein production and processing, it could not fully reactivate the immune response in cells. Interestingly, although the rescue of the "hypoxic state" of the proteome was only partial, it was sufficient to rescue A3B induction and thereby restore the anti-cccDNA effects of BS1

1779

treatment. From a clinical perspective, this could have severe consequences for the outcome of immune-stimulatory approaches for the treatment of CHB patients. The oxygen status of the liver microenvironment is not only important for parenchymal cells to be able to integrate external stimuli, but also for immune cells to exert their function properly.[14,25] Moreover, given that inflammation can trigger HIF1α stabilization, it will be mandatory to inhibit HIF1α to insure potent immune responses. Recently investigated HIF inhibitors have shown encouraging results in cancer therapies.[28] These molecules should be tested in the treatment of CHB, especially in patients with fibrosis, and thus with compromised liver oxygenation. In the context of immune-mediated A3B activation, a focus should be made on HIF1α inhibitors. Additionally, HIF1α inhibitors could be combined with immune therapies[3,5] to insure potent immune activation in the whole liver.

In summary, we have shown that HIF1α stabilization impairs NF-κB-mediated A3B induction, which is important for HBV cccDNA purging (Fig. 7). We believe that preventing the inhibitory activity of HIF1α toward RelB might represent a therapeutic window that should be considered as a support of combinatory immune therapies, to ensure a better efficacy of the treatment.

Author Contributions: Conceptualization: T.R., S.F.D., M.R., D.D., J.L., E.D., M.H. Methodology: T.R., S.F.D., M.R., D.D., J.L., E.D., M.H. Formal analysis: T.R., S.F.D., M.R. Investigation: T.R., S.F.D., M.R., S.S., Z.H., S.C., X.Z., J.W., M.A.L., R.B., V.M., S.P., D.H., C.G., M.Sc., B.H., B.S., K.R., K.U., D.T., P.S., J.L. Resources: M.Sc., B.H., K.U., B.S., I.M.W., P.S., J.M., U.P., D.D., J.L., E.D., M.H. Data curation: T.R., S.F.D., M.R. Writing, original draft: T.R., S.F.D., D.D., J.L., E.D., M.H. Visualization: T.R., S.F.D., M.R., E.D., M.H. Supervision: E.D., M.H. Project administration: E.D., M.H. Funding acquisition: D.D., J.L., E.D., M.H.

REFERENCES

1) https://www.who.int/news-room/fact-sheets/detail/hepatitis-b. Accessed August 2021.
2) Fanning GC, Zoulim F, Hou J, Bertoletti A. Therapeutic strategies for hepatitis B virus infection: towards a cure. Nat Rev Drug Discov 2019;18:827-844.
3) **Lucifora J**, **Bonnin M**, Aillot L, Fusil F, Maadadi S, Dimier L, et al. Direct antiviral properties of TLR ligands against HBV replication in immune-competent hepatocytes. Sci Rep 2018;8:5390.
4) Du K, Liu J, Broering R, Zhang X, Yang D, Dittmer U, et al. Recent advances in the discovery and development of TLR ligands as novel therapeutics for chronic HBV and HIV infections. Expert Opin Drug Discov 2018;13:661-670.
5) Niu C, Li LI, Daffis S, Lucifora J, Bonnin M, Maadadi S, et al. Toll-like receptor 7 agonist GS-9620 induces prolonged inhibition of HBV via a type I interferon-dependent mechanism. J Hepatol 2018;68:922-931.
6) **Lucifora J**, **Xia Y**, Reisinger F, Zhang K, Stadler D, Cheng X, et al. Specific and nonhepatotoxic degradation of nuclear hepatitis B virus cccDNA. Science 2014;343:1221-1228.
7) Koh S, Kah J, Tham CYL, Yang N, Ceccarello E, Chia A, et al. Nonlytic lymphocytes engineered to express virus-specific T-cell receptors limit HBV infection by activating APOBEC3. Gastroenterology 2018;155:180-193.e6.
8) Covino DA, Gauzzi MC, Fantuzzi L. Understanding the regulation of APOBEC3 expression: current evidence and much to learn. J Leukoc Biol 2018;103:433-444.
9) **Wang D**, **Li X**, **Li J**, **Lu Y**, Zhao S, Tang X, et al. APOBEC3B interaction with PRC2 modulates microenvironment to promote HCC progression. Gut 2019;68:1846-1857.
10) Dejardin E. The alternative NF-kappaB pathway from biochemistry to biology: pitfalls and promises for future drug development. Biochem Pharmacol 2006;72:1161-1179.
11) Dejardin E, Droin NM, Delhase M, Haas E, Cao Y, Makris C, et al. The lymphotoxin-β receptor induces different patterns of gene expression via two NF-κB pathways. Immunity 2002;17:525-535.
12) Mitchell S, Vargas J, Hoffmann A. Signaling via the NFκB system. Wiley Interdiscip Rev Syst Biol Med 2016;8:227-241.
13) D'Ignazio L, Bandarra D, Rocha S. NF-κB and HIF crosstalk in immune responses. FEBS J 2016;283:413-424.
14) Balamurugan K. HIF-1 at the crossroads of hypoxia, inflammation, and cancer. Int J Cancer 2016;138:1058-1066.
15) Gripon P, Rumin S, Urban S, Le Seyec J, Glaise D, Cannie I, et al. Infection of a human hepatoma cell line by hepatitis B virus. Proc Natl Acad Sci U S A 2002;99:15655-15660.
16) **Lucifora J**, **Arzberger S**, Durantel D, Belloni L, Strubin M, Levrero M, et al. Hepatitis B virus X protein is essential to initiate and maintain virus replication after infection. J Hepatol 2011;55:996-1003.
17) Seitz S, Iancu C, Volz T, Mier W, Dandri M, Urban S, et al. A slow maturation process renders hepatitis B virus infectious. Cell Host Microbe 2016;20:25-35.
18) **Faure-Dupuy S**, **Delphin M**, Aillot L, Dimier L, Lebossé F, Fresquet J, et al. Hepatitis B virus-induced modulation of liver macrophage function promotes hepatocyte infection. J Hepatol 2019;71:1086-1098.
19) Isorce N, Testoni B, Locatelli M, Fresquet J, Rivoire M, Luangsay S, et al. Antiviral activity of various interferons and pro-inflammatory cytokines in non-transformed cultured hepatocytes infected with hepatitis B virus. Antiviral Res 2016;130:36-45.
20) **Haybaeck J**, **Zeller N**, Wolf MJ, Weber A, Wagner U, Kurrer MO, et al. A lymphotoxin-driven pathway to hepatocellular carcinoma. Cancer Cell 2009;16:295-308.

21) Bersten DC, Sullivan AE, Peet DJ, Whitelaw ML. bHLH-PAS proteins in cancer. Nat Rev Cancer 2013;13:827-841.

22) Millet P, McCall C, Yoza B. RelB: an outlier in leukocyte biology. J Leukoc Biol 2013;94:941-951.

23) Wright CW, Duckett CS. The aryl hydrocarbon nuclear translocator alters CD30-mediated NF-kappaB-dependent transcription. Science 2009;323:251-255.

24) Gradin K, McGuire J, Wenger RH, Kvietikova I, Whitelaw ML, Toftgård R, et al. Functional interference between hypoxia and dioxin signal transduction pathways: competition for recruitment of the Arnt transcription factor. Mol Cell Biol 1996;16:5221-5231.

25) Palazon A, Goldrath AW, Nizet V, Johnson RS. HIF transcription factors, inflammation, and immunity. Immunity 2014;41:518-528.

26) Baud V, Collares D. Post-translational modifications of RelB NF-κB subunit and associated functions. Cells 2016;5:22.

27) Villa J, Chiu D, Brandes A, Escorcia F, Villa C, Maguire W, et al. Nontranscriptional role of Hif-1α in activation of γ-secretase and notch signaling in breast cancer. Cell Rep 2014;8:1077-1092.

28) Fallah J, Rini BI. HIF inhibitors: status of current clinical development. Curr Oncol Rep 2019;21:6.

Author names in bold designate shared co-first authorship.

Supporting Information

Additional Supporting Information may be found at onlinelibrary.wiley.com/doi/10.1002/hep.31902/suppinfo.

1781